Smithsonian
Scholarly Press

SMITHSONIAN CONTRIBUTIONS TO PALEOBIOLOGY • NUMBER 105

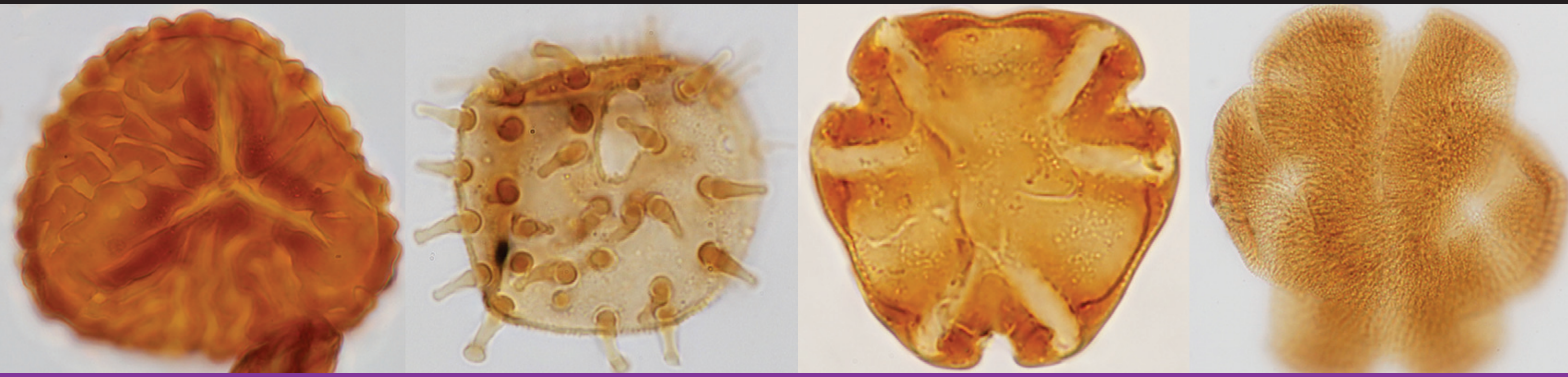

Miocene Palynology of the Solimões Formation (Well 1-AS-105-AM), Western Brazilian Amazonia

Carlos D'Apolito,
Carlos Jaramillo, and
Guy Harrington

SERIES PUBLICATIONS OF THE SMITHSONIAN INSTITUTION

Emphasis upon publication as a means of "diffusing knowledge" was expressed by the first Secretary of the Smithsonian. In his formal plan for the Institution, Joseph Henry outlined a program that included the following statement: "It is proposed to publish a series of reports, giving an account of the new discoveries in science, and of the changes made from year to year in all branches of knowledge." This theme of basic research has been adhered to through the years in thousands of titles issued in series publications under the Smithsonian imprint, commencing with Smithsonian Contributions to Knowledge in 1848 and continuing with the following active series:

Smithsonian Contributions to Anthropology
Smithsonian Contributions to Botany
Smithsonian Contributions to History and Technology
Smithsonian Contributions to the Marine Sciences
Smithsonian Contributions to Museum Conservation
Smithsonian Contributions to Paleobiology
Smithsonian Contributions to Zoology

In these series, the Smithsonian Institution Scholarly Press (SISP) publishes small papers and full-scale monographs that report on research and collections of the Institution's museums and research centers. The Smithsonian Contributions Series are distributed via exchange mailing lists to libraries, universities, and similar institutions throughout the world.

Manuscripts intended for publication in the Contributions Series undergo substantive peer review and evaluation by SISP's Editorial Board, as well as evaluation by SISP for compliance with manuscript preparation guidelines (available at https://scholarlypress.si.edu). SISP open access publications are licensed under Creative Commons licenses based on copyright status of content. Each is published initially online at https://smithsonian.figshare.com/ScholarlyPress and in print format in limited quantities.

SMITHSONIAN CONTRIBUTIONS TO PALEOBIOLOGY • NUMBER 105

Miocene Palynology of the Solimões Formation (Well 1-AS-105-AM), Western Brazilian Amazonia

Carlos D'Apolito,
Carlos Jaramillo, and
Guy Harrington

Smithsonian
Scholarly Press
WASHINGTON, D.C.
2021

ABSTRACT

D'Apolito, Carlos, Carlos Jaramillo, and Guy Harrington. *Miocene Palynology of the Solimões Formation (Well 1-AS-105-AM), Western Brazilian Amazonia*. Smithsonian Contributions to Paleobiology, number 105, viii + 134 pages, 16 figures, 31 plates, 3 tables, 2021. — During the Miocene, Andean tectonism caused the development of a vast wetland across western Amazonia. Palynological studies have been the main source of chronological and paleobotanical information for this region, including several boreholes in the Solimões Formation in western Brazilian Amazonia. Here, a palynological study of well core 1-AS-105-AM drilled in Tabatinga (Amazonas, Brazil) is presented: 91 new taxa are erected (25 spores and 66 pollen, including one new genus), 16 new combinations are proposed, and a list of botanical/ecological affinities is updated. We recorded 23,880 palynomorphs distributed in 401 different types. Among pollen and spores, 62 extant families and 99 extant genera were identified, which accounts for 39% and 30% of known botanical affinities to the family and genus level, respectively. Individual samples have pollen/spore counts with approximately 25% to 95% of known affinities to the family level. Pollen associations are sourced primarily from the wetland environments and to a minor extent from nonflooded forests. Palynological diversity analyses indicate an increase from the early to the middle/early late Miocene in core 1-AS-105-AM. Probable scenarios to explain this diversity increase include a higher degree of environmental complexity from the middle Miocene onwards, that is, a more heterogeneous riverscape, including broader extensions of nonflooded forests, as opposed to the swamp-dominated early Miocene. Additionally, the positive effects of the Miocene Climatic Optimum on plant richness could explain the increase in pollen richness. We posit hypotheses of forest diversification that can be tested as more botanical affinities are established along with a longer Miocene record.

Recommended citation:
D'Apolito, Carlos, Carlos Jaramillo, and Guy Harrington. 2021. *Miocene Palynology of the Solimões Formation (Well 1-AS-105-AM), Western Brazilian Amazonia*. Smithsonian Contributions to Paleobiology, No. 105. Washington, D.C.: Smithsonian Institution Scholarly Press.

Cover images: Plate parts 4b (*Crassoretitriletes vanraadshoovenii*), 10d (*Grimsdalea magnaclavata*), 15o (*Margocolporites carinae*), and 24i (*Perfotricolpites hexacolpatus sp. nov.*).

Published by SMITHSONIAN INSTITUTION SCHOLARLY PRESS
P.O. Box 37012, MRC 957, Washington, D.C. 20013-7012
https://scholarlypress.si.edu

Library of Congress Control Number: 2021940771

ISSN: 1943-6688 (online); 0081-0266 (print)

Contents

Figures

Tables

Miocene Palynology of the Solimões Formation (Well 1-AS-105-AM), Western Brazilian Amazonia

Carlos D'Apolito,[1,2*] *Carlos Jaramillo,*[2,3,4] *and Guy Harrington*[1]

INTRODUCTION

The landscape of western Amazonia underwent drastic changes as a result of Andean tectonism during the Miocene (Hoorn et al., 2010). During the Paleogene and most of the Neogene, drainages developed on cratonic areas (Guyana and Brazilian shields) and foothills of the Andes. These watersheds flowed into western Amazonia, where a high subsidence regime contributed to the development of the Pebas system, a continental-scale environment with no modern analogue, approximately 23–10 million years ago (Ma) (Hoorn, 1993; Hoorn et al., 2010; Wesselingh, 2006; Wesselingh et al., 2006a, 2006b). The Pebas was composed mostly of a mixture of deltaic plains; low-energy wetlands with swamps, ponds, and channels; extensive floodplains; and shallow freshwater lakes. Most of the drainage of western Amazonia ultimately was discharged into the Caribbean Sea via the Orinoco/Llanos region in Colombia and Venezuela (Jaramillo et al., 2017). Two short-lived marine floodings occurred during the Miocene that flooded most of western Amazonia (Jaramillo et al., 2017).

Rainforests covered most of the Pebas system (Hoorn, 1993, 1994a, 1994b; Jaramillo et al., 2010a; Silva-Caminha et al., 2010; Salamanca-Villegas et al., 2016; Leite et al., 2017) and a rich fauna of vertebrates developed (Lundberg et al., 1998, 2010; Monsch, 1998; Cozzuol, 2006; Salas-Gismondi et al., 2006, 2015; Antoine et al., 2007, 2016; Latrubesse et al., 2010; Negri et al., 2010; Riff et al., 2010; Aureliano et al., 2015; Cadena et al., 2020), together with a highly diverse community of invertebrates (Wesselingh et al., 2002, 2006a; Antoine et al., 2006; Wesselingh and Ramos, 2010; Gross et al., 2013, 2015; Linhares et al., 2017). By approximately 9.5–8.3 Ma, an Amazonian river flowing to the east was established for the first time (Gorini et al., 2014; Hoorn et al., 2017), subsidence in western Amazonia slowed, and there was a general collapse of the Pebas system and gradual transformation into the modern region that is dominated by terra firme (Wesselingh et al., 2002; Hoorn et al., 2010; Sacek, 2014).

Most of western Amazonia is covered with thick rainforests; most outcrops are only accessible along rivers and strata are often nearly flat. In such context, boreholes are fundamental tools to understanding the stratigraphy of the region. In the region near Leticia (Colombia) and Tabatinga (Brazil), dozens of cores were drilled in the 1970s, which have become an important source of information (e.g., Hoorn, 1993; Silva-Caminha et al., 2010; Kachniasz and Silva-Caminha, 2016; Jaramillo et al., 2017; Leite et al., 2017, 2021; Linhares et al., 2017, 2019; Leandro et al., 2019; Kern et al., 2020; Sá et al., 2020; Gomes et al., 2021). Nonetheless, a lot more work is necessary to address central questions about the evolution of the Amazon landscape and biota.

---

[1] Earth Sciences, University of Birmingham, Edgbaston, Birmingham, B15 2TT, UK.

[2] Smithsonian Tropical Research Institute, Box 0843-03092, Ancon, Panama.

[3] Institut des Sciences de l'Évolution de Montpellier, University of Montpellier, Montpellier, France.

[4] Department of Geology, Faculty of Sciences, University of Salamanca, Salamanca, Spain.

[*] Correspondence: carlosdapolito@gmail.com

Keywords: Amazonia; Miocene; Solimões Formation; palynology; new species; new genus.

Manuscript received: 24 November 2020; accepted 23 April 2021.

Most chronology in western Amazonia is derived from palynology. Hoorn (1993) proposed a pollen zonation adapted from Venezuela. This zonation was the basis of a molluscan zonation by Wesselingh et al. (2006b) and an ostracod zonation by Muñoz-Torres et al. (2006). More recently, a palynological zonation from the Llanos Basin in Colombia (Jaramillo et al., 2011) was applied to outcrops and cores in the Miocene of Peru, southern Colombia, and Brazil (Boonstra et al., 2015; Salamanca-Villegas et al., 2016; Jaramillo et al., 2017). Here, we present the palynological content of well core 1-AS-105-AM, review its taxonomy of pollen and spores, assess its diversity and ecological groups, and compare it with extant pollen assemblages to reconstruct depositional settings.

The Solimões Formation

The Solimões Formation in Brazil is located within the Solimões Basin (Figure 1). In Peru and southeastern Colombia, the formation is called Pebas and Amazonas, respectively. This system is bound on the north by the Guyana Shield, to the south by the Brazilian shields of Precambrian basement rocks, and to the east by a structural high called the Purus arch, interpreted as dividing the Solimões from the Amazonas Basin in central Amazonia. To the west, the Iquitos arch separates the Solimões/Pebas system from other Andean foreland basins (see Figure 1). Toward the Acre region, the Solimões Formation is thicker, more than 2,000 m in stratigraphic thickness (Maia et al., 1977; Silva-Caminha et al., 2020; Figure 1).

The Solimões Formation deposits accumulated predominantly in fluvio-lacustrine environments (Maia et al., 1977; Hoorn, 1993, 1994a; Latrubesse et al., 2007, 2010; Gross et al., 2011) with few shallow marine episodes (Hoorn, 1993; Boonstra et al., 2015; Salamanca-Villegas et al., 2016; Jaramillo et al., 2017). Lithofacies are dominated by gray to green muds and clays, silts, sands, and less abundantly layers of lignite and limestones. Age ranges from early Miocene to Pliocene (Cruz, 1984; Hoorn, 1993; Cozzuol, 2006; Wesselingh, 2006; Latrubesse et al., 2010; Silva-Caminha et al., 2010; Nogueira et al., 2013; Kachinasz and Silva-Caminha, 2016; Jaramillo et al., 2017; Leite et al., 2017, 2021; Linhares et al., 2019). The formation overlies the Alter do Chão Formation in the east and the Ramon Formation in the west, and it is overlain by either the Pleistocene Içá Formation, modern fluvial sediments, or it is exposed (Caputo, 1973; Maia et al., 1977; Eiras et al., 1994). In the 1970s, the Brazilian Geological Survey (CPRM) drilled 84 shallow cores (~50–400 m), some of which were studied for palynology, and only 17 of them are still preserved.

Core 1-AS-105-AM

Core 1-AS-105-AM (Figure 1; hereafter 105-AM) was drilled near Tabatinga, Brazil, (–4.5, –69.933) and reached 404.8 m deep. The core is composed almost entirely of the Solimões Formation, from 26.2 to 332.7 m deep. The lower-most 72.5 m belong to the Ramon Formation. Overall, sediments are poorly consolidated, mostly massive, with few preserved structures or bioturbation. Fossil content is seen as fragmented carbonized plant remains of millimetric scale, fragmented shell bits, but also some layers have rich, very well-preserved shells in life position. Beds sit conformably on each other, and there is no evidence for discontinuities. Lithologies do not vary much and are mostly composed of alternating clays, silts, and muds of gray, green, and dark colors, and sands of yellowish, cream, and grayish colors. Black peats and lignites are sporadic, never exceeding a meter in thickness and mostly of a few centimetres. Very thin (~10 cm) reddish paleosols and dark green biomicrite (~20–40 cm) are also present. The bottom core associated with the Ramon Formation is similar in composition, but thicker beds of quartzose white or cream sand prevail. The sedimentological analysis of core 105-AM (Jaramillo et al., 2017) revealed three informal members: from base to 267 m, there are thick beds of claystone and siltstone beds, and thinner, less frequent sands and lignites; from 267 to 168 m, the beds are still characterized by thick clay and siltstone accumulations but with thicker lignite beds (up to meter-scale) and paleosols; from 168 m to the top, there are mollusc-rich, bioturbated to massive fine-grained beds and thickening sandstone beds upsection (Figure 1).

Jaramillo et al. (2017) established ages of core 105-AM based on a graphic correlation analysis using the palynological zonation of the Llanos Orientales of Colombia as the Composite Section (Jaramillo et al., 2011). This correlation was done with first and last appearance events of key taxa as well as marine levels, which were detected on the Saltarin core in the Llanos Basin. The 105-AM core spans from about 18.7 to about 10.7 Ma, thus spanning the upper Burgidalian to the lower Tortonian (Figure 1). Two marine intervals were identified in 105-AM, 18–17.8 Ma and 14.1–13.7 Ma, respectively (Jaramillo et al., 2017; Figure 1). Overall, lithofacies associations are interpreted as a set of floodplains, small lakes, and swamps for most of the core (Jaramillo et al., 2017).

MATERIALS AND METHODS

Palynological Processing and Analyses

Ninety-five pollen samples from core 105-AM (one sample per ~4 stratigraphic meters on average) were processed as follows: approximately 10 cm^3 of sediments were macerated and washed in hydrochloric acid for at least 12 hours to remove carbonates; the remaining sediment was then washed in hydrofluoric acid for 24 hours to eliminate silicate materials (Wood et al., 1996). Each acid wash step is followed by washing with distilled water for neutralization. Finally, the residues were sieved in 250 and 10 μm meshes to eliminate coarse and very fine particles. The >10 μm fraction was further disintegrated in ultrasonic bath so that the less dense organic matter could be recovered and cleaned in ultrasonic bath. Panning was used to recover the fraction rich in palynomorphs, and centrifuging was avoided to prevent breaking delicate palynomorphs like algae

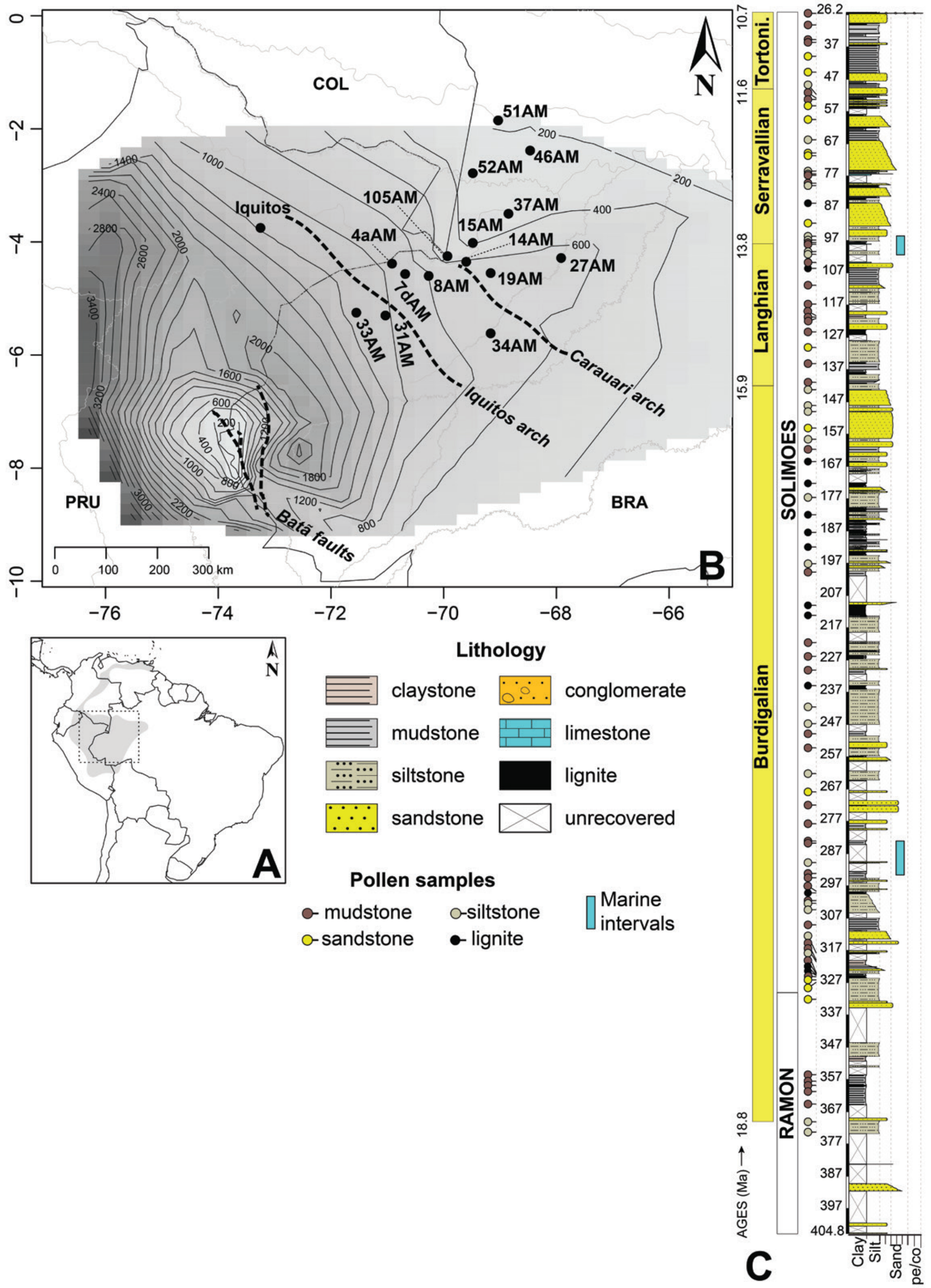

FIGURE 1. (A) Location map showing approximate coverage of the Solimões/Pebas deposits (gray shading) and the connection between western Amazonia and the Caribbean (after Jaramillo et al., 2017). (B) Study area: solid circles are cores (4aAM, Hoorn, 1993; 19-AM and 27-AM, Silva-Caminha et al., 2010; 31-AM and 34-AM, Kachniasz and Silva-Caminha, 2016; 51-AM and 52-AM, Leandro et al., 2019; 7d-AM and 8-AM, Linhares et al., 2019; 14-AM, Kern et al., 2020; 46-AM, Sá et al. 2020; 33-AM and 37-AM, Leite et al., 2021; 15-AM, Gomes et al., 2021; 105-AM, this study); isopach lines for the Miocene show depozones in the Acre region in Brazil and northern Peru (Maia et al., 1977, modified by Silva-Caminha et al., 2020). (C) Lithological column of core 105-AM (produced with R package SDAR, Ortiz and Jaramillo, 2019). The extension of the Solimões and Ramon Formations is shown along the column; ages follow Jaramillo et al. (2017).

and dinoflagellate cysts (see Plates 30, 31). Slides were mounted with polyvinyl alcohol and sealed with Canada balsam. Samples were processed at the laboratories of Paleoflora, Bucaramanga, Colombia. Palynomorphs were counted aiming for a minimum of 300 specimens per slide. Reworked palynomorphs were also counted but kept outside the 300 count.

Identifications followed local and regional publications that describe and illustrate the palynology of upper Cenozoic deposits (Germeraad et al., 1968; Lorente, 1986; Muller et al., 1987; Hoorn, 1993; Silva-Caminha et al., 2010; Leite et al., 2021) and the online electronic morphological database of Jaramillo and Rueda (2020). We also compiled an updated list of botanical affinities and the most likely ecology of each fossil taxon. The list of affinities was primarily based on previous compilations by Jaramillo et al. (2010a, 2014), Salamanca-Villegas et al. (2016), Hoorn et al. (2017), and D'Apolito et al. (2019) together with additional references that can be found in Table 1. Affinities established in the present study are based on comparisons with extant collections and with pollen atlases from western Amazonia (Colinvaux et al., 1999; Fontes et al., 2020) and other tropical areas (Roubik and Moreno, 1991; Dessaune-Rodrigues et al., 2016; Lorente et al., 2017).

Species ecology followed original descriptions that were complemented with the Flora do Brasil (Brazilian flora) project (Flora do Brasil, 2020) plus some references for specific taxa (Gentry, 1993; Punyasena et al., 2011; D'Apolito et al., 2017). Ecological affinity refers to the most likely parental habitat, terra firme (unfloodable forests), *várzea* (floodable forests that also includes riparian vegetation), and swamps represented by the *Mauritia* palm tree. Herbaceous plants were separated, when possible, into hydroseral (aquatic, semiaquatic, waterlogged, facultatively waterlogged) or terrestrial. When not assignable an ecology but of arboreal life form (e.g., Myrtaceae), the taxon was considered as undifferentiated lowland tree, and when habit was uncertain (e.g., Euphorbiaceae), the ecology was considered unknown.

TABLE 1. Botanical and ecological affinities for pollen and spores from the Miocene Solimões Formation, core 105-AM, western Amazonia. Ecological affinity abbreviations: dry forests (df), hydroseral (hy), undifferentiated lowland (lo), mangrove (ma), montane (mo), riparian (ri), terrestrial (te), white sand (ws), varzea (va). A dash (—) indicates lack of information. Bombac. = Bombacoideae; Caesalpin. = Caesalpinioideae; Mimos. = Mimosoideae; Papilion. = Papilionoideae.

Taxon (fossil)	Author^{a}	Family (Subfamily or Tribe)	Genera (with species if known)	Life form	Ecology	Reference^{a}
		Gymnosperms				
Cyclusphaera scabrata	1	Araucariaceae	—	Tree	lo	45
Podocarpidites sp. (informal)	2	Podocarpaceae	*Podocarpus*	Tree	lo, mo	2
		Angiosperms				
Arecipites 22522 (informal)	2	Arecaceae	—	Tree	—	2
Arecipites invaginatus sp. nov.	2	Arecaceae	—	Tree	—	2
Arecipites perfectus	3	Arecaceae	*Geonoma*	Tree	lo	2
Arecipites regio	4	Arecaceae	—	Tree	—	28
Bombacacidites 22293 (informal)	2	Malvaceae (Bombac.)	—	Tree	—	2
Bombacacidites araracuarensis	5	Malvaceae (Bombac.)	*Ceiba*	Tree	lo, va	5
Bombacacidites baculatus	6	Malvaceae (Bombac.)	*Pachira aquatica*	Tree	lo, va	46
Bombacacidites brevis	7	Malvaceae (Bombac.)	—	Tree	—	7
Bombacacidites hooghiemstrae sp. nov.	2	Malvaceae (Bombac.)	—	Tree	—	2
Bombacacidites lorenteae	8	Malvaceae (Bombac.)	*Bombax*	Tree	lo, va	9
Bombacacidites muinaneorum	9	Malvaceae (Bombac.)	*Bombacopsis*, *Pseudobombax*	Tree	lo, va	9; 2
Bombacacidites nacimientoensis	10	Malvaceae (Bombac.)	*Bombax*	Tree	lo, va	10

(*continued*)

TABLE 1. (*Continued*)

Taxon (fossil)	Author[a]	Family (Subfamily or Tribe)	Genera (with species if known)	Life form	Ecology	Reference[a]
Bombacacidites sp. (informal)	2	Malvaceae (Bombac.)	—	Tree	—	2
Byttneripollis ruedae	3	Malvaceae	*Byttneria*	Tree	lo	3
Cichoreacidites longispinosus	11	Asteraceae	*Piptocoma*, *Vernonanthura*, *Vernonia*	Herb	te, hy	32; 2
Clavainaperturites microclavatus	12	Chloranthaceae	*Hedyosmum*	Tree	mo, ri	5
Clavamonocolpites lorentei	6	Arecaceae	*Iriartea*?	Tree	lo	21
Corsinipollenites collaris	3	Onagraceae	*Ludwigia*	Herb	hy	2
Corsinipollenites oculusnoctis	13	Onagraceae	*Ludwigia*	Herb	hy	47
Corsinipollenites scabratus	3	Onagraceae	*Ludwigia*	Herb	hy	2
Crassiectoapertites columbianus	14	Fabaceae (Papilion.)	*Dioclea*, *Canavalia*	Liana	lo, ri	46; 2
Crotonoidaepollenites reticulatus	3	Euphorbiaceae	*Croton*	—	lo	2
Crototricolpites annemariae	15	Euphorbiaceae	*Glycydendron*	Tree	te	2
Crototricolpites finitus	3	Euphorbiaceae	*Glycydendron*	Tree	te	2
Ctenolophonidites suigeneris	3	Apocynaceae	*Geissospermum*	Tree	lo	3
Cyperaceaepollis wesselinghii sp. nov.	2	Cyperaceae	—	Herb	te, hy	2
Dicolpopollis? *costatus* sp. nov.	2	Apocynaceae	*Macoubea*	Tree	lo	2
Echidiporites barbeitoi	16	Arecaceae (Mauritiinae)	—	Tree	lo	32; 57
Echiperiporites estelae	18	Malvaceae	*Hampea*, *Hibiscus*, *Thespesia*	Tree	lo	18; 46
Echiperiporites lophatus	3	Convolvulaceae?	—	Liana	lo	2
Echiperiporites titanicus	19	Malvaceae	*Malachra*	Herb	te	19
Echitricolporites mcneillyi	18	Asteraceae	*Ambrosia*	Herb	te, hy	18
Echitricolporites spinosus	20	Asteraceae	—	Herb	te, hy	18
Echitriporites jolyi	19	Cucurbitaceae	*Cayaponia*	Liana	lo	19
Ericipites annulatus	21	Ericaceae	—	—	—	21
Florschuetzia impostora sp. nov.	2	Lythraceae?	—	—	—	2
Foveotricolpites simplex	22	Euphorbiaceae	*Sapium*	Tree	lo, va, ri	46
Glencopollis curvimuratus	3	Polygonaceae	*Polygonum*	Herb	te, hy	3; 2
Grimsdalea magnaclavata	18	Arecaceae (Mauritiinae)	Extinct genus	Tree	lo, hy	18; 49
Heterocolpites incomptus	9	Melastomataceae	*Miconia*?	Tree	lo	9
Heterocolpites rotundus	9	Melastomataceae	*Combretum*, *Terminalia*	Tree	lo, va	9; 46
Heterocolpites verrucosus	9	Melastomataceae	—	Tree	lo	9
Ilexpollenites 22438 (informal)	2	Aquifoliaceae	*Ilex*	Tree	lo, ws	2
Ilexpollenites tropicalis	3	Aquifoliaceae	*Ilex*	Tree	lo, ws	2
Jandufouria minor	1	Malvaceae	*Catostemma*?	Tree	lo, va	18
Ladakhipollenites campbellii sp. nov.	2	Lamiaceae	*Vitex*	Tree	lo, va	2
Ladakhipollenites? *caribbiensis*	23	Euphorbiaceae	*Sapium*	Tree	lo, va	2
Ladakhipollenites? *lolongatus*	24	Polygonaceae	*Symmeria*	Tree	va	24
Ladakhipollenites? *pseudocolpiconstrictus* sp. nov.	2	Fabaceae (Caesalpin.)	*Cassia, Senna*	Tree	lo	2

(*continued*)

TABLE 1. (*Continued*)

Taxon (fossil)	Author[a]	Family (Subfamily or Tribe)	Genera (with species if known)	Life form	Ecology	Reference[a]
Lakiapollis costatus	3	Chrysobalanaceae	*Couepia*, *Hirtella*, *Licania*, *Parinari*	Tree	lo	2
Lanagiopollis crassa	25	Tetrameristaceae	*Pelliciera*	Tree	ma	48; 50
Longapertites microfoveolatus	26	Arecaceae	—	Tree	—	50
Loranthacites tabatingensis sp. nov.	2	Loranthaceae	*Struthanthus*	Herb	lo	2
Luminidites amazonicus sp. nov.	2	Arecaceae	*Bactris*?	Tree	lo	2
Lymingtonia splendida sp. nov.	2	Convolvulaceae	*Evolvulus*, *Jacquemontia*	Liana	lo	2
Malvacipollis spinulosa	17	Picrodendraceae	*Piranhea* cf. *trifoliata*	Tree	te, hy	2
Malvacipolloides echibaculatus	19	Malvaceae?	—	—	—	2
Malvacipolloides maristellae	23	Malvaceae	*Allosidastrum*, *Sphaeralcea*, *Monteiroa*, *Malvella*, *Wissadula*	Herb	lo, df	51; 52
Margocolporites carinae	19	Apocynaceae	*Rauvolfia*	Tree	lo	2
Margocolporites vanwijhei	18	Fabaceae (Caesalpin.)	*Caesalpinia*	Tree	lo, va, ri	18
Mauritiidites franciscoi franciscoi	27	Arecaceae	*Mauritia*	Tree	hy	20
Mauritiidites franciscoi minutus	28	Arecaceae	*Mauritia*	Tree	hy	28
Mauritiidites franciscoi pachyexinatus	28	Arecaceae	*Mauritia*, *Mauritiella*	Tree	hy	28
Monoporopollenites annulatus	29	Poaceae	—	Herb	te, hy	53
Monoporopollenites scabratus	19	Poaceae	—	Herb	te, hy	19
Multiareolites? *reticulatus*	19	Acanthaceae	*Justicia*, *Dicliptera*	Herb	lo, va	19
Multimarginites vanderhammeni	18	Acanthaceae	*Trichanthera*, *Bravaisia*, *Sanchezia*	Tree	lo	18
Multiporopollenites crassinexinatus	3	Amaranthaceae	—	Herb	te, hy	2
Myrtaceidites spp. (informal)	2	Myrtaceae	*Myrtaceae*	Tree	lo	2
Paleosantalaceaepites kaarsii	8	Euphorbiaceae	*Dalechampia*	Liana	lo	9
Parsonsidites? *brenacii*	3	Amaranthaceae	—	Herb	te, hy	2
Parsonsidites? *minibrenacii* sp. nov.	2	Amaranthaceae	—	Herb	te, hy	2
Passifloriidites pseudoperculatus gen. et sp. nov.	2	Passifloraceae	*Passiflora* subgen. *Passiflora*	Liana	lo	2
Perfotricolpites digitatus	21	Convolvulaceae	*Merremia*	Liana	lo	48
Perfotricolpites hexacolpatus sp. nov.	2	Convolvulaceae	*Merremia*	Liana	te	2
Perisyncolporites pokornyi	18	Malpighiaceae	—	—	lo	18
Polyadopollenites macroreticulatus	30	Hippocrateaceae	*Hippocratea* (*volubilis*?)	Tree	lo	30
Polyadopollenites mariae	31	Fabaceae (Mimos.)	*Acacia*	Tree	lo, va, df	31
Polyadopollenites minimus sp. nov.	2	Fabaceae (Mimos.)	*Mimosa*	Herb	te	2

(*continued*)

TABLE 1. (*Continued*)

Taxon (fossil)	Author[a]	Family (Subfamily or Tribe)	Genera (with species if known)	Life form	Ecology	Reference[a]
Proteacidites poriscabratus sp. nov.	2	Sapindaceae	*Serjania*, *Paullinia*	Liana	te	2
Proteacidites pseudodehaanii sp. nov.	2	Proteaceae	*Roupala*, *Gevuina*	Tree	te	2
Proteacidites triangulatus	32	Sapindaceae, Proteaceae	*Allophylus*	Tree	lo	46; 32
Proxapertites psilatus	33	Nymphaeaceae	*Nymphaea*	Herb	hy	2
Proxapertites tertiaria	28	Annonaceae	*Crematosperma*	Tree	lo	54
Psilabrevitricolporites devriesii	11	Humiriaceae	*Humiria*	Tree	lo, ri, ws	32
Brevicolporites molinae	56	Apocynaceae?	—	—	—	56
Psiladiporites minimus	17	Moraceae	*Ficus*, *Sorocea*	Tree	lo	18; 2
Psiladiporites redundantis	21	Moraceae	—	Tree	lo	2
Psilamonocolpites amazonicus	9	Arecaceae	*Euterpe*?, *Geonoma*?, *Chelyocarpus*?	Tree	lo, va	9; 54
Psilamonocolpites medius	35	Arecaceae	—	Tree	lo	28
Psilamonocolpites nanus	9	Arecaceae	*Euterpe*?	Tree	lo, va	9; 54
Psilastephanocolporites fissilis	15	Polygalaceae	*Polygala*, *Monnina*?	Herb	hy	32; 54
Psilastephanocolporites marinamensis	5	Sapotaceae	—	Tree	lo	5
Psilastephanoporites herngreenii	9	Apocynaceae	*Forsteronia*, *Mandevilla*, *Odontadenia*	Liana	te	46; 2
Psilatriporites desilvae	9	Fabaceae (Caesalpin.)	—	Tree	lo	9
Psilatriporites minimus sp. nov.	2	Cannabaceae	*Celtis*	Tree	lo	2
Ranunculacidites operculatus	34	Euphorbiaceae	*Alchornea*	Tree	lo, va	17
Retimonocolpites absyae	9	Myristicaceae	*Virola*	Tree	lo, va	9
Retimonocolpites maximus	9	Arecaceae	—	Tree	lo	9
Retistephanoporites crassiannulatus	32	Malvaceae	*Quararibea*	Tree	lo, va	32
Retitrescolpites? *irregularis*	34	Phyllanthaceae	*Amanoa*	Tree	lo, va, ri	18
Retitrescolpites? *traversei*	3	Acanthaceae	*Teliostachya*	Tree	lo	3
Retitricolporites crassicostatus	17	Rubiaceae	—	—	—	54
Retitriporites crotonicolumellatus	36	Rubiaceae	*Chomelia*?	Tree	lo	2
Rhoipites caputoi	8	Araliaceae	—	Tree	—	54
Rhoipites guianensis	34	Malvaceae	*Vasivaea*, *Trichospermum*	Tree	lo	51
Rhoipites manausensis	24	Araliaceae	*Schefflera*	Tree	lo	2
Rugutricolporites arcus	9	Chrysobalanaceae	*Licania*, *Chrysobalanus*	Tree	lo	9; 2
Spirosyncolpites spiralis	21	Bignoniaceae?	—	—	—	54
Striatopollis catatumbus	37	Fabaceae (Caesalpin.)	*Crudia*	Tree	lo, va	12; 46
Striatopollis crassitectatus sp. nov.	2	Fabaceae (Caesalpin.)	*Macrolobium*	Tree	lo	2; 55
Syncolporites foveolatus sp. nov.	2	Fabaceae (Papilion.)	*Swartzia*	Tree	lo	2

(*continued*)

TABLE 1. (*Continued*)

Taxon (fossil)	Author[a]	Family (Subfamily or Tribe)	Genera (with species if known)	Life form	Ecology	Reference[a]
Syncolporites tenuicolpatus sp. nov.	2	Sapindaceae	*Serjania*	Liana	lo	2
Tetracolporopollenites labiatus	8	Sapotaceae	*Chrysophyllum*, *Micropholis*, *Pouteria*	Tree	lo, va	9; 2
Tetracolporopollenites magniporatus	8	Fabaceae?	—	—	—	9
Tetracolporopollenites obesus	8	Sapotaceae	—	Tree	lo	9
Tetracolporopollenites silvaticus	8	Burseraceae, Sapotaceae	*Protium*	Tree	lo	9; 2
Thymelipollis amazonicus sp. nov.	2	Thymelaeaceae	*Daphnopsis*?	—	—	2
Trichotomosulcites normalis sp. nov.	2	Arecaceae	—	Tree	lo	2
Verrustephanoporites circularis sp. nov.	2	Malpighiaceae	*Mascagnia*	Liana	lo	2
Verrustephanoporites intraverrucosus sp. nov.	2	Apocynaceae	*Forsteronia*, *Odontadenia*, *Prestonia*	Liana	lo	50
Verrutricolporites pusillus sp. nov.	2	Lythraceae?	—	—	—	2
Verrutricolporites rotundiporus	17	Lythraceae	*Crenea*	Tree	lo	50
Verrutricolporites simplex sp. nov.	2	Simaroubaceae	*Simarouba*?	Tree	lo	2
Zonocostites ramonae	18	Rhizophoraceae	*Rhizophora*	Tree	ma	18
		Ferns, Lycopsids, and Bryophytes				
Azolla sp. (informal)	2	Salviniaceae	*Azolla*	Fern	hy	2
Camarozonosporites fossulatus sp. nov.	2	Lycopodiaceae	*Lycopodium*, *Lycopodiella*	Fern	lo	2
Cicatricosisporites baculatus	38	Anemiaceae	*Anemia*	Fern	lo	38
Cicatricosisporites pseudograndiosus sp. nov.	2	Parkeriaceae	*Ceratopteris*	Fern	hy	2
Cingulatisporites cristatus sp. nov.	2	Selaginellaceae	*Selaginella*	Fern	lo	2
Cingulatisporites matisiensis sp. nov.	2	Notothyladaceae	*Phaeoceros*	Brio	lo	2
Crassoretitriletes vanraadshooveni	18	Schizaeaceae	*Lygodium microphyllum*	Fern	hy	18
Deltoidospora adriennis	39	Pteridaceae	*Acrostichum aureum*	Fern	hy, ma	48
Echinatisporis circularis	3	Selaginellaceae	*Selaginella*	Fern	lo	2
Echinatisporis muelleri	40	Selaginellaceae	*Selaginella*	Fern	lo	2
Echinatisporis sp. (informal)	2	Selaginellaceae	*Selaginella*	Fern	lo	2
Echinosporis densiechinatus sp. nov.	2	Marattiaceae	*Danaea*	Fern	lo	2
Foraminisporis connexus sp. nov.	2	Anthocerotaceae	*Anthoceros*	Brio	lo	2
Foveotriletes ornatus	38	Lycopodiaceae	*Huperzia*	Fern	lo	2
Hydrosporis minor	3	Salviniaceae	*Salvinia*, *Azolla*	Fern	hy	3
Kuylisporites waterbolkii	41	Cyatheaceae	*Hemitelia*, *Cnemidaria*	Fern	lo	46
Laevigatosporites cultellus sp. nov.	2	Polypodiaceae	*Vittaria?*	Fern	lo	2
Lycopodiumsporites amazonicus sp. nov.	2	Lycopodiaceae	*Lycopodium*	Fern	lo	2
Magnastriatites grandiosus	42	Pteridaceae	*Ceratopteris*	Fern	hy	18; 31
Nijssenosporites fossulatus	32	Adianthaceae	*Pityrogramma*	Fern	lo	32
Polypodiaceoisporites pseudopsilatus	32	Pteridaceae	*Pteris*	Fern	lo	32
Polypodiaceoisporites? *fossulatus*	1	Pteridaceae	—	Fern	lo	50
Polypodiisporites aff *specious*	43	Polypodiaceae	*Polypodium*	Fern	lo	43; 2

(*continued*)

TABLE 1. (*Continued*)

Taxon (fossil)	Author[a]	Family (Subfamily or Tribe)	Genera (with species if known)	Life form	Ecology	Reference[a]
Polypodiisporites densus sp. nov.	2	Polypodiaceae	*Polypodium*	Fern	lo	2
Polypodiisporites fossulatus sp. nov.	2	Lomariopsidaceae	*Nephrolepis*	Fern	lo	2
Polypodiisporites usmensis	44	Polypodiaceae	*Polypodium*	Fern	lo	20; 2
Psilatriletes marginatus sp. nov.	2	Cyatheaceae	*Cyathea*	Fern	lo	2
Pteridaceoisporis gemmatus	3	Pteridaceae	*Pteris*	Fern	lo	2
Reticulosporis diversus sp. nov.	2	Polypodiaceae	*Asplenium*	Fern	lo	2
Retitriletes altimuratus	3	Ricciaceae	*Riccia*	Brio	lo	2

[a] References:
1. Jaramillo and Dilcher, 2001
2. This study
3. Silva-Caminha et al., 2010
4. (Van der Hammen and García, 1966) Jaramillo and Dilcher, 2001
5. Hoorn, 1994b
6. Muller et al., 1987
7. (Duenãs, 1980) Muller et al., 1987
8. (Hoorn, 1993) nov. comb.
9. Hoorn, 1993
10. (Anderson, 1960) Elsik, 1968
11. (Lorente, 1986) Silva-Caminha et al., 2010
12. Hoorn, 1994a
13. (Thiergart, 1940) Nakoman, 1965
14. Dueñas, 1980 emend. Lorente, 1986
15. Leidelmeyer, 1966
16. (Muller et al., 1987) emend.
17. Van der Hammen and Wymstra, 1964
18. Germeraad et al., 1968
19. Leite et al., 2021
20. Van der Hammen, 1956a
21. González-Guzmán, 1967
22. (González-Guzman, 1967) nov. comb.
23. (Muller et al., 1987) Silva-Caminha et al., 2010
24. D'Apolito et al., 2019
25. (Van der Hammen and Wymstra, 1964) Frederiksen 1988
26. Jan du Chêne and Adegoke, 1978 (in Adegoke et al., 1978)
27. (Van der Hammen, 1956a) Van Hoeken–Klinkenberg, 1964
28. Van der Hammen and García, 1966
29. (Van der Hammen, 1954) Jaramillo and Dilcher, 2001
30. Salard-Cheboldaeff, 1974
31. Dueñas, 1980
32. Lorente, 1986
33. Sarmiento, 1992
34. (Van der Hammen and Wymstra, 1964) Jaramillo and Dilcher, 2001
35. (Van der Hammen, 1956b) Van der Hammen and García, 1966
36. (Jaramillo et al., 2011) nov. comb.
37. (González-Guzmán, 1967) Takahashi and Jux, 1989
38. Regali et al., 1974
39. (Potonié and Gelletich, 1933) Frederiksen, 1983
40. (Regali et al., 1974) Silva-Caminha et al., 2010
41. Potonié, 1956
42. (Kedves and Solé de Porta, 1963) Dueñas, 1980
43. Sah, 1967
44. (Van der Hammen, 1956a) Khan and Martin, 1972
45. Jaramillo et al., 2013
46. Jaramillo et al., 2014
47. Traverse, 1955
48. Hoorn et al., 2017
49. Pocknall and Jarzen, 2012
50. Jaramillo and Rueda, 2020
51. Hoorn et al., 2019
52. Espinosa et al., 2020
53. Van der Hammen, 1954
54. Salamanca-Villegas et al., 2016
55. Romero et al., 2020
56. (Schuler and Doubinger, 1970) Salard-Cheboldaeff, 1978
57. Bogotá-Ángel et al., 2021

Diversity Analyses

Within-sample pollen diversity (here used as the total number of species) was estimated using three approaches. First, we used rarefaction (Sanders, 1968), which standardizes sample sizes to a count number lower than the actual sample size. This is necessary because the total number of species in a sample is controlled by the number of specimens counted. Second, we used a sample-coverage rarefaction (Chao and Jost, 2012; Chao et al., 2014), which estimates richness based on completeness of sampling rather than on size. Sized-based rarefaction can be biased if samples with different species-abundance distributions are compared because they will have different degrees of sample completeness. A small size will be sufficient to correctly estimate a lower richness community but insufficient in a species richer community (Chao and Jost, 2012). Size-based and coverage-based rarefaction estimates were obtained using package iNEXT version 2.0.19 (Hsieh et al., 2019) for the R computing environment (R Core Team, 2019). We also used the Shannon index (H′) that accounts for abundances and evenness of species and was calculated with R package "vegan" version 2.5-5 (Oksanen et al., 2019). Sample sizes (*n*) less than 169 were excluded from analysis because they were determined to be too small to be informative. The final number of analyzed samples was about 78% of the total number of samples counted.

Species accumulation curves were also produced to investigate among-sample diversity, that is, how diversity increases as new samples were included (Gilinsky, 1991). These analyses were performed with R package "vegan" (Oksanen et al., 2019).

Multivariate Analyses

Two multivariate analyses were performed to explore similarities in pollen/spore composition of samples. First, a nonparametric multidimensional scaling (nMDS) was calculated using the Chao similarity index (Chao et al., 2005), with singletons excluded. The Chao index incorporates unseen shared species and thus is ideal for species-rich data sets like pollen counts from tropical areas. Second, a detrended component analysis (DCA) was run on a range-through version of the data, excluding singletons, to explore major palynofloristic gradients along time. Both analyses were performed in R package "vegan" (Oksanen et al., 2019).

TAPHONOMY

We used analyses of variance (Kruskal–Wallis test and post hoc Dunn's test) to assess the taphonomic control of lithofacies on diversity metrics. Post hoc analyses were run using R package "dunn.test" version 1.3.5 (Dinno, 2017). For multivariate metrics, we obtained the Euclidean distances within and among lithologies from the nMDS biplot, then we tested each combination of within versus among lithology differences with *t*-tests bootstrapped 10,000 times to account for different sample sizes. Among lithology distances were the distances of every pair of samples from two different lithologies. Four main types of lithology predominated in the samples: mudstones, siltstones, sandstones and lignites (Figure 1).

We also investigated differences in diversity and multivariate metrics for samples that were classified as palm swamps. They consisted of those samples that contained either *Mauriitidites* or *Grimsdalea magnaclavata* with a minimum abundance of 5% (*Mauriitiitides* samples = 11; *G. magnaclavata* samples = 20). This value was chosen based on the amount of *Mauritia* pollen found in modern *Mauritia* swamps or *Mauritia*-dominated forests (e.g., flooded/riparian forests) (e.g., Muller, 1959; Ferraz-Vicentini and Salgado-Labouriau, 1996; Behling et al., 1999; Weng et al., 2004; Cassino et al., 2015).

DISTRIBUTION MODELS

We tested which species distribution models were the best fit for palynological counts. Abundance distributions can vary among communities (Magurran, 2004) and could represent shifts in vegetation assemblages or paleoenvironments. Five models were investigated (broken stick, preemption, log-normal, Zipf, and Zipf-Mandelbrot), and their fit was evaluated with the AIC (Akaike information criterion). Fitting models was done with function radfit() from R package "vegan" (Oksanen et al., 2019).

COMPARISON WITH EXTANT POLLEN ASSEMBLAGES

For a comparison of the Solimões Formation and extant environments of Amazonian lowland plains, we used available data from two Holocene localities. In western Amazonia, Behling et al. (1999) analyzed three short sections from the Pantano de Mónica (−0.7, −72.06, 160 meters above sea level [masl]), which is a swamp system on the low terrace of the Caquetá River in Colombia and does not undergo inundation during the river's high stands. In central Amazonia, Absy (1979) analyzed várzea lakes Surara (−4.15, −61.54, ~15 masl), along the Purus River, and Terra Nova (−3.08, −59.72, ~15 masl), along the Amazonas River near Manaus; both lakes are associated with the main river courses and flood periodically during high stands. Pollen data from these localities were categorized similarly to the fossil data regarding ecological groups, combined into one data set (Holocene) and compared to Miocene data.

Palynological raw counts and R codes for analyses, figures, map, and stratigraphical section of core 105-AM can be downloaded at https://doi.org/10.25573/data.14374121.v1.

RESULTS

A total of 23,880 palynomorphs were counted in 95 samples (only 3 were completely barren). We recorded 401 pollen and spore fossil taxa (318 angiosperms, 2 gymnosperms, 78 pteridophytes, and 3 bryophytes); 59 Paleozoic and Cretaceous reworked taxa; 2 freshwater algal cysts, foraminiferal organic linings; and 21 dinoflagellate cyst taxa. Among the angiosperms, 124 taxa were assigned to 45 extant families and 77 genera. Among the gymnosperms, 2 taxa were assigned to 2 extant families and 1 genus. Among the pteridophytes, 27 taxa were assigned to 12 extant families and 18 genera (Table 1). We also recorded 3 bryophyte families and 3 genera (Table 1). In total, about 39% of all pollen and spore taxa had a known biological affinity at least to the family level and 30% to the genus level. When abundances were taken into account, the proportion of known botanical affinities to the family level ranged from about 25.1% to 95% (median of 59.3%) of the pollen counts per sample.

The richest families recorded are Arecaceae (n = 17 taxa), Malvaceae (n = 16 [9 of which are Bombacoid]), Fabaceae (n = 9), Euphorbiaceae (n = 7), Apocynaceae (n = 5), and Polypodiaceae (n = 5) among others (Figure 2A,B). A great majority of families (n = 41) were represented by a single species (Figure 2A,B). A total of 247 types (61%) could not be assigned any affinity, representing an average of 36% unknown types per sample (ranging from 20 to 68%).

The top-ranked families by grain abundance were palm trees (Arecaceae), herbaceous elements like Poaceae and ferns (Polypodiaceae, Salviniaceae, Pteridaceae) as well as aquatic plants (Cyperaceae, Amaranthaceae) (Figure 2C). Top-ranked woody elements were Picrodendraceae (*Piranhea* cf. *trifoliata*), Euphorbiaceae (*Sapium* spp.), Melastomataceae, Malvaceae (including many Bombacoid trees), Rhizophoraceae (*Rhizophora* sp.), and Podocarpaceae (*Podocarpus* sp.).

TAPHONOMIC EFFECT

There was a significant effect of lithology on all diversity metrics (Table 2). Lignites had a significantly lower diversity

TABLE 2. The effect of lithology on diversity metrics of core 105-AM: summary results of variance analyses (Kruskal–Wallis [KW], in parentheses) and Dunn's post hoc tests searching variance among groups; df = degrees of freedom. Numbers shown are *P*-values. Order of significance: *** = 0–0.001; ** = 0.001–0.01; * = 0.01–0.05; + = 0.05–0.1 (marginally significant). A dash (—) indicates the same lithology, hence no comparison performed.

Diversity metric and statistics	Lithology	Lignite	Mudstone	Sandstone
Size-based diversity	Mudstone	0.12	—	—
(KW chi-square = 20.58,	Sandstone	0.0008***	0.0480*	—
DF = 3, *P* = 0.000128***)	Siltstone	0.0004***	0.0039**	0.74
Coverage-based diversity	Mudstone	0.1976	—	—
(KW chi-square = 21.05,	Sandstone	0.0006***	0.0224*	—
DF = 3, *P* = 0.000102***)	Siltstone	0.0006***	0.0306*	0.69
Shannon diversity	Mudstone	0.3379	—	—
(KW chi-square = 14.97,	Sandstone	0.0074**	0.1103	—
DF = 3, *P* = 0.001842**)	Siltstone	0.0034**	0.0691+	0.98
Sample coverage	Mudstone	0.0684+	—	—
(KW chi-square = 20.58,	Sandstone	0.0004***	0.0493*	—
DF = 3, *P* = 0.000006***)	Siltstone	0.0002***	0.0417*	0.63

TABLE 3. Median Euclidean distances within samples of core 105-AM by lithological group. Distances were extracted from the nonparametric multidimensional scaling (nMDS) biplot (Figure 8A) and bootstrapped 10,000 times using 10 samples, the lowest number of samples of any given lithology (sandstones). Within- versus among-lithology comparisons were performed using t-tests (significance based on median P-value bootstrapped 10,000 times). Only significant tests are shown; percentage in parentheses is amount of iterations below the 0.05 significance threshold. Order of significance: *** = 0–0.001; ** = 0.001–0.01; * = 0.01–0.05; + = 0.05–0.1. A dash (—) indicates nonsignificant results.

Lithology	Euclidean distances	Mudstone–sandstone	Mudstone–lignite	Siltstone–lignite	Sandstone–lignite
Mudstone	0.33±0.2	—	—	—	—
Siltstone	0.23±0.17	—	—	—	—
Sandstone	0.22±0.13	*P*=0.07+ (43%)	—	—	*P*<0.001*** (93%)
Lignite	0.22±0.11	—	*P*<0.02* (72%)	*P*=0.06+ (43%)	*P*<0.01** (93%)

(Figure 3A–C) and higher sample coverage (Figure 3D) compared to other lithologies (Figure 3; Table 2). Sandstones had significantly higher diversity indices and lower coverage compared to mudstones and lignites (Table 2). The nMDS analysis revealed that lignites and sandstones differed significantly between each other in pollen/spore composition (Table 3; see Figure 8A) and that lignites also differed from mudstones (Table 3). Moreover, the stratigraphic distribution of sandstones and lignites was uneven: when the core was split into two segments (upper and lower ~200 m, see section below), there were 11 lignites in the lower block while there were 2 lignites in the upper block, and there was 1 sandstone in the lower while 9 were in the upper block (Figure 1). Therefore, we excluded lignite and sandstone samples from the diversity analyses given the high degree of unbalanced stratigraphic sampling, and we focused only on comparing mudstone and siltstone samples.

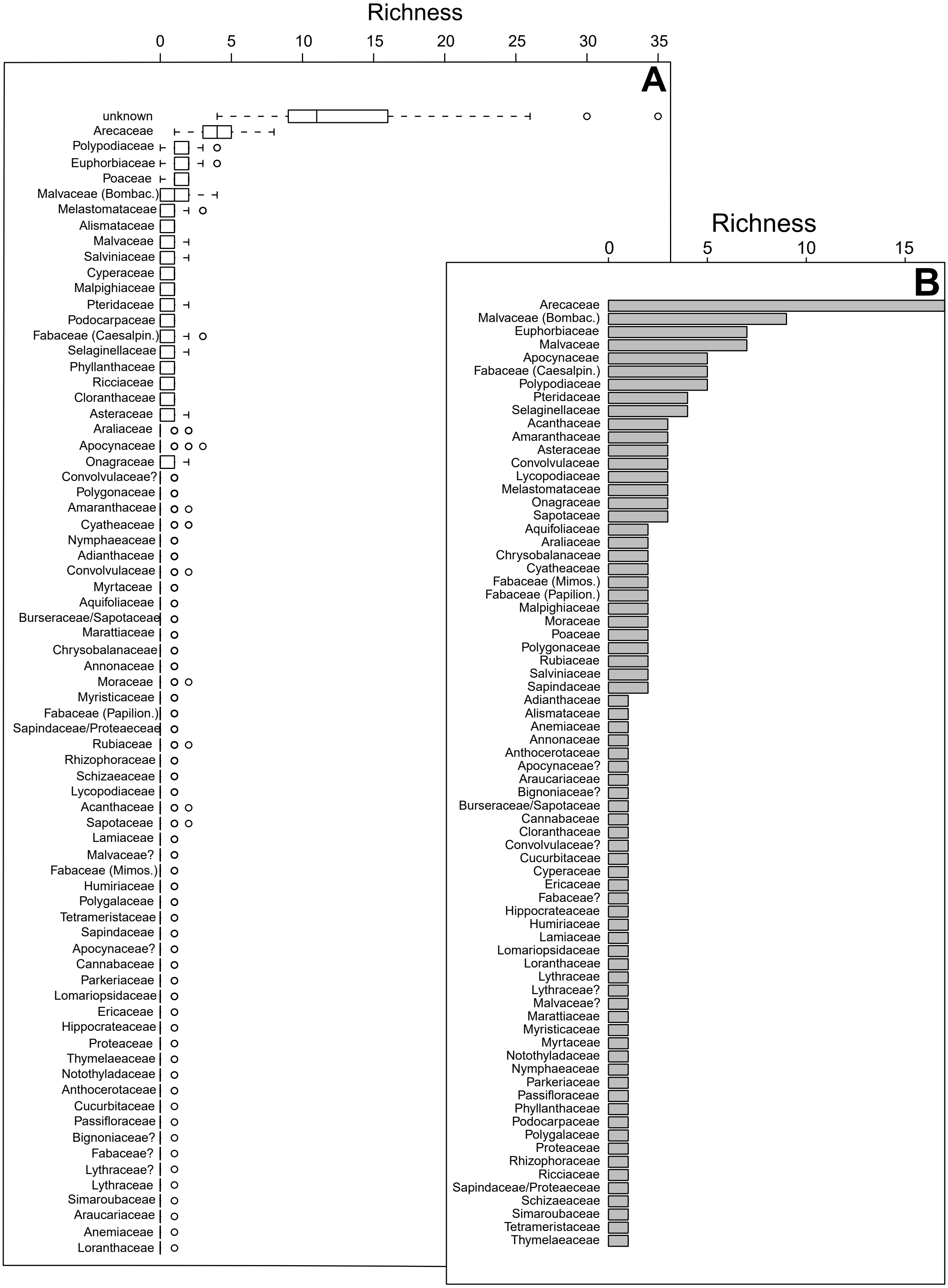
Richness
0
5
10
15
20
25
30
35
A
unknown
Arecaceae
Polypodiaceae
Euphorbiaceae
Poaceae
Malvaceae (Bombac.)
Melastomataceae
Alismataceae
Malvaceae
Salviniaceae
Cyperaceae
Malpighiaceae
Pteridaceae
Podocarpaceae
Fabaceae (Caesalpin.)
Selaginellaceae
Phyllanthaceae
Ricciaceae
Cloranthaceae
Asteraceae
Araliaceae
Apocynaceae
Onagraceae
Convolvulaceae?
Polygonaceae
Amaranthaceae
Cyatheaceae
Nymphaeaceae
Adianthaceae
Convolvulaceae
Myrtaceae
Aquifoliaceae
Burseraceae/Sapotaceae
Marattiaceae
Chrysobalanaceae
Annonaceae
Moraceae
Myristicaceae
Fabaceae (Papilion.)
Sapindaceae/Proteaeceae
Rubiaceae
Rhizophoraceae
Schizaeaceae
Lycopodiaceae
Acanthaceae
Sapotaceae
Lamiaceae
Malvaceae?
Fabaceae (Mimos.)
Humiriaceae
Polygalaceae
Tetrameristaceae
Sapindaceae
Apocynaceae?
Cannabaceae
Parkeriaceae
Lomariopsidaceae
Ericaceae
Hippocrateaceae
Proteaceae
Thymelaeaceae
Notothyladaceae
Anthocerotaceae
Cucurbitaceae
Passifloraceae
Bignoniaceae?
Fabaceae?
Lythraceae?
Lythraceae
Simaroubaceae
Araucariaceae
Anemiaceae
Loranthaceae
Richness
0
5
10
15
B
Arecaceae
Malvaceae (Bombac.)
Euphorbiaceae
Malvaceae
Apocynaceae
Fabaceae (Caesalpin.)
Polypodiaceae
Pteridaceae
Selaginellaceae
Acanthaceae
Amaranthaceae
Asteraceae
Convolvulaceae
Lycopodiaceae
Melastomataceae
Onagraceae
Sapotaceae
Aquifoliaceae
Araliaceae
Chrysobalanaceae
Cyatheaceae
Fabaceae (Mimos.)
Fabaceae (Papilion.)
Malpighiaceae
Moraceae
Poaceae
Polygonaceae
Rubiaceae
Salviniaceae
Sapindaceae
Adianthaceae
Alismataceae
Anemiaceae
Annonaceae
Anthocerotaceae
Apocynaceae?
Araucariaceae
Bignoniaceae?
Burseraceae/Sapotaceae
Cannabaceae
Cloranthaceae
Convolvulaceae?
Cucurbitaceae
Cyperaceae
Ericaceae
Fabaceae?
Hippocrateaceae
Humiriaceae
Lamiaceae
Lomariopsidaceae
Loranthaceae
Lythraceae
Lythraceae?
Malvaceae?
Marattiaceae
Myristicaceae
Myrtaceae
Notothyladaceae
Nymphaeaceae
Parkeriaceae
Passifloraceae
Phyllanthaceae
Podocarpaceae
Polygalaceae
Proteaceae
Rhizophoraceae
Ricciaceae
Sapindaceae/Proteaeceae
Schizaeaceae
Simaroubaceae
Tetrameristaceae
Thymelaeaceae

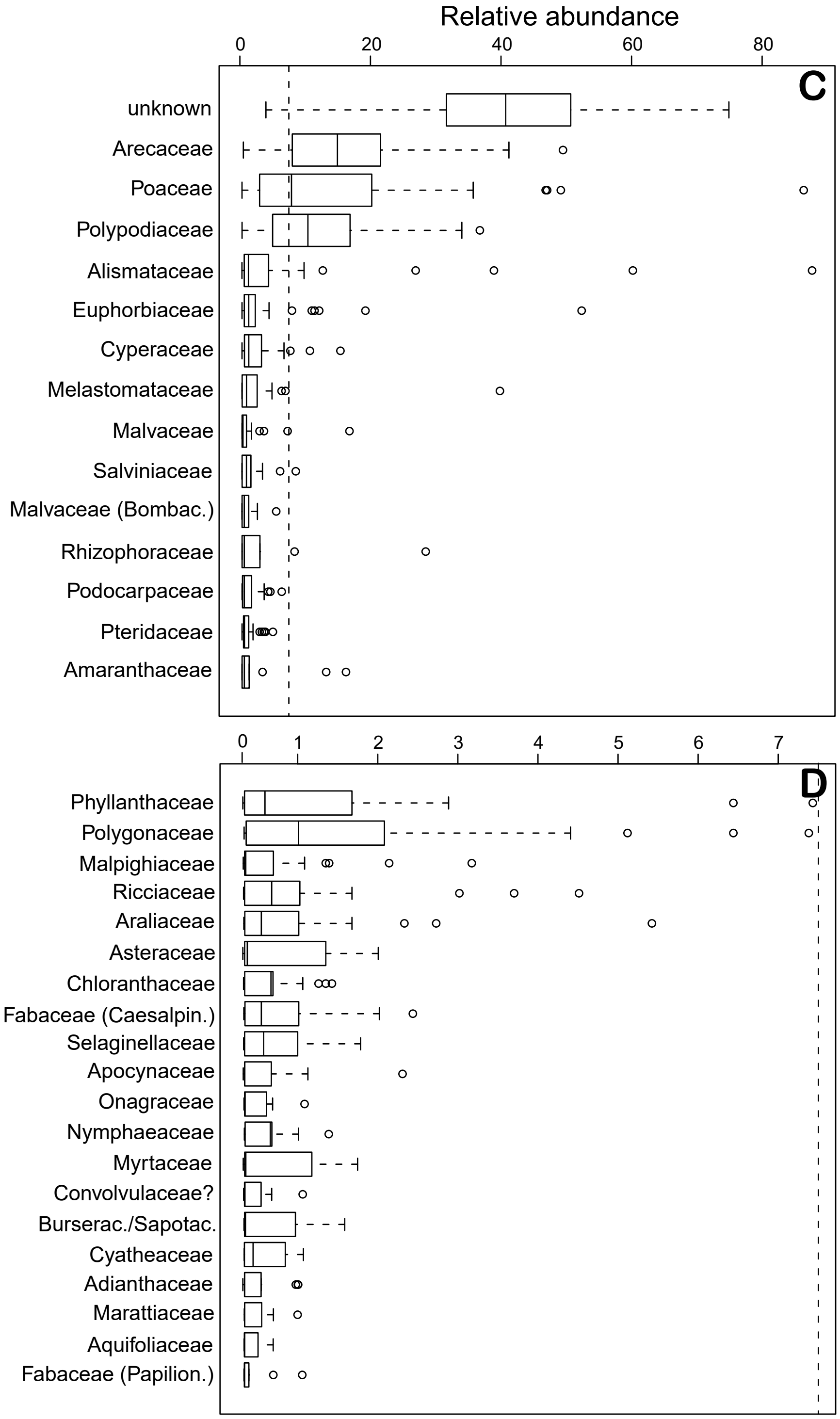

FIGURE 2. (*Facing page and above*) Richness and relative abundance of botanical families/subfamilies from core 105-AM, western Brazilian Amazonia. (A) Boxplots with richness per sample, (B) richness data for the entire data set, (C–D) boxplots with relative abundance data per sample. Selected families were ordered by mean abundances, notice scale change from right to left panel. The list of botanical affinities can be found in Table 1.

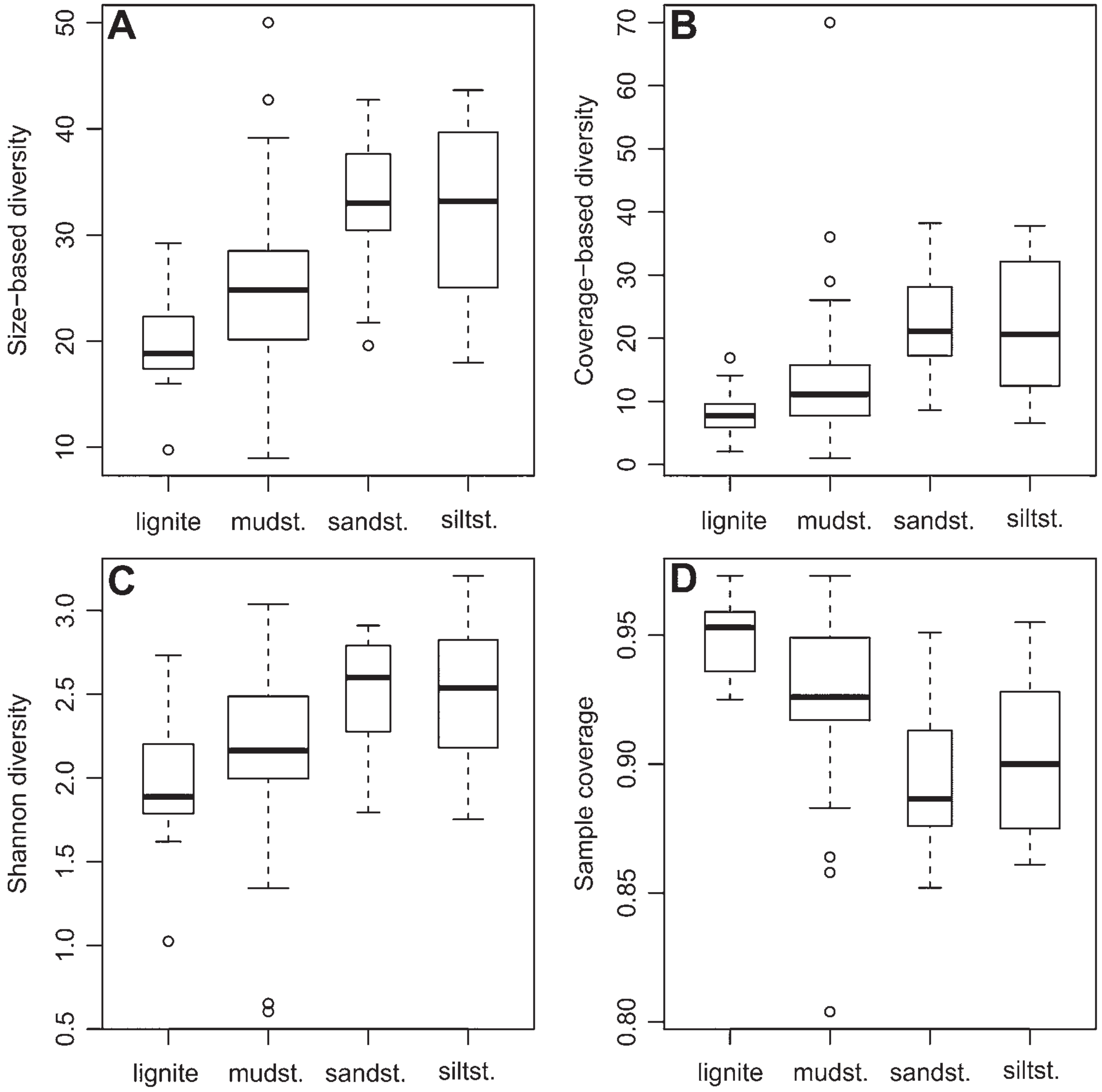

FIGURE 3. Boxplots of diversity metrics by lithological types from core 105-AM, western Brazilian Amazonia. (A) Size-based rarefied diversity, (B) coverage-based rarefied diversity, (C) Shannon H′ index, and (D) sample coverage. For statistical comparisons, see Table 2.

Diversity Analyses

Estimates of pollen/spore diversity showed an increase from bottom to top of the 105-AM core. To find out where the most significant break is, consecutive *t*-tests were run on comparing groups of samples (lower core versus upper core): two bottommost samples versus remaining upper samples, three bottommost samples versus remaining upper samples minus one, and so on. The lowest *P*-value for all three diversity metrics (size rarefaction, coverage rarefaction, and H′) was found to be at 197.2 m (Figure 4A). This depth had an age of about 16.6 Ma (Jaramillo et al., 2017), and it split the core into two main blocks, early Miocene (~18.7–16.6 Ma) and middle to early late Miocene (~16.1–10.7 Ma). Further analyses will consider these two blocks for comparisons (Lower 16 and Upper 16, respectively). The subset of mudstones + siltstones created a sampling gap between 161.7 and 197.2 m (Figure 4A). A test of the most significant difference including all lithologies showed for all metrics the depth 165.5 m to be the break point (Figure 4B), with an estimated age of 16.1 Ma.

The estimate of sampling completeness (sample coverage) was high, varying from 0.804 to 0.973. The lowest value (0.804) was used for the sample coverage-based rarefaction cut off. There was a significant decrease in coverage from Lower 16 (0.938±0.02) to Upper 16 (0.904±0.03) (Figure 5B; *t*-test, df =

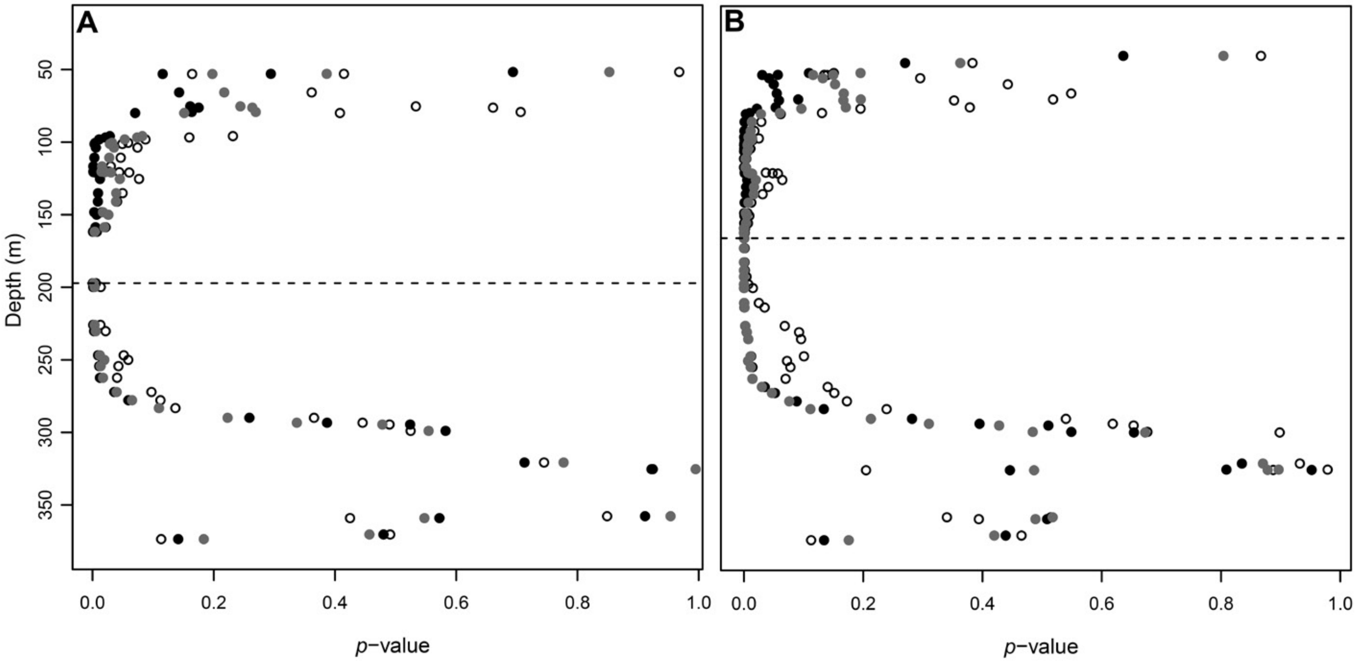

FIGURE 4. The *P*-values from *t*-tests comparing diversity metrics along core 105-AM. Shannon (open symbols), size-based rarefaction (solid symbols), coverage-based rarefaction (gray). (A) Mudstones and siltstones, dashed line is the lowest *P*-value found for all three metrics at 197.2 m (age = 16.6 Ma). (B) All samples, dashed line indicates 165.5 m (age = 16.1 Ma).

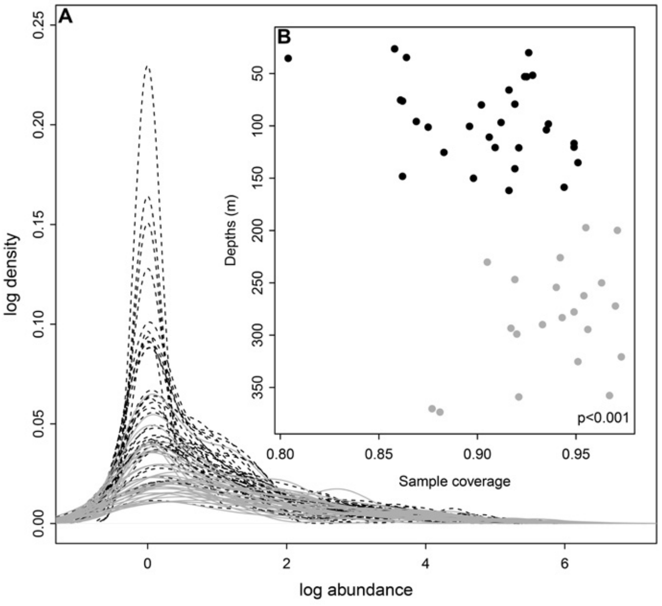

FIGURE 5. (A) Density distributions for abundance data of all pollen samples of core 105-AM; gray lines are samples from the lower group, black dashed lines are samples from the upper group. (B) Sample coverage values along core 105-AM; *P*-value refers to *t*-test comparing mudstone and siltstone samples of the lower (373.5–197.2 m) and upper (161.7 to 26.2 m) groups.

47.9, $P < 0.001$). Upper 16 samples were richer in singletons (from 12.5±5.9 to 20.2±8.5, *t*-test, df = 49, $P < 0.001$) and doubletons (from 3.8±2.3 to 5.7±2.3, *t*-test, df = 45, $P < 0.04$).

The Shannon index H′ increased from of 2.01±0.6 in Lower 16 to 2.43±0.3 in Upper 16 (Figure 6A) (*t*-test, df = 28.7, $P < 0.02$). Size-based rarefaction (Figure 6B) increased significantly by 38%, from 22.4±8.9 in Lower 16 to 30.9±7.7 in Upper 16 (*t*-test, df = 39.3, $P < 0.01$, rarefaction cutoff = 169). Sample coverage-based rarefaction (Figure 6C) had a similar trend, with a significant increase from 11±8.8 to 20.3±12.8 (*t*-test, df = 49, $P < 0.01$), an increase of about 84%.

The species accumulation curves show that an asymptote was not reached (Figure 7). The Lower 16 accumulated species at a lower rate than the Upper 16 block (Figure 7B). There were 94 taxa restricted to the Lower 16 group (or ~23% of the total richness), 149 taxa were restricted to the Upper 16 (or ~37%), while 158 (or ~39%) of the taxa range through both blocks.

MULTIVARIATE ANALYSES

The nMDS reached a solution with 3 dimensions and 100 runs and had a stress value of 0.200, which is at the limit of fit (Clarke, 1993) (Figure 8A). Mudstones occupied a greater extent of the biplot space (Table 3), and lignites and sandstones differed from each other (Table 3). The DCA with range-through transformed data displayed a shifting trend against depth (Figure 8B), with a break around 157 m (Figure 8) that corresponded to

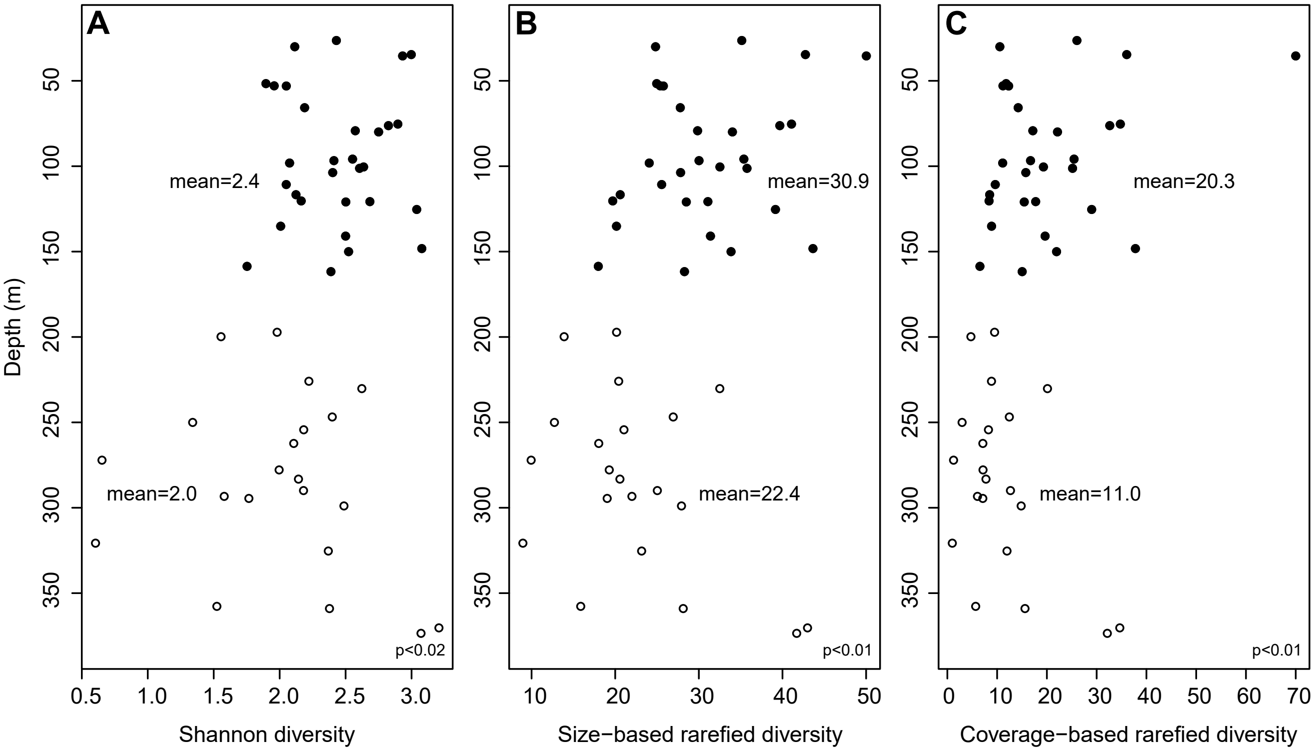

FIGURE 6. Diversity estimates for pollen samples (mudstones and siltstones) from core 105-AM, western Amazonia. (A) Shannon H′ index; (B) size-based rarefied diversity at a sample size of 169; (C) coverage-based rarefied diversity at a sample coverage of 0.804. The *P*-values refer to comparisons between the lower (373.5–197.2 m; open symbols) and upper (161.7–26.2 m; solid symbols) group.

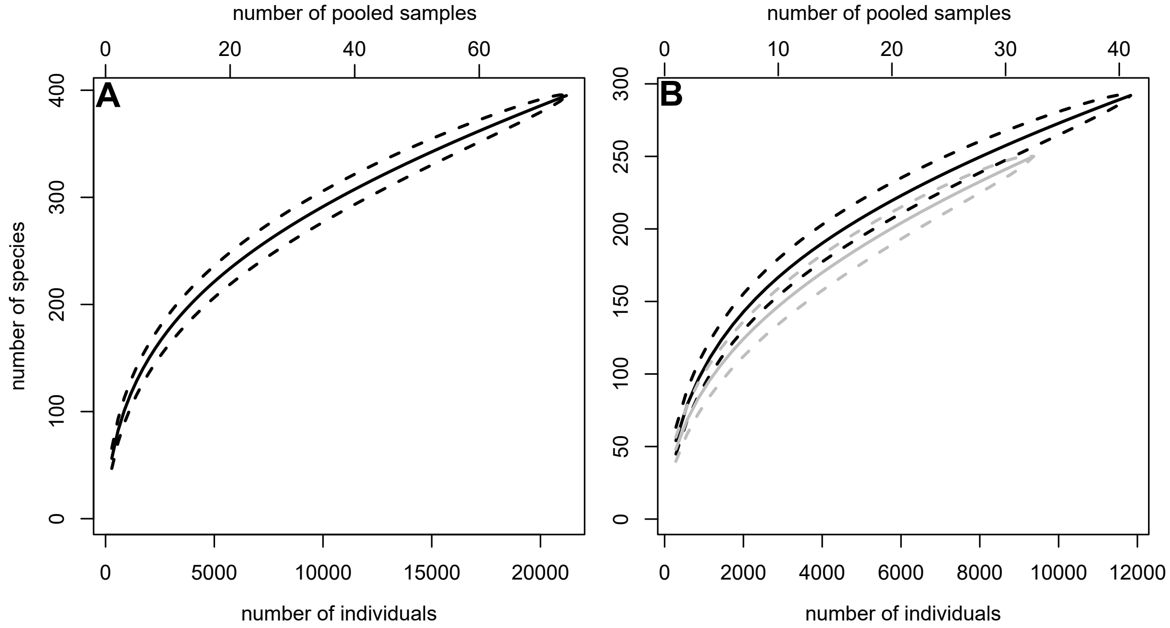

FIGURE 7. Species accumulation curves for all pollen samples from core 105-AM. (A) All samples, and (B) samples from lower group (373.5–165.5 m) in gray, and the upper group (165.5 to 26.2 m) in black. Total number of samples = 74; total number of individuals counted = 21,194. Dashed lines are 95% confidence intervals.

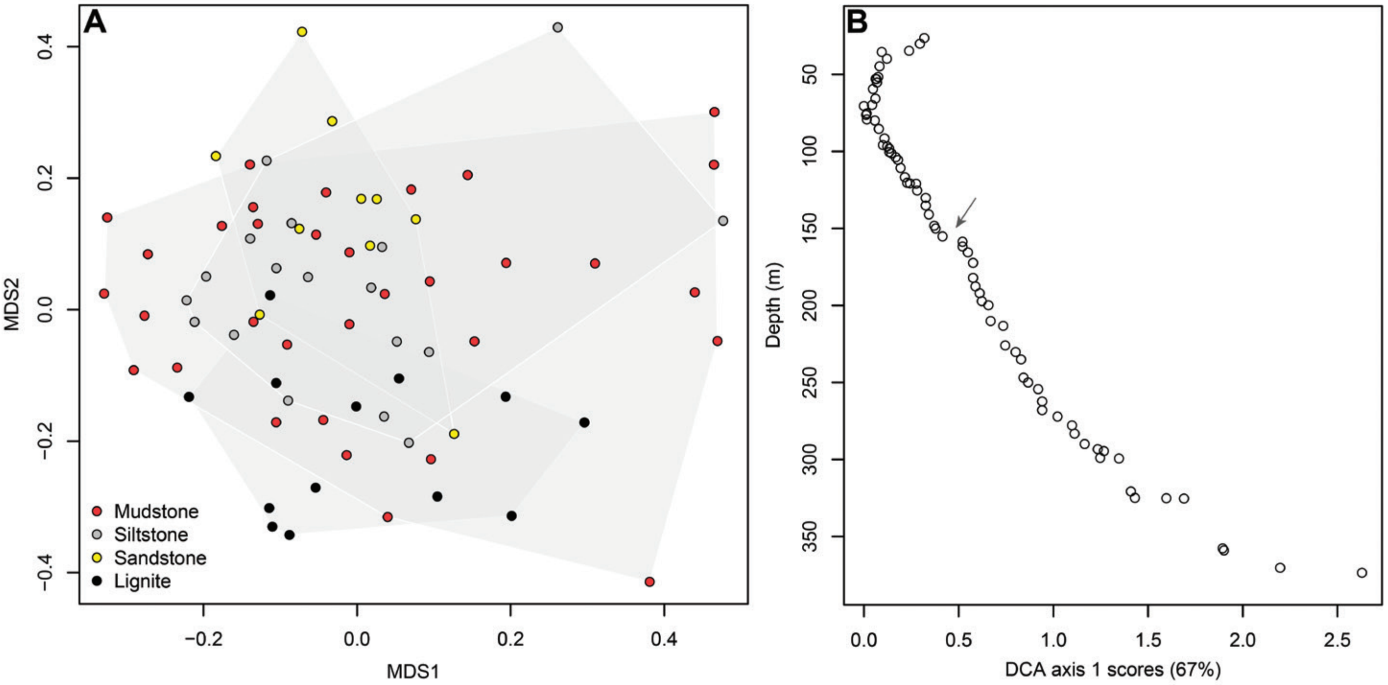

FIGURE 8. (A) Nonmetric multidimensional scaling (nMDS) biplot (k = 3; nonmetric fit, $R^2 = 0.96$; stress = 0.200); (B) scores from axis one of DCA (detrended component analysis) along core 105-AM. The DCA was performed on a range-through version of the pollen matrix, with singletons excluded. Arrow indicates 157 m (~16 Ma).

approximately 16 Ma. The breaks at the bottom and top parts of the section will not be considered due to edge effect (Foote, 2000).

Distribution Models

Fitting abundance distribution models to the data resulted in the same sequence of best fits for all lithologies (Figure 9A–D), with Zipf-Mandelbrot and Zipf performing better and Brokenstick and preemption performing worse. There was no difference among the best fitted models (post hoc tests, P-values > 0.05), which was also the case between Zipf and preemption for lignites (Figure 9C) ($P > 0.2$).

The Lower 16 and Upper 16 groups (Figure 9E, F) had the same sequence of model fits, not differing from individual lithologies. The null model was the least fit in both groups. In the Lower 16 group (Figure 9F), the preemption model had similar values to the log-normal ($P > 0.05$), which in turn was not different from the best fitted models, Mandelbrot and Zipf ($P > 0.05$). In the Upper 16 group (Figure 9E), Brokenstick and preemption models did not differ ($P > 0.05$).

Vegetation

Tree-pollen abundance decreased significantly, Lower 16 = 39% ± 22.7% versus Upper 16 = 23% ± 8.4% (t-test, df = 23.9, $P < 0.01$) (Figure 10A). On the other hand, herbaceous elements did not change significantly, Lower 16 = 17.8% ± 19.4% versus Upper 16 = 17.6% ± 11.4% (t-test, df = 29, $P = 0.9$) (Figure 10B). Fern spores increased from 32.2% ± 26.5% to 52.3% ± 13.8% (t-test, df = 27.6, $P < 0.01$) (Figure 10C). This increase was observed across the most important fern taxa ($P < 0.05$); for example, *Echinomonoletes* spp., *Echinatisporis* spp, *Magnastriatites grandiosus*, *Polypodiisporites* spp, *Psilatriletes* spp., and *Verrucatriletes* spp., with the exception of *Laevigatosporites* spp. The quantity of unknown life forms did not change from the Lower 16 to the Upper 16 group (t-test, df = 22.2, $P > 0.05$) (Figure 10D).

The main ecological groups (Table 1) were also explored (Figure 11). Flooded vegetation elements (i.e., várzea/riparian forests, hydroseral herbs, the swamp palm *Mauritia*, and *Rhizophora*) dominated the assemblage ranging from 6% to 95.7%, with a mean of 39.5% (Figure 11A). Unflooded vegetation (e.g., terra firme forests) were a smaller component ranging from 0% to 35.3.9%, with a mean of 15.2% (Figure 11B). Flooded forests did not vary significantly from the Lower 16 to Upper 16 (t-test, df = 25.3, $P > 0.08$). Unflooded forests increased from 11.4%±9.3% to 17.8%±7.3% (t-test, df = 36.4, $P < 0.02$). Palynomorphs with unknown ecological affinities ranged from 4% to 65.5% (mean of 43.3%) and did not vary significantly from the lower to the upper group (t-test, df = 28.9, $P > 0.2$) (Figure

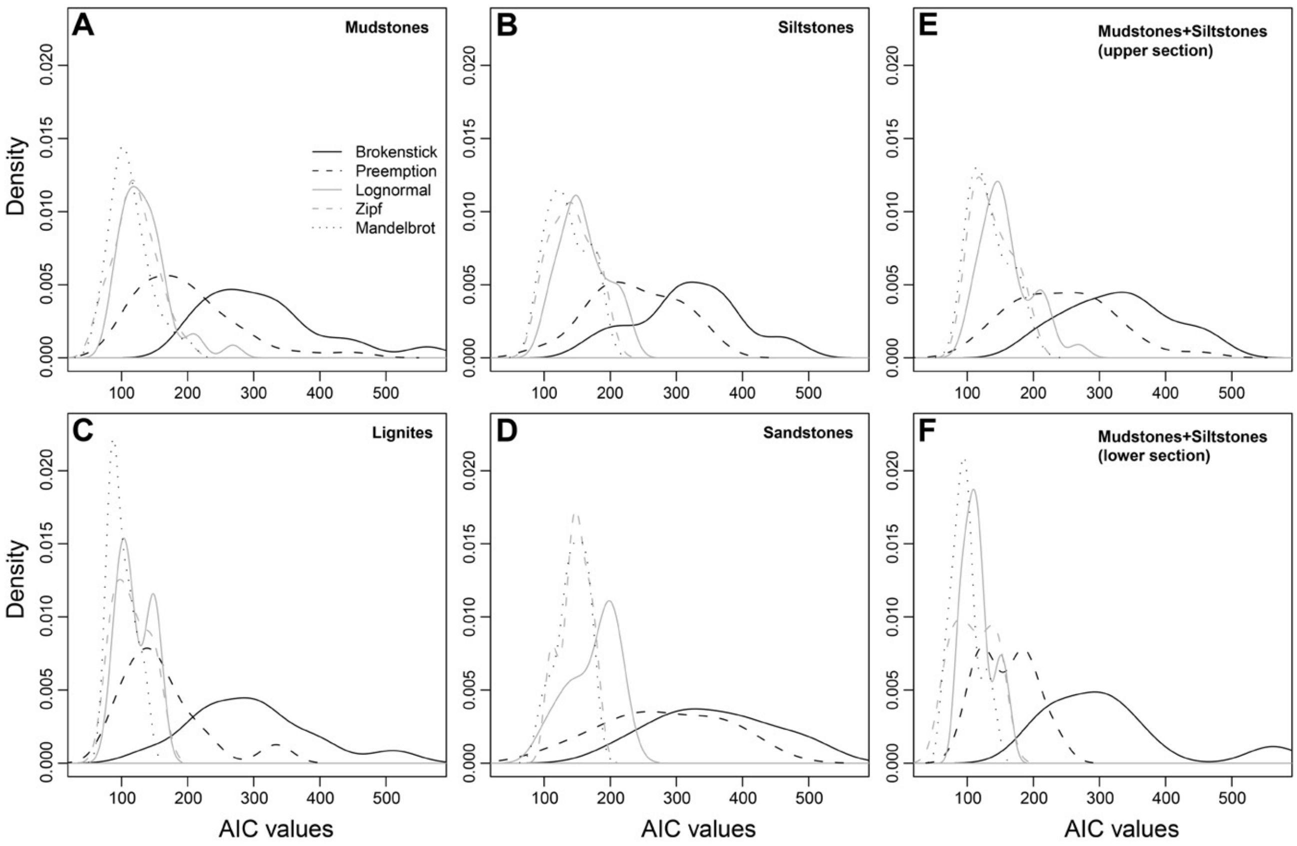

FIGURE 9. Density distribution plots with Akaike's information criterion (AIC) values for five abundance distribution models for core 105-AM. The AIC measured the model fit to the pollen counts of individual samples, with lower values indicating better fits. For statistical comparisons, see text. Samples were divided by lithology (A) mudstones, (B) siltstones, (C) lignites, and (D) sandstones. Combined AIC values for mudstones + siltstones divided by upper (161.7–26.2 m) and lower (373.5–197.2 m) groups are shown in (E) and (F), respectively.

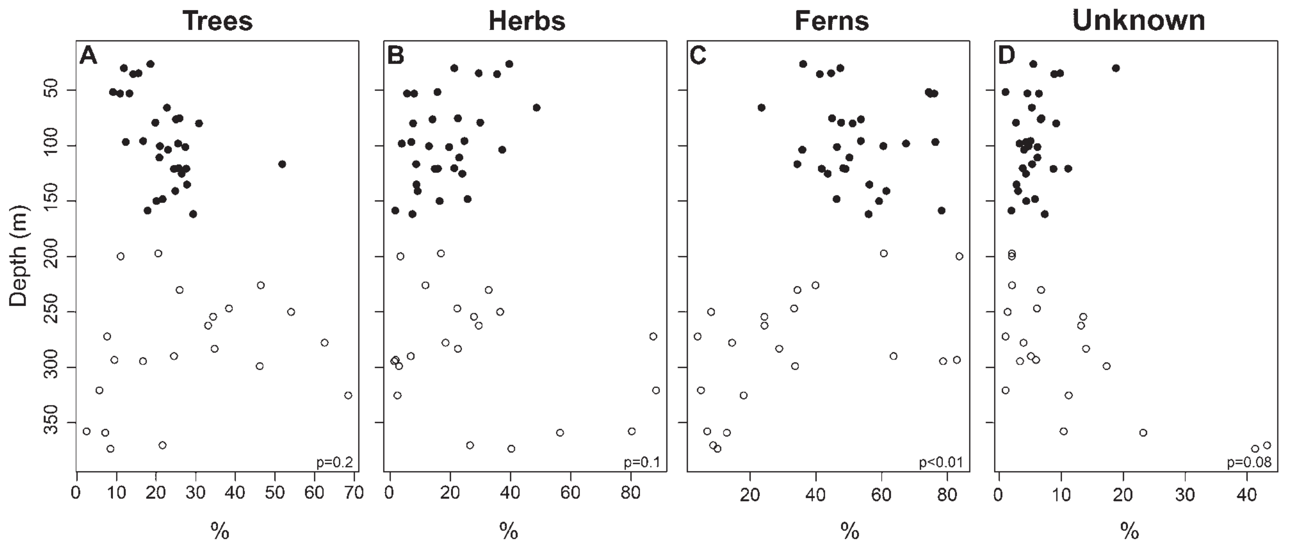

FIGURE 10. Relative abundances of life forms along core 105-AM, for mudstone and sandstone samples. (A) Arboreal, (B) herbaceous, (C) fern spores, and (D) unknown life forms. The *P*-values refer to *t*-test comparisons between samples from lower (373.5–197.2 m; open symbols) and upper group (161.7–26.2 m; solid symbols). The list of life forms can be found in Table 1.

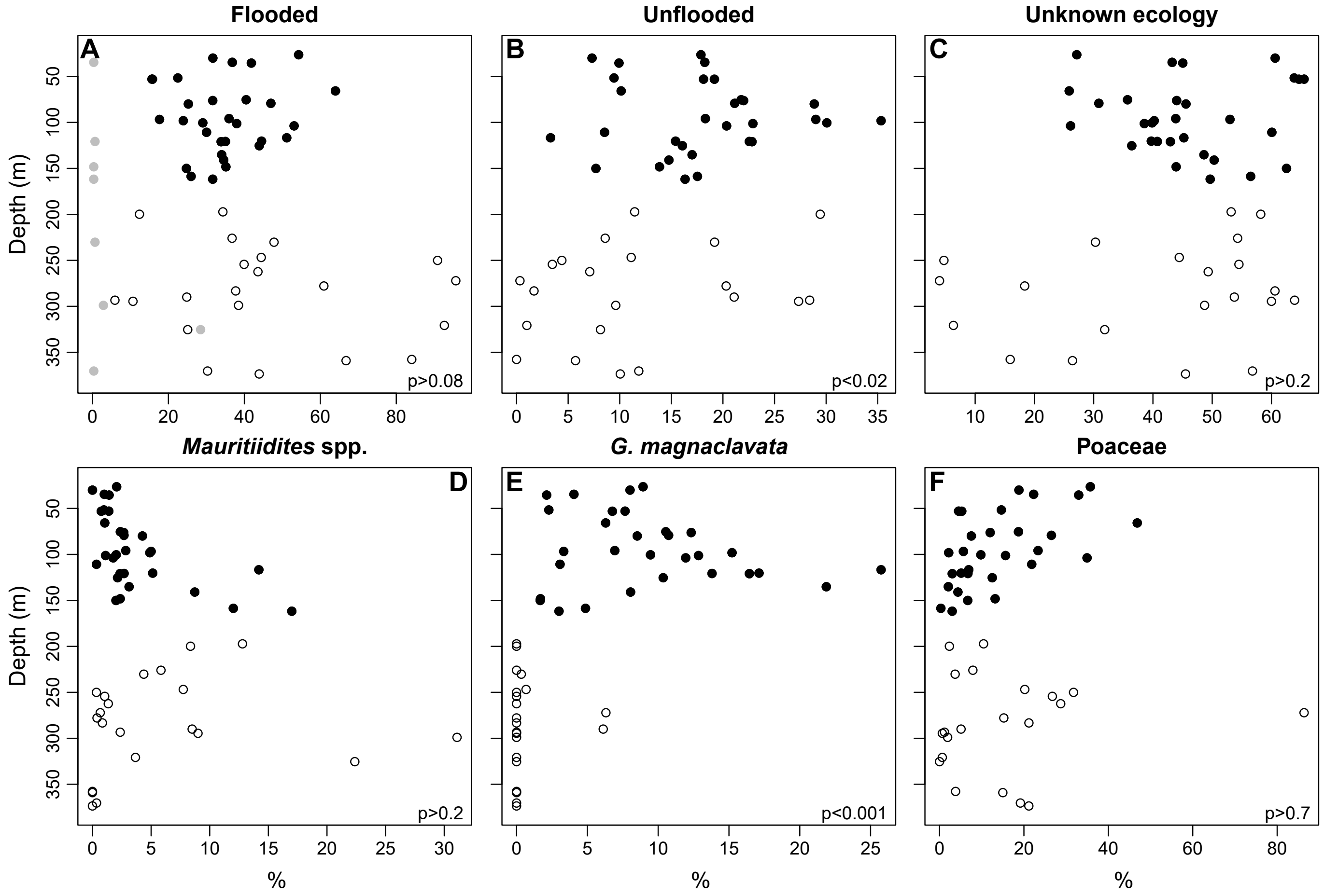

FIGURE 11. Relative abundances of ecological groups along core 105-AM, for mudstones and siltstone samples. (A) Flooded elements (várzea/riparian forests, hydroseral herbs, and trees including *Mauritiidites*, *Rhizophora* pollen), *Rizophora* pollen (= *Zonocostites ramonae*) is also plotted separately (gray symbols); (B) unflooded elements (terra firme, montane, and forests on white sand soils); (C) unknown ecological affinities; (D) *Mauritiidites* spp., (E) *Grimsdalea magnaclavata*; and (F) Poaceae (*Monoporopollenites* spp.). The *P*-values refer to *t*-tests comparing between samples from lower (373.5–197.2 m; open symbols) and upper group (161.7–26.2 m; solid symbols). The list of ecological affinities can be found in Table 1.

11C). To further explore the higher abundance of unflooded elements in the Upper 16 group (Figure 11B), we looked at taxa restricted to this group (n = 149 in 30 samples) and compared richness among ecological groups (Figure 12). Richness of unknown ecology dominated (mean = 68%), and unflooded types made up an average 20% of the richness against 11% of the flooded types (t-test, df = 54.2, $P < 0.02$).

Some of the most abundant pollen types in the whole assemblage included the palm trees *Mauritiidites franciscoi* and *Grimsdalea magnaclavata* and the Poaceae *Monoporopollenites* spp. The abundance of *M. franciscoi* did not change significantly (Lower 16 = 5.7% versus Upper 16 = 3.7%, t-test, df = 27.2, $P > 0.2$) (Figure 11D). In contrast, the abundance of *G. magnaclavata* increased significantly (Lower 16 = 0.6% versus Upper 16 = 9.2%, t-test, df = 36.6, $P < 0.001$) (Figure 11D). The abundance of *Monoporopollenites* spp. did not change significantly (Lower 16 = 15.4% versus Upper 16 = 14%, t-test, df = 30.6, $P > 0.7$) (Figure 11E).

Finally, we also tested the control of lithology on ecological groups. Significant effects (Kruskal–Wallis tests, $P < 0.05$) were observed for flooded forests, *Mauritiidites* spp. and *M. annulatus*. In all cases, lignites and sandstones explained the variations: lignites had lower abundance of flooded elements and *M. annulatus* and higher abundance of *Mauritiidites* spp. when compared to sandstones.

We found that palm swamp samples were more similar to each other in species composition when compared to nonpalm swamp samples (Figure 13). Distances among *Mauritiidites* samples were slightly higher than distances among *Grimsdalea* samples (bootstrapped t-test, $P < 0.05$, 58%) (Figure 13).

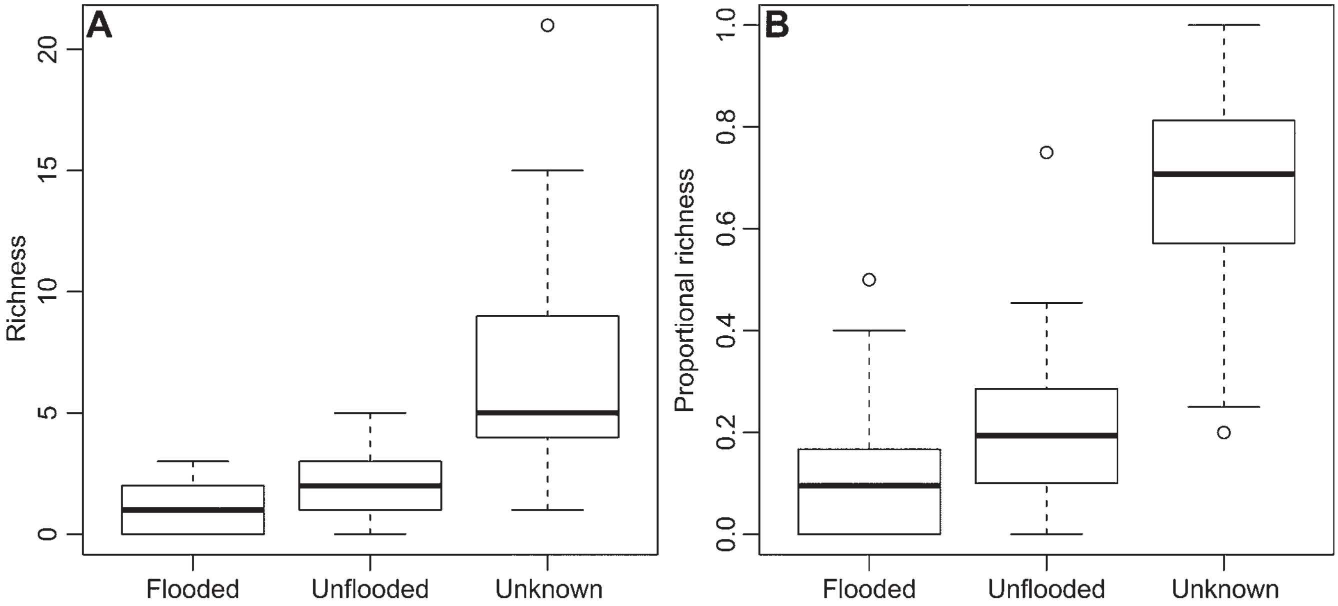

FIGURE 12. Boxplots showing palynological richness by ecological group for the upper phase (161.7–26.2 m; middle to early late Miocene). (A) Raw richness and (B) proportional richness.

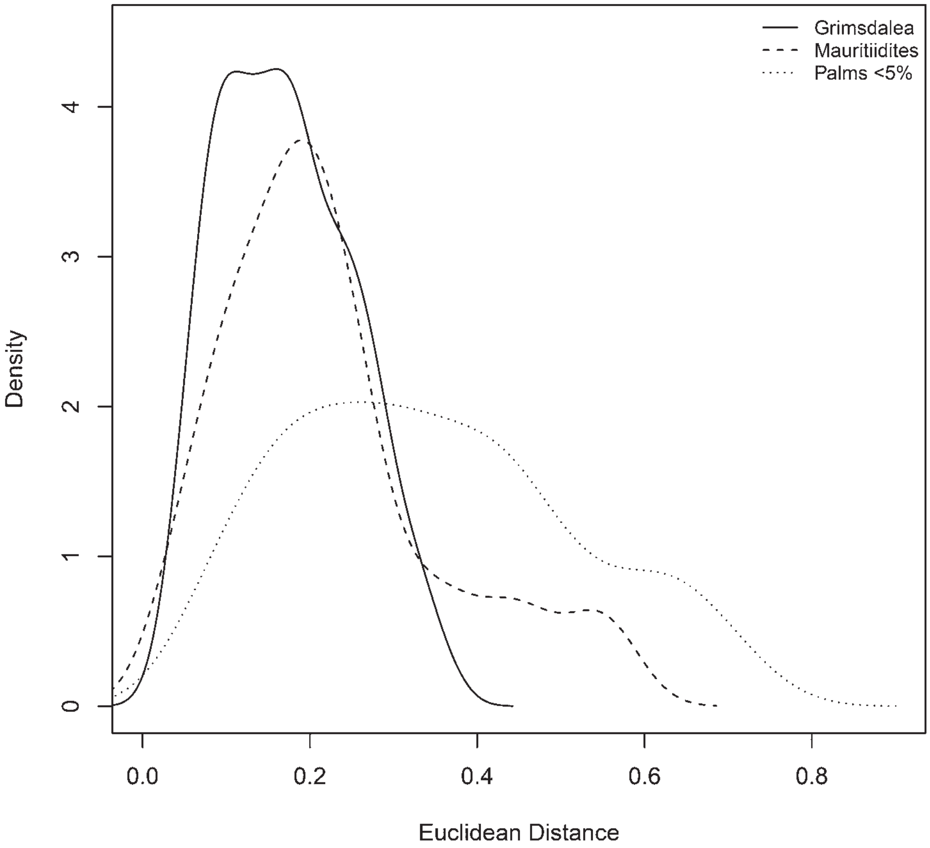

FIGURE 13. Density distributions of Euclidean distances taken from the multivariate space (Figure 8A), for samples classified as *Mauritiidites* swamps (>5%), *Grimsdalea* swamps (>5%), and nonpalm swamps (palms <5%).

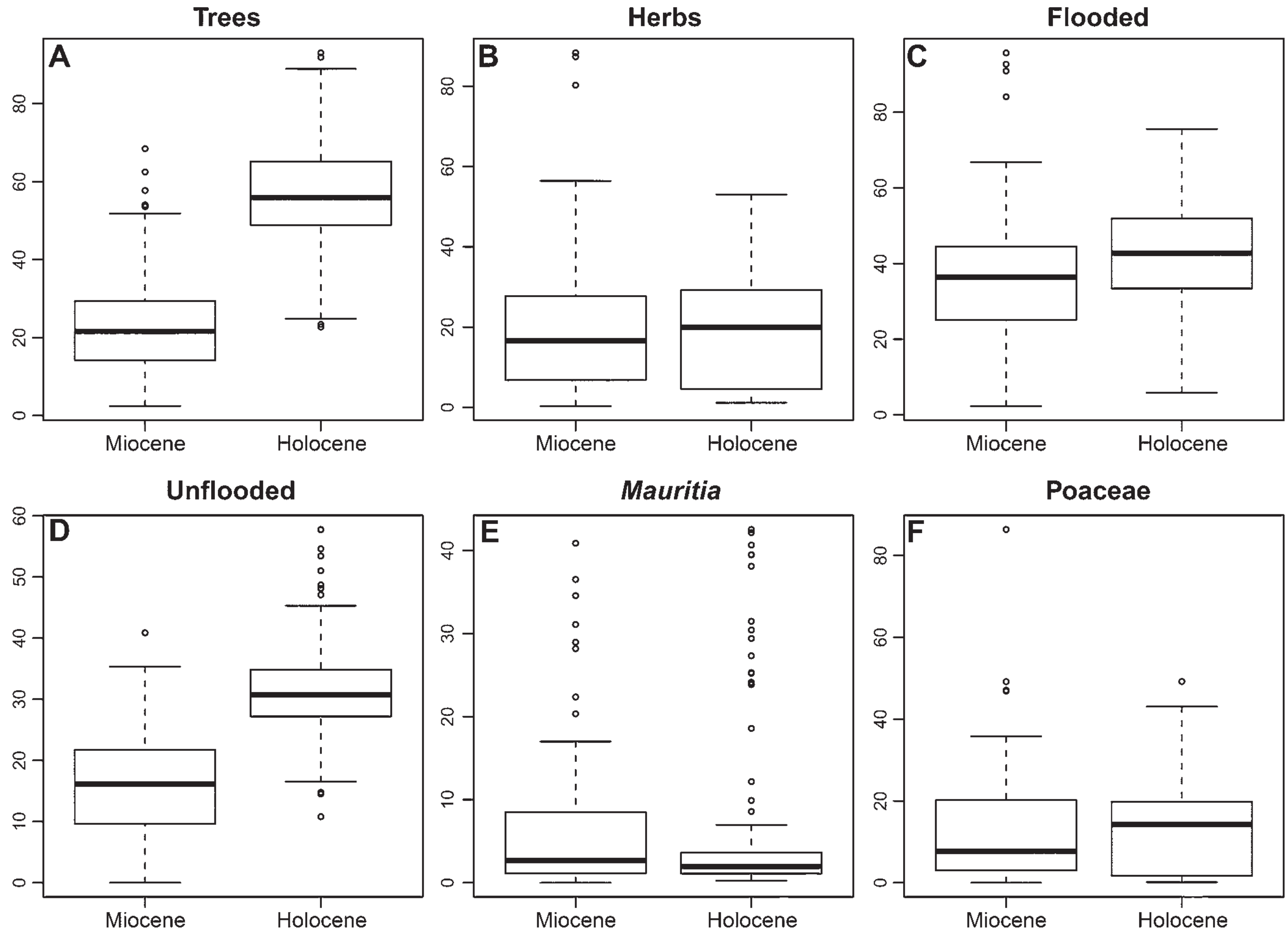

FIGURE 14. Boxplots showing comparison between Miocene and Holocene pollen assemblages, grouped by life form and ecological affinities. All samples from the Miocene data set were used; *y*-axis is relative abundance data. (A) Arboreal, (B) herbaceous, (C) flooded elements, (D) unflooded elements, (E) *Mauritiidites*/*Mauritia*, and (F) Poaceae. See text for statistical comparisons.

Diversity estimates were compared among Lower 16 *Mauritiidites* samples, Upper 16 *Grimsdalea* samples, and both Lower 16 and Upper 16 nonpalm samples. There were not enough samples for statistical comparisons in the Upper 16 *Mauritiidites* and Lower 16 *Grimsdalea* groups. All differences were nonsignificant, except when *Grimsdalea* and *Mauritiidites* were compared, in which case *Grimsdalea* samples had higher diversity estimates.

MIOCENE VERSUS HOLOCENE COMPARISONS

Holocene samples had higher proportions of trees than the Miocene (*t*-test, df = 121.8, $P < 0.001$; Figure 14A), but the proportion of herbs was not significantly different (*t*-test, df = 130.4, $P > 0.4$; Figure 14B). Spore abundance was lower in Holocene than in Miocene samples (mean = 12.1% versus 48%; *t*-test, df = 80.5, $P < 0.001$). The percentage of unknown life form was higher for the Holocene samples (mean = 13%, from 0 to 64.7%) than for Miocene samples (mean = 7.1% from 0.9 to 43%) (*t*-test, df = 212, $P < 0.001$).

Flooded elements were similar in both Miocene and Holocene assemblages (*t*-test, df = 122.4, $P > 0.1$; Figure 14C), but unflooded elements had significantly higher proportions in the Holocene samples (*t*-test, df = 140, $P < 0.001$; Figure 14D). There were no significant differences for the proportions of *Mauritia*/*Mauritiidites* or Poaceae (*P*-values > 0.5; Figure 14E, F). Finally, the percentage of the unknown ecology group was higher for the Miocene samples (mean = 44.3%, from 4 to 75%) than for the Holocene samples (mean = 21.5%, from 0 to 76.2%) (*t*-test, df = 163.2, $P > 0.001$).

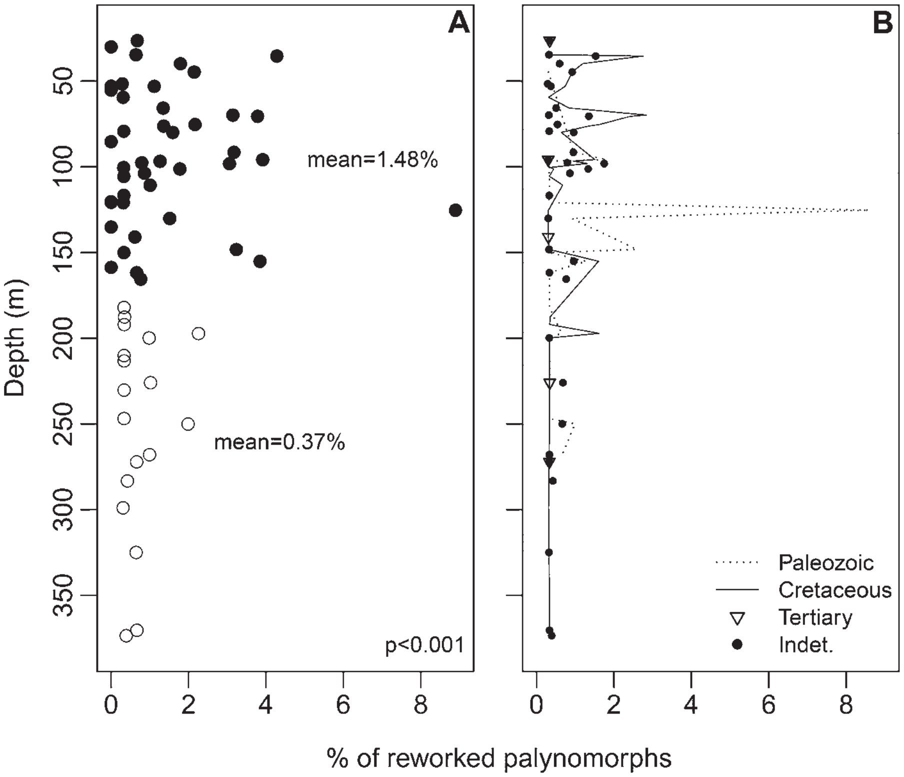

FIGURE 15. Relative abundance data of reworked palynomorphs along core 105-AM. Percentages were calculated for all samples with counts ≥100. Only samples with reworking >0% are plotted. The *P*-value refers to *t*-test comparison between samples from the lower (373.5–165.5 m; open symbols) and upper group (165.5–26.2 m; solid symbols). (A) All reworked palynomorphs; (B) palynomorphs divided by age group.

Reworked Palynomorphs

The percentage of reworked (RW) palynomorphs in the Miocene samples reached up to 8.9%. The Lower 16 had a significantly lower proportion of RW taxa than the Upper 16 (0.37% versus 1.48 %, *t*-test, df = 51.9, $P < 0.001$) (Figure 15). Sandstones had significantly higher proportions of RW taxa when compared to lignites and mudstones (Kruskal–Wallis chi-squared = 10.6, df = 3, $P < 0.02$), while lignites had the lowest proportion of RW (mean = 0.26%). Among the RW grains identified, the majority were Paleozoic acritarchs and Cretaceous pollen, spores, and dinocysts (the Cretaceous being significantly more abundant in the Upper 16: *t*-test, df = 56.6, $P < 0.001$; while there was no difference for the Paleozoic RW: *t*-test, df = 45.3, $P > 0.1$).

DISCUSSION

Our data suggest that core 105-AM had two distinct palynoflora phases, early and middle to early late Miocene (Figures 4, 8). The early Miocene (~18.8 to ~16.1 Ma) had lower diversity than the middle Miocene, regardless of the metric used (Figure 6), and it was also accompanied by higher coverage estimates (Figure 5), which was achieved in less diverse communities (Chao and Jost, 2012; Chao et al., 2014); the early Miocene palynoflora also had a non-neglectable contribution of the preemption abundance distribution model, reflecting species poor or harsh environments (Magurran, 2004). By contrast, the middle to early late Miocene phase (~16.1 to ~10.7 Ma) had significantly higher diversity, lower coverage, and best-fit abundance models (Mandelbrot and Zipf) that suggest assemblages in nonextreme environments (Sugihara, 1980; Magurran, 2004). Taken altogether, this evidence revealed a change along the core, the causes of which are explored in the following sections.

Taphonomic Effect

The diversity difference could be a taphonomic effect, for example, more restricted environments were sampled in the lower Miocene compared to the middle Miocene. The early Miocene phase was primarily characterized by low-energy wetlands dominated by swamps, which allowed the formation of lignites, together with floodplains cut by fluvial channels (Jaramillo et al., 2017). Swamps are restricted environments that tend to collect the local pollen signal (Sugita, 1994) leading to lower pollen richness. By contrast, there were more floodplains and larger lakes in the middle Miocene with a stronger signal of fluvial activity interpreted from thicker sandstone beds (Figure 1; Jaramillo et al., 2017). However, the analysis of an isotaphonomic subset of the data (Figure 6) showed the difference in diversity as observed in the entire dataset, suggesting that taphonomy did not drive the observed diversity pattern. Furthermore, when comparing *Mauritiidites* with *Grimsdalea* swamp samples, the latter were more diverse despite being less dissimilar (Figure 13), indicating that even with the potential contribution of more ex-situ pollen, the *Mauritiidites* swamps were not as diverse as the *Grimsdalea* swamps.

Increase in Unflooded Forests

A second idea to explain why the middle to late Miocene had higher diversity than the early Miocene was a shift to broader bands of unflooded forest (e.g., terra firme) at the expense of flooded environments. Unflooded forests in western Amazonia are richer in species when compared to flooded environments (Wittmann et al., 2006; Draper et al., 2018). Our data showed a significant increase of unflooded elements in the middle Miocene (Figure 11), in support of this hypothesis. However, a large portion of the morphotypes had unknown ecologies (Figure 12), so the magnitude of the increase in unflooded elements in the middle Miocene may change if additional taxa are identified.

Increase in Environmental Complexity

A third hypothesis to explain diversity changes from early to middle late Miocene relates to physiographic processes. The emerging river system of the middle Miocene could have created a larger number of interfluves and more complex fluvial subenvironments with a varied degree of connectivity among lakes. Fluvial and topographic variation translates into environments that were more spatially heterogeneous than the swamp-dominated early Miocene landscape. Environmental diversity offers more niche possibilities thus explaining increased diversity (Pianka, 1966; Tews et al., 2004; Stein et al., 2014). Furthermore, a diversity of fluvial subenvironments likely also produced a larger variety of edaphic conditions, which are important controls on plant distribution in Amazonia (Higgins et al., 2011; Quesada et al., 2012; Tuomisto et al., 2016; Figueiredo et al., 2018).

Many lines of evidence support dynamic and more environmentally heterogeneous settings in the middle and especially late Miocene in western Amazonia. For instance, sedimentary reconstructions point to avulsive systems in the late Miocene (Latrubesse et al., 2010; Gross et al., 2011). Furthermore, there was a stronger Andean signal in sediments from the upper part of many cores, which was interpreted from Cretaceous reworking, stable minerals, and Neodymium isotopes (Figure 15; Hoorn, 1993; Horbe et al., 2019) and potentially indicates effective sediment transport in a broad geographical area. Finally, there is evidence of local uplifts, like the Iquitos arch (Roddaz et al., 2005) that is believed to have impacted deposition of the Solimões Formation (Latrubesse et al., 2010; Silva-Caminha et al., 2010).

A quantitative comparison of the sedimentary environments in core 105-AM was not performed because the early Miocene had a much larger proportion of the stratigraphy that was not recovered during the core drilling (~33% against ~10% in the upper phase; Figure 1). However, the available sedimentary data (Jaramillo et al., 2017) supported the change from swamp-dominated to more active-fluvial settings, and such change had also been observed in core 33AM (Leite et al., 2017, 2021), although with a slight difference in ages (~12–13 Ma). Future work with a focus on sedimentary facies could help test this environmental heterogeneity hypothesis.

Miocene Climatic Optimum

A final hypothesis relates to climate (Figure 16). Global temperatures rose by 3°C to 4°C (You et al., 2009; Goldner et al., 2014) during the Miocene Climatic Optimum (MCO), which lasted from about 17 to 14.7 Ma. Warmings have been shown to prompt plant diversification in northern South America during most of the Cenozoic (Jaramillo et al., 2006, 2010b). For the Miocene, a positive effect of the MCO on plant diversity was suggested by Hoorn et al., (2010) with data from the Llanos Basin in Colombia. Jaramillo et al. (2014) also inferred an increase in palynological richness from early to late Miocene in Panama, although with large gaps in the record. Furthermore, there is no evidence that rainforests lived above their heat tolerance during the Miocene; for instance, experiments have shown that tropical plants tolerate temperatures higher than those estimated for the Miocene (Krause et al., 2010; León-García and Lasso, 2019). Widespread neotropical species have molecular age estimates in the Miocene, demonstrating tolerance of different plant lineages at the species level to warmer climates (Dick et al., 2013).

Many Miocene CO_2 estimates are greater than 400 ppm (parts per million; e.g., Beerling and Royer, 2011; Zhang et al., 2013; Londoño et al., 2018). High CO_2 increases water use efficiency and overall plant performance (Lloyd and Farquhar, 2008; Cernusak et al., 2011, 2019), a mechanism that has been shown to promote forest fertilization in the warmer early Miocene (Reichgelt et al., 2020). This could have favored plants during the Miocene in western Amazonia. There was no evidence for hydric stress in the study site, the sedimentological data from the Solimões Formation, including core 105-AM (Jaramillo et al., 2017), suggested high water availability in a wet tropical climate with a seasonal monsoonal system (Kaandorp et al., 2005).

The 105-AM is a short record that needs to be compared with more cores in western Amazonia to generate a more continuous Miocene data set. This will allow testing of the hypothesis that originations and extinctions were related to the MCO (Figure 16).

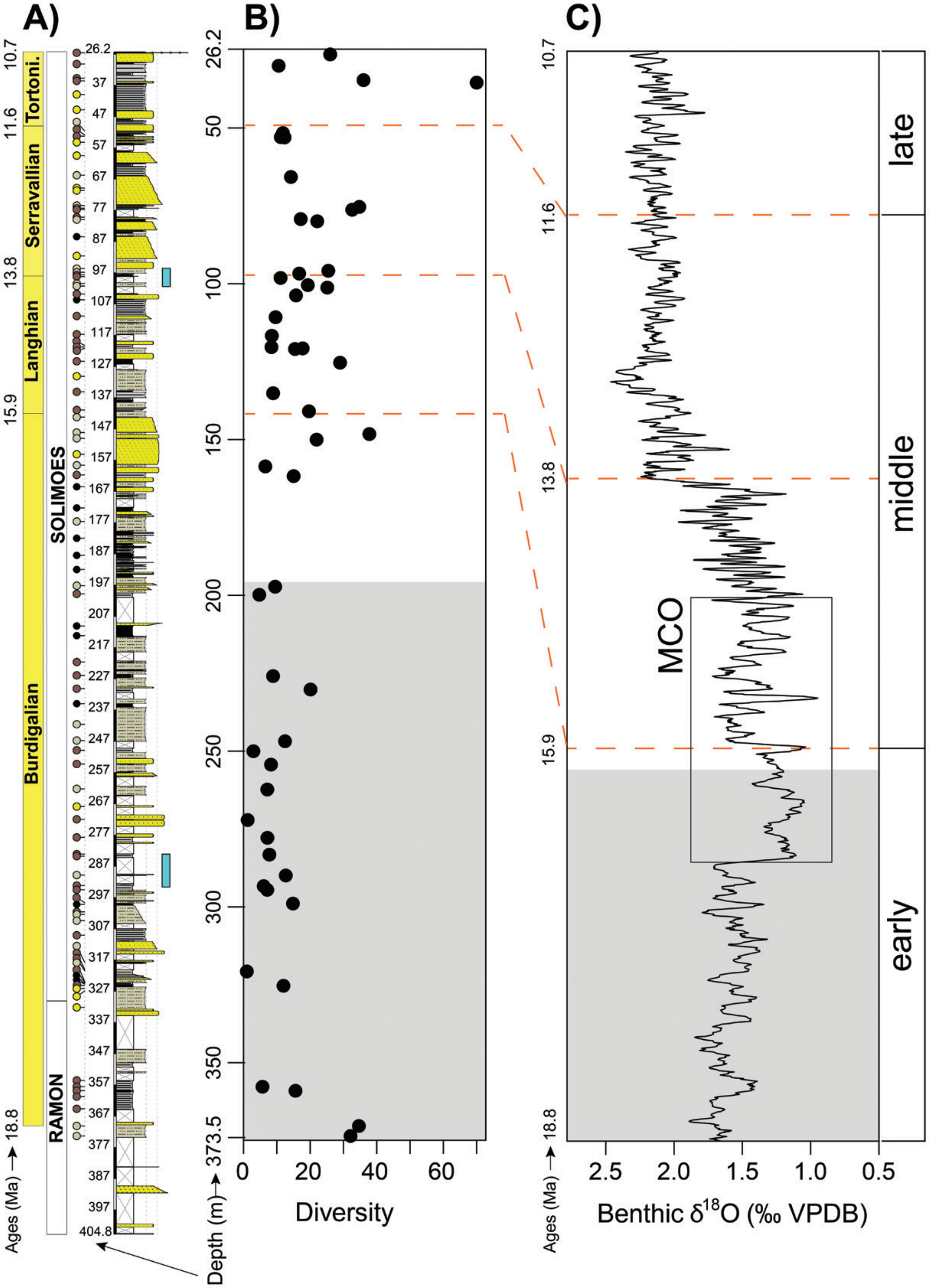

FIGURE 16. Summary data showing main changes along core 105-AM and comparison with global temperature data. (A) Sedimentary log from core 105-AM; (B) coverage-based rarefied diversity of pollen/spores; (C) benthic δ^{18}O data compiled by De Vleeschouwer et al. (2017), used as a proxy for paleotemperature; MCO = Miocene Climatic Optimum.

NOTES ON SOME MIOCENE VEGETATION TYPES

Palm Swamps

Arecaceae was the top ranked family in relative abundance and richness of pollen types along core 105-AM (Figure 2). Most of the high palm counts were from *Mauritiidites franciscoi*, the fossil type of *Mauritia*. This palm cannot tolerate deep seasonal flooding as it requires permanently waterlogged conditions (Rull, 1998); *Mauritia* pollen is not transported long distances, thus indicating local swampy vegetation (Rull, 1998) and the relation of its pollen abundance with vegetation reflects population density (Rull, 1998). Pollen from *Mauritia* has been successfully used to interpret peat-forming swamps in western Amazonia (Behling et al., 1999; Roucoux et al., 2013). Modern *Mauritia* pollen dominance in peats/lignites was comparable to the swamp-dominated environment reconstructed for the early Miocene and was particularly expressed in lignites that were more frequent and thicker in the lower section of core 105-AM (Jaramillo et al., 2017) and had higher abundances of *Mauritia*. Various localities in the Pebas system record lignite and organic-rich clay deposits with high counts of *Mauritia*, for instance, southeastern Colombia (Hoorn, 1994a, 2006; Salamanca-Villegas et al., 2016) and northeastern and eastern Peru (Hoorn, 1994b; Antoine et al., 2016), both with late early to early middle Miocene ages. Palynology in these sites frequently reconstructs *Mauritia* swamps in backswamp settings, implying wide geographical extensions of floodplains with associated palm swamps (e.g., Contamana in Peru and Mariñame in Colombia are ~800 km apart).

During the middle to late Miocene, *Grimsdalea magnaclavata* replaced *Mauritiidites* as the dominant pollen type. *G. magnaclavata* is an extinct palm tree with probable affinities with *Mauritia* (Pocknall and Jarzen, 2012), and it is assumed to be of coastal backswamps (Germeraad et al., 1968), upper coastal plain swamps (Lorente, 1986; Rull, 1997), and coastal forests (Pocknall and Jarzen, 2012). For the Solimões Formation, high *Grimsdalea* abundances have been reconstructed in shallow lake surroundings (Hoorn, 1994a) in higher energy settings when compared to *Mauritiidites* (Jorge et al., 2019). Pollen associations in *Grimsdalea* swamps were more similar to each other than *Mauritia* swamps were to each other (Figure 13). A similar result was found in extant *Mauritia* swamp forests in western Amazonia—they were more dissimilar to each other and less diverse than other forest types like várzeas and terra firme (Draper et al., 2018). Furthermore, the vast majority of the diversity (~80%) of *Mauritia* swamps could be associated with small woody and herbaceous vegetation (Householder and Wittmann, 2016). It could be the case that the higher diversity in *Grimsdalea* swamps was derived from a higher proportion of arboreal vegetation and that there was a fundamental difference in what controlled *Grimsdalea* and *Mauritia* swamps (e.g., flooding dynamics). However, the large amount of unknown life forms and parental habitats hamper a better understanding of such differences. More precise botanical affinities and larger sample sets may provide answers to this and other questions related to Miocene palm swamps.

Mangroves

In some localities of the Pebas deposits, high abundances of *Zonocostites ramonae* (fossil *Rhizophora*) have been recorded along with dinoflagellate cysts, indicating the possible effects of marine influence on vegetation in the early Miocene (Hoorn, 1993; Salamanca-Villegas et al., 2016). In core 105-AM, one spike of *Z. ramonae* (~28.5%) was found at approximately 18.4 Ma, then lower abundance (2.9%) at about 18.2 Ma (Figure 11A), both preceding the marine event onset at about 18 Ma (Jaramillo et al., 2017). Pollen rain studies have suggested that the dominance of *Rhizophora* indicated high seasonal influxes of freshwater but not a direct tidal influence (Urrego et al., 2010), which is in line with low salinity levels expected for the Pebas marine events (Jaramillo et al., 2017). In other samples of core 105-AM, *Z. ramonae* was recorded below 1%. *Rhizophora* pollen has been recorded regularly in low percentages upstream of its source area due to high pollen production and effective wind dispersal (Muller, 1959). For these reasons, the presence of *Z. ramonae* in the Solimões Formation should be interpreted with caution (especially if in low abundances) and not used as direct marine evidence without further support of dinocysts or other marine microfossils.

Fern Spores

Throughout core 105-AM, spore counts were quite high (Figure 10C), which was similar to other palynological analysis in the Solimões Formation (e.g., Silva-Caminha et al., 2010; Kern et al., 2020). This abundance contrasted with much less fern spores in the Holocene localities compared herein (Absy, 1979; Behling et al., 1999) and elsewhere in Amazonia (e.g., Irion et al., 2006; Sá et al., 2016; Rodríguez-Zorro et al., 2018). However, a pollen study in western Amazonia near the 105-AM site by Roucoux et al. (2013) found high fern spore abundances during the formation of a peat deposit in the Late Holocene. The site included sedge fen and floating mats, closed canopy flooded forests, and *Mauritia* palm swamp, all of which were in a restricted flooding system unlike várzea lakes but still with sporadic riverine connections. This setting fits the general reconstructions of the Pebas system in core 105-AM. Today, floating mats are common in many lakes in Amazonian river systems and can harbor diverse fern species (Junk and Piedade, 1997). However, lakes are a minor component of the Amazon landscape in present times (e.g., ~1% in western Amazonia; Toivonen et al., 2007). In extensive lakes and swamps of the Pantanal Basin in central South America, the largest tropical wetland (Por, 1995) and a possible analogue to the Pebas System (Latrubesse et al., 2010), floating mats can be massive and alone comprise on average >2% of the entire landscape and up to >10% in some regions (Silva et al., 2000; but probably still underestimated, see Merino and Assine, 2020). In these gigantic mats, some fern species can be frequent and abundant (Pott et al., 2011; Cunha et al., 2012) just like in Amazonian floating mats (Junk and Piedade, 1997) and include pioneer ferns during colonization of areas disturbed by fluvial processes (Pott and Pott, 2000). These ferns include, for instance, Salviniaceae that are also found abundantly as massulae in lake-dominated palynofacies of the Solimões Formation (Sá et al., 2020). Altogether, this evidence points to fern abundance primarily associated with the lacustrine settings of the Pebas system, which could explain their higher counts in the middle to late Miocene phase (Figure 10C).

Miocene versus Holocene Comparisons

Comparisons of the extant and Miocene palynofloras are hindered by the different taxonomical approach of modern versus paleopalynology (Gomes et al., 2021). To date, the only study to partially overcome this issue for Amazonia (Gomes et al., 2021) showed that both Miocene and extant pollen assemblages from floodplain sediments were dominated by plant groups associated with the floodable flora (e.g., várzeas). In our 105-AM assemblage, floodable elements also prevailed (Figure 11A). When comparing the Miocene with Holocene samples, the most remarkable difference was a higher abundance of trees in the Holocene (Figure 14A), which reflected also a higher abundance of unflooded elements (Figure 14D) (>90% of the Holocene unflooded abundance was made up of trees). This result lends support to the hypothesis of a less-forested Pebas System in comparison to the recent western Amazonia. Today in western Amazonia, most area is forested (Toivonen et al., 2007; Melack and Hess, 2010), in contrast to vast aquatic ecosystems during the Miocene (Hoorn et al., 2010).

The different extant environments sampled explain the similar amounts of *Mauritia* and Poaceae among Miocene and Holocene samples (Figure 13E, F). The palm swamp in western Amazonia (Behling et al., 1999) had on average 11.3% (0%–42.5%) of *Mauritia* pollen, in contrast to 0.9% (0%–4.7%) in the central Amazon fluvial lakes (Absy, 1979). On the other hand, Poaceae was almost absent in the palm swamp (<2%) but abundant in the lakes (18.9%, from 0 to 50%). These differences support our interpretations of swamps in the early to early middle Miocene and a more dynamic fluvial system in the middle to late Miocene part of the 105-AM record. Scanty *Mauritia* and high Poaceae pollen were common features in surface river sediments (Gomes et al., 2021; Akabane et al., 2020) and Holocene records from fluvial lakes in Amazonia (Absy, 1979; Irion et al., 2006; Sá et al., 2016). Furthermore, high Poaceae counts in these settings can be an indicative of várezas (Akabane et al., 2020); in the 105-AM samples, Poaceae abundance correlated reasonably with abundance of floodable elements ($r^2 = 0.31$, $P < 0.001$).

The comparisons presented herein are tentative and constrained by a) how much is known of botanical affinities with the extant plant diversity, b) comparability of Cenozoic and Quaternary pollen taxonomy, and c) the coverage of different depositional settings in the modern data. Better comparisons will be possible when these issues are tackled properly.

SYSTEMATIC PALYNOLOGY

Descriptions are provided here for 91 new species (25 spores and 66 pollen, including 1 new genus). Sixteen new combinations are proposed along with one emendation. Species formally named are also illustrated but not described. Descriptions of new species were ordered by major morphological groups (e.g., monoletes, triletes, monocolpate, trilcolpate, etc.), then alphabetical within each section. New species and genera were erected and compared to existing species in the literature using the online morphological database of Jaramillo and Rueda (2020), which hosts updated taxonomic information on pollen and spores of Cretaceous–Cenozoic ages in northern South America. The terminology used in descriptions follows Punt et al. (2007), with some modifications from Jaramillo and Dilcher (2001).

All grains were located using the England Finder coordinate system. Slides were deposited in the collection of the Palaeontology and Palynology Laboratory of the Federal University of Mato Grosso, in Cuiabá-Brazil.

Abbreviations:

CEi	calculated in pollen polar view: colpi length/equatorial diameter
CPi	calculated in pollen equatorial view: colpi length/polar diameter
EF	England Finder coordinate system
MLI	monolete index = laesura length/spore length
nm	number of specimens measured
no	number of specimens observed
TLI	trilete index = radius length/(spore diameter/2)

PTERIDOPHYTE AND BRYOPHYTE SPORES

Monolete Spores

Echinosporis Krutzsch, 1967

TYPE SPECIES. *ECHINOSPORIS ECHINATUS* KRUTZSCH, 1967

Echinosporis densiechinatus sp. nov.

PLATE 1A–D

HOLOTYPE. Plate 1a, b, sample 22140, EF P-40-1/2.

PARATYPE. Plate 1c, d, sample 22326, EF V-37.

TYPE LOCALITY. Well 1-AS-105-AM, Solimões Formation, Amazonas, Brazil.

DESCRIPTION. Spores single, symmetry radial, lateral shape oval; monolete, curvatura absent, laesura midsized, 15 µm, MLI 0.6, margo absent, commissure indistinct; exospore

1–2 μm, echinate, echinae densely and evenly distributed over the entire surface of the spore, conical shaped, 2–3 μm high, 1–1.5 μm wide at base, and 1–2 μm spaced.

DIMENSIONS. Equatorial diameter, 15–(17.6)–18 μm; polar diameter, 26–(25.3)–25 μm; polar/equatorial = 1.43; nm = 3, no = 14.

COMPARISONS. *Echinosporis* sp. Raine, 1981, has shorter and sparser echinae. *Polypodiisporites echinatus* Jaramillo and Dilcher, 2001, has much longer and wider conical spines and less dense spines.

ETYMOLOGY. After the dense echinate pattern.

BOTANICAL AFFINITY. *Danaea* (Marattiaceae).

Laevigatosporites **Ibrahim, 1933**

TYPE SPECIES. *LAEVIGATOSPORITES VULGARIS* IBRAHIM, 1933

Laevigatosporites indigestus **sp. nov.**

PLATE 1E,F

HOLOTYPE. Plate 1e, sample 22287, EF H-5-1/2.

PARATYPE. Plate 1f, sample 22272, EF J-11.

TYPE LOCALITY. Well 1-AS-105-AM, Solimões Formation, Amazonas, Brazil.

DESCRIPTION. Spores single, symmetry radial, lateral shape reniform; monolete, curvatura absent, laesura midsized, 20 μm, MLI 0.5, margo indistinct, commissure indistinct; exospore 1 μm, scabrate, scabrae densely distributed over the entire surface of the spore, short, <0.5 μm, scabrate pattern irregular, sometimes anastomosing, creating small rugulae.

DIMENSIONS. Equatorial diameter, 27 μm; polar diameter, 40 μm; polar/equatorial = 1.48 μm; nm = 2, no = 55.

COMPARISONS. *Punctatosporites* sp. A Brenner and Bickoff, 1992, is smaller, and scabration is almost indistinct; *P. scabratus* (Couper, 1958) Singh, 1971, is granulate–scabrate. *Laevigatosporites catanejensis* Muller et al., 1987, is granular.

ETYMOLOGY. After the word *indigestus* (disordered), in reference to the irregular scabrate surface.

Laevigatosporites cultellus **sp. nov.**

PLATE 1G, H

HOLOTYPE. Plate 1g, sample 22279, EF K-24.

PARATYPE. Plate 1h, sample 22158, EF K-6-1.

TYPE LOCALITY. Well 1-AS-105-AM, Solimões Formation, Amazonas, Brazil.

DESCRIPTION. Spores single, symmetry radial, lateral shape elliptic; monolete, curvatura absent, laesura long, 58 μm, MLI 0.78, margo raised as a blade along the entire laesura, 4–6 μm wide, commissure straight, exospore 1–1.5 μm, laevigate.

DIMENSIONS. Equatorial diameter, 46 μm; polar diameter, 74–(65)–56 μm; polar/equatorial = 1.41; nm = 2, no = 2.

COMPARISON. *Laevigatosporites belfordii* Burger, 1976, has a depression in the laesura area.

ETYMOLOGY. After the bladelike margo, from the word *cultellus* (dagger).

BOTANICAL AFFINITY. *Vittaria?* (Polypodiaceae).

Microfoveolatosporis **Krutzsch, 1959**

TYPE SPECIES. *MICROFOVEOLATOSPORIS PSEUDODENTATUS* KRUTZSCH, 1959

Microfoveolatosporis simplex **sp. nov.**

PLATE 1K

Microfoveolatosporis sp.1 Silva-Caminha et al. 2010

HOLOTYPE. Plate 1k, sample 22354, EF Q-26-4.

TYPE LOCALITY. Well 1-AS-105-AM, Solimões Formation, Amazonas, Brazil.

DESCRIPTION. Spores single, symmetry radial, lateral shape reniform; monolete, curvatura absent, laesura distinct, midsized, 15 μm, MLI 0.36, margo distinct, 2 μm wide, segmented to granulate, commissure distinct, straight; exospore 1 μm, foveolate, foveolae circular to elongate, 0.7–1.5 μm wide, 1.2 μm apart, homobrochate, uniformly distributed over the entire surface of the spore.

DIMENSIONS. Equatorial diameter, 26 μm; polar diameter, 41 μm; equatorial/polar diameter = 1.57; nm = 1, no = 1.

COMPARISON. *M. skottsbergii* (Selling, 1946) Srivastava, 1971, is larger and has larger foveolae.

ETYMOLOGY. After the simple morphology.

Polypodiisporites **Potonié, 1956**

TYPE SPECIES. *POLYPODIISPORITES FAVUS* POTONIÉ, 1956

Polypodiisporites densus **sp. nov.**

PLATE 1M, N

HOLOTYPE. Plate 1m, sample 22277, EF D-45-4.

PARATYPE. Plate 1n, sample 22158, EF W-9-2.

TYPE LOCALITY. Well 1-AS-105-AM, Solimões Formation, Amazonas, Brazil.

DESCRIPTION. Spores single, symmetry radial, lateral shape oval; monolete, curvatura absent, laesura midsized, 20 μm, MLI 0.47, margo indistinct, commissure indistinct; exospore 2 μm, verrucate, verrucae densely and evenly distributed over the entire surface, closely spaced and of constant height, 1 μm high, 1–4 μm wide, and 1 μm spaced, subpolygonal in plain view.

DIMENSIONS. Equatorial diameter, 24–(29.5)–35 μm; polar diameter, 42–(46)–50 μm; polar/equatorial = 1.55; nm = 2, no = 8.

COMPARISONS. *Polypodiisporites* aff. *specious* Sah, 1967, is laevigate on the proximal face and has larger irregular verrucae with bases that sometimes connect; *P. pachyexinatus* has a thicker sporoderm and laevigate proximal side; *P. usmensis* (Van der Hammen, 1956b) Khan and Martin, 1972, is gemmate; *P.? planus* Silva-Caminha et al., 2010, has flat verrucae.

ETYMOLOGY. After the dense verrucate pattern.

BOTANICAL AFFINITY. *Polypodium* (Polypodiaceae).

Polypodiisporites discretus **sp. Nov.**

PLATE 2A, B

HOLOTYPE. Plate 2a, sample 22140, EF N-5-2/4.

PARATYPE. Plate 2b, sample 22140, EF G-23-4.

TYPE LOCALITY. Well 1-AS-105-AM, Solimões Formation, Amazonas, Brazil.

DESCRIPTION. Spores single, symmetry radial, lateral shape reniform; monolete, curvatura absent, laesura midsized, 20 µm, MLI 0.52, margo indistinct, commissure indistinct; exospore 1 µm, verrucate, verrucae sparsely distributed over the entire surface, very short, <0.5 µm high, 2 µm wide, and 3–5 µm apart.

DIMENSIONS. Equatorial diameter, 25–(25.5)–26 µm; polar diameter, 38 µm; polar/equatorial = 1.49 µm; nm = 2, no = 68.

COMPARISONS. *Polypodiisporites* aff. *specious* Sah, 1967, is laevigate on the proximal face and has larger irregular verrucae; *P. scabraproximatus* Silva-Caminha et al., 2010, has a scabrate proximal face.

ETYMOLOGY. After the inconspicuous (discrete) verrucate pattern.

Polypodiisporites fossulatus **sp. nov.**

PLATE 2C, D

HOLOTYPE. Plate 2c, d, sample 22418, EF V-43-1/3.

TYPE LOCALITY. Well 1-AS-105-AM, Solimões Formation, Amazonas, Brazil.

DESCRIPTION. Spores single, symmetry radial, lateral shape reniform; monolete, curvatura absent, laesura midsized, 13 µm, MLI 0.54, margo absent, commissure indistinct; exospore 1.5 µm, foveo-fossulate, foveolae and fossulae irregularly distributed over the surface of the spore, foveolae sometimes fused together creating fossulae, fossulae of variable size and distribution, sometimes seen as long ridges, very short, <0.5 µm high, 0.5–1 µm wide, and 1–1.5 µm apart. Where fossulae are wider, small verrucae or granulae can be present.

DIMENSIONS. Equatorial diameter, 15 µm; polar diameter, 24 µm; polar/equatorial = 1.6 µm; nm = 1, no = 5.

COMPARISON. *Microfoveolatosporis* Krutzsch, 1959, species are solely foveolate.

ETYMOLOGY. After the fossulate pattern.

BOTANICAL AFFINITY. *Nephrolepis* (Lomariopsidaceae).

Punctatosporites **Ibrahim, 1933**

TYPE SPECIES. *PUNCTATOSPORITES MINUTUS* IBRAHIM, 1933

Punctatosporites latrubessei **sp. nov.**

PLATE 2J–M

HOLOTYPE. Plate 2j, k, sample 22354, EF J-19.

PARATYPE. Plate 2l, m, sample 22402, EF E-11-3/4.

TYPE LOCALITY. Well 1-AS-105-AM, Solimões Formation, Amazonas, Brazil.

DESCRIPTION. Spores single, symmetry radial; monolete, lateral shape reniform, curvatura absent, laesura midsized, 18 µm, MLI 0.58, simple, commissure distinct, invaginated, ends pointed; exospore 1 µm, scabrate, scabrae very densely and evenly distributed over the entire surface of the spore, forming a mat-like layer, 1.5–2 µm high.

DIMENSIONS. Equatorial diameter, 18–(18.5)–19 µm; polar diameter, 31–(31.5)–32 µm; polar/equatorial = 1.7 µm; nm = 2, no = 4.

COMPARISONS. *Puncatosporites minutus* Ibrahim, 1933, *P. scabratus* (Couper, 1958) Singh, 1971, *P. walkomii* de Jersey, 1962, and *Laevigatosporites granulatus* Jaramillo et al., 2007, all have considerably less dense scabrae and thinner exospore. *Gabonisporis* Boltenhagen, 1967, is trilete.

ETYMOLOGY. After Argentinian geologist Edgardo M. Latrubesse.

Reticulosporis **Krutzsch, 1959**

TYPE SPECIES. *RETICULOSPORIS MIOCENICUS*
(SELLING, 1944) KRUTZSCH, 1959

Reticulosporis diversus **sp. nov.**

PLATE 2N–Q

HOLOTYPE. Plate 2n, o, sample 22354, EF G-7.

PARATYPE. Plate 2p, q, sample 22354, EF T-13.

TYPE LOCALITY. Well 1-AS-105-AM, Solimões Formation, Amazonas, Brazil.

DESCRIPTION. Spores single, symmetry radial, lateral shape reniform; monolete, curvatura absent, laesura distinct, straight, 20 µm long, tapering, margo distinct, 1.5 µm wide, also tapering, commissure distinct; exospore 1–2 µm, reticulate, few lumina, very broad and of irregular shape, curvy and sometimes lobed, lumina 10–20 µm wide, muri 1 µm thick, lumina 2 µm apart. Occasionally, lumina are thin, having a canaliculated appearance, intrareticulate surface laevigate to sparsely granulose, with circular granules, 1–2 µm wide.

DIMENSIONS. Equatorial diameter, 21–(23)–25 µm; polar diameter, 36–(38)–40 µm; polar/equatorial = 1.65; nm = 2, no = 2.

Comparisons. All other monolete-reticulate spores have a much narrower and polygonal reticulate patterns.

Etymology. After its different/unique morphology, from the word *diversus* (different).

Botanical affinity. *Asplenium* (Polypodiaceae).

Trilete spores

Camarozonosporites Pant, 1954, ex Potonié, 1956, emend. Klaus, 1960

TYPE SPECIES. *CAMAROZONOSPORITES CRETACEOUS* (WEYLAND & KRIEGER, 1953) POTONIÉ, 1956

Camarozonosporites fossulatus sp. nov.

PLATE 3D, E

Holotype. Plate 3d, e, sample 22277, EF S-39.

Type locality. Well 1-AS-105-AM, Solimões Formation, Amazonas, Brazil.

Description. Spores single, symmetry radial, polar shape circular to subcircular; trilete, curvatura absent, laesura distinct, straight, radii middle sized, 8 µm, TLI 0.61, margo distinct, very thin, 0.5–1 µm wide, commissure distinct, straight, ends pointed; interradial crassitude, exospore 3 µm at the interradial area and 1 µm at corners, fossulate over the entire surface of the spore, fossulae long, curvy, and irregular, 1 µm wide, 2–3 µm apart, sometimes bifurcating.

Dimensions. Equatorial diameter length, 26 µm; equatorial diameter width, 25 µm; length/width = 1.04; nm = 1, no = 1.

Comparisons. *Camarozonosporites* Pant ex Potonié, 1956, emend. Klaus, 1960, accommodates verrucate spores with interradial crassitude; *C. crassus* Silva-Caminha et al., 2010, is verrucate. *Camarozonosporites* sp. 1 Jaramillo and Dilcher, 2001, has thinner interradial crassitude, is laevigate proximally, and its fossulae are smaller.

Etymology. After fossulate ornamentation.

Botanical affinity. *Lycopodium*/*Lycopodiella* (Lycopodiaceae).

Camarozonosporites trilobatus sp. nov.

PLATE 3F–I

Holotype. Plate 3f, g, sample 22277, EF U-35-4.

Paratype. Plate 3h, i, sample 22278, EF H-37-1.

Type locality. Well 1-AS-105-AM, Solimões Formation, Amazonas, Brazil.

Description. Spores single, symmetry radial, polar shape triangular–obtuse–convex; trilete, curvatura absent, laesura distinct, straight, radii middle sized, 10 µm, TLI 0.83, margo distinct, very thin, 0.5–1 µm wide, commissure distinct, straight; exospore 5–6 µm at interradial area and 1 µm at corners, verrucate, verrucae distributed on the entire surface of the spore, verrucae larger and irregular on the distal face, and smaller and circular on the proximal face, verrucae can be very large and irregular. Around the equator, verrucae merge and form interradial crassitude that can sometimes resemble lobes. Verrucae are 2–7 µm wide, 2–5 µm high, 1–4 µm apart.

Dimensions. Equatorial diameter length, 24–(24.5)–25 µm; equatorial diameter width, 20–(20.5)–22 µm; length/width = 1.19; nm = 2, no = 2.

Comparison. *C. crassus* Silva-Caminha et al., 2010, has smaller and more regular verrucae and thinner interradial crassitude.

ETymology. After lobate appearance of the interradial crassitude.

Cicatricosisporites Potonié & Gelletich, 1933, emend. Potonié, 1966

TYPE SPECIES. *CICATRICOSISPORITES DOROGENSIS* POTONIÉ & GELLETICH, 1933

Cicatricosisporites pseudograndiosus sp. nov.

PLATE 3L, M

Holotype. Plate 3l, m, sample 22278, EF H-8-3.

Type locality. Well 1-AS-105-AM, Solimões Formation, Amazonas, Brazil.

Description. Spores single, symmetry radial, polar shape triangular–obtuse–convex; trilete, curvatura absent, laesura distinct, straight, radii long, reaching equator, 40 µm, TLI 1, margo indistinct, commissure distinct, straight; exospore 0.7 µm, cicatricose over the entire surface of the spore, distal ribs 5–7 µm wide, flat, straight, separated by thin grooves 1 µm wide, ribs arranged in one set on the distal face, running parallel to the equator, sometimes bifurcating. Rib extremities pinch out gently toward the equator and coalesce at the apices. On the proximal face, ribs are similar to the distal face but are disposed in three sets, one in each interradial area.

Dimensions. Equatorial diameter length, 51–(63)–75 µm; equatorial diameter width, 45–(52.5)–60 µm; length/width = 1.2; nm = 2, no = 4.

Comparisons. *Cicatricosisporites subrotundus* Brenner, 1963, has ribs arranged parallel to the equator in the distal face. *Magnastriatites* Germeraad et al., 1968, does not have ridges/ribs on the proximal contact area; *M. grandiosus* (Kedves and Solé de Porta, 1963) Dueñas, 1980, and other species of *Cicatricosisporites* have shorter and nonflat ribs, and a lower rib-groove width ratio.

Etymology. After resemblance with *Magnastriatites grandiosus*.

Botanical affinity. *Ceratopteris* (Parkeriaceae).

Cingulatisporites **Thomson in Thomson & Pflug, 1953, emend. Potonié, 1956**

TYPE SPECIES. *CINGULATISPORITES LEVISPECIOSUS* PFLUG IN THOMSON AND PFLUG, 1953

Cingulatisporites cristatus **sp. nov.**

PLATE 3N

Holotype. Plate 3n, sample 22279, EF U-43.

Type locality. Well 1-AS-105-AM, Solimões Formation, Amazonas, Brazil.

Description. Spores single, symmetry radial, polar shape circular to triangular–obtuse–convex; trilete, curvatura absent, laesura distinct, curvy, radii long, 10 µm, reaching equator, TLI 0.9, margo distinct, very thin <0.5 µm wide, commissure indistinct; exospore 1 µm, laevigate with scarce small verrucae on the surface; cingulum cristate, 2–5 µm thick, cingulum sculptural elements 1 µm wide, 1 µm high. Thickness of the cingulum can vary, but there is not a clear interradial crassitude.

Dimensions. Equatorial diameter length, 22–(22.5)–23 µm; equatorial diameter width, 20–(20.5)–21 µm; length/width = 1.09; nm = 2, no = 2.

Comparisons. Other species of *Cingulatisporites* do not present a cristate cingulum.

Etymology. After cristate cingulum.

Botanical affinity. *Selaginella* (Selaginellaceae).

Cingulatisporites matisiensis **sp. nov.**

PLATE 3O–R

Holotype. Plate 3o, p, sample 22278, EF S-19.

Paratype. Plate 3q, r, sample 22278, EF E-12-4.

Type locality. Well 1-AS-105-AM, Solimões Formation, Amazonas, Brazil.

Description. Spores single, symmetry radial, polar shape circular, cingulate; trilete, curvatura imperfecta, laesura distinct, straight, radii long, reaching equator, 12 µm long, TLI 0.8, margo distinct, 2 µm wide, serrulate border, commissure distinct, straight, cingulum 2–3 µm thick; exospore thin, ~0.5 µm, verrucate–rugulate, verrucae sparse and often clustered in the proximal face, circular, 1–2 µm wide; distal face with sparse and irregular rugulae, 4–6 µm wide, 2–3 µm thick.

Dimensions. Equatorial diameter length, 30–(32.5)–35 µm; equatorial diameter width, 30 µm; length/width = 1.08; nm = 2, no = 2.

Comparisons. *Cingulatisporites verrucatus* Regali et al., 1974, has a much wider cingulum and laevigate proximal face. *Polypodiaceoisporites pseudopsilatus* Lorente, 1986, has a triangular prominence on the distal face. *Pteridaceoisporis gemmatus* Silva-Caminha et al., 2010, has thicker cingulum, shorter radii and denser and more diverse verruca–rugulae. *Cingulatisporites rugulatus* Silva-Caminha et al., 2010, has waving commissure, thinner margo, proximal rugulae, and distal scabrae.

Etymology. After the Amazon indigenous people Matis.

Botanical affinity. *Phaeoceros* (Notothyladaceae).

Echinatisporis **Krutzsch, 1959**

TYPE SPECIES. *ECHINATISPORIS LONGECHINUS* KRUTZSCH, 1959

Echinatisporis infantulus **sp. nov.**

PLATE 4E–G

Holotype. Plate 4e, f, sample 22140, EF S-51-2.

Paratype. Plate 4g, sample 22170, EF F-32-2/4.

Type locality. Well 1-AS-105-AM, Solimões Formation, Amazonas, Brazil.

Description. Spores single, symmetry radial, circular; trilete, curvatura absent, laesura distinct, straight, radii middle sized, 10 µm long, TLI 0.66, marginate, margo very thin, 0.7 µm wide, commissure straight; exospore 0.5 µm, echinate, spines evenly distributed over the entire surface; 0.5 µm wide at base, 1 µm high, 2–3 µm apart, short, conical.

Dimensions. Equatorial diameter length, 30 µm; equatorial diameter width, 26 µm; length/width = 1.15; nm = 1, no = 2.

Comparisons. *Planisporites* sp. 2 Jaramillo and Dilcher, 2001, has larger spines and margo is raised. *Acanthotriletes levidensis* Balme, 1957, has larger spines and radii that reaches equator; and *E. circularis* Silva-Caminha et al., 2010, is thicker and has larger spines.

Etymology. After the reduced size of spines, from word *infantulus* (little infant).

Foraminisporis **Krutzsch, 1959**

TYPE SPECIES. *FORAMINISPORIS FORAMINIS* KRUTZSCH, 1959

Foraminisporis connexus **sp. nov.**

PLATE 4I–L

Holotype. Plate 4i, j, sample 22278, EF P-24.

Paratype. Plate 4k, l, sample 22140, EF L-13.

Type locality. Well 1-AS-105-AM, Solimões Formation, Amazonas, Brazil.

Description. Spores single, symmetry radial, polar shape circular; trilete, curvatura absent, laesura distinct, irregular, radii reach the equator, 20 µm long, TLI 0.8, marginate, margo 1 µm wide, commissure irregular; exospore slightly zonate, 2–3 µm, echinate, echinae distributed over the entire surface but denser on the distal face, 2 µm wide at base, 2 µm high, conical shape, closely spaced, 1–2 µm apart. Spines tend to connect to each other and sometimes create a rugulate appearance.

Dimensions. Equatorial diameter length, 50–(51)–52 µm; equatorial diameter width, 46–(48)–50 µm; length/width = 1.06 µm; nm = 2, no = 2.

Comparisons. *Foraminisporis foraminis* Krutzsch, 1959, and *F. wonthaggiensis* (Cookson and Dettmann, 1958) Dettmann, 1963, are also foraminate (=foveolate); *F. asymmetricus* (Cookson and Dettmann, 1958) Dettmann, 1963, is verrucate; *F. dailyi* (Cookson and Dettmann, 1958) Dettmann, 1963, is foveolate and verrucate. *Echinatisporis brevispinosus* Jaramillo and Dilcher, 2001, *E. muelleri* (Regali et al., 1974) Silva-Caminha et al., 2010, and *E. circularis* Silva-Caminha et al., 2010, are smaller, differ in spine morphology, and lack zona.

Etymology. After connection between spines.

Botanical affinity. *Anthoceros* (Anthocerotaceae).

Hamulatisporis Krutzsch, 1959

TYPE SPECIES. *HAMULATISPORIS CAPERATUS* (VAN HOEKEN-KLINKENBERG, 1964) SCHRANK, 1994

Hamulatisporis bareanus sp. nov.

PLATE 5C, D

Holotype. Plate 5c, d, sample 22140, EF V-9-1.

Type locality. Well 1-AS-105-AM, Solimões Formation, Amazonas, Brazil.

Description. Spores single, symmetry radial, polar shape circular to triangular–obtuse–convex; trilete, curvatura absent, laesura distinct, straight, radii middle sized, 15 µm long, TLI 0.75, margo thin, 1 µm wide, commissure distinct, straight; exospore 1–2 µm, rugulate (hamulate) over the entire surface of the spore, slightly coarser distally, rugula 1 µm wide, curvy, mostly connected, and sometimes forming isolated foveolae, fossula 1.5 µm wide.

Dimensions. Equatorial diameter length, 36–(38)–40 µm; equatorial diameter width, 33–(35)–37 µm; length/width = 1.08 µm; nm = 2, no = 2.

Comparisons. *Hamulatisporis caperatus* (Van Hoeken-Klinkenberg, 1964) Schrank, 1994, has a thinner hamulate pattern; *H. insignis* (Norris, 1967) Kedves, 1995, has interradial crassitude, rugulae have a radial arrangement, and amb is more circular.

Etymology. After the Amazon indigenous group Baré.

Ischyosporites Balme, 1957

TYPE SPECIES. *ISCHYOSPORITES CRATERIS* BALME, 1957

Ischyosporites dubius sp. nov.

PLATE 5G–J

Holotype. Plate 5g, h, sample 22140, EF Q-6-1.

Paratype. Plate 5i, j, sample 22293, EF U-11.

Type locality. Well 1-AS-105-AM, Solimões Formation, Amazonas, Brazil.

Description. Spores single, symmetry radial, polar shape triangular–obtuse–convex; trilete, curvatura absent, laesura distinct, straight, radii midsized, 12 µm long, TLI 0.52, marginate, margo 2–3 µm wide, undulating to straight, thinning outward, commissure distinct, straight; exospore 1.5 µm, verrucate, verrucae present over the entire surface. Most verrucae anastomose to form a rugulate pattern; verrucae very variable, 5 µm wide, 0.5–1 µm high, with fossulae separating them, of irregular shape.

Dimensions. Equatorial diameter length, 27–(36.5)–46 µm; equatorial diameter width, 21–(33)–45 µm; length/width = 1.1; nm = 2, no = 7.

Comparisons. *Ischyosporites problematicus* Jaramillo and Dilcher, 2001, has a higher proportion of fossula compared to verrucae; *I. variegatus* (Couper, 1958) Jansonius and Hills, 1990, is distally foveo–reticulate and proximally granulose to verrucose; *I. badagriensis* Jan du Chêne et al., 1978, has broad reticulum; and *I. crateris* Balme, 1957, is thicker and foveolate. *Verrucatotriletes* spp. lack anastomosing verrucae and fossula.

Etymology. After the large variation of sculptural elements.

Ischyosporites granulatus sp. nov.

PLATE 5K, L

Holotype. Plate 5k, l, sample 22303, EF J-37.

Type locality. Well 1-AS-105-AM, Solimões Formation, Amazonas, Brazil.

Description. Spores single, symmetry radial, polar shape triangular to triangular–obtuse–convex; trilete, curvatura absent, laesura distinct, straight, radii long, almost reaching the equator, 14 µm long, TLI 0.73, marginate, margo thick, 2–3 µm, with an irregular outer border, commissure distinct, straight; exospore 2–3 µm, granular to verrucate in proximal face, granules on proximal face sparse, circular, 1–3 µm wide; rugulate in distal face, rugulae irregular, long and bifurcating, 4–5 µm wide, and of variable length, connecting to each other, sometimes bounded by fossulae or circular lumina, 4–5 µm wide and of variable length.

Dimensions. Equatorial diameter length, 29–(33.5)–38 µm; equatorial diameter width, 26–(31)–36 µm; length/width = 1.08; nm = 2, no = 2.

Comparisons. Other species of *Ischyosporites* have a well-defined fossulate or reticulate sculpture.

Etymology. After granulate ornamentation.

Lycopodiumsporites Thiergart, 1938

TYPE SPECIES. *LYCOPODIUMSPORITES AGATHOECUS* (POTONIÉ, 1934) THIERGART, 1938

Lycopodiumsporites amazonicus **sp. nov.**

PLATE 5N, O

Holotype. Plate 5n, o, sample 22279, EF T-16.

Type locality. Well 1-AS-105-AM, Solimões Formation, Amazonas, Brazil.

Description. Spores single, symmetry radial, triangular–obtuse–convex; trilete, curvatura absent, laesura distinct, straight, radii middle sized, 12 µm long, TLI 0.8, margo indistinct, commissure indistinct; exospore 3–4 µm; reticulate over the entire surface, lumina circular, 2–3 µm wide, muri thin, 0.7 µm wide, very high, 3 µm high.

Dimensions. Equatorial diameter length, 30–(34.5)–39 µm; equatorial diameter width, 29–(34)–36 µm; length/width = 1.01; nm = 2, no = 2.

Comparisons. *L. novomexicanum* Drugg, 1967, and *Retitriletes austroclavatidites* (Cookson, 1953) Döring et al. in Krutzsch, 1963, have shorter muri and larger lumina. *Retitriletes altimuratus* Silva-Caminha et al., 2010, has shorter muri and indistinct laesura. *Retitriletes baqueroense* Archangelsky and Villar de Seoane, 1998, and *L. fastigioides* (Couper, 1953) Boltenhagen, 1967, are laevigate on proximal face.

Etymology. After the Amazon forest.

Botanical affinity. *Lycopodium* (Lycopodiaceae).

Neoraistrickia **Cookson ex. Potonié, 1956**

TYPE SPECIES. *NEORAISTRICKIA TRUNCATA*
(COOKSON, 1953) POTONIÉ, 1956

Neoraistrickia dubia **sp. nov.**

PLATE 6A–D

Holotype. Plate 6a, b, sample 22293, EF K-50-1/2.

Paratype. Plate 6c, d, sample 22326, EF J-14.

Type locality. Well 1-AS-105-AM, Solimões Formation, Amazonas, Brazil.

Description. Spores single, symmetry radial, circular; trilete, aculite absent, laesura distinct, irregular to straight, radii short, 8 µm long, TLI 0.66, marginate, margo very thin <1 µm wide, commissure distinct; exospore 1–1.5 µm, aculite, baculae densely and evenly distributed over the entire surface; 1–1.5 µm wide at base, 1.5–3 µm high, 1 µm apart, some baculae constricted at the base.

Dimensions. Equatorial diameter length, 24–(24.5)–25 µm; equatorial diameter width, 22–(23)–24 µm; length/width = 1.06; nm = 2, no = 3.

Comparison. *Neoraistrickia truncata* (Cookson, 1953) Potonié, 1956, has larger, less dense bacula and shape is more triangular.

Etymology. After the variation of baculae, constricted and nonconstricted.

Psilatriletes **Van der Hammen, 1954, ex Potonié, 1956**

TYPE SPECIES. *PSILATRILETES DETORTUS*
(WEYLAND & KRIEGER, 1953) POTONIÉ, 1956

Psilatriletes delicatus **sp. nov.**

PLATE 6I, J

Holotype. Plate 6i, sample 22257, EF P-39-2.

Paratype. Plate 6j, sample 22148, EF M-6-3/4.

Type locality. Well 1-AS-105-AM, Solimões Formation, Amazonas, Brazil.

Description. Spores single, symmetry radial, circular; trilete, curvatura absent, laesura distinct, radii long almost reaching the equator, 10 µm long, TLI 0.69, slightly marginate, margo 0.5 µm wide, commissure straight, ends pointed; exospore 0.7 µm, laevigate. Spore easily folded especially around the equator, often creating a false cingulate appearance.

Dimensions. Equatorial diameter length, 22–(25.5)–29 µm; equatorial diameter width, 19–(22)–25 µm; length/width = 1.15; nm = 2, no = 8.

Comparisons. *Cyathidites minor* Couper, 1953, and *C. australis* Couper, 1953, are triangular–subtriangular and with thicker exospore. *Biretisporites potoniaei* Delcourt and Sprumont, 1955, has radii reaching the equator and thicker exospore and margo. *Hydrosporis minor* Silva-Caminha et al., 2010, is smaller and exospore is thicker (1.5 µm).

Etymology. After the thin and foldable exospore.

Psilatriletes marginatus **sp. nov.**

PLATE 6L–N

Holotype. Plate 6l, m, sample 22277, EF D-50-2.

Paratype. Plate 6n, sample 22277, EF H-25-3/4.

Type locality. Well 1-AS-105-AM, Solimões Formation, Amazonas, Brazil.

Description. Spores single, symmetry radial, polar shape triangular–obtuse–straight to slightly convex; trilete, curvatura absent, laesura distinct, straight, radii medium sized, 10 µm long, TLI 0.76, marginate, margo 3–4 µm wide, well-defined, wider toward the center of the Y-mark, commissure straight, ends pointed; exospore 1.5–2 µm, laevigate or micropitted. When micropitted, exospore densely perforated. Margo is characteristic; it can be straight or constricted at the central point of the trilete mark, forming two segments.

Dimensions. Equatorial diameter length, 26–(31.5)–37 µm; equatorial diameter width, 25–(28.5)–32 µm; length/width = 1.1; nm = 2, no = 12.

Comparisons. *Dictyophyllidites impensus* (Hedlund, 1966) Singh, 1983, is circular and has thinner margo. *Hydrosporis minor* Silva-Caminha et al., 2010, is smaller, granulate, more circular and has thinner margo.

Etymology. After the presence of a margo.

Botanical affinity. *Cyathea* (Cyatheaceae).

Rotverrusporites Döring, 1964

TYPE SPECIES. *ROTVERRUSPORITES OBSCURILAESURATUS* (POCOCK, 1962) DÖRING, 1964

Rotverrusporites amazonicus sp. nov.

PLATE 7E–H

Holotype. Plate 7e, f, sample 22277, EF E-49-1.

Paratype. Plate 7g, h, sample 22279, EF G-8-4.

Type locality. Well 1-AS-105-AM, Solimões Formation, Amazonas, Brazil.

Description. Spores single, symmetry radial, polar shape circular to subcircular; trilete, curvatura absent, laesura distinct, straight, radii long, 12 µm long, almost reaching equator, TLI 0.80, margo distinct, 1 µm wide, straight, commissure distinct, straight; exospore 2 µm thick, verrucate, verrucae distributed over the entire surface, varying in width throughout the grain in a random pattern, 0.5–2 µm wide, 1 µm high, circular, 0.5 µm apart, wider verrucae are more frequent.

Dimensions. Equatorial diameter length, 30–(33)–36 µm; equatorial diameter width, 30–(33)–36 µm; length/width = 1; nm = 2, no = 2.

Comparisons. *Rotverrusporites rupununiensis* Van der Hammen and Burger, 1966, is larger, much thicker and has larger verrucae. *Rotverrusporites obscurilaesuratus* (Pocock, 1962) Döring, 1964, does not have distinct laesura.

Etymology. After the Amazon forest.

Verrucatotriletes Van Hoeken-Klinkenberg, 1964

TYPE SPECIES. *VERRUCATOTRILETES BULLATUS* VAN HOEKEN-KLINKENBERG, 1964

Verrucatotriletes pseudovirueloides sp. nov.

PLATE 7K, L

Holotype. Plate 7k, l, sample 22278, EF O-9-3/4.

Type locality. Well 1-AS-105-AM, Solimões Formation, Amazonas, Brazil.

Description. Spores single, symmetry radial, polar shape circular to subcircular; trilete, curvatura absent, laesura distinct, radii middle sized, 17 µm long, TLI 0.73, margo absent, commissure distinct, straight; exospore 2 µm, verrucate, verrucate sparse and unevenly distributed over the entire surface, very short, 1 µm wide, <0.5 µm high, circular, 0.5–2 µm apart.

Dimensions. Equatorial diameter length, 46 µm; equatorial diameter width, 44 µm; length/width = 1.04; nm = 1, no = 2.

Comparison. *Verrucatotriletes virueloides* Jaramillo et al., 2007, has smaller and denser verrucae and thinner exospore.

Etymology. After similarity with *V. virueloides* Jaramillo et al., 2007.

Pollen

Inaperturate

Inaperturopollenites (Pflug & Thomson in Thomson & Pflug, 1953) Potonié, 1958

TYPE SPECIES. *INAPERTUROPOLLENITES DUBIUS* (POTONIÉ & VENITZ, 1934) PFLUG & THOMSON IN THOMSON & PFLUG, 1953

Inaperturopollenites tectatus sp. nov.

PLATE 8D

Holotype. Plate 8d, sample 22278, EF T-50.

Type locality. Well 1-AS-105-AM, Solimões Formation, Amazonas, Brazil.

Description. Monad, radial, isopolar, amb circular, inaperturate; tectate, exine 1 µm, nexine 0.3 µm, columellae distinct, 0.4 µm, tectum 0.3 µm thick, micropitted, lumina <0.5 µm wide, circular, homobrochate; grain often folded.

Dimensions. Polar diameter length, 24 µm; nm = 1, no = 21.

Comparisons. *Inaperturopollenites cursis* Sarmiento, 1992, and *I. curvimuratus* Regali et al., 1974, are reticulate; *I. dubius* (Potonié and Venitz, 1934) Pflug and Thomson in Thomson and Pflug, 1953, and *I. simplex* Regali et al., 1974, are atectate and psilate.

Etymology. After tectate exine.

Polyadopollenites Pflug & Thomson in Thomson & Pflug, 1953

TYPE SPECIES. *POLYADOPOLLENITES MULTIPARTITUS* PFLUG IN THOMSON & PFLUG, 1953

Polyadopollenites minimus sp. nov.

PLATE 8L–N

Holotype. Plate 8l, m, sample 22158, EF H39/3.

Paratype. Plate 8n, sample 22140, EF T8/1-2.

Type locality. Well 1-AS-105-AM, Solimões Formation, Amazonas, Brazil.

Description. Polyad of 12 monads, polyad circular and isopolar, arranged in 3 planes of 4 monads, monads subcircular to trapezoidal, inaperturate; atectate, exine 0.5–1 µm, psilate. Grain probably porate; however, pores seemed indistinct.

Dimensions. Polyad diameter, 16 µm; monad diameters 6–8 × 4–5 µm; nm = 2, no = 2.

Comparisons. *P. mariae* Dueñas, 1980, and *P. vancampoi* Salard-Cheboldaeff, 1978, are much larger.

Etymology. After its minute size.

Botanical affinity. *Mimosa* (Fabaceae).

Monosulcate

Arecipites Wodehouse, 1933, emend. Nichols et al., 1973

TYPE SPECIES. *ARECIPITES PUNCTATUS*
WODEHOUSE, 1933, EX POTONIÉ, 1958

Arecipites invaginatus sp. nov.

PLATE 8O

Holotype. Plate 8o, sample 22460, EF P-20-4.

Type locality. Well 1-AS-105-AM, Solimões Formation, Amazonas, Brazil.

Description. Monad, bilateral, heteropolar, prolate to perprolate; monocolpate, colpus long, 36 µm long, CPi 0.92, reaching poles, ends rounded, borders straight, slightly tapered, colpus simple, deeply invaginated creating a membranous appearance; tectate, exine 1.5 µm, nexine 0.5 µm, columellae 0.5 µm, distinct and dense, tectum 0.5 µm thick; micropitted, lumina <0.5 µm wide, circular, homobrochate, densely distributed.

Dimensions. Polar diameter, 35–(37)–39 µm; equatorial diameter, 18–(18.5)–19 µm; polar/equatorial = 2; nm = 2, no = 2.

Comparison. *Arecipites regio* (Van der Hammen and García, 1966) Jaramillo and Dilcher, 2001, is marginate.

Etymology. After the invaginating colpus.

Botanical affinity. Arecaceae.

Trichotomosulcate

Luminidites amazonicus sp. nov.

PLATE 10A

Holotype. Plate 10a, sample 22140, EF D-32-3.

Type locality. Well 1-AS-105-AM, Solimões Formation, Amazonas, Brazil.

Description. Monad, radial, heteropolar, amb triangular–obtuse–straight to slightly concave; trichotomosulcate, colpi long, radii 19 µm, reaching equator, ends usually open to rounded, simple; semitectate, exine 1.5 µm, nexine 0.5 µm, columellae 0.5 µm, distinct, <0.5 µm apart, tectum 0.5 µm thick; reticulate, lumina <0.5 µm wide, circular, muri ~0.5 µm wide, homobrochate.

Dimensions. Equatorial diameter length, 26–(32)–38 µm; equatorial diameter width, 26–(32)–38; length/width = 1; nm = 2, no = 10.

Comparisons. *Trichotomosulcites ornatus* Boltenhagen, 1976, has wider reticulum; *T. laevigatus* Boltenhagen, 1976, is psilate. *Luminidites colombianensis* Jaramillo and Dilcher, 2001, is heterobrochate.

Etymology. After the Amazon forest.

Botanical affinity. Arecaceae (*Bactris*?).

Trichotomosulcites Couper, 1953

TYPE SPECIES. *TRICHOTOMOSULCITES*
SUBGRANULATUS COUPER, 1953

Trichotomosulcites normalis sp. nov.

PLATE 10B

Holotype. Plate 10b, sample 22405, EF Q-42-1.

Type locality. Well 1-AS-105-AM, Solimões Formation, Amazonas, Brazil.

Description. Monad, radial, heteropolar, triangular-obtuse-convex amb; trichotomosulcate, colpi long, radii 14 µm long, 3–4 µm wide, almost reaching equator, ends rounded, simple; tectate, exine 2.1 µm, nexine 0.7 µm, columellae 0.7 µm, distinct, dense, but not packed and very thin, tectum 0.7 µm thick; psilate, columellae tips seen through tectum, giving a micropitted appearance.

Dimensions. Equatorial diameter length, 37–(38)–39 µm; equatorial diameter width, 35–(36.5)–38 µm; length/width = 1.04; nm = 2, no = 3.

Comparison. *Trichotomosulcites laevigatus* Boltenhagen, 1976, has a narrower colpus with wide margo and seems to be atectate.

Etymology. After the rather simple morphology.

Botanical affinity. Arecaceae.

Dicolpate

Dicolpopollis Pflanzl, 1956, emend Potonié, 1966

TYPE SPECIES. *DICOLPOPOLLIS KOCKELI* PFLANZL, 1965

Dicolpopollis? costatus sp. nov.

PLATE 10H–J

Holotype. Plate 10h, sample 22460, EF D-48-2.

Paratype. Plate 10i, j, sample 22460, EF S-20.

Type locality. Well 1-AS-105-AM, Solimões Formation, Amazonas, Brazil.

Description. Monad, radial, isopolar, amb subcircular; dicolporate, ectocolpi short, ends rounded, 12 µm long, costate, costa produced by a thickening of the exine around colpi, 2 μm thick, 8 μm wide; endopores, pores simple, 4 μm wide; atectate, exine 1–2 μm thick, psilate.

DIMENSIONS. Equatorial diameter length, 22–(24.6)–26 μm; equatorial diameter width, 21–(22.6)–25 μm; length/width = 1.08; nm = 3, no = 2.

COMPARISON. *Dicolpopollis*, Pflanzl, 1956, accommodates dicolpate grains; therefore, we place the present fossil type provisionally in this genus.

ETYMOLOGY. After costate aperture.

BOTANICAL AFFINITY. *Macoubea* (Apocynaceae), which is tricolporate and dicolporate (Colinvaux et al., 1999).

Diporate

Echidiporites **Muller et al., 1987**

TYPE SPECIES. *ECHIDIPORITES BARBEITOENSIS* MULLER ET AL., 1987

Echidiporites barbeitoi **Muller et al., 1987, emend.**

PLATE 10M–O

BASIONYM. *Echidiporites barbeitoensis* Muller et al., 1987, p. 40, pl. 2, figs. 2–3.

SPECIMEN. Plate 10m, sample 22290, EF J-18-3.

SPECIMEN. Plate 10n, o, sample 22282, EF T-14-3.

EXPANDED DESCRIPTION. Monad, radial, isopolar, suboblate, amb oval; porate, pores oval to quadrangular, 6–9 μm wide, costate, costa 1–2 μm wide; tectate, exine 1.5–2 μm thick, nexine 0.5 μm, columella 1 μm, indistinct, tectum 0.5 μm; echinate, echinae conical, 2–3 μm high, 1 um wide at the base, base of echinae deeply rooted, sunken in the exine.

DIMENSIONS. Equatorial diameter, 32 μm; polar diameter, 27 μm; P/E ratio 0.84; equatorial diameter length, 32–(35.3)–38 μm; equatorial diameter width, 30 μm; length/width = 1.06–1.17; nm = 2, no = 22.

COMPARISON. *Mauritiidites* Van Hoeken-Klinkenberg, 1964, is monoporate/monocolpate (see Plate 9d–g).

NOTE. The epithet *barbeitoensis* was coined in honour of P. Barbeito. Because this is a personal name and the Latin termination *-ensis* is designed for geographical locations, we emend the epithet to reflect the correct personal masculine and singular termination (Article 60 and 60.8[a] of the International Code of Nomenclature [Turland et al., 2018]).

BOTANICAL AFFINITY. Arecaceae (Mauritiinae).

Tricolpate

Foveotricolpites **Pierce, 1961**

TYPE SPECIES. *FOVEOTRICOLPITES SPHAEROIDES* PIERCE, 1961

Foveotricolpites colpiconstrictus **Hoorn, 1994b, comb. nov.**

PLATE 11A, B

BASIONYM. *Retitricolpites colpiconstrictus* Hoorn 1994b, p. 38, pl. 4, fig. 2.

SPECIMEN. Plate 11a, b, sample 22140, EF T-9-1.

DESCRIPTION. Monad, radial, isopolar, prolate; tricolpate, endo and ectocolpi coinciding, colpi long, 22 μm long, CPi 0.73, simple, invaginating, ends pointed, constriction present at mesocolpia area of colpi; polar area small, 10 μm wide; tectate, exine 2 μm thick, slightly thicker at apocolpia, nexine 0.5 μm thick, columellae 0.5 μm thick, distinct, packed, tectum 1 μm thick; micropitted, lumina 0.5 μm wide, 0.5 μm apart, evenly and densely distributed over the entire grain.

DIMENSIONS. Polar diameter, 30 μm; equatorial diameter, 22 μm; polar/equatorial = 1.36; nm = 1, no = 10.

COMPARISONS. *Retitricolpites* Van der Hammen, 1956b, ex Pierce, 1961, is illegitimate and a later synonym of *Neea* (Jansonius and Hills, 1976, card 2401). *Foveotricolpites* Pierce, 1961, accommodates subprolate tricolpate pollen with foveolate ornamentation.

Foveotricolpites simplex **González-Guzmán, 1967 comb. nov.**

PLATE 11C–E

BASIONYM. *Retitricolpites simplex* González-Guzmán, 1967, p. 31, pl. 2, fig. 1.

SPECIMENS. Plate 11c, d, sample 22418, EF X-17.

SPECIMENS. Plate 11e, sample 22436, EF L-10-1/2.

DESCRIPTION. Monad, radial, isopolar, prolate, tricolpate, sometimes tricolporate, endo and ectocolpi coinciding, 32 μm long, CPi 0.78, CEi 0.68, almost reaching poles, slightly costate, costa 0.5 μm wide, borders straight, ends pointed, polar area very small, 6 μm wide; endopores circular, simple, 10 μm wide; tectate, exine 2.4 μm thick, nexine 0.7 μm thick, columellae 1 μm thick, distinct, 0.5 μm wide, 0.5 μm apart, tectum 0.7 μm thick; foveolate to reticulate, lumina 0.5 μm wide, muri 0.5 μm thick, homobrochate, densely and evenly distributed over the entire grain.

DIMENSIONS. Equatorial view: polar diameter, 36–(38.5)–41 μm; equatorial diameter, 20–(24)–28; polar/equatorial = 1.60; polar view: polar diameter length, 41 μm; polar diameter width, 41 μm; length/width = 1; nm = 3, no = 216.

COMPARISONS. *Retitricolpites* Van der Hammen, 1956b, ex Pierce, 1961, is invalid and is a later synonym of *Neea* (Jansonius and Hills, 1976, card 2401). *Foveotricolpites* Pierce, 1961, accommodates subprolate tricolpate pollen with foveolate ornamentation.

BOTANICAL AFFINITY. *Sapium* (Euphorbiaceae).

Ladakhipollenites Mathur & Jain, 1980

TYPE SPECIES. *LADAKHIPOLLENITES LEVIS*
(SAH & DUTTA, 1966) MATHUR & JAIN, 1980

Ladakhipollenites campbellii sp. nov.

PLATE 11F–H

Holotype. Plate 11f, g, sample 22257, EF K-45-3.

Paratype. Plate 11h, sample 22140, EF D-16-1/2.

Type locality. Well 1-AS-105-AM, Solimões Formation, Amazonas, Brazil.

Description. Monad, radial, isopolar, prolate to subprolate, amb circular; tricolpate, colpi long, 16 μm long, CPi 0.58, CEi 0.47, borders slightly invaginating, ends rounded, ectocolpi marginate and costate, margo 5 μm wide, 1 μm thick, formed by the thinning of columellae near colpi, costae 1 μm wide, 1–1.5 μm thick; polar area small, 6 μm wide; tectate, exine 2 μm thick, nexine 0.5 μm thick, columellae 1 μm thick, distinct, 0.5 μm wide, 0.5 μm apart, tectum 0.5 μm thick; psilate, tips of columellae seen through tectum, giving a foveolate appearance.

Dimensions. Equatorial view: polar diameter, 34 μm; equatorial diameter, 25–(27)–29 μm; polar/equatorial = 1.25; polar view: equatorial diameter length, 32 μm; equatorial diameter width, 32 μm; length/width = 1; nm = 3, no = 7.

Comparisons. *Psilatricolpites acerbus* González-Guzmán, 1967, has packed columellae; *P. anconis* Hoorn, 1993, has indistinct columellae and is smaller; *P. clarissimus* (Van der Hammen, 1954) Van der Hammen and Wymstra, 1964, lacks margo; *P. colpiconstrictus* Van Hoeken-Klinkenberg, 1966, has constriction of the colpi; *P. polaroides* González-Guzmán, 1967, has thicker exine at poles; and *P. hammenii* Boltenhagen, 1976, is atectate.

Etymology. After geologist Kenneth E. Campbell Jr.

Botanical affinity. *Vitex* (Lamiaceae).

Ladakhipollenites colpiconstrictus Van Hoeken-Klinkenberg, 1966, comb. nov.

PLATE 11K, L

Basionym. *Psilatricolpites colpiconstrictus* Van Hoeken-Klinkenberg, 1966, p. 41, pl. 1, fig. 13.

Specimens. Plate 11k, l, sample 22445, EF U-35.

Description. Monad, radial, isopolar, prolate-spheroidal; tricolpate, endo and ectocolpi coinciding, 18 μm long, CPi 0.66, borders straight, ends rounded, polar area small, 5 μm wide, costate, costae 1 μm wide, colpi constriction at mesocolpia area; tectate, exine 2 μm thick, nexine 0.5 μm thick, columellae 1 μm thick, distinct, 0.3 μm wide, 0.2 μm apart, tectum 0.5 μm thick; psilate, tips of columellae seen through tectum.

Dimensions. Polar diameter, 27 μm; equatorial diameter, 25 μm; polar/equatorial = 1.08; nm = 1, no = 10.

Comparisons. *Psilatricolporites* Van der Hammen, 1956a, ex Pierce, 1961, is an obligate later synonym of *Tricolporites* Van der Hammen, 1954, because they have the same type species; as *Tricolpites* is not validly published and is a later synonym of *Clethra*, so is *Psilatricolporites* (Jansonius and Hills, 1976, card 2234). *Ladakhipollenites* Mathur and Jain, 1980, accommodates tricolpate psilate pollen grains.

Ladakhipollenites nanus sp. nov.

PLATE 11M, N

Holotype. Plate 11m, n, sample 22148, EF G-12.

Type locality. Well 1-AS-105-AM, Solimões Formation, Amazonas, Brazil.

Description. Monad, radial, isopolar, prolate to perprolate; tricolpate, colpi 15–18 μm long, CPi 0.78–0.81, borders straight, ends pointed, simple, polar area small, 5 μm wide; tectate, exine 1.1 μm thick, nexine 0.3 μm thick, columellae 0.5 μm thick, indistinct, tectum 0.3 μm thick; psilate.

Dimensions. Polar diameter, 19–(19.5)–20 μm; equatorial diameter, 9–(10.5)–12 μm; polar/equatorial = 1.85; nm = 2, no = 7.

Comparison. *Psilatricolpites minutus* González-Guzmán, 1967, has distinct constriction at mesocolpi.

Etymology. After the small size.

Loranthacites Mtchedlishvili in Samoilovich & Mtchedlishvili, 1961

TYPE SPECIES. *LORANTHACITES MACROSOLENSIDES*
SAMOILOVICH & MTCHEDLISHVILI, 1961

Loranthacites tabatingensis sp. nov.

PLATE 11 O, P

Synonymy. *Loranthacites* sp. 1 Silva-Caminha et al., 2010

Holotype. Plate 11o, sample 22375, EF K9/1.

Paratype. Plate 11p, sample 22445, EF R49/3.

Type locality. Well 1-AS-105-AM, Solimões Formation, Amazonas, Brazil.

Description. Monad, radial, isopolar, amb triangular–obtuse–straight to slightly convex; tricolpate, syncolpate, colpi 18 μm long, CEi 1, colpi marginate; margo produced by thinning of the sexine, margo 4–5 μm wide, 1 μm thick, borders slightly invaginating, polar area absent; tectate, exine thicker in the mesocolpia, thinning toward colpi, where it becomes atectate, exine 2 μm thick at mesocolpia, nexine 1 μm thick, columellae 0.5 μm thick, distinct, tectum 0.5 μm thick, exine 1 μm near colpi; psilate.

Dimensions. Equatorial diameter length, 30–32 µm; equatorial diameter width, 30–32 µm; length/width = 1; nm = 2, no = 2.

Remarks. *Loranthacites digitatus* Silva-Caminha et al., 2010, has columellae arranged longitudinally like striae; *L. macrosolenoides* Samoilovitch and Mtchedlishvili, 1961, is striate/reticulate.

Etymology. After the town of Tabatinga in Amazonas state, Brazil.

Botanical affinity. *Struthanthus* (Loranthaceae).

Retibrevitricolpites Van Hoeken-Klinkenberg, 1966

TYPE SPECIES. *RETIBREVITRICOLPITES TRIANGULATUS* VAN HOEKEN-KLINKENBERG, 1966

Retibrevitricolpites pseudoretibolus sp. nov.

PLATE 12A, B

Synonymy. *Retibrevitricolpites* sp. 1 Silva-Caminha et al., 2010.

Holotype. Plate 12a, sample 22140, EF W-13-2.

Paratype. Plate 12b, sample 22287, EF H-8-1/2.

Type locality. Well 1-AS-105-AM, Solimões Formation, Amazonas, Brazil.

Description. Monad, radial, isopolar, amb circular; tricolpate, colpi simple, very short, 4 µm long, CEi 0.18, borders straight, ends pointed, polar area large, 14 µm wide; semitectate, exine 1.82 µm thick, nexine 0.6 µm thick, columellae 0.6 µm thick, distinct, tectum 0.6 µm thick; reticulate, lumina 0.51 µm wide, circular, muri 0.51 µm wide, homobrochate. Nexine endocracks can be seen in different degrees of intensity.

Dimensions. Equatorial diameter length, 22–(25)–28 µm; equatorial diameter width, 22–(24.75)–27.5 µm; length/width = 1.01; nm = 2, no = 36.

Comparisons. *Retibrevitricolpites retibolus* Leidelmeyer, 1966, is tricolp(or)ate and has shorter colpi; *R. distinctus* Van Hoeken-Klinkenberg, 1966, is heterobrochate; *R. triangulatus* Van Hoeken-Klinkenberg ,1966, and *R. deltoides* Dueñas, 1986, have strong triangular amb.

Etymology. After its similarity with *R. retibolus*.

Rhoipites Wodehouse, 1933

TYPE SPECIES. *RHOIPITES BRADLEYI* WODEHOUSE, 1933

Rhoipites? colpiverrucosus sp. nov.

PLATE 12F, G

Holotype. Plate 12f, g, sample 22522, EF H-10-2.

Type locality. Well 1-AS-105-AM, Solimões Formation, Amazonas, Brazil.

Description. Monad, radial, isopolar, amb circular; tricolpate, colpi midsized, 28 µm long, CEi 0.7, borders straight, ends pointed, marginate, margo produced by slight decrease in columellae thickness towards colpi, 2 µm wide, 1 µm thick, marginate, margo formed by small and irregular verrucae distributed along colpi, 1–2 µm wide, polar 12 µm wide; semitectate, exine 1 µm thick, nexine 0.4 µm thick, columellae 0.2 µm thick, tectum 0.4 µm thick; stratification is not very clear, and the wall sometimes appears intectate; reticulate, lumina 0.5 µm, circular to slightly elongate, 0.5 µm wide, muri 0.5 µm wide, homobrochate.

Dimensions. Equatorial diameter length, 35–(37.5)–40 µm; equatorial diameter width, 31–(32)–33 µm; polar/equatorial diameter = 1.17; nm = 2, no = 3.

Comparisons. *Rhoipites* Wodehouse, 1933, accommodates tricolporate grains. We provisionally assign *R.*? *colpiverrucosus* to this genus as it does not contain pores. *Retitricolpites scabratus* Herngreen, 1975, has a colpus membrane and thicker exine (1.8–3 µm).

Etymology. After scabrae–verrucae lining colpi.

Tricolporate

Bombacacidites Couper, 1960

TYPE SPECIES. *BOMBACACIDITES BOMBAXOIDES* COUPER, 1960

Bombacacidites hooghiemstrae sp. nov.

PLATE 13A, B

Holotype. Plate 13a, b, sample 22522, EF S-41-4.

Type locality. Well 1-AS-105-AM, Solimões Formation, Amazonas, Brazil.

Description. Monad, radial, isopolar, amb triangular–obtuse–straight; tricolpate, planaperturate, colpi short, 18µm long, CEi 0.45, straight, ends pointed, costate, costae 1.5 µm wide, 2 µm thick, surrounding the entire colpi, having a horseshoe appearance and slightly protruding; polar area large, 16 µm wide; semitectate, exine 2 µm thick, nexine 0.7 µm thick, columellae 0.6 µm thick, distinct, 0.5 µm wide, 0.5 µm apart, tectum 0.7 µm thick; reticulate, lumina circular to slightly elongate, 0.5 µm wide, muri 0.5 µm wide, homobrochate.

Dimensions. Polar diameter length, 40 µm; polar diameter width, 33–(36.5)–40 µm; length/width = 1.09; nm = 2, no = 16.

Comparisons. *Bombacacidites soleaformis* Muller et al., 1987, is micropitted and has concave sides; *B. brevis* (Dueñas, 1980) Muller et al., 1987, is smaller, has a circular to triangular–convex amb and thinner wall, and lacks bulging costae.

Etymology. After Dutch palynologist Henry Hooghiemstra.

Botanical affinity. Malvaceae (Bombacoideae).

***Bombacacidites lorenteae* Hoorn, 1993 comb. nov.**

PLATE 13C

Basionym. *Retitricolpites lorenteae* Hoorn, 1993, p. 301, pl. 1, fig. 27.

Specimens. Plate 13c, sample 22140, EF P-11-3.

Description. Monad, radial, isopolar, amb triangular–obtuse–concave; tricolpate, planaperturate, colpi midsized, 18 µm long, CEi 0.39, borders straight, rounded pointed, costae thin, 1 µm wide, 1 µm thick; polar area 15 µm wide; semitectate, exine 2.1 µm thick, nexine 0.7 µm thick, columellae 0.7 µm thick, distinct, 0.7 µm apart, tectum 0.7 µm thick; reticulate, lumina circular to elongate, 1–0.5 µm wide, muri 1 µm wide, heterobrochate, lumina increases in size slightly (0.5 to 1 µm) toward apocolpia, simplicolumellate.

Dimensions. Polar diameter length, 46–(49)–52 µm; polar diameter width, 43–(46)–49 µm; length/width = 1.06; nm = 2, no = 9.

Comparisons. *Retitricolpites* Van der Hammen, 1956b, ex Pierce, 1961, is invalid and a later synonym of *Neea* (Jansonius and Hills, 1976, card 2401). *Bombacacidites* Couper, 1960, accommodates planaperturate pollen grains with a Bombacoideae pollen type.

Botanical affinity. *Bombax* (Malvaceae/Bombacoideae).

***Ladakhipollenites* Mathur & Jain, 1980**

TYPE SPECIES. *LADAKHIPOLLENITES LEVIS*
(SAH & DUTTA, 1966) MATHUR & JAIN, 1980

***Ladakhipollenites*? *pseudocolpiconstrictus* sp. nov.**

PLATE 14G–I

Holotype. Plate 14g, sample 22140, EF L-9.

Paratype. Plate 14h, i, sample 22518, EF N-6-3.

Type locality. Well 1-AS-105-AM, Solimões Formation, Amazonas, Brazil.

Description. Monad, radial, isopolar, prolate spheroidal; tricolporate, endo and ectocolpi coinciding, long, 19 µm long, CPi 0.79, strongly constricted at equator, ends rounded; colpi costate, costae thin, 1 µm wide, 1 µm thick, sometimes indistinct, pores lalongate, simple, 2 µm wide, 1 µm long, indistinct; polar area 8 µm wide; tectate, exine 1.6 µm thick, nexine 0.6 µm thick, columellae 0.4 µm long, sometimes indistinct, tectum 0.6 µm thick; psilate, sometimes wall structure cannot be seen, giving an atectate appearance.

Dimensions. Polar diameter, 24 µm; equatorial diameter, 21–(22.5)–24 µm; polar/equatorial = 1.06; nm = 2, no = 19.

Comparisons. *Psilatricolporites costatus* Dueñas, 1980, has much thicker costa; *P. vanus* González-Guzmán, 1967, is spherical, has nexine = sexine, and colpi are simple; *L. colpiconstrictus* (Van Hoeken-Klinkenberg, 1966) comb. nov. is colpate and has thicker exine with columellae tips clearly visible through tectum.

Etymology. After resemblance with *L. colpiconstrictus*.

Botanical affinity. *Cassia/Senna* (Fabaceae).

***Ladakhipollenites*? *corvattatus* sp. nov.**

PLATE 14J, K

Holotype. Plate 14j, k, sample 22278, EF H-11-3.

Type locality. Well 1-AS-105-AM, Solimões Formation, Amazonas, Brazil.

Description. Monad, radial, isopolar, prolate to spheroidal; tricolporate, ectocolpi midsized, 13 µm long, CPi 0.72, ends pointed, constricted at equator, costate, costae 1 µm wide, not extending until the end of colpi and gently fading away, giving the colpi the appearance of a bow tie; endopores very small and narrow, simple, lalongate, 2 µm wide, 0.5 µm long; polar area 7 µm wide; tectate, exine 1.5 µm thick, nexine 0.5 µm thick, columellae indistinct, 0.5 µm thick, tectum 0.5 µm thick; psilate.

Dimensions. Polar diameter, 18–(19)–20 µm; equatorial diameter, 16–(17)–18 µm; polar/equatorial = 1.11; nm = 2, no = 2.

Comparisons. *Psilatricolporites costatus* Dueñas, 1980, has much thicker costa and longer colpi; *P. cassioides* nov. sp. has continuous costae along entire colpi; *P. constrictus* Van Hoeken-Klinkenberg, 1966, is colpate and has thicker exine.

Etymology. After the word *corvatta* (tie), for the appearance of the costa endocolpi.

***Ladakhipollenites*? *endoporatus* sp. nov.**

PLATE 14L, M

Holotype. Plate 14l, m, sample 22522, EF P-13-1.

Type locality. Well 1-AS-105-AM, Solimões Formation, Amazonas, Brazil.

Description. Monad, radial, isopolar, prolate; tricolporate, ectocolpi long, 33 µm long, CPi 0.86, ends pointed, borders straight, costate, costae 2 µm wide, 1.5 µm thick near mesocolpia decreasing to 1 µm thick toward apocolpia, polar area small, 10 µm, endopores slightly lalongate, simple, 4 µm long, 5 µm wide; tectate, exine 1.8 µm thick, nexine 0.5 µm thick, columellae packed, indistinct, 0.8 µm thick, tectum 0.5 µm thick; psilate.

Dimensions. Polar diameter, 35–(36.5)–38 µm; equatorial diameter, 22–(23.5)–25 µm; polar/equatorial = 1.55; nm = 2, no = 11.

Comparisons. *Ladakhipollenites? caribbiensis* (Muller et al., 1987) Silva-Caminha et al., 2010, has simple colpi, much larger pores and thick, distinct columellae.

Psilatricolporites costatus Dueñas, 1980, has thicker costae and equatorial constriction; *P. atalayensis* Hoorn, 1993, has perforated exine, equatorial constriction and larger pore; *P. crassoexinatus* Hoorn, 1993, has thicker exine, with short columella and lalongate pores; *L.? magniporatus* (Hoorn, 1993) comb. nov. has much wider pores and thicker tectum.

Etymology. After distinct endopores.

Ladakhipollenites? *garzonii* Hoorn, 1993, comb. nov.

PLATE 14N–P

Basionym. *Psilatricolporites garzonii* Hoorn, 1993, p. 304, pl. 2, figs. 7, 8.

Specimens. Plate 14n, o, sample 22140, EF M-11-3/4.

Specimens. Plate 14p, sample 22140, EF U-12.

Description. Monad, radial, isopolar, oblate to spheroidal, amb triangular–obtuse–convex; tricolporate, endocolpi short, 10 µm long, CPi 0.71, CEi 0.71, costate, costae 1.5 µm wide, 1.5 µm thick, ectocolpi simple, very thin, borders slightly invaginated, ends pointed, polar area small, 7 µm, endopores lalongate, simple, 1 µm long, 2 µm wide; tectate, exine 1.5–2 µm thick, nexine 1 µm thick, columellae distinct, 0.5 µm thick, tectum 0.5 µm thick; psilate to very finely micropitted.

Dimensions. Polar view: equatorial diameter length, 14 µm; equatorial diameter width, 14 µm; length/width = 1; equatorial view: polar diameter, 14 µm; equatorial diameter, 15 µm; polar/equatorial = 0.93; nm = 2, no = 7.

Comparisons. *Psilatricolporites* Van der Hammen, 1956a, ex Pierce, 1961, is an obligate later synonym of *Tricolporites* Van der Hammen, 1954, because they have the same type species; as *Tricolpites* is not validly published and is a later synonym of *Clethra*, so is *Psilatricolporites* (Jansonius and Hills, 1976, card 2234). *Ladakhipollenites* Mathur and Jain, 1980, accommodates tricolpate psilate pollen grains. The grain is provisionally placed in *Ladakhipollenites* as it cannot be satisfactorily placed in any other genus.

Ladakhipollenites? *sphaericus* sp. nov.

PLATE 14S, T

Holotype. Plate 14s, t, sample 22140, EF X-7-1.

Type locality. Well 1-AS-105-AM, Solimões Formation, Amazonas, Brazil.

Description. Monad, radial, isopolar, spheroidal; tricolporate, endocolpi long, 14 µm long, CPi 0.73, slightly costate, costae 0.5 µm wide, 0.5 µm thick, ends pointed, polar area small, 5 µm, rounded, ectopores circular, simple, large in relation to total size, 5 µm long, 5 µm wide; tectate, exine about 1 µm, nexine 0.3 µm thick, columellae 0.3 µm thick, barely distinct, tectum 0.3 µm thick; psilate to micropitted.

Dimensions. Polar diameter, 16–(17.5)–19 µm; equatorial diameter, 16–(17.5)–9 µm; polar/equatorial = 1; nm = 2, no = 2.

Comparisons. *Psilatricolporites vanus* González-Guzmán, 1967, has midsized colpi and small pores; *P. atalayensis* Hoorn, 1993, has much thicker costa and lalongate pores; *P. crassoexinatus* Hoorn, 1993, has thicker exine and lalongate pores; and *P. magniporatus* Hoorn, 1993, has much thicker exine and is more prolate.

Etymology. After circular pores.

Margocolporites (Ramanujam, 1966, ex Srivastava, 1969) Pocknall & Mildenhall, 1984

TYPE SPECIES. *MARGOCOLPORITES TSUKADAI* (RAMANAJUAN, 1966) SRIVASTAVA, 1969

Margocolporites bilinearis sp. nov.

PLATE 15K–M

Holotype. Plate 15k–m, sample 22290, EF L-45-2.

Type locality. Well 1-AS-105-AM, Solimões Formation, Amazonas, Brazil.

Description. Monad, radial, isopolar, subprolate to prolate; tricolporate, ectocolpi long, 18 µm long, CPi 0.75, ends pointed, marginate, margo produced by fading of the sexine along colpi, margo 2 µm wide, endocolpi costate, costae 1–1.5 µm wide and 1 µm thick, thinning out toward apocolpia; endopores circular 3 µm long, 3 µm wide, simple; semitectate, exine 1.5 µm thick, nexine 0.5 µm thick, columellae 0.5 µm thick, distinct, tectum 0.5 µm thick; sculpture reticulate, lumina 0.5–1.5 µm wide, circular, muri 0.5 µm wide, homobrochate.

Dimensions. Polar diameter, 24–(25)–26 µm; equatorial diameter, 16–(19)–22 µm; polar/equatorial = 1.31; nm = 2, no = 5.

Comparisons. *Margocolporites vanwijhei* Germeraad et al., 1968, has much wider margo and is baculate near colpi. *Siltaria hammenii* Silva-Caminha et al., 2010, has indistinct columellae and is micropitted.

Etymology. After margo running along colpi, resembling two lines.

Margocolporites incertus sp. nov.

PLATE 15P, Q

Holotype. Plate 15p, q, sample 22434, EF N-52-4.

Type locality. Well 1-AS-105-AM, Solimões Formation, Amazonas, Brazil.

Description. Monad, radial, isopolar, circular; tricolporate, ectocolpi long, 20 µm long, CEi 0.83, ends rounded, marginate, margo produced by absence of the sexine around colpi, 2 μm wide, colpi characteristics not very clear; pores circular, 2 μm long, 2 μm wide, simple; tectate, exine 1.5 μm thick, nexine 0.5 μm thick, columellae 0.5 μm thick, barely distinct, very thin, tectum 0.5 μm thick; psilate.

DIMENSIONS. Polar diameter length, 24 μm; polar diameter width, 23 μm; length/width = 1; nm = 1, no = 3.

COMPARISONS. *Margocolporites vanwijhei* Germeraad et al., 1968, *M. bilinearis* sp. nov., and *Siltaria hammenii* Silva-Caminha et al., 2010, are reticulate and micropitted.

ETYMOLOGY. After uncertain colpi characteristics.

Paleosantalaceaepites Biswas, 1962, ex Dutta & Sah, 1970

TYPE SPECIES. *PALEOSANTALACEAEPITES DINOFLAGELLATUS* BISWAS, 1962, EX DUTTA & SAH, 1970

Paleosantalaceaepites kaarsii Hoorn, 1993, comb. nov.

PLATE 16F, G

BASIONYM. *Retitricolporites kaarsii* Hoorn, 1993, p. 305, pl. 1, figs. 11, 12.

SPECIMENS. Plate 16f, g, sample 22434, EF E-40.

DESCRIPTION. Monad, radial, isopolar, spheroidal; tricolporate, ectocolpi very short, 12 μm long, CPi 0.27, very thin, almost imperceptible, colpi ends pointed, polar area rounded and broad, 38 μm wide, marginate, margo produced by a decrease in lumina size around colpi; endopores anastomose forming an endocingulum, 2.5 μm wide, costate, costae 2 μm thick, 4 μm wide, thinning out toward apocolpia; semitectate, exine 3.5 μm thick, nexine 1.5 μm thick, columellae 1.5 μm thick, distinct, 1 μm wide, 1 μm apart, tectum 0.5 μm thick; reticulate, lumina circular to curvimurate, 1–5 μm wide, muri 1–1.5 μm wide, simplicolumellate, often smaller lumina ~1 μm wide present on the corners of large reticulae (5 μm wide).

DIMENSIONS. Polar diameter, 30–(36.5)–43 μm; equatorial diameter, 30–(36)–42 μm; polar/equatorial = 1.01; nm = 2, no = 11.

COMPARISONS. *Retitricolporites* (Van der Hammen, 1956b) Van der Hammen and Wymstra, 1964, is invalid and a later synonym of *Viburnum* (Jansonius and Hills, 1976, card 2402). *Paleosantalaceaepites* Biswas, 1962, ex Dutta and Sah, 1970, accommodates tricolporate pollen grains with long or short colpi and endocingulum. The original description of the holotype indicates a lumina variation from 0.5 μm to 2.5 μm, but we have observed grains with larger lumina.

BOTANICAL AFFINITY. *Dalechampia* (Euphorbiaceae).

Ranunculacidites Sah, 1967

TYPE SPECIES. *RANUNCULACIDITES COMMUNIS* SAH, 1967

Ranunculacidites pontoreticulatus sp. nov.

PLATE 16Q–S

HOLOTYPE. Plate 16q, r, sample 22518, EF L-16-1.

PARATYPE. Plate 16s, sample 22518, EF L-9-3.

TYPE LOCALITY. Well 1-AS-105-AM, Solimões Formation, Amazonas, Brazil.

DESCRIPTION. Monad, radial, isopolar, subprolate to prolate; tricolpate, ecto- and endocolpi coinciding, 17 μm long, CPi 0.56, simple; polar area, 7 μm, pontoperculate, pontoperculum as long as colpi, 4 μm wide; semitectate, exine 2 μm, nexine 1 μm, columellae 0.5 μm, distinct, 0.5 μm wide, 0.5 μm apart, tectum 0.5 μm; reticulate, lumina circular, elongate to slightly polygonal, 1 μm wide, muri 0.5 μm thick, homobrochate. Pontoperculum ornamentation does not differ from remainder of the grain. Pontoperculum often well preserved.

DIMENSIONS. Polar diameter, 29–(29.5)–30 μm; equatorial diameter, 26–(27)–28 μm; polar/equatorial = 1.09; nm = 2, no = 18.

COMPARISONS. *Ranunculacidites* Sah, 1967, accommodates small, tricolp(or)ate with variable exine ornamentation and operculum covering colpi entirely or partially. *Ranunculacidites operculatus* (Van der Hammen and Wymstra, 1964) Jaramillo and Dilcher, 2001, is psilate–micropitted. *Retitricolpites operculatus* Herngreen, 1973, is smaller and has a larger lumina in comparison to grain size and operculum is psilate.

ETYMOLOGY. After reticulate ornamentation and pontoperculum.

Retibrevitricolporites Legoux, 1978

TYPE SPECIES. *RETIBREVITRICOLPORITES OBODOENSIS* LEGOUX, 1978

Retibrevitricolporites solimoensis Hoorn, 1993, comb. nov.

PLATE 17C–F

BASIONYM. *Retitricolporites solimoensis* Hoorn, 1993, p. 305, pl. 2, fig. 12.

SPECIMENS. Plate 17c, d, sample 22140, EF H-25.

SPECIMENS. Plate 17e, f, sample 22140, EF D-10-1/3.

DESCRIPTION. Monad, radial, isopolar, spheroidal, amb circular; tricolporate, ectocolpi very short, 4 μm long, CEi 0.28, simple, borders straight, colpi ends rounded, polar area broad, 11 μm wide; endopores lalongate, 1.5 μm long, 3 μm wide, costate, costae 1 μm wide, restricted to the bottom and top of endocolpi; semitectate, exine about 1 μm thick, nexine 0.3 μm thick, columellae 0.3 μm thick, distinct, tectum 0.3 μm thick, reticulate, lumina circular, <0.5 μm wide, muri <0.5 μm wide, homobrochate.

DIMENSIONS. Equatorial diameter length, 14–(14.6)–15 μm; equatorial diameter width, 14–(14.6)–15 μm; length/width = 1; nm = 3, no = 5.

Comparisons. *Retitricolporites* (Van der Hammen, 1956b) Van der Hammen and Wymstra, 1964, is invalid and is a later synonym of *Viburnum* (Jansonius and Hills 1976, card 2402). *Retibrevitricolporites* Legoux, 1978, accommodates retibrevitricolporate pollen grains.

Retitrescolpites Sah, 1967

TYPE SPECIES. *RETITRESCOLPITES TYPICUS* SAH, 1967

Retitrescolpites benjaminensis sp. nov.

PLATE 17I–L

Holotype. Plate 17i, j, sample 22506, EF H-14.

Paratype. Plate 17k, l, sample 22522, EF G-12-4.

Type locality. Well 1-AS-105-AM, Solimões Formation, Amazonas, Brazil.

Description. Monad, radial, isopolar, oblate–spheroidal amb; tricolporate, colpi 16 µm long, CPi 0.55, CEi 0.87, ectocolpi simple, borders straight, ends rounded, polar area 8 µm wide; endopores costate, costae 2 µm wide, 2 µm thick, slightly lolongate, 3 µm long, 2 µm wide; semitectate, exine 3 µm thick, nexine <1 µm thick, columellae 2 µm thick, distinct, 0.5 µm wide, 0.5 µm apart, increasing in thickness at apocolpia to 4 µm thick, tectum very thin, 0.5 µm thick, almost not visible, giving the wall a retipilate appearance on cross section; reticulate, lumina 0.5 µm, elongate to curvimurate, muri 0.5 µm wide, simplicolumellate, homobrochate.

Dimensions. Equatorial view: polar diameter, 29 µm; equatorial diameter, 29 µm; polar/equatorial = 1; polar view: polar diameter length, 32 µm; polar diameter width, 32 µm; length/width = 1; nm = 2, no = 44.

Comparisons. *Retitrescolpites* Sah, 1967, accommodates retitricolp(or)ate with coarse retipilate or reticulate exine. Its type species, *R. typicus* Sah, 1967, is curvimurate; *R. baculatus* Jaramillo and Dilcher, 2001, is much larger and thicker and tricolpate; *R.? irregularis* (Van der Hammen and Wymstra, 1964) Jaramillo and Dilcher, 2001, *R. magnus* (González-Guzmán, 1967) Jaramillo and Dilcher, 2001, *R. peculiaris,* and *R. saturum* Jaramillo and Dilcher, 2001, have much coarser reticulum; *R. definidus* Jaramillo et al., 2007, has a well-defined costa around the colpi.

Etymology. After the town Benjamin Constant in Amazonas state, Brazil.

Retitrescolpites brevicolpatus sp. nov.

PLATE 17M

Holotype. Plate 17m, sample 22506, EF R-5-2.

Type locality. Well 1-AS-105-AM, Solimões Formation, Amazonas, Brazil.

Description. Monad, radial, isopolar, circular amb; tricolpate, ecto- and endocolpi coinciding, colpi 14 µm long, CEi 0.4, short, borders straight, ends pointed, polar area 20µm wide, costate, costae 2 µm wide, 2 µm thick; semitectate, exine 2.5 µm thick, nexine 0.5 µm thick, columellae distinct, 1.5 µm thick, 1 µm wide, 1 µm apart, tectum very thin, 0.5 µm thick, almost not visible, giving the wall a retipilate appearance on cross section; reticulate, lumina 3–4 µm wide, curvimurate to irregular, muri 1 µm wide, simplicolumellate, homobrochate.

Dimensions. Polar diameter length, 35–(37.3)–41 µm; polar diameter width, 27–(30)–33 µm; length/width = 1.24; nm = 3, no = 13.

Comparisons. *R. typicus* Sah, 1967, is curvimurate; *R.? irregularis* (Van der Hammen and Wymstra, 1964) Jaramillo and Dilcher, 2001, is colporate, and nexine is thicker than the sexine; *R. magnus* (González-Guzmán, 1967) Jaramillo and Dilcher, 2001, and *R. saturum* Jaramillo and Dilcher, 2001, are longicolpate.

Etymology. After the short colpi.

Retitrescolpites grossus sp. nov.

PLATE 17N, O

Holotype. Plate 17n, o, sample 22503, EF U-8-1.

Type locality. Well 1-AS-105-AM, Solimões Formation, Amazonas, Brazil.

Description. Monad, radial, isopolar, subspheroidal, circular amb; tricolporate, ecto- and endocolpi coinciding, 30 µm long, CPi 0.83, borders invaginated, ends pointed, marginate, margo 2 µm wide, produced by a decrease in columellae thickness and lumina size towards colpi, costate, costae 2 µm wide, thinning out toward apocolpia; polar area small; endopores lolongate, 6 µm long, 3 µm wide, costate, costae 1.5 µm wide, 1 µm thick; semitectate, exine 2.5 µm thick, nexine 1 µm thick, columellae 0.5 µm thick, distinct, 1 µm wide, 1 µm apart, tectum 1 µm thick; reticulate, lumina 1.5–3 µm, elongate to curvimurate, muri 1 µm wide, simplicolumellate, homobrochate.

Dimensions. Equatorial view: polar diameter, 36 µm; equatorial diameter, 35 µm; polar/equatorial = 1.02; polar view: polar diameter length, 25–(32)–39 µm; polar diameter width, 24–(31)–38 µm; length/width = 1.03; nm = 3, no = 32.

Comparisons. *Retitrescolpites baculatus* Jaramillo and Dilcher, 2001, is colpate and larger; *R.? irregularis* (Van der Hammen and Wymstra, 1964) Jaramillo and Dilcher, 2001, has wider lumina and costate colpi; *R. magnus* (González-Guzmán, 1967) Jaramillo and Dilcher, 2001, and *R. saturum* (González-Guzmán, 1967) Jaramillo and Dilcher, 2001, are colpate.

Etymology. After its thick wall.

Retitrescolpites kriptoporus sp. nov.

PLATE 17P–R

Holotype. Plate 17p–r, sample 22445, EF Q9/3.

Type locality. Well 1-AS-105-AM, Solimões Formation, Amazonas, Brazil.

Description. Monad, radial, isopolar, subprolate; tricolpate, ectocolpi simple, 30 μm long, CPi 0.8, reaching poles, polar area very small; endopores circular, 2 μm wide, simple; exine 2.5-3 μm thick, nexine ~0.8 μm thick, columellae distinct, 1.2 μm thick, 1.5 μm wide, 1 μm apart, tectum 0.5 μm thick; reticulate, lumina 2–4 μm wide, curvimurate to polygonal, muri 1 μm wide, simplicolumellate, homobrochate.

Dimensions. Polar diameter, 37 μm; equatorial diameter, 30 μm; length/width = 1.23; nm = 1, no = 1.

Comparisons. *Retitrescolpites*? *irregularis* (Van der Hammen and Wymstra, 1964) Jaramillo and Dilcher, 2001, has nexine thicker than the sexine; *R. magnus* (González-Guzmán, 1967) Jaramillo and Dilcher, 2001, has thin muri and is colpate.

Etymology. After internal and simple pores.

Retitrescolpites marginatus **sp. nov.**

PLATE 17S–U

Holotype. Plate 17s–u, sample 22518, EF N-25-2.

Type locality. Well 1-AS-105-AM, Solimões Formation, Amazonas, Brazil.

Description. Monad, radial, isopolar, subprolate; tricolporate, colpi 22 μm long, CPi 0.70, ectocolpi marginate and costate, thin, borders straight, ends rounded, polar area small, 16 μm wide, margo 2 μm wide, produced by a decrease in lumina size near colpi, costae 2 μm wide, 1 μm thick, interrupted around pores; endopores lalongate, 2 μm long, 5 μm wide; tectate, exine 2 μm thick, nexine 1 μm thick, columellae 0.5 μm thick, distinct, tectum 0.5 μm thick, hardly visible; suprareticulate, lumina 2–5 μm, highly curvimurate, muri 1 μm wide and 0.5 μm tall, heterobrochate; reticulum is created by a septum on top of tectum, meaning muri is not sustained by columellae but solid.

Dimensions. Polar diameter, 31 μm; equatorial diameter, 27 μm; polar/equatorial = 1.14; nm = 1, no = 5.

Comparisons. The combination of suprareticulum with curvimuri has not been described. *Rhoipites guianensis* (Van der Hammen and Wymstra, 1964) Jaramillo and Dilcher, 2001, has elongated reticulum with different shape.

Etymology. After margin of colpi.

Rhoipites **Wodehouse, 1933**

TYPE SPECIES *RHOIPITES BRADLEYI* WODEHOUSE, 1933

Rhoipites caputoi **Hoorn, 1993, comb. nov.**

PLATE 18C, D

Basionym. *Retitricolporites caputoi* Hoorn, 1993, p. 305, pl. 3, figs. 1, 2.

Specimens. Plate 18c, d, sample 22412, EF P-12-4.

Description. Monad, radial, isopolar, prolate; tricolporate, ectocolpi midsized, 21 μm long, CPi 0.66, borders straight, ends rounded, polar area medium, 13 μm wide, costate, costae 1 μm thick, 2 μm wide; endopores slightly lalongate, 4 μm long, 5 μm wide, simple; semitectate, exine 2 μm thick, nexine 0.6 μm thick, columellae 0.8 μm thick, distinct and packed, tectum 0.6 μm thick; reticulate, lumina circular to slightly elongate, 1 μm wide, muri 1 μm wide; heterobrochate, lumina decrease slightly toward mesocolpium.

Dimensions. Polar diameter, 29–(30.8)–32 μm; equatorial diameter, 18–(20.3)–22 μm; polar/equatorial = 1.51; nm = 3, no = 44.

Comparisons. *Retitricolporites* (Van der Hammen, 1956b) Van der Hammen and Wymstra, 1964, is invalid and a later synonym of *Viburnum* (Jansonius and Hills 1976, card 2402). *Rhoipites* Wodehouse, 1933, accommodates tricolporate pollen grains that are reticulate–pitted, prolate, with marginate/costate colpi (Jansonius and Hills, 1976, card 2421; Pocknall and Crosbie, 1982; Frederiksen, 1983).

Botanical affinity. Araliaceae.

Rhoipites vilis **sp. nov.**

PLATE 18E–H

Holotype. Plate 18e, f, sample 22164, EF P-7.

Paratype. Plate 18g, h, sample 22272, EF S-39.

Type locality. Well 1-AS-105-AM, Solimões Formation, Amazonas, Brazil.

Description. Monad, radial, isopolar, prolate spheroidal, amb circular; tricolporate, ectocolpi long, 14 μm long, CEi 0.77, CPi 0.68, marginate, margo 2 μm wide, 1 μm thick, produced by thinning of columellae thickness toward colpi, borders slightly invaginated, colpi ends rounded, polar area small, 3 μm wide, costate, costae 1 μm thick, 1 μm wide; endopores circular to slightly lalongate, 2 μm long, 2.5 μm wide, slightly costate, costae 0.5 μm thick, 0.5 μm wide; semitectate, exine 2.1 μm thick, nexine 0.7 μm thick, columellae 0.7 μm thick, distinct, tectum 0.7 μm thick; reticulate, lumina circular to elongate, 0.5–1 μm wide, muri 0.5–1 μm wide, homobrochate.

Dimensions. Equatorial view: polar diameter, 16–(17.5)–19 μm; equatorial diameter, 15–(15.5)–16 μm; polar/equatorial = 1.12; polar view: equatorial diameter length, 18 μm; equatorial diameter width, 16 μm; length/width = 1.12; nm = 3, no = 9.

Comparisons. *Retitricolporites milnei* Hoorn, 1993, has shorter colpi, lalongate pores, and smaller reticulum. *Siltaria dilcheri* Silva-Caminha et al., 2010, is micropitted and has pores with well-developed costae, slightly protruding. *Rhoipites crassicostatus* Van der Hammen and Wymstra, 1964, comb. nov. is heterobrochate.

Etymology. After the very common tricolporate morphology, from *vilis* (cheap, inexpensive).

Rhoipites crassicostatus Van der Hammen and Wymstra, 1964, comb. nov.

PLATE 18I, J

Basionym. *Retitricolporites crassicostatus* Van der Hammen and Wymstra, 1964, p. 236.

Specimens. Plate 18i, j, sample 22140, EF T-17/3.

Description. Monad, radial, isopolar, prolate spheroidal; tricolporate, ectocolpi midsized, 11 µm, CPi 0.68, simple, borders straight, ends pointed, polar area 7 µm wide, costate, costae 2 µm wide, 1 µm thick, nexine surrounding costae thinner, creating a sharp contour of costae; endopores lalongate, 1.5 µm long, 3 µm wide, simple; semitectate, exine 1.5 µm thick, nexine 0.5 µm thick, columellae 0.5 µm thick, distinct, tectum 0.5 µm thick; foveoreticulate, lumina circular, <0.5 µm wide, muri 1–1.5 µm wide, reticulate at apocolpia, foveolate at mesocolpia, heterobrochate.

Dimensions. Polar diameter, 16 µm; equatorial diameter, 14 µm; polar/equatorial = 1.14; nm = 1, no = 2.

Comparison. *Retitricolporites* (Van der Hammen, 1956b) Van der Hammen and Wymstra, 1964, is invalid and is a later synonym of *Viburnum* (Jansonius and Hills, 1976, card 2402).

Rhoipites crassinexinicus sp. nov.

PLATE 18K–N

Holotype. Plate 18k–m, sample 22158, EF P-46-4.

Paratype. Plate 18n, sample 22158, EF N-38-3/4.

Type locality. Well 1-AS-105-AM, Solimões Formation, Amazonas, Brazil.

Description. Monad, radial, isopolar, prolate spheroidal; tricolporate, ectocolpi 18 µm long, CPi 0.81, borders straight, ends rounded, polar area small, 8 µm wide, costate, costae 2 µm wide, 1.5 µm thick, thinning out gradually toward apocolpia, absent surrounding the endopore at mesocolpia; endopores lalongate, simple, 1.5 µm long, 4 µm wide; semitectate, exine 1.5 µm thick at apocolpia and 3 µm thick at mesocolpia, nexine 1 µm thick at apocolpia and 2 µm thick at mesocolpia, columellae 0.3–0.5 µm thick, distinct, tectum 0.3–0.5 µm thick; reticulate, lumina circular to elongate, 0.5 µm wide, muri 0.5 µm wide; homobrochate.

Dimensions. Polar diameter, 22–(23)–24 µm; equatorial diameter, 20 µm; polar/equatorial = 1.15; nm = 2, no = 2.

Comparison. *Foveotricolpites colpiconstrictus* Hoorn, 1994b, comb. nov. is tricolpate, and exine is thicker at apocolpia.

Etymology. After thick nexine.

Rhoipites crassitectatus sp. nov.

PLATE 18O, P

Holotype. Plate 18o, p, sample 22290, EF M-17.

Type locality. Well 1-AS-105-AM, Solimões Formation, Amazonas, Brazil.

Description. Monad, radial, isopolar, subprolate; tricolporate, ectocolpi 25 µm long, CPi 0.86, borders straight, ends rounded, polar area small, 4 µm wide, costate, costae 2 µm wide, 1.5 µm thick; endopores circular, 4 µm long, 4 µm wide, simple; tectate, exine ~3 µm thick, nexine 0.7 µm thick, columellae 0.7 µm thick, distinct, ~0.5 µm apart, tectum 1.5 µm thick; micropitted, lumina circular, <0.5 µm wide, muri 0.5 µm wide, homobrochate.

Dimensions. Polar diameter, 29 µm; equatorial diameter, 24 µm; polar/equatorial = 1.2; nm = 1, no = 1.

Comparisons. *Retitricolporites crassopolaris* Hoorn, 1994b, has thicker exine at apocolpia; *R. poriconspectus* Hoorn, 1994b, has indistinct columellae and broader apocolpia. *Foveotricolporites crassiexinus* Van Hoeken-Klinkenberg, 1966, is foveolate and has wider lumina.

Etymology. After thick tectum.

Rhoipites grossomurus sp. nov.

PLATE 18Q–T

Holotype. Plate 18q–s, sample 22422, EF Q-21-2.

Paratype. Plate 18t, sample 22386, EF L-43-2.

Type locality. Well 1-AS-105-AM, Solimões Formation, Amazonas, Brazil.

Description. Monad, radial, isopolar, prolate spheroidal to spheroidal; tricolporate, ectocolpi midsized, 15 µm long; CPi 0.5, simple, sometimes not visible; borders straight, ends rounded; polar area large, 10 µm wide; endopores lalongate, 2 µm long, 9 µm wide, costate, costae restricted to bottom and top of pores, 3 µm wide, 2 µm wide thick; semitectate, exine 2.5 µm thick, nexine 1 µm, columellae 1 µm thick, distinct, very thin, and regularly distributed, tectum 0.5 µm thick, slightly cristate, coarse reticulation, lumina large, circular, 2–3 µm wide, muri thick, 1.5 µm wide, homobrochate, smaller lumina (1 µm wide) appear within the muri, usually at lumen corners, pluricolumellate, lumina surface psilate.

Dimensions. Polar diameter, 30–(36)–42 µm; equatorial diameter, 30–(33.5)–37 µm; polar/equatorial = 1–1.07; nm = 2, no = 5.

Comparisons. This grain bears resemblance to *Retibrevitricolporites*? *toigoae* Leite et al., 2021, but has thicker exine and reticulation. *Retitricolporites wijmstrae* Hoorn, 1994b, has long costate colpi, and the wall structure is different.

Etymology. After thick muri.

Rhoipites guttatus sp. nov.

PLATE 18W, X

Holotype. Plate 18w, x, sample 22277, EF H-39-1.

Type locality. Well 1-AS-105-AM, Solimões Formation, Amazonas, Brazil.

Description. Monad, radial, isopolar, spheroidal; tricolporate, ectocolpi midsized, 12 µm long, CPi 0.54, borders straight, ends rounded, polar area broad, 10 µm wide, simple; endopores large, lalongate, 6 x 3.5 µm wide, costate, costae 1.5 µm wide, 2.5 µm thick, turned inward, restricted to the bottom and top side of pore; semitectate, exine 1.6 µm thick, nexine 1 µm, columellae 0.3 µm thick, distinct, well spaced, tectum 0.3 µm thick; reticulate, lumina circular to elongate, 1–2 µm wide, muri <1 µm wide, homobrochate.

Dimensions. Polar diameter, 22–(24)–26 µm; equatorial diameter, 22–(24)–26 µm; polar/equatorial = 1; nm = 2, no = 2.

Comparisons. *Rhoipites oblatus* Hoorn, 1994b, comb. nov. is micropitted and has narrow pores. *Retibrevitricolporites solimoensis* Hoorn, 1993, comb. nov. is much smaller.

Etymology. From the word *gutta* (drop), after the costa shape in lateral view.

***Rhoipites apertus* sp. nov.**

PLATE 19A, B

Holotype. Plate 19a, b, sample 22506, EF N14/1-2.

Type locality. Well 1-AS-105-AM, Solimões Formation, Amazonas, Brazil.

Description. Monad, radial, isopolar, subprolate, small; tricolporate, ectocolpi midsized, 11 µm long, CPi 0.61, borders rounded, ends pointed, polar area 10 µm wide, costate, costae <0.5 µm wide, 0.5–1 µm thick; endopores lenslike, lalongate, 2 µm long, 6 µm wide, slightly costate, costae very thin, <0.5 µm thick, 1 µm wide, absent at equatorial ending of the pore; semitectate, exine ~1.5 µm thick, nexine 1 µm, columellae 0.7 µm thick, thin, indistinct, tectum 0.7 µm thick; psilate to finely reticulate, lumina circular, <0.5 µm wide, homobrochate.

Dimensions. Polar diameter, 18–(18.5)–19 µm; equatorial diameter, 16 µm; polar/equatorial = 1.15; nm = 2, no = 4.

Comparisons. *Ladakhipollenites*? *porolenticularis* D'Apolito et al., 2019, is psilate and atectate. *Foveotricolporites lenticuloides* Silva-Caminha et al., 2010, is foveolate and larger. *Retiricolporites milnei* Hoorn, 1993, has slit-like pores.

Etymology. From word *apertus* (open), after costa being open in extremities.

***Rhoipites oblatus* Hoorn, 1994b, comb. nov.**

PLATE 19C, D

Basionym. *Retitricolporites oblatus* Hoorn, 1994b, p. 39, pl. 3, figs. 11, 12.

Specimens. Plate 19c, d, sample 22290, EF S-45.

Description. Monad, radial, isopolar, oblate to oblate spheroidal; tricolporate, ectocolpi midsized, 12 µm long, CPi 0.63, borders slightly invaginated, ends pointed, polar area broad, 6 µm wide, costate, costae 0.5–2 µm wide, 1–2.5 µm thick, much thicker around equator, turned inward and gradually thinning out toward apocolpia, almost conical shaped and partially extending around pores; endopores lalongate, 2 µm long, 4.5 µm wide, simple; semitectate, exine 1.5 µm thick, nexine 0.6 µm thick, columellae 0.3 µm thick, distinct, tectum 0.6 µm thick; reticulate, lumina circular, 0.5 µm wide, muri 0.5 µm wide, homobrochate.

Dimensions. Polar diameter, 18–(19.5)–21.5 µm; equatorial diameter, 16–(17.5)–18.5 µm; polar/equatorial = 1.11; nm = 3, no = 17.

Comparison. *Retitricolporites* (Van der Hammen, 1956b) Van der Hammen and Wymstra, 1964, is invalid and is a later synonym of *Viburnum* (Jansonius and Hills, 1976, card 2402).

***Rhoipites pseudoscabratus* sp. nov.**

PLATE 19E, F

Holotype. Plate 19e, f, sample 22518, EF G9.

Type locality. Well 1-AS-105-AM, Solimões Formation, Amazonas, Brazil.

Description. Monad, radial, isopolar, prolate, medium sized; tricolporate, ectocolpi long, 32 µm long, CPi 0.8, ends rounded, polar area small, 9 µm wide, costate, costae 2 µm wide, 1.5 µm thick, fading towards poles; pores slightly lolongate, simple, 4.5 µm long, 3.5 µm wide; semitectate, exine 2 µm thick, nexine 0.5 µm, columellae 0.5 µm thick, distinct, thin, tectum 1 µm thick; reticulate, lumina circular, 1 µm wide, muri 1 µm wide, homobrochate, muri scabrate.

Dimensions. Polar diameter, 36 µm; equatorial diameter, 24 µm; polar/equatorial = 1.5; nm = 1, no = 3.

Comparisons. *Foveotricolporites rugulatus* Jaramillo and Dilcher, 2001, has thick tectum and rugulate/fussulate ornamentation. *Foveotricolporites* sp. 3 Jaramillo and Dilcher, 2001, is foveolate and micropitted. *Rhoipites guianensis* (Van der Hammen and Wymstra, 1964) Jaramillo and Dilcher, 2001, has wider reticulum arranged in a loose mesh and is heterobrochate.

Etymology. After scabrate muri.

***Rhoipites lolongatus* sp. nov.**

PLATE 19G, H

Holotype. Plate 19g, h, sample 22386, EF T-10-2.

Type locality. Well 1-AS-105-AM, Solimões Formation, Amazonas, Brazil.

Description. Monad, radial, isopolar, prolate; tricolporate, ectocolpi long, 32 µm long, CPi 0.76, borders straight, ends rounded, polar area small, 4 µm wide, costate, costae 1 µm wide, 1 µm thick; endopores discrete, lolongate, simple, 4 µm long, 3 µm wide, part of costae runs through pores, giving the impression that pores are split in two; semitectate, exine 2 µm thick, nexine 1 µm, columellae 0.7 µm thick, distinct, tectum

0.3 µm thick; reticulate, lumina circular to polygonal, 1 µm wide, muri 1 µm wide, homobrochate.

Dimensions. Polar diameter, 42 µm; equatorial diameter, 30 µm; polar/equatorial = 1.4; nm = 1, no = 1.

Comparison. *Retitricolporites wijmstrae* Hoorn, 1994b, has large, lalongate pores and is thicker.

Etymology. After lolongate pores.

Rhoipites protoguttatus **sp. nov.**

PLATE 19I–K

Holotype. Plate 19i, sample 22518, EF M-17-3.

Paratype. Plate 19j-k, sample 22522, EF O-13-2.

Type locality. Well 1-AS-105-AM, Solimões Formation, Amazonas, Brazil.

Description. Monad, radial, isopolar, oblate spheroidal to prolate spheroidal, amb circular; tricolporate, ectocolpi midsized, 20 µm long, CPi 0.64, CEi 0.66, very thin, borders slightly invaginating, ends rounded, polar area broad, 13–15 µm wide, marginate, margo discrete, only seen in polar view, created by a thickening of columellae near colpi, 0.3 to 0.5 µm thick, 6 µm wide; endopores very large, lalongate, lens shaped with beak-like endings, 6 µm long, 10 µm wide, costate, costae restricted to bottom and top of pores, 1 µm wide and 2 µm thick, costa deflected inward; semitectate, exine 2 µm thick, nexine 1 µm, columellae 0.5 µm thick, distinct, tectum 0.5 µm thick; reticulate to micropitted, lumina circular, 0.5 µm wide, muri 0.5–1 µm wide, homobrochate.

Dimensions. Equatorial view: polar diameter, 31–(33)–35 µm; equatorial diameter, 32–(32.5)–33 µm; polar/equatorial = 1.01; polar view: equatorial diameter length, 36 µm; equatorial diameter width, 36 µm; length/width = 1; nm = 3, no = 6.

Comparisons. *Retitricolporites wijmstrae* Hoorn, 1994b, has long costate colpi and exine is thicker; *R. crassopolaris* Hoorn, 1994b has thicker wall at apocolpia; *R. guttatus* sp. nov. is smaller and has coarser reticulum.

Etymology. After resemblance to *R. guttatus* sp. nov.

Rhoipites pseudocrassopolaris **sp. nov.**

PLATE 19L, M

Holotype. Plate 19l, m, sample 22140, EF W-10-4.

Type locality. Well 1-AS-105-AM, Solimões Formation, Amazonas, Brazil.

Description. Monad, radial, isopolar, prolate; tricolporate, ectocolpi long, 17 µm long, CPi 0.7, borders straight, ends rounded, polar area small, 3 µm wide, costate, costae 1.5 µm wide, 1.5 µm thick, thinning out toward apocolpia; endopores lalongate, 2 µm long, 4 µm wide, simple, abruptly protruding; semitectate, exine 1.5 µm thick at mesocolpia and 2.5 µm thick at apocolpia, nexine 0.5 µm, columellae 0.5 µm thick at mesocolpia gradually thickening to 1.5 µm thick at apocolpia, distinct, <0.5 µm wide, tectum 0.5 µm thick; micropitted, lumina circular, 0.5 µm wide, muri 0.5–1 µm wide, homobrochate.

Dimensions. Polar diameter, 24 µm; equatorial diameter, 16 µm; polar/equatorial = 1.5; nm = 1, no = 1.

Comparison. *Retitricolporites crassopolaris* Hoorn, 1994b, lacks protruding pores; nexine thickens at apocolpia.

Etymology. After resemblance to *Retitricolporites crassopolaris* Hoorn, 1994b.

Rhoipites pseudopilatus **sp. nov.**

PLATE 19N, O

Holotype. Plate 19n, o, sample 22320, EF L-44-3/4.

Type locality. Well 1-AS-105-AM, Solimões Formation, Amazonas, Brazil.

Description. Monad, radial, isopolar, prolate; tricolporate, ectocolpi long, 16 µm long, CPi 0.69, borders invaginated, ends rounded, polar area small, 4 µm wide, costate, costae 2 µm wide, 2 µm thick; endopores large, lolongate, 9 µm long, 4 µm wide, simple; semitectate, exine 1 µm thick, nexine 0.3 µm, columellae 0.4 µm thick, distinct, 0.3 µm wide, 0.3 µm apart, tectum 0.3 µm thick, in cross section, wall appears to be pilate, but there is a tectum; reticulate, lumina circular, 0.5–1 µm wide, muri 0.5–1 µm wide, homobrochate.

Dimensions. Polar diameter, 21–(22)–23 µm; equatorial diameter, 16–(17)–18 µm; polar/equatorial = 1.29–1.43; nm = 2, no = 2.

Comparison. *Ladakhipollenites? lolongatus* D'Apolito et al., 2019, is psilate–micropitted with different wall structure.

Etymology. After false pilate appearance.

Rhoipites quantulus **sp. nov.**

PLATE 19P, Q

Holotype. Plate 19p, q, sample 22287, EF T-17-3.

Type locality. Well 1-AS-105-AM, Solimões Formation, Amazonas, Brazil.

Description. Monad, radial, isopolar, prolate, very small; tricolporate, ectocolpi long, 12 µm long, CPi 0.75, borders straight, ends pointed, polar area small, 2 µm wide, costate, costae 0.5–1 µm wide, 0.5–1 µm thick; endopores very large in relation to grain size, slightly lalongate, simple, 2.5 µm long, 3 µm wide; semitectate, exine 1 µm thick, nexine 0.4 µm, columellae 0.2 µm thick, indistinct, tectum 0.4 µm thick; reticulate, lumina circular to elongate, 1 µm wide, muri 1 µm wide, homobrochate.

Dimensions. Polar diameter, 16–(17)–18 µm; equatorial diameter, 10–(11)–12 µm; polar/equatorial = 1.54; nm = 2, no = 4.

Comparison. *Rhoipites minuticirculus* D'Apolito et al., 2019, has circular simple pores and a different polar–equatorial aspect ratio.

Etymology. After the small size, from the word *quantulus* (little).

Rhoipites ticuneorum Hoorn, 1993, comb. nov.

PLATE 19R, S

Basionym. *Retitricolporites ticuneorum* Hoorn, 1993, p. 306, pl. 2, figs. 17, 18.

Specimen. Plate 19r, s, sample 22140, EF L14/2.

Type locality. Well 1-AS-105-AM, Solimões Formation, Amazonas, Brazil.

Description. Monad, radial, isopolar, amb triangular, very small; tricolporate, ectocolpi long, 12 µm long, CEi 0.58, borders straight, ends rounded, polar area 6 µm wide, marginate, margo produced by decreasing exine thickness toward colpi, margo 1 µm wide; endopores indistinct; semitectate, exine ~2 µm thick, nexine 0.7 µm, columellae 0.7 µm thick, distinct, tectum 0.7 µm thick; reticulate, lumina circular, 1 µm wide, muri 1 µm wide, homobrochate.

Dimensions. Polar diameter length, 20.5 µm; equatorial diameter length, 18 µm; nm = 1, no = 1.

Comparisons. *Horniella* sp. 1 Jaramillo and Dilcher, 2001, is larger with larger reticulum. *Horniella* sp. 2 Jaramillo and Dilcher, 2001, has a more circular amb and distinct costate pores. *Retibrevitricolporites speciosus* Jaramillo and Dilcher, 2001, has wider lumina and is strongly heterobrochate.

Striatopollis Krutzsch, 1959

TYPE SPECIES. *STRIATOPOLLIS SARSTEDTENSIS* KRUTZSCH, 1959

Striatopollis crassitectatus sp. nov.

PLATE 20J–L

Holotype. Plate 20j, k, sample 22140, EF Q-7-3.

Paratype. Plate 20l, sample 22282, EF H-11-4.

Type locality. Well 1-AS-105-AM, Solimões Formation, Amazonas, Brazil.

Description. Monad, radial, isopolar, prolate; tricolporate, ectocolpi very long, 30 µm long, CPi 0.9, borders invaginated, ends open, polar area very small to absent, simple; endopores circular, 3–4 µm long, 3–4 µm wide, simple, indistinct; semitectate, exine ~2.5 µm thick, nexine 0.3 µm, columellae 0.3 µm thick, distinct, very short in relation to tectum, dense and regularly distributed, tectum 2 µm thick; striate, striae solid, running parallel to polar axis, 1.5 µm wide, 0.5 µm apart, interstriae surface psilate, some striae are shorter near the colpi and do not reach apocolpia.

Dimensions. Polar diameter, 29.5–(31.25)–33 µm; equatorial diameter, 17–(19)–21 µm; polar/equatorial = 1.64; nm = 2, no = 13.

Comparison. *Striatopollis catatumbus* (González-Guzmán, 1967) Takahashi and Jux, 1989, has a thinner tectum.

Etymology. After thick tectum.

Botanical affinity. *Macrolobium* (Fabaceae).

Syncolporites Van der Hammen, 1954

TYPE SPECIES. *SYNCOLPORITES LISAMAE* VAN DER HAMMEN, 1954

Syncolporites foveolatus sp. nov.

PLATE 20O, P

Holotype. Plate 20o, p, sample 22354, EF N-9.

Type locality. Well 1-AS-105-AM, Solimões Formation, Amazonas, Brazil.

Description. Monad, radial, isopolar, triangular–obtuse–straight amb; tricolporate, syncolpate, ectocolpi 24 µm long, CEi 0.5, borders rounded, apocolpial field absent, marginate, margo created by thinning of sexine near colpi, margo 4 µm wide; endopores large, 8 µm wide, simple; semitectate, exine 3 µm thick, nexine 1 µm, columellae 0.5 µm thick, distinct, packed, short in relation to tectum, tectum 1.5 µm thick; foveolate, distributed over entire surface, foveolae circular, 1 µm wide, >1–2 µm apart.

Dimensions. Polar diameter length, 24 µm; equatorial diameter width, 24 µm; nm = 1, no = 1.

Comparisons. *Syncolporites anibalii* Hoorn, 1993, is micropitted and has a smaller pore; *S. incomptus* Van Hoeken-Klinkenberg, 1964, *S. minutus* Van Hoeken-Klinkenberg, 1964, and *S. poricostatus* Van Hoeken-Klinkenberg, 1966, are psilate; *S. lisamae* Van der Hammen, 1954, is scabrate–psilate; *S. marginatus* Van Hoeken-Klinkenberg, 1964, is densely reticulate; *S. triangularis* Regali et al., 1974, is parasyncolporate. *Crassiectoapertites columbianus* Dueñas 1980 emend. Lorente, 1986, has ectoapertures with asymmetrical hemispheres.

Etymology. After foveolate ornamentation.

Botanical affinity. *Swartzia* (Fabaceae).

Syncolporites tenuicolpatus sp. nov.

PLATE 20Q–S

Holotype. Plate 20q, r, sample 22290, EF E11/4.

Paratype. Plate 20s, sample 22386, EF D23.

Type locality. Well 1-AS-105-AM, Solimões Formation, Amazonas, Brazil.

Description. Monad, radial, isopolar, amb triangular–acute–straight to slightly convex, syncolporate, ectocolpi 24 long, CEi 0.5, simple, very thin, almost indistinct, borders rounded, apocolpial field absent, simple; endopores atriate, pore canal 2 µm long, 3 µm wide; semitectate, exine ~2 µm thick, nexine 0.7 µm, columellae 0.7 µm thick, distinct, tectum 0.7 µm thick; reticulate, lumina circular, >1 µm wide, homobrochate.

Dimensions. Polar diameter length, 25–(26.5)–28 µm; equatorial diameter width, 28 µm; nm = 2, no = 2.

Comparisons. *Syncolporites anibalii* Hoorn, 1993, is micropitted and has well-defined colpi; *S. incomptus* Van Hoeken-Klinkenberg, 1964, *S. minutus* Van Hoeken-Klinkenberg, 1964, and *S. poricostatus* Van Hoeken-Klinkenberg, 1966, are psilate; *S. lisamae* Van der Hammen, 1954, is scabrate–psilate; *S. marginatus* Van Hoeken-Klinkenberg, 1964, is densely reticulate; *S. triangularis* Regali et al., 1974, is parasyncolporate.

Etymology. After almost indistinct (tenuous) colpi.

Botanical affinity. *Serjania* (Sapindaceae).

Tetracolporopollenites Pflug & Thomson in Thomson & Pflug, 1953

TYPE SPECIES. *TETRACOLPOROPOLLENITES SAPOTOIDES*
PFLUG & THOMSON IN THOMSON AND PFLUG, 1953

Tetracolporopollenites labiatus Hoorn, 1993, comb. nov.

PLATE 21A

Basionym. *Psilatricolporites labiatus* Hoorn, 1993, p. 304, pl. 2, fig. 14.

Specimens. Plate 21a, sample 22140, EF L-16-4.

Description. Monad, radial, isopolar, prolate; tricolporate, endo- and ectocolpi coinciding, short, 12 µm long, CPi 0.44, very thin, almost indistinct, borders straight, ends pointed, simple, polar area broad, 12 µm, endopores lalongate, 2.5 µm long, 5 µm wide, costate, costae 5 µm wide, restricted to area on top and bottom of pores, pores areas protruding; atectate, exine 1 µm thick; psilate.

Dimensions. Polar diameter, 27 µm; equatorial diameter, 20 µm; polar/equatorial = 1.35; nm = 1, no = 1.

Comparisons. *Psilatricolporites* Van der Hammen, 1956b, ex Pierce, 1961, is an obligate later synonym of *Tricolporites* Van der Hammen, 1954, because they have the same type species; as *Tricolpites* is not validly published and is a later synonym of *Clethra*, so is *Psilatricolporites* (Jansonius and Hills, 1976, card 2234). *Tetracolporopollenites* Pflug and Thomson in Thomson and Pflug, 1953, accommodates tri- and tetracolporate grains with an ovoid egg shape and flattened poles.

Botanical affinity. *Chrysophyllum*/*Micropholis*/*Pouteria* (Sapotaceae).

Tetracolporopollenites magniporatus Hoorn, 1993, comb. nov.

PLATE 21B, C

Basionym. *Psilatricolporites magniporatus* Hoorn, 1993, p. 304, pl. 2, fig. 24.

Specimen. Plate 21b, c, sample 22336, EF E-43-4.

Description. Monad, radial, isopolar, prolate; tricolporate, endo- and ectocolpi coinciding, colpi long, 31 µm long, CPi 0.88, borders straight, simple, polar area 10 µm wide, rounded; endopores costate, large, 8 µm long, forming almost a continuous equatorial band, costate, costae 2 µm wide, 2 µm thick, developed at the intersection of endopore and ectocolpi; tectate, thick exine, exine 2 µm thick, nexine 1 µm thick, columellae distinct, 0.5 µm thick, tectum 0.5 µm thick; psilate to reticulate, homobrochate.

Dimensions. Polar diameter, 35 µm; equatorial diameter, 20–(22)–24 µm; polar/equatorial = 1.59; nm = 2, no = 2.

Tetracolporopollenites nanus sp. nov.

PLATE 21D

Holotype. Plate 21d, sample 22320, EF D-48.

Type locality. Well 1-AS-105-AM, Solimões Formation, Amazonas, Brazil.

Description. Monad, radial, isopolar, subprolate to prolate; tricolporate, ectocolpi 8 µm long, CPi 0.61, borders straight, ends pointed, slightly costate, costae 0.5 µm wide, polar area small, 6 µm wide; endopores circular, simple, rather large in proportion to total grain size, 1–2 µm wide, 1–2 µm long; atectate, exine 0.7 µm thick; psilate.

Dimensions. Polar diameter, 12–(12.5)–13 µm; equatorial diameter, 9–(9.5)–10 µm; polar/equatorial = 1.31; nm = 2, no = 19.

Comparison. *Psilatricolporites vanus* González-Guzmán, 1967, is larger (19–29 µm) and has much smaller pores in proportion to the grain size.

Etymology. After its diminutive size.

Tetracolporopollenites obesus Hoorn, 1993, comb. nov.

PLATE 21E, F

Basionym. *Psilatricolporites obesus* Hoorn, 1993, p. 304, pl. 2, fig. 20.

Specimen. Plate 21e, f, sample 22140, EF V-22-2.

Description. Monad, radial, isopolar, prolate spheroidal; tricolporate, ectocolpi short, 8 µm long, CPi 0.47, very thin and almost not visible, borders straight, simple, ends pointed, polar area large, 9 µm; endopores almost joining in an equatorial band as an endocingulum, lalongate, 6 µm long, costate, costae 1 µm wide, 1 µm thick; tectate, exine ~1 µm thick, nexine 0.3 µm thick, columellae indistinct, 0.3 µm thick, tectum 0.3 µm thick; psilate.

Dimensions. Polar diameter, 17 µm; equatorial diameter, 16 µm; polar/equatorial = 1.06; nm = 2, no = 3.

Botanical affinity. Sapotaceae.

Tetracolporopollenites silvaticus Hoorn, 1993, comb. nov.

PLATE 21G–J

Basionym. *Psilatricolporites silvaticus* Hoorn, 1993, p. 304, pl. 2, fig. 21.

Specimens. Plate 21g, h, sample 22320, EF R13.

Specimens. Plate 21i, j, sample 22170, EF R33-1.

Description. Monad, radial, isopolar, subprolate to prolate spheroidal, pore area slightly protruding; tricolporate, ectocolpi short, 6–8 μm long, CPi 0.5, sometimes costate, costa 1 μm thick, polar area broad, 8 μm, endopores lalongate, narrow, 5 μm wide, 2 μm long, sometimes costate, costae 1 μm wide, encircling and darkening the entire mesocolpia, tapering poleward; tectate, exine ~1 μm thick, nexine 0.3 μm thick, columellae 0.3 μm thick, sometimes indistinct, tectum 0.3 μm thick; psilate to slightly micropitted.

Dimensions. Polar diameter, 15–(17.7)–22 μm; equatorial diameter, 14–(15.7)–19 μm; polar/equatorial = 1.12; nm = 4, no = 23.

Botanical affinity. *Protium* (Burseraceae)/Sapotaceae.

Tetracolporopollenites xatanawensis sp. nov.

PLATE 21K–N

Holotype. Plate 21k–m, sample 22140, EF W-35-1.

Paratype. Plate 21n, sample 22256, EF O-40-3/4.

Type locality. Well 1-AS-105-AM, Solimões Formation, Amazonas, Brazil.

Description. Monad, radial, isopolar, prolate, almost flat apocolpia; tricolporate, ectocolpi midsized, 25 μm long, CPi 0.67, ends rounded, costate, costae 1 μm wide, 1 μm thick, narrowing toward apocolpia, polar area large, 14 μm, endopores lalongate, oval to lens shaped, simple, 3–4 μm long by 5–8 μm wide; tectate, exine 1.5 μm, nexine 0.5 μm, columellae 0.5 μm, indistinct, tectum 0.5 μm, stratification not very clear; psilate. Some grains appear to have atectate psilate apocolpia, whereas the mesocolpia is slightly micropitted.

Dimensions. Polar diameter, 36.5–(36.75)–37 μm; equatorial diameter, 20–(20.5)–21 μm; polar/equatorial = 1.79; nm = 2, no = 3.

Comparisons. *Psilatricolporites cyamus* Van der Hammen and Wymstra, 1964, is smaller and has thicker exine and an equatorial constriction; *P. atalayensis* Hoorn, 1993, has thicker exine, apocolpia is acute, and pores have a different shape; *P. magniporatus* Hoorn, 1993, has thicker exine, distinct columellae, and larger pore. *Retitricolporites poriconspectus* Hoorn, 1993, is micropitted, of different shape, and smaller, and it has circular pores.

Etymology. After the indigenous people Xatanawa of western Amazonia.

Verrutricolporites Van der Hammen and Wymstra, 1964

TYPE SPECIES. *VERRUTRICOLPORITES ROTUNDIPORUS* VAN DER HAMMEN & WYMSTRA, 1964

Verrutricolporites pusillus sp. nov.

PLATE 21 O, P

Holotype. Plate 21o, p, sample 22140, EF N-37.

Type locality. Well 1-AS-105-AM, Solimões Formation, Amazonas, Brazil.

Description. Monad, radial, isopolar, subprolate; tricolporate, ectocolpi midsized, 10 μm long, CPI 0.64, borders straight, ends pointed, polar area broad and rounded, 4 μm wide, simple; endopores lalongate, relatively large, 2.5 μm long, 4 μm wide, simple; tectate, exine relatively thick, 2.1 μm thick, nexine 1.5 μm, columellae 0.3 thick, barely distinct, tectum 0.3 μm thick; verrucate, verrucae very short and of irregular shape, 1 μm wide, <0.5 μm high, 0.5–1 μm apart, a few larger verrucae are scattered over the surface.

Dimensions. Polar diameter, 15.5–(15.75)–16 μm; equatorial diameter, 13–(13.5)–14 μm; polar/equatorial = 1.16; nm = 2, no = 2.

Comparison. *Verrutricolporites rotundiporus* Van der Hammen and Wymstra, 1964, has smaller and circular pore and verrucae are larger.

Etymology. After the small size, from word *pusillus* (tiny or very small).

Botanical affinity. Lythraceae?

Verrutricolporites simplex sp. nov.

PLATE 21Q–T

Holotype. Plate 21q, r, sample 22482, EF F-10.

Paratype. Plate 21s, t, sample 22481, EF F-48.

Type locality. Well 1-AS-105-AM, Solimões Formation, Amazonas, Brazil.

Description. Monad, radial, isopolar, prolate spheroidal, subtriangular amb; tricolporate, ectocolpi long, 14 μm long, CPi 0.77, borders slightly invaginated, ends rounded, simple; endopores lolongate, 4 μm long, 3 μm wide, simple; tectate, exine 2–3 μm thick, nexine 1 μm, columella thin, ~0.5 μm thick, indistinct, tectum 1.5–2 μm thick; verrucate, verrucae evenly distributed and shaped, circular, 1–2 μm wide, 1–2 μm high, 1 μm apart.

Dimensions. Polar diameter, 18 μm; equatorial diameter, 17 μm; polar/equatorial = 1.05; polar diameter length, 16 μm; equatorial diameter width, 20 μm; length/diameter = 0.8; nm = 2, no = 3.

Comparisons. *Verrutricolporites haplites* González-Guzmán, 1967, is larger, has costate colpi and irregular verrucae; *V. rotundiporus* Van der Hammen and Wymstra, 1964, is tectate, with distinct columellae, has shorter verrucae, indistinct colpi, and circular pore; *V. pusillus* sp. nov. is tectate and has larger lalongate pore.

Etymology. After the rather simple morphology.

Botanical affinity. *Simarouba*? (Simaroubaceae).

Triporate

***Byttneripollis* Konzalová, 1976**

TYPE SPECIES. *BYTTNERIPOLLIS CORONARIUS* KONZALOVÁ, 1976

***Byttneripollis rugulatus* sp. nov.**

PLATE 21Y–BB

Holotype. Plate 21y, z, sample 22277, EF L-13-3.

Paratype. Plate 21aa, bb, sample 22158, EF G-20-1.

Type locality. Well 1-AS-105-AM, Solimões Formation, Amazonas, Brazil.

Description. Monad, radial, isopolar, amb circular; triporate, pores circular, 4–5 μm long, 4–5 μm wide, aspidate, aspis 2 μm thick; tectate, exine 1.8 μm thick, nexine 0.6 μm thick, columellae 0.6 μm thick, indistinct, tectum 0.6 μm thick, undulating; rugulate, rugulae 0.5 μm wide, 0.5 μm high, very short and of irregular length, interrugulate area is fossulate, fossula thin, 2 μm wide.

Dimensions. Polar diameter length, 26–(27)–28 μm; polar diameter width, 25–(25.5)–26 μm; length/width = 1.05; nm = 2, no = 3.

Comparisons. *Byttneripollis* Konzalová, 1976, accommodates 3–6 porate grains with a fringe-like aspis; *B. ruedae* Silva-Caminha et al., 2010, is triangular–obtuse in shape, reticulate, endopores costate and has thicker aspis.

Etymology. After rugulate pattern.

***Florschuetzia* Germeraad et al., 1968**

TYPE SPECIES. *FLORSCHUETZIA TRILOBATA*
GERMERAAD ET AL., 1968

***Florschuetzia impostora* sp. nov.**

PLATE 22G–K

Holotype. Plate 22g, h, sample 22460, EF X-8-3.

Paratype. Plate 22i, sample 22460, EF V-7-3.

Specimen. Plate 22j, k, sample 22460, EF C-8-3.

Type locality. Well 1-AS-105-AM, Solimões Formation, Amazonas, Brazil.

Description. Monad, radial, isopolar, subprolate, amb triangular; triporate, pores circular, 2.5 μm long, 2.5 μm wide, simple, slightly protruding, colpi absent, but there seems to be colpi as well, with invaginated mesocolpia; tectate, exine 1.5 μm thick, nexine 0.5 μm thick, columellae distinct, 0.5 μm thick, tectum 0.5 μm thick; psilate to micropitted.

Dimensions. Polar diameter, 20–(20.5)–21 μm; equatorial diameter, 17 μm; polar/equatorial = 1.20; nm = 2, no = 51.

Comparisons. *Florschuetzia trilobata* Germeraad et al., 1968, is strongly lobate. *Psilatriporites sarimentoi* and *P. corstanjei* Hoorn, 1993, are circular; *P. desilvae* Hoorn, 1993, has pseudocolpi along with pores.

Etymology. From the word *impostor* (deceiver), as the grain appears tricolporate, but colpis are absent.

Botanical affinity. Lythraceae?

***Proteacidites* Cookson, 1950, ex Couper, 1953, emend.**

TYPE SPECIES. *PROTEACIDITES ADENANTHOIDES* COOKSON, 1950

***Proteacidites poriscabratus* sp. nov.**

PLATE 22L–N

Holotype. Plate 22l, m, sample 22330, EF G-41-1.

Paratype. Plate 22n, sample 22326, EF C-20-3.

Type locality. Well 1-AS-105-AM, Solimões Formation, Amazonas, Brazil.

Description. Monad, radial, isopolar, amb triangular–obtuse–convex; triporate, pores distinct, circular, 3 μm wide; annulate, annulus produced by a dense scabrate cover around pores, 2 μm wide, 1 μm thick; intectate, exine 0.8 μm thick, nexine 0.5; scabrate, scabrae 0.3 μm high, <0.5 μm wide, densely and evenly distributed.

Dimensions. Polar diameter length, 30–(32.5)–35 μm; polar diameter width, 24–(27.5)–31 μm; length/width = 1.18; nm = 2, no = 2.

Comparisons. *Proteacidites triangulatus* Lorente, 1986, has large, clear pores and thicker exine; *P. dehaani* Germeraad et al., 1968, is reticulate; *P. miniporatus* Van Hoeken-Klinkenberg, 1966, has very slight scabration and simple, smaller pores.

Etymology. After scabrae around apertures.

Botanical affinity. *Serjania*/*Paullinia* (Sapindaceae).

***Proteacidites pseudodehaanii* sp. nov.**

PLATE 22O

Holotype. Plate 22o, sample 22412, EF L-9-1/3.

Type locality. Well 1-AS-105-AM, Solimões Formation, Amazonas, Brazil.

Description. Monad, radial, isopolar, amb triangular; triporate, pores distinct, circular, 7 μm wide, costate, costae 3 μm wide, produced by an irregular thickening of the nexine ~1 μm thick and then by a thinning 2 μm wide in such a way that only the sexine borders the outer part of the pores; semitectate, exine 1.5 µm thick, nexine 1 µm thick, columellae 0.3 µm thick, barely distinct, tectum 0.3 µm thick; reticulate, lumina circular, 0.5–1 µm wide, muri 0.5–1 µm wide, homobrochate.

DIMENSIONS. Polar diameter length, 31–(34.5)–38 µm; polar diameter width, 28–(31)–34 µm; length/width = 1.11; nm = 2, no = 3.

COMPARISONS. *Proteacidites dehaani* Germeraad et al., 1968, has smaller pores and thicker annulus and is heterobrochate; *P. miniporatus* Van Hoeken-Klinkenberg, 1966, is scabrate and has smaller pores; *P. triangulatus* Lorente, 1986, is thicker and micropitted.

ETYMOLOGY. After similarity to *P. dehaani* Germeraad et al., 1968.

BOTANICAL AFFINITY. *Roupala/Gevuina* (Proteaceae).

***Psilatriporites* (Van der Hammen 1956b) Mathur, 1966**

TYPE SPECIES. *PSILATRIPORITES INORNATUS*
(VAN DER HAMMEN) MATHUR, 1966

***Psilatriporites minimus* sp. nov.**

PLATE 23B–D

HOLOTYPE. Plate 23b, sample 22506, EF S-4-3.

PARATYPE. Plate 23c, d, sample 22303, EF U-22-2.

TYPE LOCALITY. Well 1-AS-105-AM, Solimões Formation, Amazonas, Brazil.

DESCRIPTION. Monad, radial, isopolar, spheroidal, amb circular; triporate, pores distinct, circular, 3 µm wide, slightly sunken; costate, costae ~0.5 µm thick, 0.5 µm wide; atectate, exine 1 µm thick; psilate.

DIMENSIONS. Equatorial view: polar diameter, 14 µm; equatorial diameter, 13 µm; polar/equatorial = 1.07; polar view: polar diameter length, 19 µm; polar diameter width, 15 µm; length/width = 1.26; nm = 2, no = 3.

COMPARISONS. *Momipites* and *Triporopollenites* have triangular amb and slightly protruding pores. *Psilatriporites sarmientoi* Hoorn, 1993, has much larger pores in proportion to grain size; *P. corstanjei* Hoorn, 1993, has larger pores with thick annulus.

ETYMOLOGY. After diminutive size.

BOTANICAL AFFINITY. *Celtis* (Cannabaceae).

***Retitriporites* Ramanujam, 1966**

TYPE SPECIES *RETITRIPORITES CURVIMURATI* RAMANUJAM, 1966

***Retitriporites crotonicolumellatus* comb. nov. et emend.**

PLATE 23F–I

BASIONYM. *Retipollenites crotonicolumellatus* Jaramillo et al., 2011, p. 74, pl. 9, figs. 1–3.

SPECIMEN. Plate 23f, g, sample 22436, EF N13/3.

SPECIMEN. Plate 23h, i, sample 22436, EF S21/4.

TYPE LOCALITY. Well 1-AS-105-AM, Solimões Formation, Amazonas, Brazil.

DESCRIPTION. Monad, radial, isopolar, amb circular; triporate, pores simple, sometimes indistinct, probably circular; semitectate, exine ~2.5 µm thick, nexine 0.7 µm thick, columellae 1 µm thick, distinct, tectum 0.7 µm thick, ~1 µm wide, 0.5-2 µm apart; reticulate, reticulum coarse, curvimurate, simplicolumellate, columellae resemble a croton pattern, lumina 3–7 µm wide, muri 1.5 µm wide, homobrochate.

DIMENSIONS. Polar diameter length, 27–(26)–25 µm; equatorial diameter width, 24–24 µm; length/width = 1.08; nm = 2, no = 8.

COMPARISON. *Retipollenites crotonicolumellatus* Jaramillo et al., 2011, was originally described as inaperturate; however, the grain has three pores.

BOTANICAL AFFINITY. *Chomelia*? (Rubiaceae).

***Retitriporites discretus* sp. nov.**

PLATE 23J–M

HOLOTYPE. Plate 23j, k, sample 22518, EF V-17.

PARATYPE. Plate 23l, m, sample 22522, EF S-47-1/2.

TYPE LOCALITY. Well 1-AS-105-AM, Solimões Formation, Amazonas, Brazil.

DESCRIPTION. Monad, radial, isopolar, amb circular to subtriangular; triporate, pores 2 µm wide, circular, slightly protruding; costate, costae 3 µm wide, 2 µm thick; semitectate, exine 2 µm thick, nexine 1 µm thick, columellae distinct, 0.5 µm thick, tectum 0.5 µm thick; rugulate, rugula, 0.5–1 µm wide, and secondarily fossulate, variable in size, 0.5–1 µm wide, homobrochate.

DIMENSIONS. Polar diameter length, 23.5 µm; equatorial diameter width, 18–(19.5)–21 µm; length/width = 1.2; nm = 2, no = 2.

COMPARISONS. *Retitriporites dubiosus* González-Guzmán, 1967, *R. poricostatus* Jaramillo and Dilcher, 2001, *R. typicus* González-Guzmán, 1967, and *R. simplex* Van der Kaars, 1983, are all reticulate and have much larger lumina; *R. acostai* Dueñas, 1986, is heterobrochate and has larger pores.

ETYMOLOGY. After simple, discrete morphology.

***Retitriporites sifonis* sp. nov.**

PLATE 23N, O

HOLOTYPE. Plate 23n, o, sample 22290, EF F-42-2.

TYPE LOCALITY. Well 1-AS-105-AM, Solimões Formation, Amazonas, Brazil.

DESCRIPTION. Monad, radial, isopolar, amb triangular–obtuse–convex; triporate, pores circular, 5–6 µm long, 5–6 µm wide, simple, pore outline irregular, highly protruding resembling a tubular appendage like a labrum; semitectate, exine

1.5 µm thick, nexine 0.6 µm thick, columellae indistinct, 0.3 µm thick, tectum 0.6 µm thick; reticulate, lumina of irregular shape and size, circular to elongate, 1–3 µm wide, muri 1.5 µm wide, lumina smaller and circular at apocolpia and lumina larger and elongate at mesocolpia, heterobrochate.

Dimensions. Polar diameter length, 35–(36.5)–38 µm; equatorial diameter width, 30–(34)–38 µm; length/width = 1.07; nm = 2, no = 2.

Comparisons. *Byttneripollis* spp. have atrium, different from the simple protrusions in *R. sifonis* sp. nov.

Etymology. After highly protruding apertures, like tubes, from word *sifonis* (siphon).

Stephanocolpate

***Passifloriidites* gen. nov.**

TYPE SPECIES. *PASSIFLORIIDITES PSEUDOPERCULATUS* SP. NOV.

Description. Monad, circular–subtriangular amb, stephanocolp(or)ate, 6 or more colpi, colpi syncolpate, colpi arranged in pairs (geminicolpate); syncolpus formed by the merging of 2 colpi that are opposite, not adjacent, to each other. This arrangement creates a number of syncolpi that is half of the total number of colpi. The area between two adjacent colpi forms a pontoperculum. The mesocolpium around a syncolpus can detach completely (forming a pseudoperculum) or remain attached by a small exine bridge at the apocolpia. Exine semitectate, thick, columellae distinct, reticulate, large mesh, lumina rounded, polygonal, or curvimurate.

Comments. The genus is erected to accommodate pollen with the combination of geminicolpi, pseudoperculum/pontoperculum, and reticulate exine of the Passifloraceae type.

Etymology. After extant genus *Passiflora* (Passifloraceae).

***Passifloriidites pseudoperculatus* sp. nov.**

PLATE 24A–F

Holotype. Plate 24a, b, sample 22365, EF P10/3.

Paratype. Plate 24c, d, sample 22422, EF F35.

Specimen. Plate 24e–f, sample 22158, EF Q15/3.

Type locality. Well 1-AS-105-AM, Solimões Formation, Amazonas, Brazil.

Description. Monad, radial, isopolar, circular to subtriangular amb; stephanocolpate, 6-syncolpate, colpi arranged in pairs and merge at apocolpia, colpi simple; mesocolpia around syncolpi detaches forming pseuoperculum (Plate 24e, f) and giving the grain a false triporate appearance, apocolpia side 14 µm wide; semitectate, exine 4–5 µm thick, nexine 1.5 µm thick, columellae distinct, 1 µm thick, 1–1.5 µm wide, and 1 µm apart, tectum 1.5 µm thick; reticulate, lumina mostly curvimurate, 2–8 µm wide, muri 1–1.5 µm wide, simplicolumellate, intralumen nexine with sparse granules, 0.5–1 µm wide; heterobrochate, few smaller lumina are rounded, most lumina are large and curvy. Seen in oblique views only.

Dimensions. Polar diameter length, 40–44 µm; equatorial diameter width, 20–36 µm; pseudoperculum width, 26–30 µm; pontoperculum, 8–10 µm wide; pseudoperculum (in Plate 24e, f) is 32 × 22 µm; nm = 3, no = 3.

Comparisons. *Syncolpites* sp. (in Palazzesi et al., 2014) has a similar morphology but with more than three pseudopercula.

Etymology. After pseudopercula.

Botanical affinity. *Passiflora* subgen. *Passiflora* (Passifloraceae).

Perfotricolpites
González-Guzmán, 1967

TYPE SPECIES. *PERFOTRICOLPITES DIGITATUS*
GONZÁLEZ-GUZMÁN, 1967

Expanded description. Monad, radial, isopolar, prolate, circular amb, tricolpate to stephanocolpate, colpi long, borders straight to invaginating; tectate, columellae distinct and digitate, psilate, scabrate to finely reticulate, lumina <0.5 µm.

Comments. The genus is characterized by the presence of digitate columellae in zonocolpate grains.

***Perfotricolpites hexacolpatus* sp. nov.**

PLATE 24G–J

Holotype. Plate 24g, h, sample 22354, EF W42/2.

Paratype. Plate 24i, j, sample 22438, EF K45/1.

Type locality. Well 1-AS-105-AM, Solimões Formation, Amazonas, Brazil.

Description. Monad, radial, isopolar, circular amb, large sized; stephanocolpate, 6 colpi, 40 µm long, borders invaginating, ends rounded, slightly marginate, margo created by decreasing columellae thickness toward colpi; tectate, exine 5 µm thick, nexine 1 µm thick, columellae 3 µm thick, distinct, digitate, tectum 1 µm thick; psilate, columellae tips visible through tectum, tectum surface sparsely scabrate; grains often in oblique views.

Dimensions. Polar diameter length, 64–(67)–70 µm; equatorial diameter width, 64–64 µm; length/width = 1.04; nm = 2, no = 6.

Comparison. *Jandufouria seamrogiformis* Germeraad et al., 1968 is micropitted and columellae are not digitate.

Etymology. After number of colpi.

Botanical affinity. *Merremia* (Convolvulaceae).

Retistephanocolpites
Leidelmeyer, 1966

TYPE SPECIES. *RETISTEPHANOCOLPITES ANGELI*
LEIDELMEYER, 1966

Retistephanocolpites liberalis sp. nov.

PLATE 25D–F

Holotype. Plate 25d, e, sample 22282, EF L-14-2.

Paratype. Plate 25f, sample 22287, EF S-17-1.

Type locality. Well 1-AS-105-AM, Solimões Formation, Amazonas, Brazil.

Description. Monad, radial, isopolar, amb circular to quadrangular; stephanocolpate, 4 colpi, midsized, colpi 20 µm long, CEi 0.54, borders slightly invaginated, ends pointed, often wide open, simple; semitectate, exine 2 µm thick, nexine 0.7 µm thick, sometimes with endocracks, columellae 0.6 µm long, distinct, 0.5 µm thick, 0.5 µm apart, tectum 0.7 µm thick; reticulate, lumina 1 µm wide, rounded, elongate to angular, muri 1 µm wide, homobrochate.

Dimensions. Equatorial diameter length, 37–(37.5)–38 µm; equatorial diameter width, 33–(35)–37 µm; length/width = 1.07; nm = 2, no = 7.

Comparisons. *Retistephanocolpites angeli* Leidelmeyer, 1966, and *R. finalis* González-Guzmán, 1967, have 5 very short colpi; *R. regularis* Van Hoeken-Klinkenberg, 1966, has 5 longer colpi and smaller lumina; *R. tropicalis* Dueñas, 1980, has minute lumina (<0.5 µm) and much more invaginated colpi; *R. circularis* Silva-Caminha et al., 2010, has 5 very short marginate colpi.

Etymology. After simple and open (“liberal”) character of colpi.

Stephanocolporate

Psilastephanocolporites Leidelmeyer, 1966

TYPE SPECIES. *PSILASTEPHANOCOLPORITES FISSILIS* LEIDELMEYER, 1966

Psilastephanocolporites ectoporatus sp. nov.

PLATE 25Q–S

Holotype. Plate 25q, r, sample 22140, EF L-22-1/3.

Paratype. Plate 25s, sample 22140, EF X-32.

Type locality. Well 1-AS-105-AM, Solimões Formation, Amazonas, Brazil.

Description. Monad, radial, isopolar, subprolate to prolate; stephanocolporate, 5 colpori, endocolpi, midsized, colpi 16 µm long, CPi 0.64, ends pointed, polar area rounded, 7 µm wide, endocolpi costate, costae 1 µm wide, 1.5 µm thick; ectopores simple, circular, 5 µm long, 5 µm wide; tectate, exine 2 µm thick, nexine 1 µm thick, sexine 1 µm thick, columella indistinct; psilate.

Dimensions. Polar diameter, 25–(28.16)–31.5 µm; equatorial diameter, 20–(21)–22 µm; polar/equatorial = 1.34; nm = 2, no = 74.

Comparisons. *Psilastephanocolporites globulus* Van Hoeken-Klinkenberg, 1966, has 4 colpori, costate pores, and thicker exine; *P. marinamensis* Hoorn, 1994b, has 4 very short and indistinct colpi and lalongate pores; *P. matapiorum* Hoorn, 1994b, has 4 long colpori and lalongate pores; *P. schneideri* Hoorn, 1993, has 4 colpori, large lalongate pores and is psilate–microreticulate. *Meliapollis* sp. 1 Silva-Caminha et al., 2010, has costate pores and simple colpi.

Etymology. After ectopores.

Psilastephanocolporites pseudomarinamensis sp. nov.

PLATE 26A, B

Holotype. Plate 26a, b, sample 22282, EF T-16-1.

Type locality. Well 1-AS-105-AM, Solimões Formation, Amazonas, Brazil.

Description. Monad, radial, isopolar, prolate spheroidal to subprolate, stephanocolporate, 5 colpori, ectocolpi 16 µm long, CPi 0.51, ends pointed, polar area rounded, 18 µm wide costate, costae 2 µm wide, 1.5 µm thick; endopores lalongate, 2 µm long by 5 µm wide, simple, displaying a slight constriction, which makes them appear as 8-shaped; tectate, exine 2 µm thick, nexine 0.7 µm thick, columellae 0.6 µm thick, indistinct, tectum 0.7 µm thick; psilate to micropitted, lumina <0.5 µm, evenly distributed.

Dimensions. Polar diameter, 23–(27)–31 µm; equatorial diameter, 22–(24)–26 µm; polar/equatorial = 1.12; nm = 2, no = 4.

Comparisons. *Psilastephanocolporites marinamensis* Hoorn, 1994b, has shorter colpi and is psilate and pores are strongly lalongate; *P. schneideri* Hoorn, 1993, has much larger pores and is smaller.

Etymology. After a similarity with *Psilastephanocolporites marinamensis* Hoorn, 1994b.

Retistephanocolporites Van der Hammen & Wymstra, 1964

TYPE SPECIES. *RETISTEPHANOCOLPORITES QUADRIPORUS* VAN DER HAMMEN & WYMSTRA, 1964

Retistephanocolporites loxocolpatus sp. nov.

PLATE 26C–E

Holotype. Plate 26c–e, sample 22140, EF J-40-4.

Type locality. Well 1-AS-105-AM, Solimões Formation, Amazonas, Brazil.

Description. Monad, radial, isopolar, subprolate; stephanocolporate, loxocolporate, 4 colpori, ectocolpi midsized, 12 µm long, CPi 0.63, borders straight, ends pointed, polar area 8 µm wide, simple; endopores costate, costae discrete, 1.5 µm wide, 1.5 µm thick; lalongate, 4 by 3 µm wide; semitectate, exine

1.5 μm thick, nexine 1 μm thick, columellae 0.3 μm thick, distinct, regularly distributed, very thin tectum, 0.2 μm thick; reticulate to micropitted, lumina/foveolae circular, 0.5–1 μm wide, 0.5–1 μm apart, homobrochate.

DIMENSIONS. Polar diameter, 19 μm; equatorial diameter, 16.5 μm; polar/equatorial = 1.15; nm = 1, no = 1.

COMPARISON. Loxocolporate grains have not yet been described in northern South America.

ETYMOLOGY. From the term *loxocolp(or)ate* (Erdtman and Straka, 1961).

Stephanoporate

***Verrustephanoporites* Leidelmeyer, 1966**

TYPE SPECIES. *VERRUSTEPHANOPORITES SIMPLEX* LEIDELMEYER, 1966

***Verrustephanoporites circularis* sp. nov.**

PLATE 26L, M

HOLOTYPE. Plate 26l, m, sample 22412, EF M-13-2/4.

TYPE LOCALITY. Well 1-AS-105-AM, Solimões Formation, Amazonas, Brazil.

DESCRIPTION. Monad, radial, isopolar, circular; stephanoporate, 6 pores, pores 2.5 by 2.5 μm wide, circular, costate, costa 1 μm wide and 1 μm thick; intectate, exine 2 μm thick, nexine 0.5 μm thick, sexine 1.5 μm thick; verrucate, verrucae circular to elongate, 2–4 μm wide, 0.5 μm apart, densely distributed over the entire surface.

DIMENSIONS. Equatorial diameter length, 26 μm; equatorial diameter width, 24 μm; length/width = 1.08; nm = 1, no = 3.

COMPARISONS. *Verrustephanoporites simplex* Leidelmeyer, 1966, has four pores and rounded verrucae. *Verrustephanoporites* sp. 1 Jaramillo and Dilcher, 2001, is tectate and has smaller verrucae, bacula, and gemmae. *Verrustephanoporites intraverrucatus* sp. nov. has smooth sexine. *Ulmoideipites krempii* (Anderson, 1960) Elsik, 1968, is tectate and has 3–5 pores and smaller verrucae.

ETYMOLOGY. After circular outline.

BOTANICAL AFFINITY. *Mascagnia* (Malpighiaceae).

***Verrustephanoporites intraverrucosus* nov. sp.**

PLATE 26N, O

HOLOTYPE. Plate 26n, sample 22381, EF S-37-3.

PARATYPE. Plate 26o, sample 22381, EF G-9-2/4.

TYPE LOCALITY. Well 1-AS-105-AM, Solimões Formation, Amazonas, Brazil.

DESCRIPTION. Monad, radial, isopolar, circular; stephanoporate, 5 pores, pores circular, 2 μm long, 2 μm wide; costate, costae 2 μm wide, formed of agglomeration of verrucae around pores, pores slightly protruding; atectate, exine 1.5 μm thick; infraverrucate, that is, nexine is fragmented into verrucae and baculae, of circular shape, irregular size and distribution, 0.5–1 μm wide; verrucae of costae are larger.

DIMENSIONS. Equatorial diameter length, 30–(33.5)–37 μm; equatorial diameter width, 28 μm; length/width = 1.19; nm = 2, no = 3.

COMPARISON. *Ulmoideipites krempii* (Anderson, 1960) Elsik, 1968, has external verrucae and is tectate.

ETYMOLOGY. After internal verrucae.

BOTANICAL AFFINITY. *Forsteronia/Prestonia/Odontadenia* (Apocynaceae) and African genus *Funtumia* (Apocynaceae).

Pericolpate

***Lymingtonia* Erdtman, 1960**

TYPE SPECIES. *LYMINGTONIA RHETOR* ERDTMAN, 1960

***Lymingtonia splendida* sp. nov.**

PLATE 27A, B

HOLOTYPE. Plate 27a, b, sample 22506, EF O-48-3/4.

TYPE LOCALITY. Well 1-AS-105-AM, Solimões Formation, Amazonas, Brazil.

DESCRIPTION. Monad, radial, isopolar, circular; pantocolpate, ecto- and endocolpi coinciding, 16 colpate (8 latitudinal colpi in the equatorial band and 4 meridional colpi halfway between the mesocolpium and apocolpium on each side), small, 11 μm long, CEi 0.29, ends rounded, marginate, margo produced by a gradual thinning of the columellae until they completely disappear and hence colpi are slightly sunken; tectate, exine 3 μm thick, nexine 1 μm thick, columellae 1 μm thick, 1 μm wide, 1 μm apart, tectum 1 μm thick; psilate to echinate, echinae very short 0.1–0.2 μm high; columellae tips seen through tectum giving the impression of a negative reticulum.

DIMENSIONS. Equatorial diameter length, 54–(56)–60 μm; equatorial diameter width, 50–(52)–54 μm; length/width = 1.07; nm = 2, no = 2.

COMPARISONS. *Lymingtonia*? sp. 1 Jaramillo and Dilcher, 2001 is intectate–echinate. *Echiperiporites* spp. (Plate 28a–j) are porate with larger, more conspicuous spines.

ETYMOLOGY. After the word *splendens* (shining or brilliant), for the large size and exquisite morphology.

BOTANICAL AFFINITY. *Evolvulus/Jacquemontia* (Convolvulaceae).

Periporate

***Cyperaceaepollis* Krutzsch, 1970**

TYPE SPECIES. *CYPERACEAEPOLLIS NEOGENICUS* KRUTZSCH, 1970

Cyperaceaepollis wesselinghii **sp. nov.**

PLATE 27I–K

Holotype. Plate 27i, sample 22256, EF L-46.

Paratype. Plate 27j, k, sample 22321, EF H-8-1.

Type locality. Well 1-AS-105-AM, Solimões Formation, Amazonas, Brazil.

Description. Monad, radial, isopolar, circular, easily folded; pantoporate, 4–6 pores, one main pore always visible, other adjacent pores less clear; pores outline irregular to circular, 4 µm long, 4 µm wide, costate, costae granular, 0.5 µm thick; tectate, exine 1 µm thick, nexine 0.3 µm thick, columellae 0.3 µm thick, indistinct, tectum 0.4 µm thick; psilate to finely pitted.

Dimensions. Equatorial diameter length, 32–(33)–34 µm; equatorial diameter width, 28–(29)–30 µm; length/width = 1–1.2; nm = 2, no = 305.

Comparison. *Cyperaceaepollis neogenicus* Krutzsch, 1970, is thicker and has punctate sculpture.

Etymology. After Dutch geologist Frank Wesselingh.

Botanical affinity. Cyperaceae.

Multiporopollenites **Pflug in Thomson & Pflug, 1953**

TYPE SPECIES. *MULTIPOROPOLLENITES MACULOSUS* (POTONIÉ, 1931) PFLUG IN THOMSON & PFLUG, 1953

Multiporopollenites intermedius **sp. nov.**

PLATE 29B, C

Holotype. Plate 29b, c, sample 22164, EF J-10-1.

Type locality. Well 1-AS-105-AM, Solimões Formation, Amazonas, Brazil.

Description. Monad, radial, isopolar, circular; pantoporate, 14–16 pores, pores circular, 3 µm long, 3 µm wide, simple; semitectate, exine 2 µm thick, nexine 1 µm thick, columellae 0.5 µm thick, distinct, <0.5 µm wide, 0.5 µm apart, tectum 0.5 µm thick; reticulate, lumina 1 µm wide, elongate, muri 0.5–1 µm thick, homobrochate.

Dimensions. Equatorial diameter length, 28 µm; equatorial diameter width, 22–(23)–24 µm; length/width = 1.21; nm = 2, no = 3.

Comparisons. *Multiporopollenites crassinexinatus* Silva-Caminha et al., 2010, has 24 pores and a thicker nexine than sexine; *M. pauciporatus* Jaramillo and Dilcher, 2001, has 18–23 pores and is micropitted.

Etymology. After its generalist/intermediate morphology.

Parsonsidites **Couper, 1960**

TYPE SPECIES. *PARSONSIDITES PSILATUS* COUPER, 1960

Parsonsidites? minibrenacii **sp. nov.**

PLATE 29E, F

Holotype. Plate 29e, sample 22518, EF E-43-4.

Paratype. Plate 29f, sample 22506, EF R-6-1/2.

Type locality. Well 1-AS-105-AM, Solimões Formation, Amazonas, Brazil.

Description. Monad, radial, isopolar, circular; pantoporate, 12–14 pores, pores circular, 2 µm long, 2 µm wide; tectate, exine 1 µm thick, nexine 0.4 µm thick, columellae 0.2 µm thick, indistinct, tectum 0.4 µm thick; psilate.

Dimensions. Equatorial diameter length, 12–(12.6)–13 µm; equatorial diameter width, 11–(11.6)–12 µm; length/width = 1.08; nm = 3, no = 85.

Comparisons. *Parsonsidites? brenacii* Silva-Caminha et al., 2010, is larger and has thicker exine. *Multiporopollenites pauciporatus* Jaramillo and Dilcher, 2001, is bigger and micropitted and has 18–23 pores.

Etymology. After resemblance with *P.? brenacii* Silva-Caminha et al., 2010, but much smaller size and thickness.

Botanical affinity. Amaranthaceae.

Psilaperiporites **Regali et al., 1974**

TYPE SPECIES. *PSILAPERIPORITES ROBUSTUS* REGALI ET AL., 1974

Psilaperiporites depressus **sp. nov.**

PLATE 29G–J

Holotype. Plate 29g, h, sample 22279, EF V12.

Paratype. Plate 29i, j, sample 22278, EF O32.

Type locality. Well 1-AS-105-AM, Solimões Formation, Amazonas, Brazil.

Description. Monad, radial, isopolar, circular to slightly quadrangular amb; pantoporate, 6 pores (4 pores at mesocolpia and 1 in each apocolpium), 8 µm long, 5 µm wide, marginate, margo produced by a thinning of the sexine around pores, 1 µm wide, 0.5 µm thick, pores sunken, operculate, operculum slightly smaller than pore at the base of depressions, opercula often absent; tectate, exine 2 µm thick, nexine 1 µm thick, columellae 0.5 µm thick, very thin, tectum 0.5 µm thick; psilate, columellae tips seen through tectum.

Dimensions. Equatorial diameter length, 21–(21.5)–22 µm; equatorial diameter width, 20–(21)–22 µm; length/width = 1.02; nm = 2, no = 2.

Comparisons. *Psilaperiporites minimus* Regali et al., 1974, *P. robustus* Regali et al., 1974, and *P. multiporatus* Hoorn, 1994a, have more pores and lack sunken pore.

Etymology. After pore depressions.

Psilaperiporites circinatus nov. sp.

PLATE 29L, M

Holotype. Plate 29l, m, sample 22349, EF J-11-1.

Type locality. Well 1-AS-105-AM, Solimões Formation, Amazonas, Brazil.

Description. Monad, radial, isopolar, circular; pantoporate, 19–20 pores, pores 4 µm long, 4 µm wide, circular, simple; tectate, exine 1 µm thick, nexine very thin, 0.2 µm thick, columella 0.4 µm thick, distinct, <0.5 µm wide, <0.5 µm apart, tectum 0.4 µm thick; psilate. Columellae tips clearly seen through tectum.

Dimensions. Equatorial diameter length, 43 µm; equatorial diameter width, 33 µm; equatorial diameter length/width = 1.3; nm = 1, no = 2.

Comparisons. *Psilaperiporites multiporatus* Hoorn, 1994a, and *P. suarezi* Vajda-Santivanez, 1999, are atectate. *Parsonsidites? brenacii* Silva-Caminha et al., 2010, *Parsonsidites*? sp. 1 Jaramillo and Dilcher, 2001, and *Parsonsidites*? sp. 2 Jaramillo and Dilcher, 2001, have fewer pores. *Multiporopollenites pauciporatus* Jaramillo and Dilcher, 2001, is micropitted, and its pores are relatively smaller in comparison to grain size.

Etymology. After rounded shape of pollen and pores, from the word *circinatus* (round).

Retiperiporites Puri, 1963

TYPE SPECIES. *RETIPERIPORITES MULTIPOROIDES* PURI, 1963

Retiperiporites retiporatus sp. nov.

PLATE 29N–P

Holotype. Plate 29n–p, sample 22298, EF G12/3.

Type locality. Well 1-AS-105-AM, Solimões Formation, Amazonas, Brazil.

Description. Monad, radial, isopolar, circular; pantoporate, 12 pores, circular, 2 µm long, 2 µm wide, marginate, margo 1 µm wide, formed by muri around pores; semitectate, exine 2 µm thick, nexine 1 µm thick, columellae 0.5 µm, distinct, 0.5 µm wide and 0.5 µm apart, tectum 0.5 µm; reticulate, lumina rounded to polygonal, 0.5–1.5 µm wide, muri 1 µm, heterobrochate, lumina variation change at random over the entire grain.

Dimensions. Equatorial diameter length, 24 µm; equatorial diameter width, 22 µm; length/width = 1.09; nm = 1, no = 1.

Comparisons. *Bahiaporites reticularis* Regali et al., 1974 is larger, has a coarser reticulum and indistinct pores. *Retiperiporites piacabucuensis* Herngreen, 1975, is much larger and curvimurate. *Maravenites polyoratus* Muller et al., 1987, is larger and has one pore per lumina.

Etymology. After reticulation and porate characteristics.

Thymelipollis Krutzsch, 1966

TYPE SPECIES. *THYMELIPOLLIS RETISCULPTURIUS*
KRUTZSCH, 1966

Thymelipollis amazonicus sp. nov.

PLATE 29Q, R

Holotype. Plate 29q, r, sample 22506, EF P-17.

Type locality. Well 1-AS-105-AM, Solimões Formation, Amazonas, Brazil.

Description. Monad, radial, isopolar, circular; pantoporate, 12 pores, circular, 2 µm long, 2 µm wide, slightly costate, costae 1 µm wide, 1 µm thick; intectate, exine 2 µm thick, nexine 0.5 µm thick, sexine 1.5 µm thick, composed of clavae; sculpture croton type, rosette formed of 6–7 triangular ornaments (clavae tips), total rosette width 3–4 µm wide, circular to oval, adjoining to adjacent ones, with a circular center of ~1 µm wide, each triangular ornament is 1–1.5 µm wide. Some grains display a reticulate pattern underneath clavae tips, probably formed by anastomosing clavae bases. Croton pattern not very clear in all specimens.

Dimensions. Equatorial diameter length, 30–(32)–34 µm; equatorial diameter width, 26–(27)–28 µm; length/width = 1.18; nm = 2, no = 3.

Comparison. *Thymelipollis retisculpturius* Krutzsch, 1966, has a much thicker exine (~5 µm) and is larger.

Etymology. After the Amazon forest.

Botanical affinity. Thymelaeaceae (*Daphnopsis*?).

Acknowledgments

We thank the Brazilian Geological Survey (Departamento Nacional de Produção Mineral, DNPM, and Companhia de Pesquisa de Recursos Minerais, CPRM) for sampling permit and access to work on core 1-AS-105-AM; author C.D. thanks Coordenação de Aperfeiçoamento de Pessoal de Nível Superior (CAPES) for scholarship BEX 0376/12-4 and the Palynological Society (United States) for Student Research Grant-2013. Thanks also are owed to Smithsonian Tropical Research Institute, the National Science Foundation's Division of Earth Sciences (grant 0957679), the Anders Foundation, 1923 Fund, and Gregory D. and Jennifer Walston Johnson. We also thank the following palynologists for fruitful discussions, help with identifications, and access to extant collections for comparisons: Fátima P. R. Leite (Federal University of Mato Grosso), Silane A. F. Silva-Caminha (Federal University of Mato Grosso), Ingrid Romero (University of Illinois at Urbana–Champaign), Marcos Gonçalves Ferreira (Federal University of Acre), Maria L. Absy (National Institute for Amazon Research), and Ana Mezzonato-Pires (State University of Rio de Janeiro). We thank especially Vanessa R. Matos (Federal University of Mato Grosso) for revising many botanical affinities. We are grateful to Eduardo G. Ottone and one anonymous reviewer for their revisions that greatly improved our work.

Plates

PLATE 1. (*Opposite page*)

(**a, b**) *Echinosporis densiechinatus* sp. nov. (Holotype), sample 22140, EF P40-1;

(**c, d**) *Echinosporis densiechinatus* sp. nov. (Paratype), sample 22326, EF V37;

(**e**) *Laevigatosporites indigestus* sp. nov. (Holotype), sample 22287, EF H5-1/2;

(**f**) *Laevigatosporites indigestus* sp. nov. (Paratype), sample 22272, EF J11;

(**g**) *Laevigatosporites cultellus* sp. nov. (Holotype), sample 22279, EF K24;

(**h**) *Laevigatosporites cultellus* sp. nov. (Paratype), sample 22158, EF K6-1;

(**i**) *Laevigatosporites granulatus* Jaramillo et al., 2007, sample 22480, EF C7-1/2;

(**j**) *Laevigatosporites tibuensis* (Van der Hammen, 1956b) Jaramillo and Dilcher, 2001, sample 22278, EF D6-1/2;

(**k**) *Microfoveolatosporis simplex* sp. nov. (Holotype), sample 22354, EF Q26-4;

(**l**) *Polypodiisporites* aff. *speciosus* Sah, 1967, sample 22253, EF S13/3-4;

(**m**) *Polypodiisporites densus* sp. nov. (Holotype), sample 22277, EF D45-4;

(**n**) *Polypodiisporites densus* sp. nov. (Paratype), sample 22158, EF W9-2.

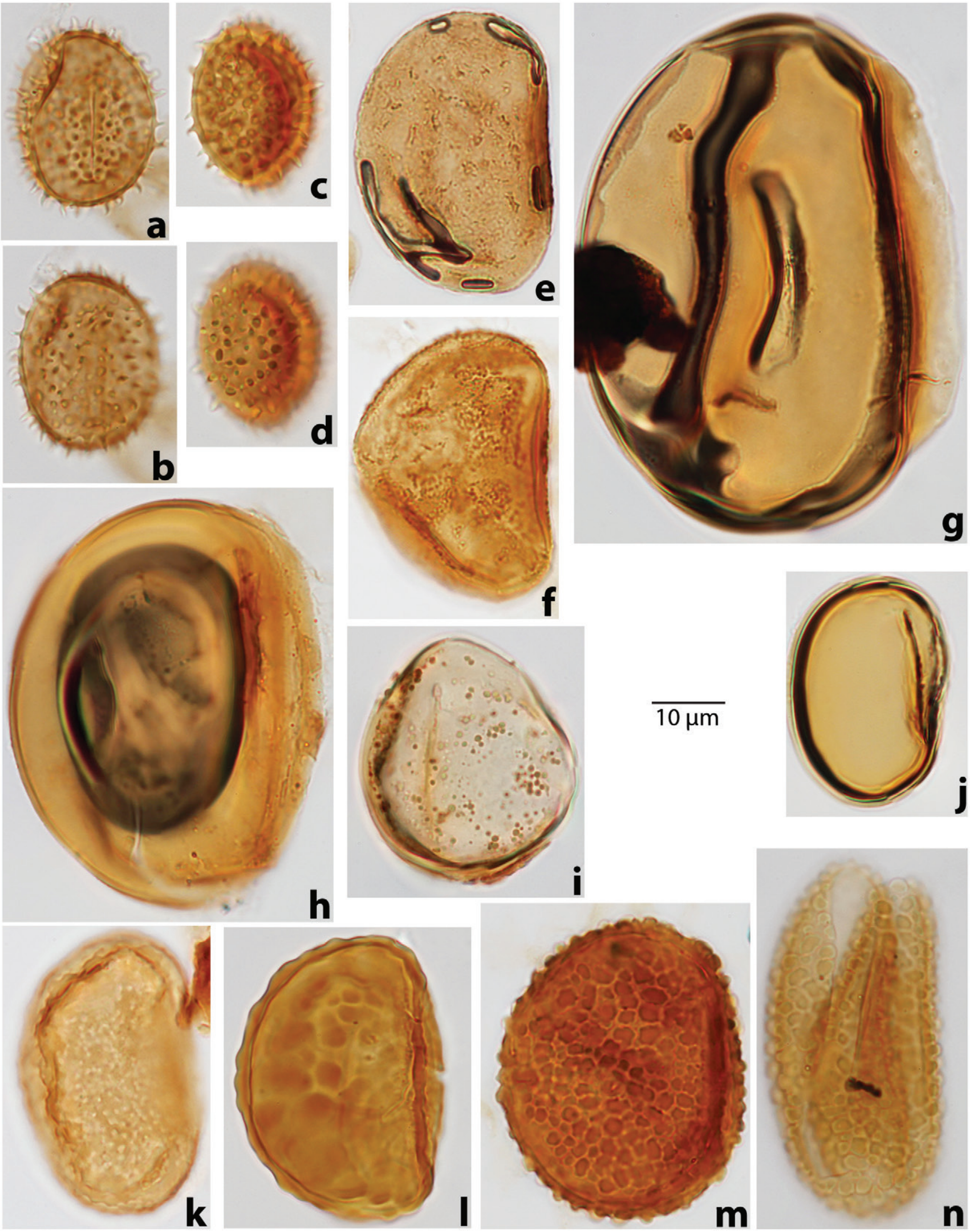
a
b
c
d
e
f
g
h
i
j
k
l
m
n
10 µm

PLATE 2. (*Opposite page*)

(**a**) *Polypodiisporites discretus* sp. nov. (Holotype), sample 22140, EF N5-2/4;

(**b**) *Polypodiisporites discretus* sp. nov. (Paratype), sample 22140, EF G23-4;

(**c, d**) *Polypodiisporites fossulatus* sp. nov. (Holotype), sample 22418, EF V43-1/3;

(**e, f***) *Polypodiisporites scabraproximatus* Silva-Caminha et al., 2010, sample 22158, EF S11-2;

(**g, h**) *Polypodiisporites usmensis* (Van der Hammen, 1956b) Khan and Martin, 1972, **g**: sample 22287, EF V39-2, **h**: sample 22300, EF Q32-2/4;

(**i**) *Polypodiisporites? planus* Silva-Caminha et al., 2010, sample 22140, EF E44;

(**j, k**) *Punctatosporites latrubessei* sp. nov. (Holotype), sample 22402, EF E11-3/4;

(**l, m**) *Punctatosporites latrubessei* sp. nov. (Paratype), sample 22290, EF S15-1/2;

(**n, o**) *Reticulosporis diversus* sp. nov. (Holotype), sample 22354, EF G7;

(**p, q**) *Reticulosporis diversus* sp. nov. (Paratype), sample 22354, EF T13.

*Taken with DIC (differential interference contrast).

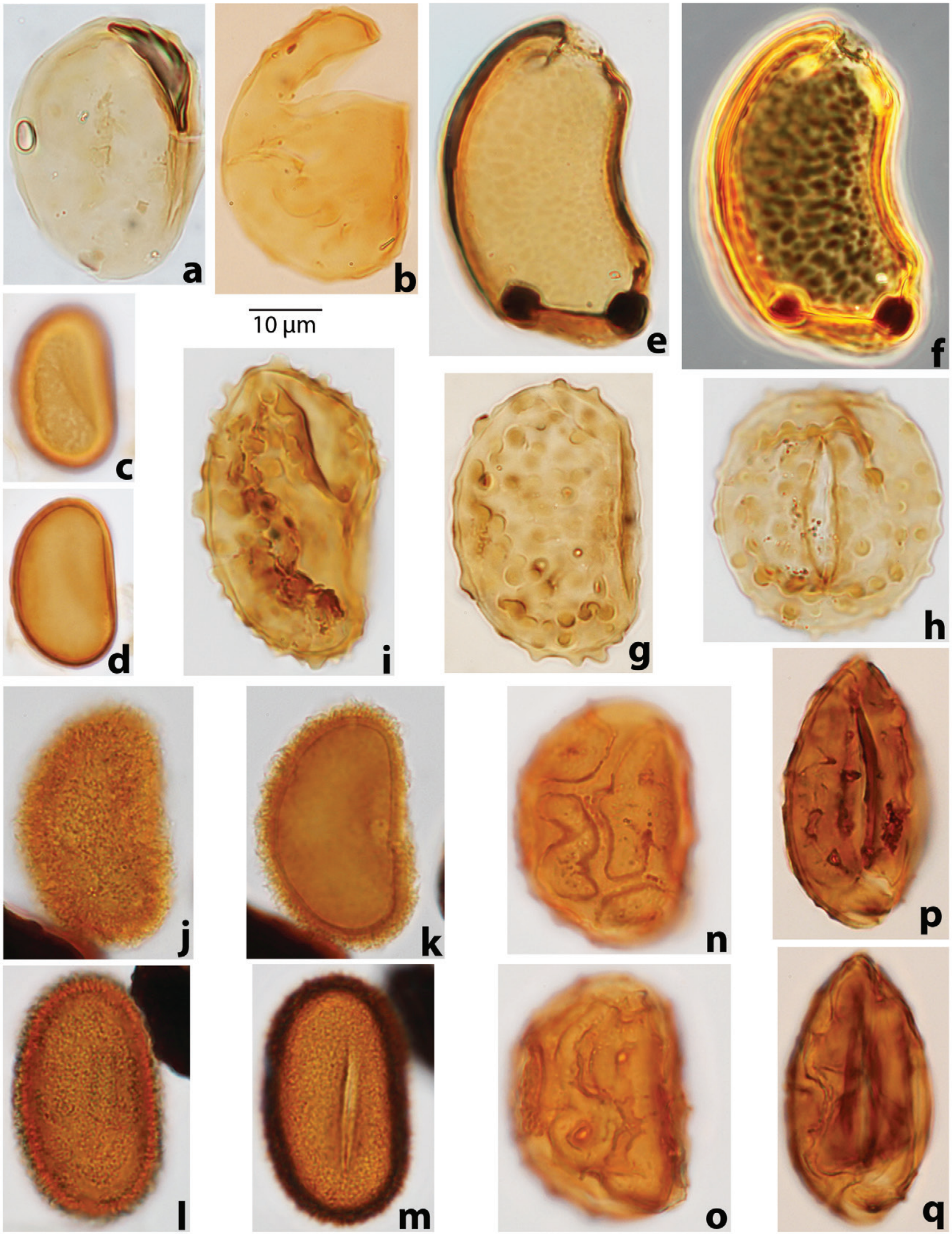
a
b
10 µm
e
f
c
d
i
g
h
j
k
n
p
l
m
o
q

PLATE 3. (*Opposite page*)

(**a**) *Azolla* sp., sample 22279, EF U21/3-4;

(**b, c**) *Camarozonosporites crassus* Silva-Caminha et al., 2010, sample 22140, EF P47;

(**d, e**) *Camarozonosporites fossulatus* sp. nov. (Holotype), sample 22277, EF S39;

(**f, g**) *Camarozonosporites trilobatus* sp. nov. (Holotype), sample 22277, EF U35-4;

(**h, i**) *Camarozonosporites trilobatus* sp. nov. (Paratype), sample 22278, EF H37-1;

(**j, k**) *Cicatricosisporites baculatus* Regali et al. 1974, sample 22330, EF O39;

(**l, m**) *Cicatricosisporites pseudograndiosus* sp. nov. (Holotype), sample 22278, EF H8-3;

(**n**) *Cingulatisporites cristatus* sp. nov. (Holotype), sample 22279, EF U43;

(**o, p**) *Cingulatisporites matisiensis* sp. nov. (Holotype), sample 22278, EF S19;

(**q, r**) *Cingulatisporites matisiensis* sp. nov. (Paratype), sample 22278, EF E12-4.

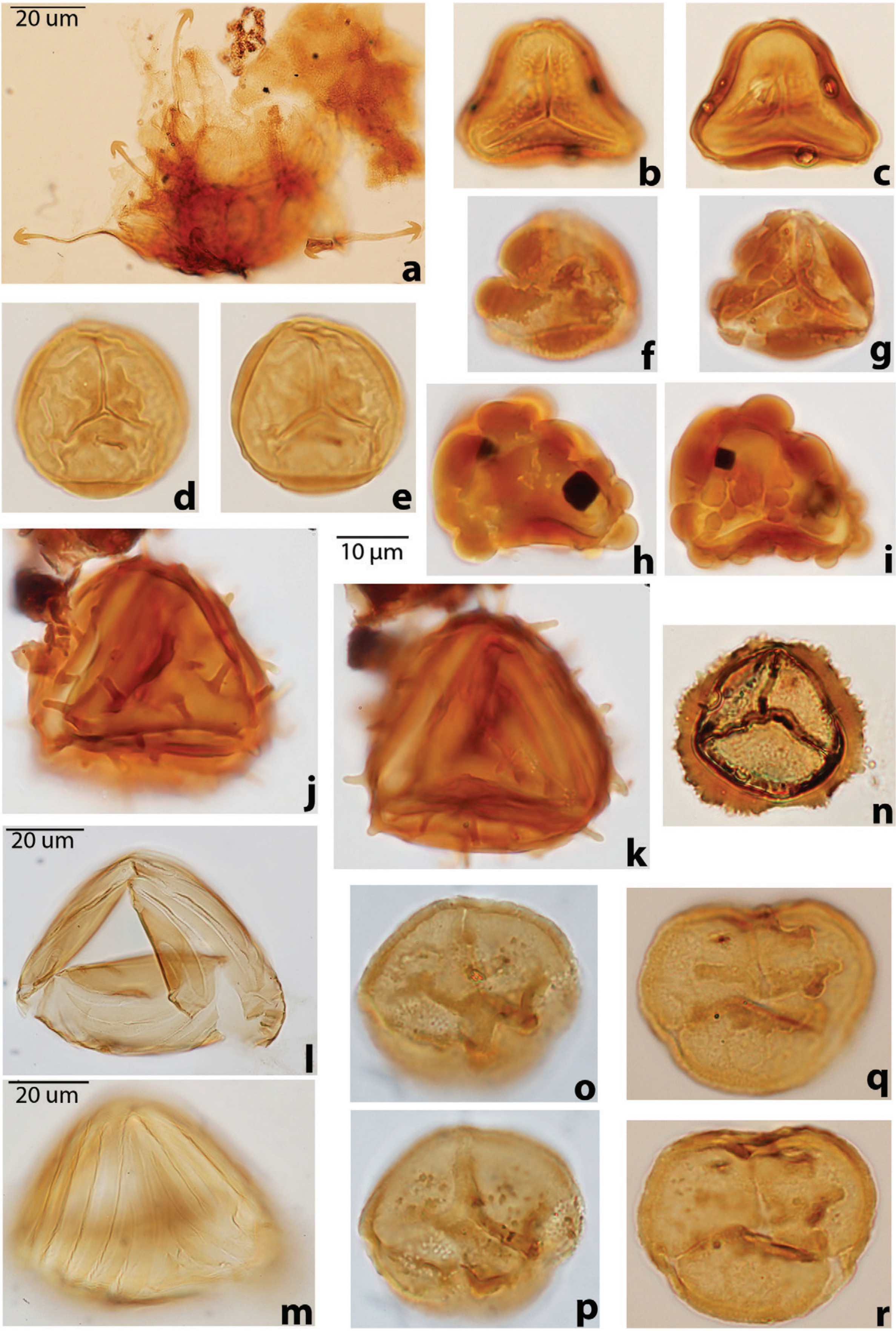
20 um
a
b
c
f
g
d
e
h
i
10 µm
j
k
n
20 um
l
o
q
20 um
m
p
r

PLATE 4. (*Opposite page*)

(**a, b**) *Crassoretitriletes vanraadshooveni* Germeraad et al., 1968, sample 22402, EF H11;

(**c**) *Deltoidospora adriennis* (Potonié and Gelletich 1933) Frederiksen, 1983, sample 22140, EF L12-4;

(**d**) *Echinatisporis circularis* Silva-Caminha et al. 2010, sample 22140, EF J6;

(**e, f**) *Echinatisporis infantulus* sp. nov. (Holotype), sample 22140, EF S51-2;

(**g**) *Echinatisporis infantulus* sp. nov. (Paratype), sample 22170, EF F32-2/4;

(**h**) *Echinatisporis muelleri* (Regali et al., 1974) Silva-Caminha et al., 2010, sample 22293, EF K17;

(**i, j**) *Foraminisporis connexus* sp. nov. (Holotype), sample 22278, EF P24;

(**k, l**) *Foraminisporis connexus* sp. nov. (Paratype), sample 22140, EF L13.

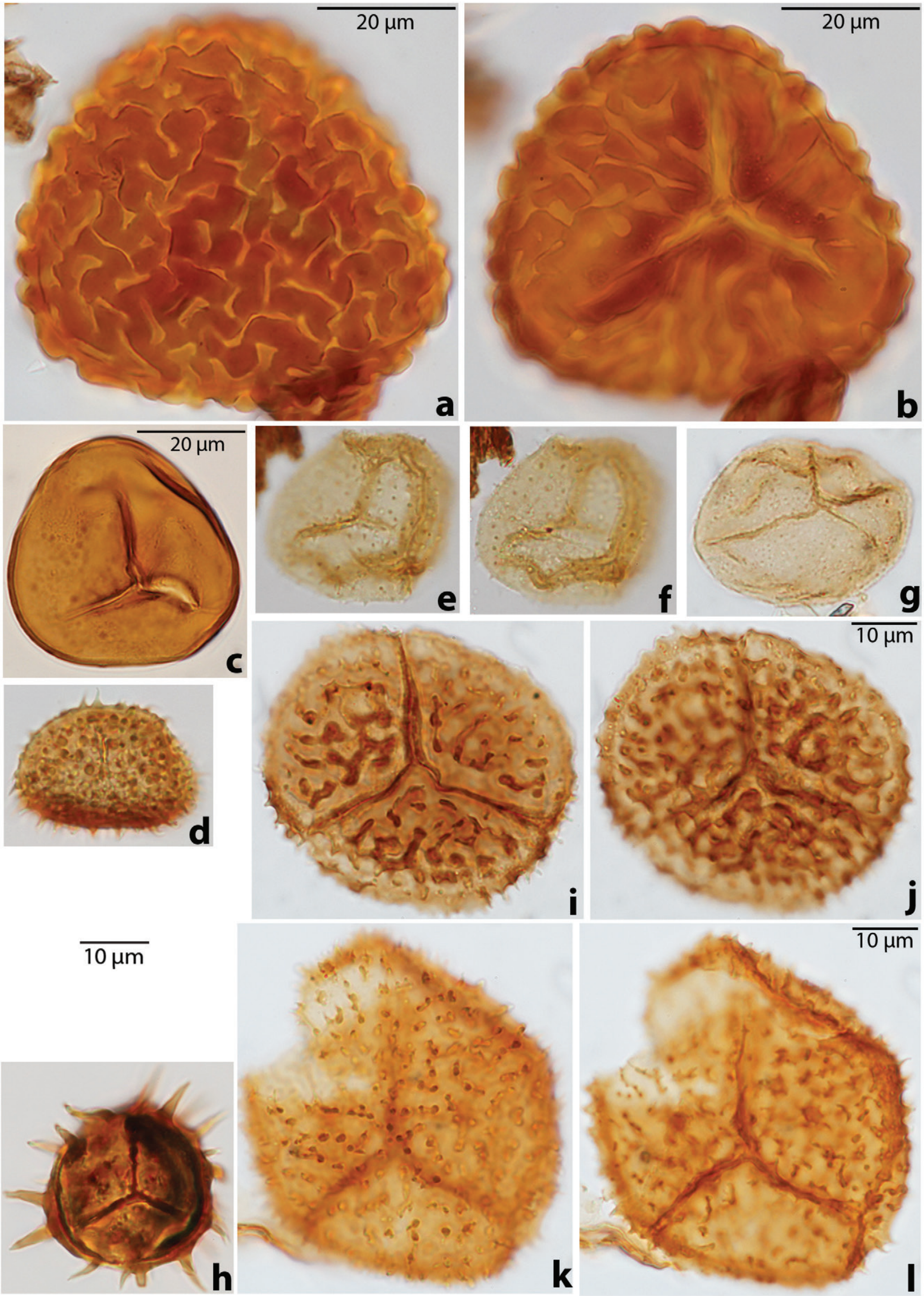
20 µm
a
20 µm
b
20 µm
c
e
f
g
d
10 µm
i
j
10 µm
h
k
10 µm
l

PLATE 5. (*Opposite page*)

(**a, b**) *Foveotriletes ornatus* Regali et al., 1974, sample 22303, EF P11;

(**c, d**) *Hamulatisporis bareanus* sp. nov. (Holotype), sample 22140, EF V9-1;

(**e, f**) *Hydrosporis minor* Silva-Caminha et al., 2010, sample 22267, EF N18-3;

(**g, h**) *Ischyosporites dubius* sp. nov. (Holotype), sample 22140, EF Q6-1;

(**i, j**) *Ischyosporites dubius* sp. nov. (Paratype), sample 22293, EF E11;

(**k, l**) *Ischyosporites granulatus* sp. nov. (Holotype), sample 22303, EF J37;

(**m**) *Kuylisporites waterbolkii* Potonié, 1956, sample 22279, EF C31-4;

(**n, o**) *Lycopodiumsporites amazonicus* sp. nov. (Holotype), sample 22279, EF T16;

(**p**) *Magnastriatites grandiosus* (Kedves and Solé de Porta, 1963) Dueñas, 1980, sample 22261, EF H10-2.

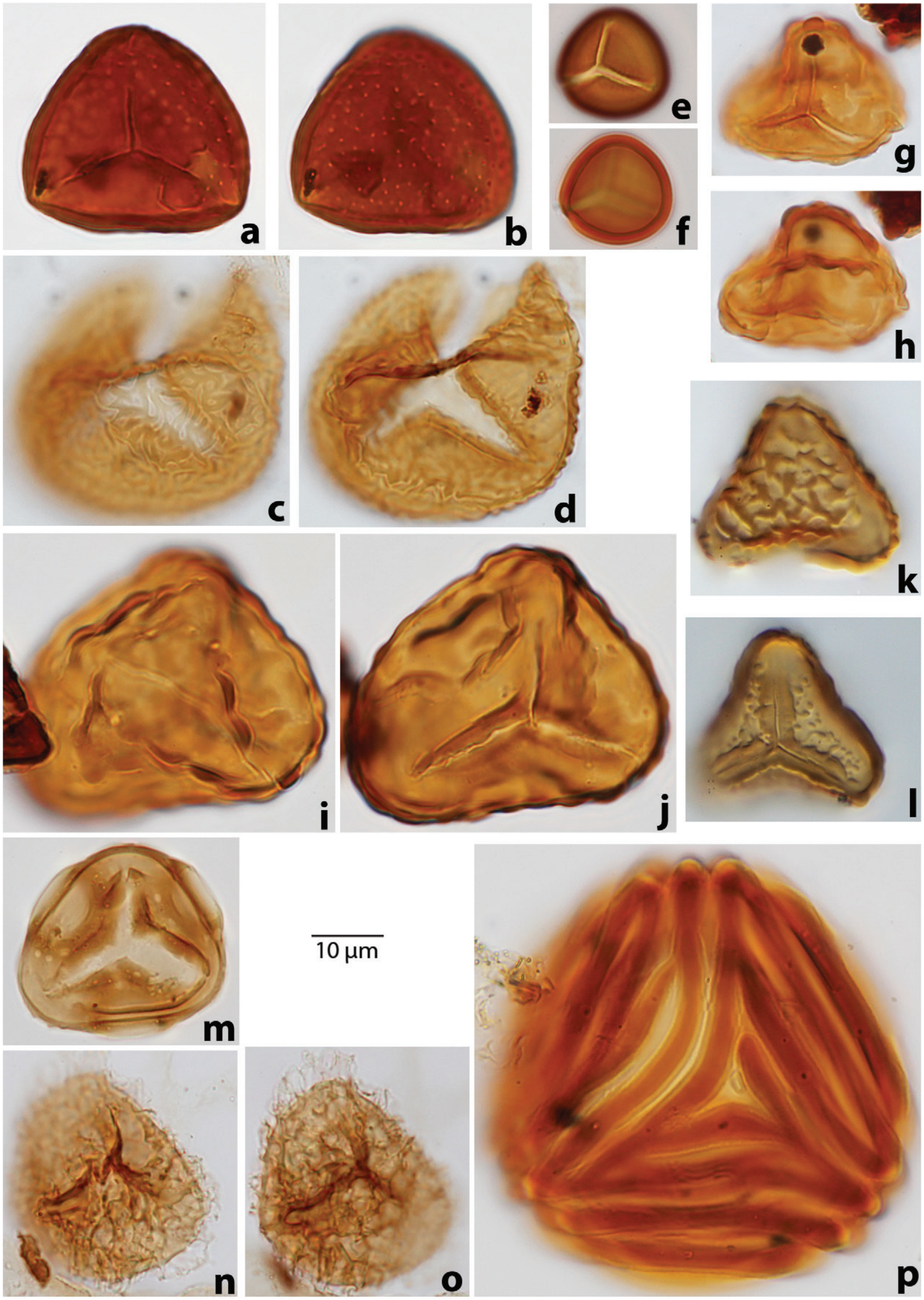
a
b
e
f
g
h
c
d
k
i
j
l
m
10 µm
n
o
p

PLATE 6. (*Opposite page*)

(**a, b**) *Neoraistrickia dubia* sp. nov. (Holotype), sample 22326, EF J14;

(**c, d**) *Neoraistrickia dubia* sp. nov. (Paratype), sample 22293, EF K50-1/2;

(**e, f**) *Nijssenosporites fossulatus* Lorente 1986, sample 22402, EF G8-1;

(**g, h**) *Polypodiaceoisporites pseudopsilatus* Lorente 1986, sample 22170, EF E9;

(**i**) *Psilatriletes delicatus* sp. nov. (Holotype), sample 22257, EF P39-2;

(**j**) *Psilatriletes delicatus* sp. nov. (Paratype), sample 22148, EF M6-3/4;

(**k**) *Psilatriletes lobatus* Hoorn 1994, sample 22446, EF M40-1/2;

(**l, m**) *Psilatriletes marginatus* sp. nov. (Holotype), sample 22277, EF D50-2;

(**n**) *Psilatriletes marginatus* sp. nov. (Paratype), sample 22277, EF H25-3/4;

(**o**) *Psilatriletes* sp. <25 µm, sample 22267, EF T46-4;

(**p**) *Psilatriletes* sp. 25–50 µm, sample 22140, EF U42-3/4;

(**q**) *Psilatriletes* sp. >50 µm, sample 22318, EF J11.

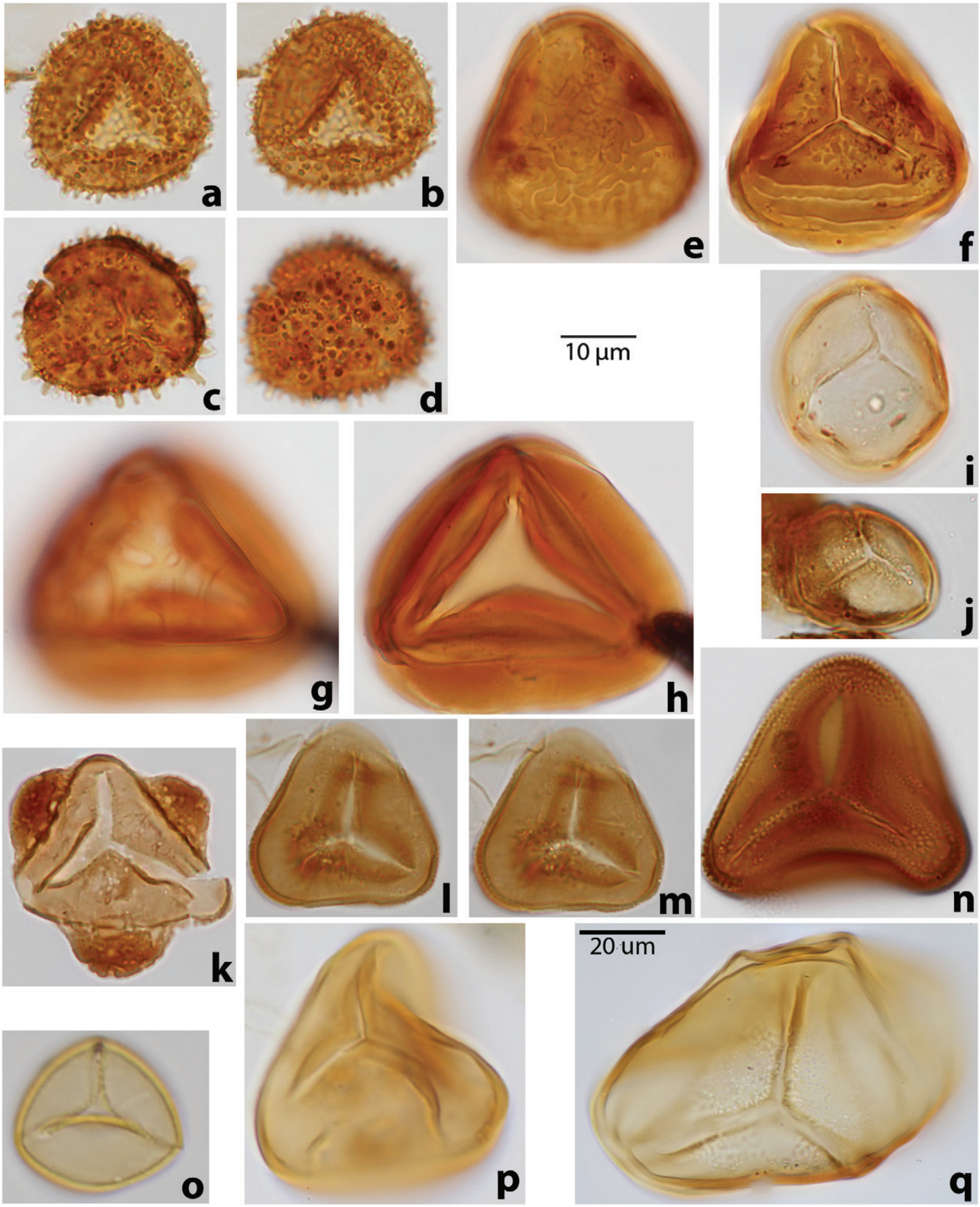
a
b
c
d
e
f
10 μm
i
j
g
h
k
l
m
n
20 um
o
p
q

PLATE 7. (*Opposite page*)

(**a, b**) *Pteridaceoisporis gemmatus* Silva-Caminha et al., 2010, sample 22278, EF N48-2;

(**c, d**) *Retitriletes altimuratus* Silva-Caminha et al., 2010, sample 22138, EF G31;

(**e, f**) *Rotverrusporites amazonicus* sp. nov. (Holotype), sample 22277, EF E49-1;

(**g, h**) *Rotverrusporites amazonicus* sp. nov. (Paratype), sample 22279, EF G8-4;

(**i, j**) *Striatriletes saccolomoides* Jaramillo et al., 2011, sample 22170, EF Q39-1/2;

(**k, l**) *Verrucatotriletes pseudovirueloides* sp. nov. (Holotype), sample 22278, EF O9-3/4;

(**m, n**) *Verrucatotriletes etayoi* Dueñas, 1980, sample 22326, EF K11-2.

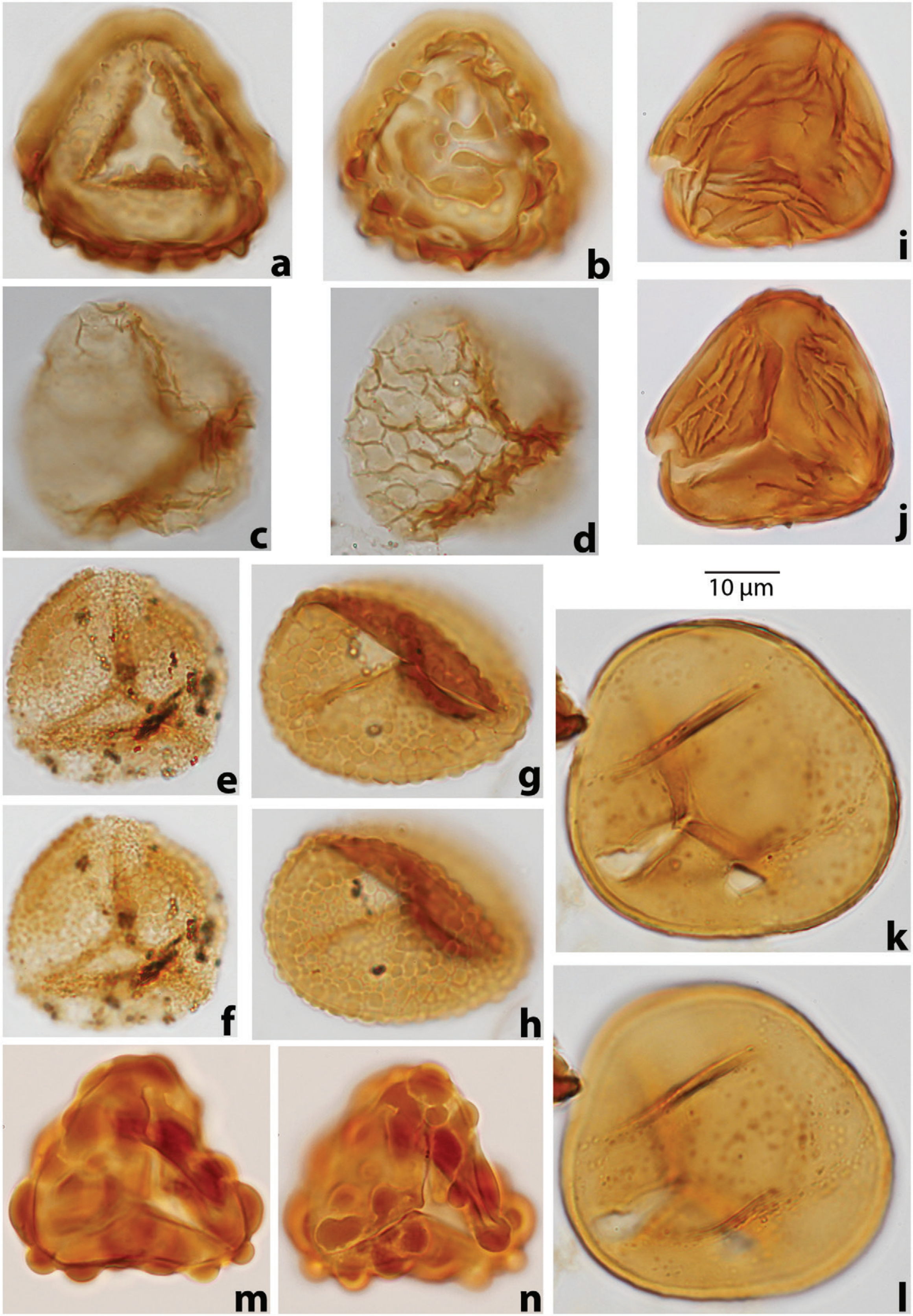
a
b
i
c
d
j
10 µm
e
g
k
f
h
m
n
l

PLATE 8. (*Opposite page*)

(**a**) *Clavainaperturites microclavatus* Hoorn, 1994a, sample 22277, EF K46-2/4;

(**b, c***) *Crotonoidaepollenites reticulatus* Silva-Caminha et al., 2010, sample 22278, EF J7;

(**d**) *Inaperturopollenites tectatus* sp. nov. (Holotype), sample 22278, EF T50;

(**e, f**) *Podocarpidites* sp., **e**: sample 22277, EF T15-1/3; **f**: sample 22276, EF J50-4;

(**g–j**) *Polyadopollenites macroreticulatus* Salard-Cheboldaeff 1974, **g, h**: sample 22358, EF C17-3; **i, j**: sample 22460, EF L10-4;

(**k**) *Polyadopollenites mariae* Dueñas, 1980, sample 22448, EF J49-1/3;

(**l, m**) *Polyadopollenites minimus* sp. nov. (Holotype), sample 22158, EF H39-3;

(**n**) *Polyadopollenites minimus* sp. nov. (Paratype), sample 22140, EFT8-1/2;

(**o**) *Arecipites invaginatus* sp. nov. (Holotype), sample 22460, EF P20-4;

(**p**) *Arecipites perfectus* Silva-Caminha et al. 2010, sample 22422, EF R20-1/3;

(**q**) *Arecipites regio* (Van der Hammen and García, 1966) Jaramillo and Dilcher, 2001, sample 22158, EF R8/4.

*Taken with DIC (differential interference contrast).

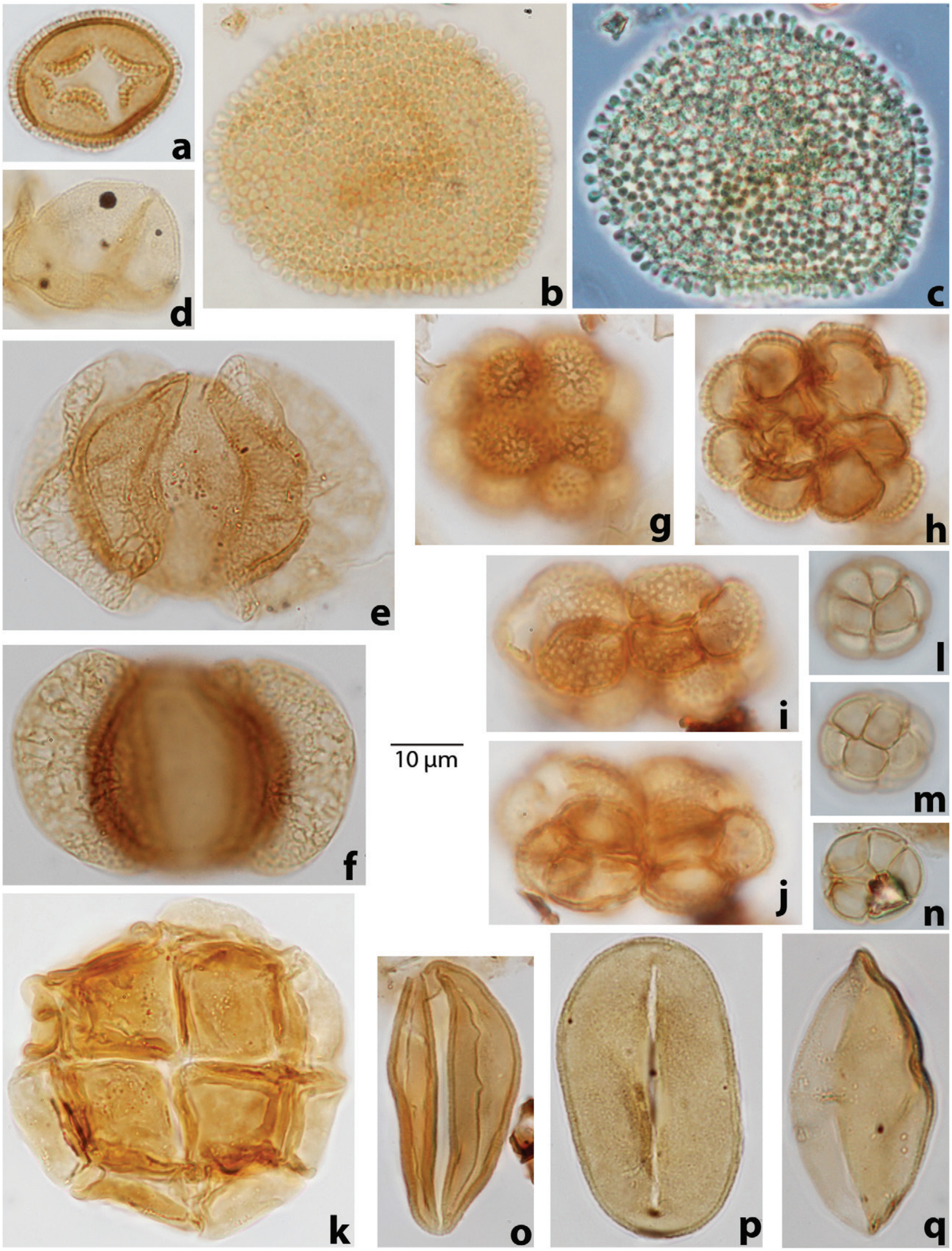
a
b
c
d
e
f
g
h
i
j
k
l
m
n
o
p
q
10 µm

PLATE 9. (*Opposite page*)

(**a, b**) *Clavamonocolpites lorentei* Muller et al. 1987, sample 22277, EF P20-2;

(**c**) *Longapertites microfoveolatus* Jan du Chêne and Adegoke, 1978 (in Adegoke et al., 1978), sample 22140, EF L5-1/3;

(**d, e**) *Mauritiidites franciscoi* var. *franciscoi* (Van der Hammen, 1956a) Van Hoeken-Klinkenberg, 1964, sample 22170, EF P32;

(**f**) *Mauritiidites franciscoi* var. *minutus* Van der Hammen and García, 1966, sample 22287, EF T8/3;

(**g**) *Mauritiidites franciscoi* var. *pachyexinatus* Van der Hammen and García, 1966, sample 22287, EF S11/1;

(**h**) *Psilamonocolpites amazonicus* Hoorn, 1993, sample 22282, EF W18-2;

(**i, j**) *Psilamonocolpites medius* (Van der Hammen, 1956a) Van der Hammen and García, 1966; **i**: sample 22278, EF K5-4; **j**: sample 22272, EF K6-3;

(**k**) *Psilamonocolpites nanus* Hoorn, 1993, sample 22418, EF D16-4;

(**l, m**) *Proxapertites psilatus* Sarmiento, 1992, **l**: 22303, EF F20-1; **m**: sample 22418, EF G20-1/2;

(**n**) *Proxapertites tertiaria* Van der Hammen and García, 1966, sample 22278, EF S23-3;

(**o–q**) *Retimonocolpites absyae* Hoorn, 1993, **o**: sample 22140, EF N12-4; **p, q**: sample 22402, EF U37-3;

(**r**) *Retimonocolpites maximus* Hoorn 1993, samples 22272, EF T6.

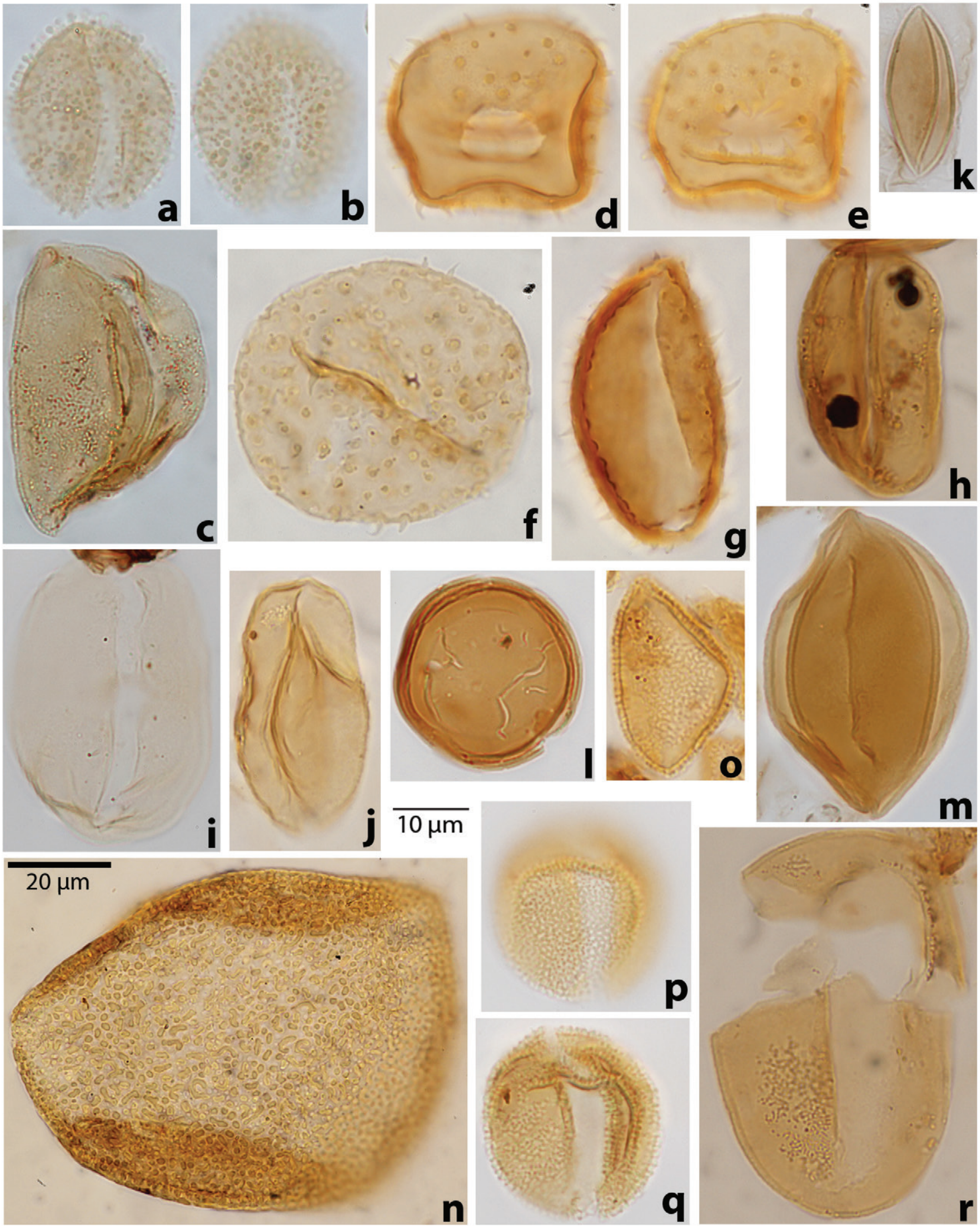
a
b
d
e
k
c
f
g
h
i
j
l
o
m
10 µm
20 µm
n
p
q
r

PLATE 10. (*Opposite page*)

(**a**) *Luminidites amazonicus* sp. nov. (Holotype), sample 22140, EF D32-3;

(**b**) *Trichotomosulcites normalis* sp. nov. (Holotype), sample 22405, EF Q42-1;

(**c, d**) *Grimsdalea magnaclavata* Germeraad et al., 1968, sample 22320, M46-4;

(**e**) *Monoporopollenites annulatus* (Van der Hammen, 1954) Jaramillo and Dilcher, 2001, sample 22140, EF K7-3/4;

(**f, g**) *Monoporopollenites scabratus* Leite et al. 2021, sample 22140, EF F36;

(**h**) *Dicolpopollis? costatus* sp. nov. (Holotype), sample 22460, EF D48-2;

(**i, j**) *Dicolpopollis? costatus* sp. nov. (Paratype), sample 22460, EF S20;

(**k**) *Multimarginites vanderhammeni* Germeraad et al. 1968, sample 22140, EF F13-3;

(**l**) *Cyclusphaera scabrata* Jaramillo and Dilcher 2001, sample 22518, EF W41-4;

(**m–o**) *Echidiporites barbeitoi* Muller et al., 1987 emend., **m**: sample 22290, EF J18-3; **n, o**: sample 22282, EF T14-3;

(**p**) *Psiladiporites minimus* Van der Hammen and Wymstra, 1964, sample 22381, EF W24;

(**q**) *Psiladiporites redundantis* González-Guzmán, 1967, sample 22170, EF E35;

(**r**) *Crototricolpites annemariae* Leidelmeyer, 1966, sample 22445, EF S9-4;

(**s**) *Crototricolpites finitus* Silva-Caminha et al. 2010, sample 22282, Q17-2/4.

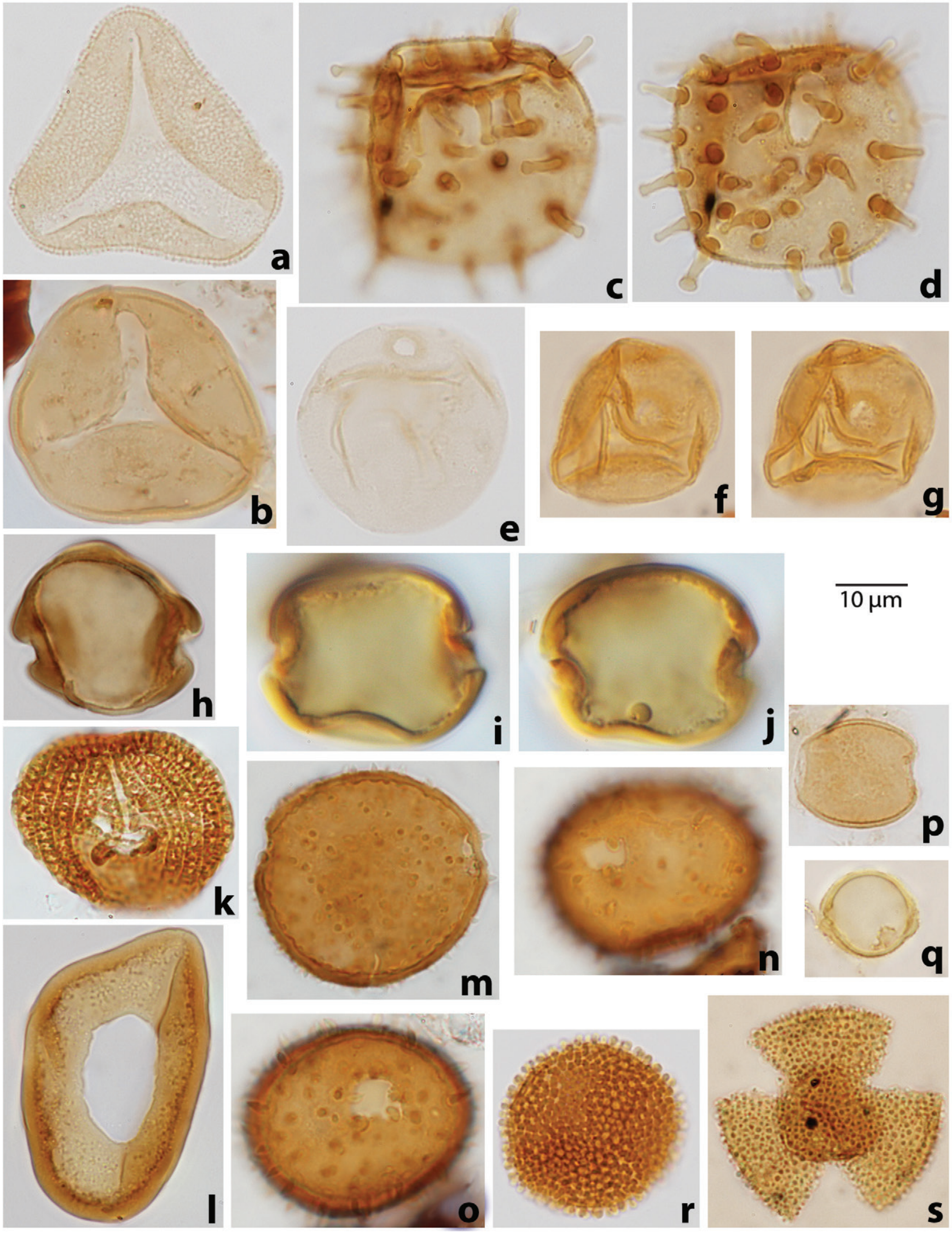
a
c
d
b
e
f
g
h
i
j
10 µm
p
k
m
n
q
l
o
r
s

PLATE 11. (*Opposite page*)

(**a, b**) *Foveotricolpites colpiconstrictus* Hoorn, 1994b, comb. nov., sample 22140, EF T9-1;

(**c–e**) *Foveotricolpites simplex* González-Guzmán, 1967 comb. nov., **c, d**: sample 22418, EF X17; **e**: 22436, EF L10-1/2;

(**f, g**) *Ladakhipollenites campbellii* sp. nov. (Holotype), sample 2257, EF K45-3;

(**h**) *Ladakhipollenites campbellii* sp. nov. (Paratype), sample 22140, EF D16-1/2;

(**i, j**) *Ladakhipollenites floratus* Silva-Caminha et al., 2010, sample 22282, EF R11-1;

(**k, l**) *Ladakhipollenites colpiconstrictus* Van Hoeken-Klinkenberg, 1966, comb. nov., sample 22290, EF U10-1/2;

(**m, n**) *Ladakhipollenites nanus* sp. nov. (Holotype), sample 22148, EF G12;

(**o**) *Loranthacites tabatingensis* sp. nov. (Holotype), sample 22375, EF K9-4;

(**p**) *Loranthacites tabatingensis* sp. nov. (Paratype), sample 22445, EF R49-3;

(**q, r**) *Perfotricolpites digitatus* González-Guzmán, 1967, **q**: sample 22318, EF H11-3/4; **r**: sample 22279, EF W31-2/4.

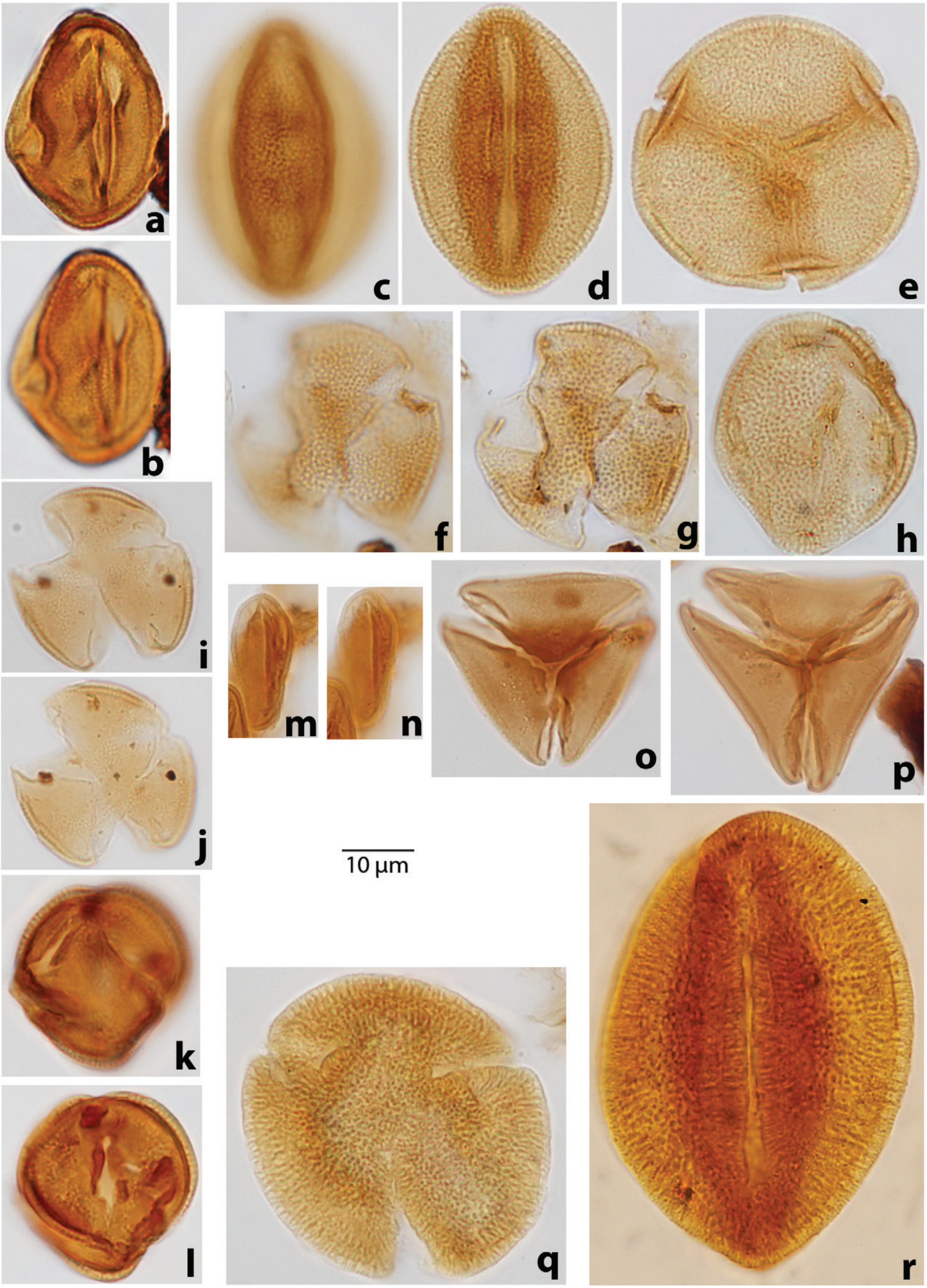
a
b
c
d
e
f
g
h
i
j
m
n
o
p
10 µm
k
l
q
r

PLATE 12. (*Opposite page*)

(**a**) *Retibrevitricolpites pseudoretibolus* sp. nov. (Holotype), sample 22140, EF W13-2;

(**b**) *Retibrevitricolpites pseudoretibolus* sp. nov. (Paratype), sample 22287, EF H8-1/2;

(**c**) *Retitrescolpites magnus* (González-Guzmán, 1967) Jaramillo and Dilcher, 2001, sample 22257, EF R42-1;

(**d, e**) *Retibrevitricolporites*? *toigoae* Leite et al., 2021, sample 22158, EF R12-3;

(**f, g**) *Rhoipites? colpiverrucosus* sp. nov. (Holotype), sample 22522, EF H10-2;

(**h**) *Spirosyncolpites spiralis* González-Guzmán, 1967, sample 22170, EF F13;

(**i, j**) *Tricolpites? pseudoclarensis* Silva-Caminha et al., 2010, **i**: sample 22278, EF O20-4; **j**: sample 22282, EF Z36;

(**k**) *Bombacacidites araracuarensis* Hoorn, 1994b, sample 22349, EF V7-3/4;

(**l**) *Bombacacidites baculatus* Muller et al., 1987, sample 22381, EF H14-3;

(**m**) *Bombacacidites brevis* (Dueñas, 1980) Muller et al., 1987, sample 22481, EF J15-1.

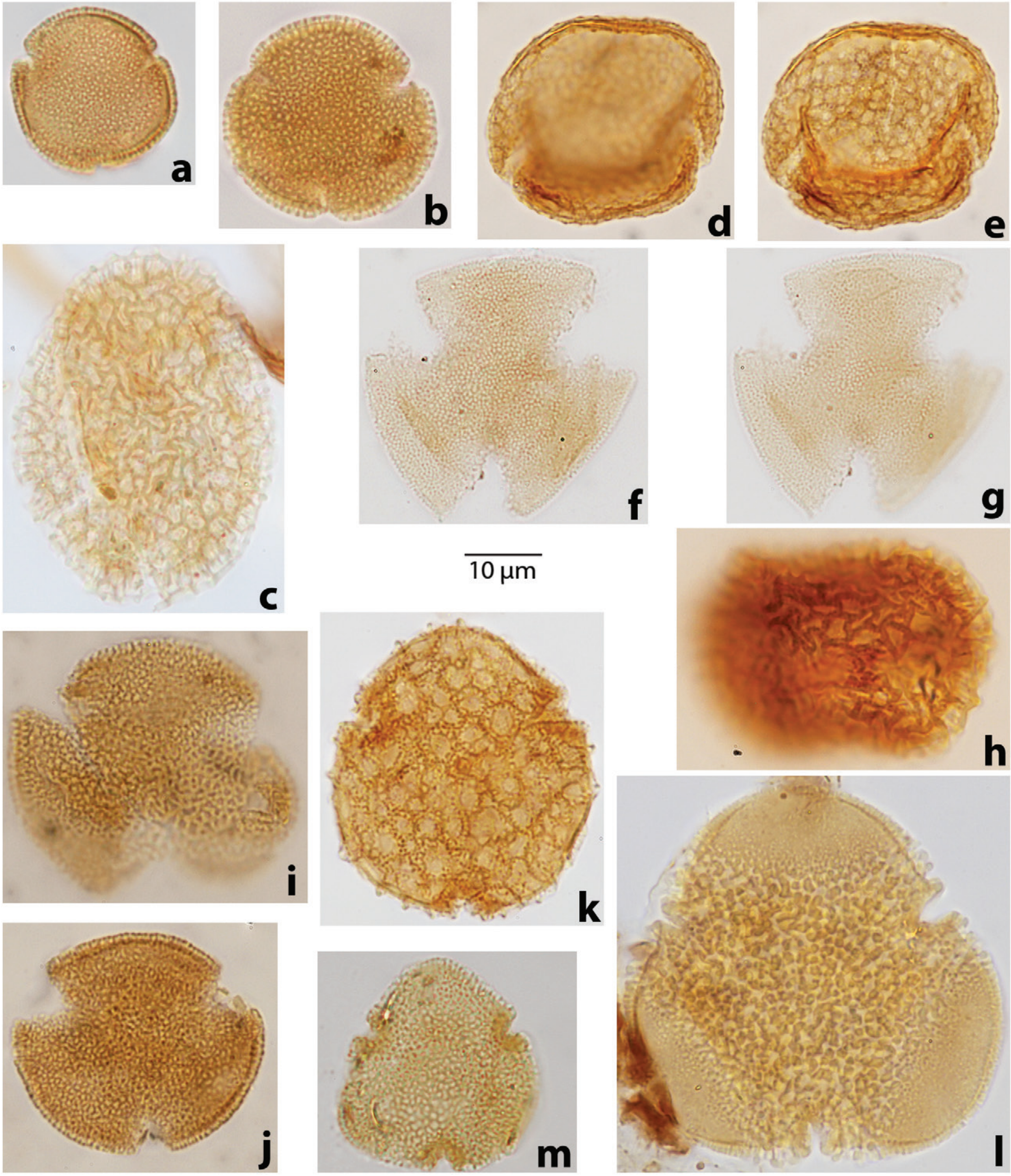
a
b
d
e
c
f
g
10 µm
h
i
k
l
j
m

PLATE 13. (*Opposite page*)

(**a, b**) *Bombacacidites hooghiemstrae* sp. nov. (Holotype), sample 22522, EF S41-4;

(**c**) *Bombacacidites lorenteae* Hoorn, 1993, comb. nov., sample 22140, EF P11-3;

(**d**) *Bombacacidites muinaneorum* Hoorn ,1993, sample 22402, EF M50-3;

(**e**) *Bombacacidites nacimientoensis* (Anderson, 1960) Elsik, 1968, sample 22398, EF L40;

(**f, g**) *Brevicolporites molinae* (Schuler and Doubinger, 1970) Salard-Cheboldaeff, 1978, sample 22412, EF M42;

(**h, i**) *Cichoreacidites*? *flammulatus* Leite et al., 2021, sample 22318, EF E46-2;

(**j**) *Cichoreacidites longispinosus* (Lorente 1986) Silva-Caminha et al., 2010, sample 22278, EF N43-1;

(**k, l**) *Crassiectoapertites columbianus* (Dueñas, 1980) Lorente, 1986, sample 22140, EF K36;

(**m, n**) *Echitricolporites mcneillyi* Germeraad et al., 1968, sample 22298, EF M46-4;

(**o, p**) *Echitricolporites spinosus* Van der Hammen, 1956b, sample 22287, EF N40-2.

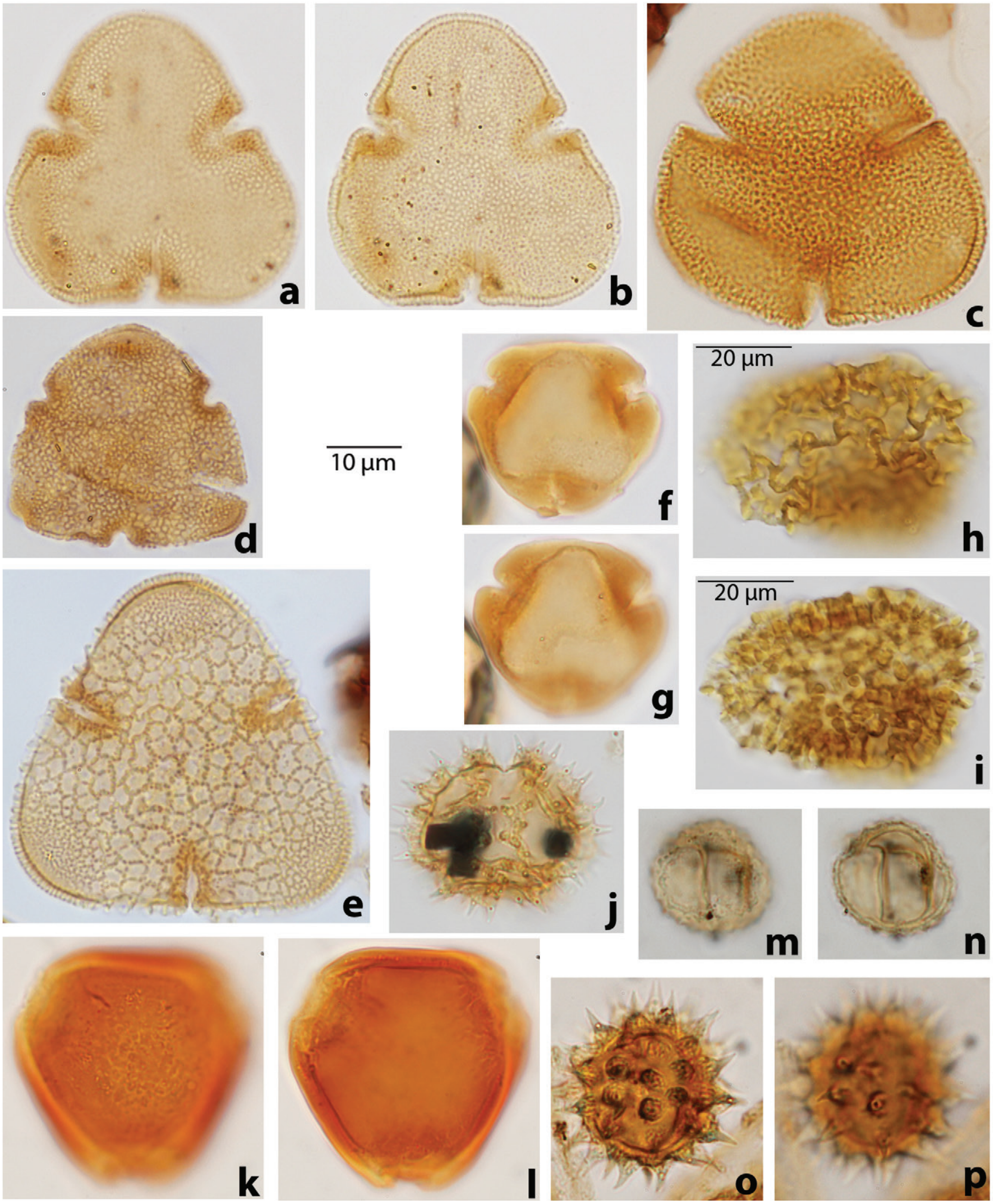
a
b
c
d
10 µm
f
20 µm
h
g
20 µm
i
e
j
m
n
k
l
o
p

PLATE 14. (*Opposite page*)

(**a, b**) *Ericipites annulatus* González-Guzmán, 1967, sample 22157, EF V42;

(**c**) *Foveotricolporites pseudodubiosus* Silva-Caminha et al., 2010, sample 22277, EF E22-1/2;

(**d, e**) *Ilexpollenites tropicallis* Silva-Caminha et al., 2010, **d**: sample 22272, EF G44-2; **e**: sample 22277, EF N7;

(**f**) *Ladakhipollenites? caribbiensis* (Muller et al., 1987) Silva-Caminha et al., 2010, sample 22344, EF P46-1;

(**g**) *Ladakhipollenites? pseudocolpiconstrictus* sp. nov. (Holotype), sample 22140, EF L-9;

(**h, i**) *Ladakhipollenites? pseudocolpiconstrictus* sp. nov. (Paratype), sample 22518, EF N6-3;

(**j, k**) *Ladakhipollenites? corvattatus* sp. nov. (Holotype), sample 22287, EF H11-3;

(**l, m**) *Ladakhipollenites? endoporatus* sp. nov. (Holotype), sample 22522, EF P13-1;

(**n–p**) *Ladakhipollenites? garzoni* Hoorn, 1993 comb. nov., **n, o**: sample 22140, EF M11-3/4; **p**: sample 22140, U12;

(**q, r**) *Ladakhipollenites*? *lolongatus* D'Apolito et al., 2019, sample 22290, EF R37;

(**s, t**) *Ladakhipollenites*? *sphaericus* sp. nov. (Holotype), sample 22140, EF X7-1;

(**u, v**) *Lakhiapollis costatus* Silva-Caminha et al., 2010, sample 22290, EF V17.

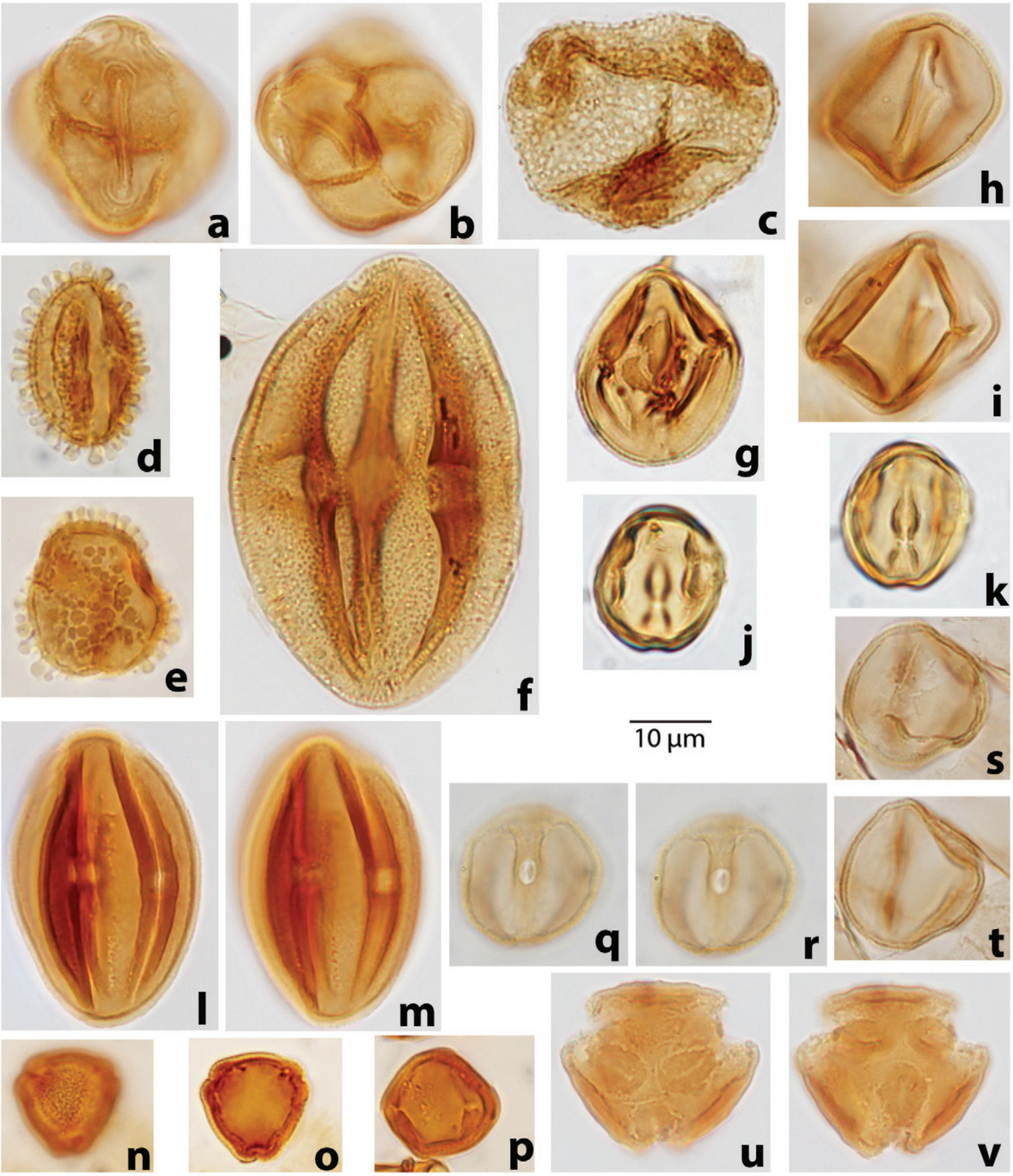
a
b
c
h
d
f
g
i
k
e
j
10 µm
s
l
m
q
r
t
n
o
p
u
v

PLATE 15. (*Opposite page*)

(**a, b**) *Lanagiopollis crassa* (Van der Hammen and Wymstra, 1964) Frederiksen, 1988, sample 22460, Q50-2;

(**c, d**) *Malvacipolloides echibaculatus* Leite et al., 2021, sample 22287, EF L8;

(**e, f**) *Malvacipolloides maristellae* (Muller et al., 1987) Silva-Caminha et al., 2010, sample 22293, EF Y42-1;

(**g–j**) *Malvacipolloides romeroae* Leite et al., 2021, **g, h**: sample 22279, EF D10-2; **i, j**: sample 22365, EF S9-2;

(**k–m**) *Margocolporites bilinearis* sp. nov. (Holotype), sample 22290, EF L45-2;

(**n, o**) *Margocolporites carinae* Leite et al., 2021, sample 22140, EF Q20-4;

(**p, q**) *Margocolporites incertus* sp. nov. (Holotype), sample 22434, EF N53-3/4;

(**r, s**) *Margocolporites vanwijhei* Germeraad et al., 1968, sample 22279, F22-4.

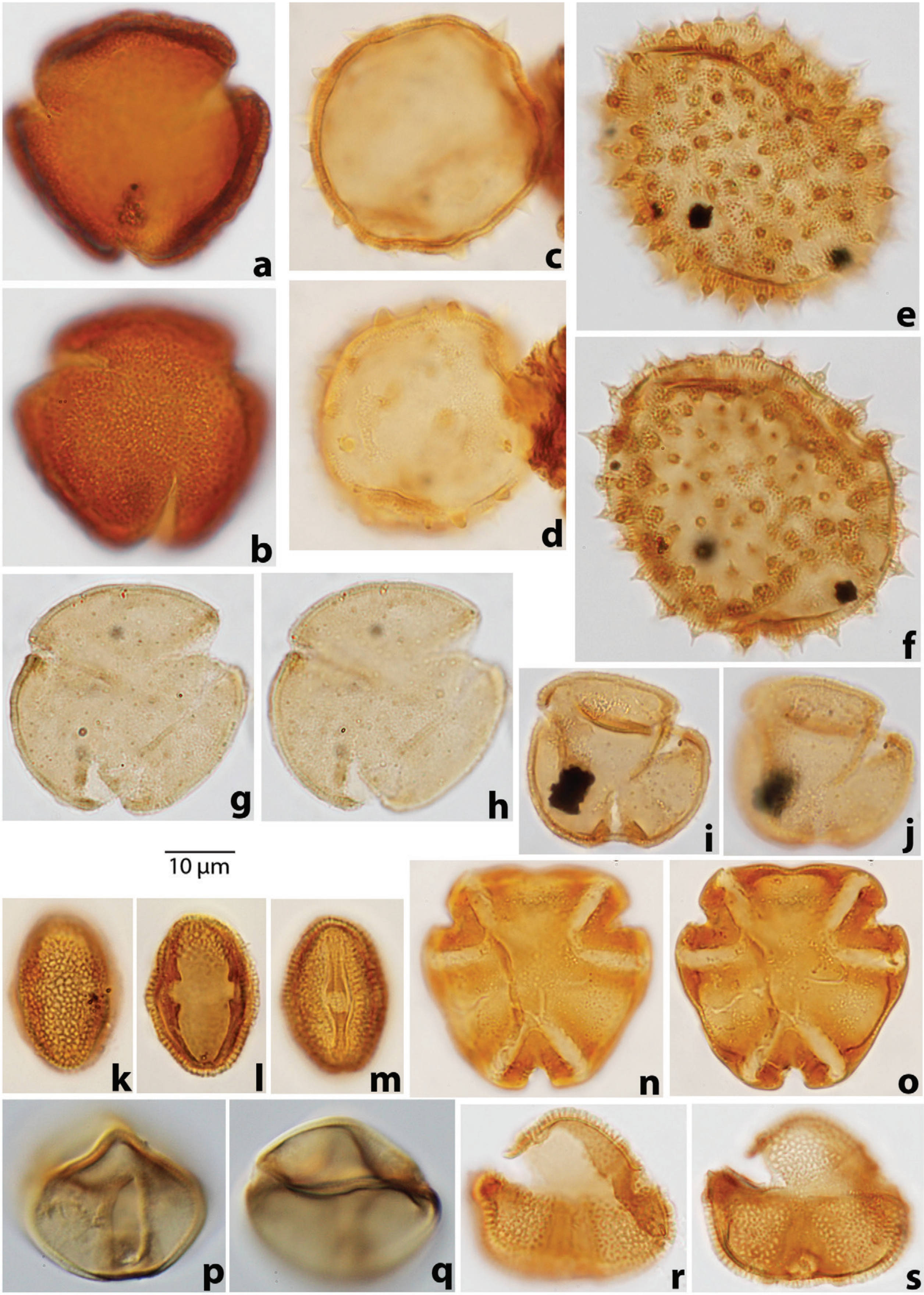
a
b
c
d
e
f
g
h
i
j
10 µm
k
l
m
n
o
p
q
r
s

PLATE 16. (*Opposite page*)

(**a–c**) *Multiareolites*? *reticulatus* Leite et al., 2021, sample 22344, EF L6;

(**d, e**) *Myrtaceidites* sp., sample 22140, EF M19-2;

(**f, g**) *Paleosantalaceaepites kaarsii* Hoorn, 1993, comb. nov., sample 22434, EF E40;

(**h–j**) *Psilabrevitricolporites devriesii* (Lorente, 1986) Silva-Caminha et al., 2010, **h**, **i**: sample 22456, EF E15-1; **j**: sample 22456, EF Q22-7;

(**k, l**) *Paleosantalaceaepites cingulatus* Jaramillo et al., 2011, sample 22277, EF L11-2;

(**m–o**) *Psilatricolporites* cf. *vanus* González-Guzmán, 1967, **m**, **n**: sample 22436, EF K37-2/4; **o**: sample 22434, EF V23-2;

(**p**) *Ranunculacidites operculatus* (Van der Hammen and Wymstra, 1964) Jaramillo and Dilcher, 2001, sample 22445, EF S6-3;

(**q, r**) *Ranunculacidites pontoreticulatus* sp. nov. (Holotype), sample 22518, EF L16-1;

(**s**) *Ranunculacidites pontoreticulatus* sp. nov. (Paratype), sample 22518, EF L9-3.

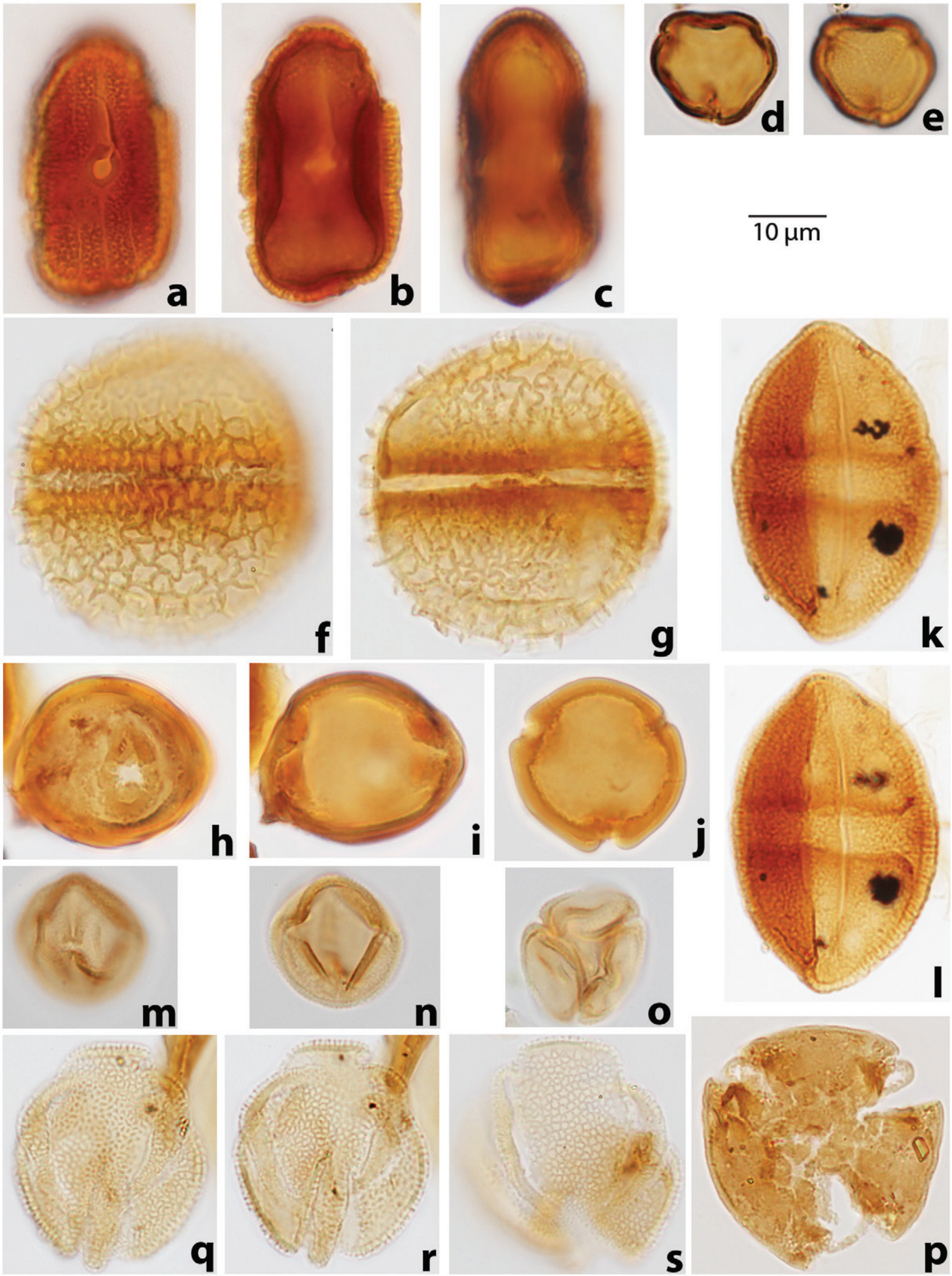
a
b
c
d
e
10 µm
f
g
k
h
i
j
l
m
n
o
q
r
s
p

PLATE 17. (*Opposite page*)

(**a, b**) *Retibrevitricolporites retibolus* Leidelmeyer, 1966, **a**: sample 22278, EF K39-4; **b**: sample 22405, EF V8;

(**c–f**) *Retibrevitricolporites solimoensis* Hoorn, 1993 comb. nov., **c, d**: sample 22140, EF H25; **e, f**: sample 22140, EF D10-1/3;

(**g, h**) *Retibrevitricolporites yavarensis* (Hoorn, 1993) Silva-Caminha et al., 2010, sample 22358, EF V44-1;

(**i, j**) *Retitrescolpites benjaminensis* sp. nov. (Holotype), sample 22522, EF G12-4;

(**k, l**) *Retitrescolpites benjaminensis* sp. nov. (Paratype), sample 22506, EF H14;

(**m**) *Retitrescolpites brevicolpatus* sp. nov. (Holotype), sample 22506, EF R5-2;

(**n, o**) *Retitrescolpites grossus* sp. nov. (Holotype), sample 22503, EF U8-1;

(**p–r**) *Retitrescolpites kriptoporus* sp. nov. (Holotype), sample 22445, EF Q9-3;

(**s–u**) *Retitrescolpites marginatus* sp. nov. (Holotype), sample 22518, EF N25-2;

(**v, w**) *Retitrescolpites? irregularis* (Van der Hammen and Wymstra, 1964) Jaramillo and Dilcher, 2001, sample 22405, EF E12.

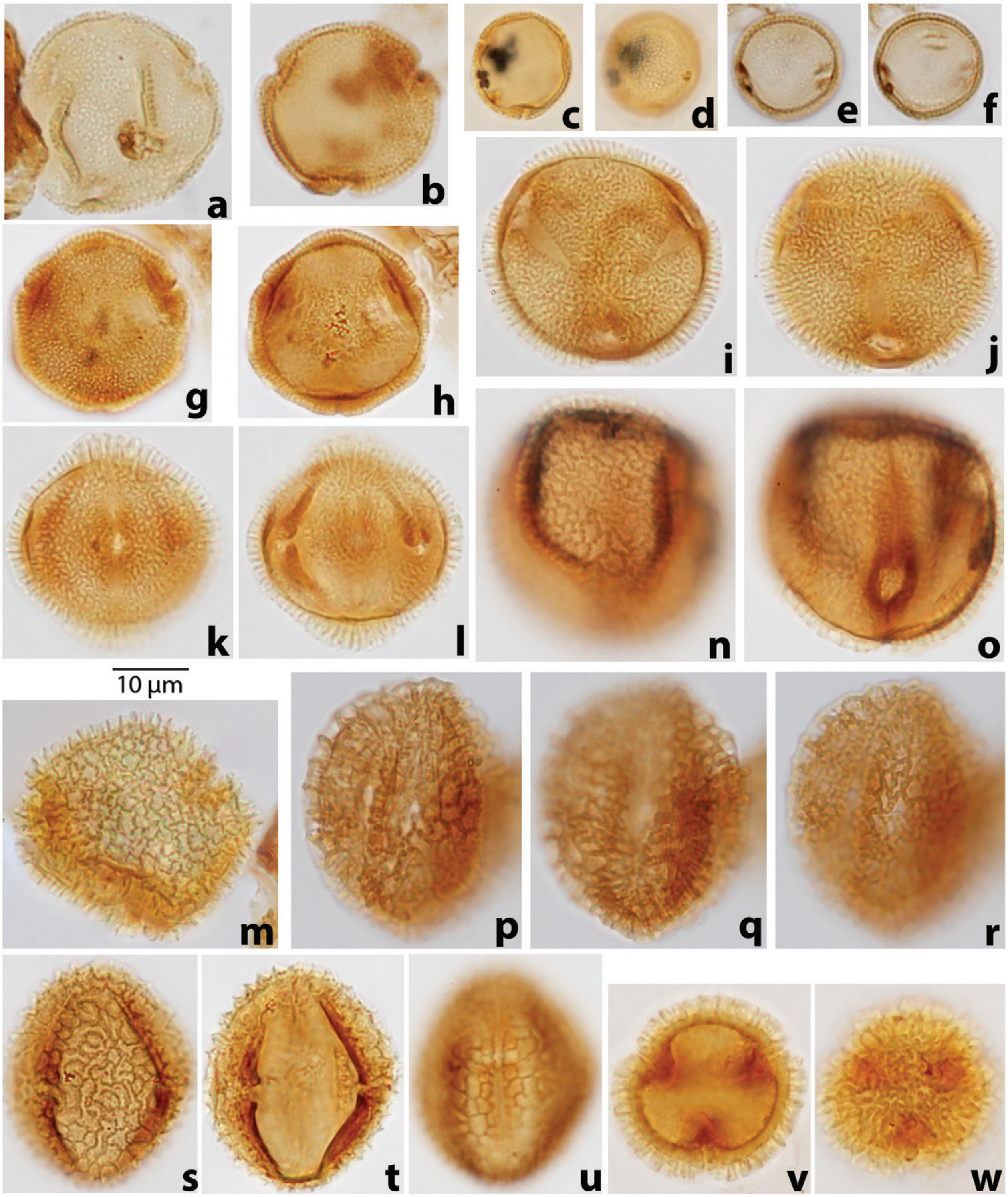
a
b
c
d
e
f
g
h
i
j
k
l
n
o
10 µm
m
p
q
r
s
t
u
v
w

PLATE 18. (*Opposite page*)

(**a, b**) *Retitrescolpites? traversei* Silva-Caminha et al., 2010, sample 22170, EF E14-3;

(**c, d**) *Rhoipites caputoi* Hoorn, 1993 comb. nov., sample 22412, EF P12-4;

(**e, f**) *Rhoipites vilis* sp. nov. (Holotype), sample 22164, EF P7;

(**g, h**) *Rhoipites vilis* sp. nov. (Paratype), sample 22272, EF S39;

(**i, j**) *Rhoipites crassicostatus* Van der Hammen and Wymstra, 1964 comb. nov., sample 22140, EF T17-3;

(**k–m**) *Rhoipites crassinexinicus* sp. nov. (Holotype), sample 22158, EF P46-4;

(**n**) *Rhoipites crassinexinicus* sp. nov. (Paratype), sample 22158, N38-3/4;

(**o, p**) *Rhoipites crassitectatus* sp. nov. (Holotype), sample 22290, EF M17;

(**q–s**) *Rhoipites grossomurus* sp. nov. (Holotype), sample 22422, EF Q21-2;

(**t**) *Rhoipites grossomurus* sp. nov. (Paratype), sample 22386, EF L43-2;

(**u, v**) *Rhoipites guianensis* (Van der Hammen and Wymstra, 1964) Jaramillo and Dilcher, 2001, sample 22456, EF G18-4;

(**w, x**) *Rhoipites guttatus* sp. nov. (Holotype), sample 22277, EF H39-1;

(**y–bb**) *Rhoipites manausensis* D'Apolito et al., 2019, **y, z**: sample 22456, EF Q7-2; **aa, bb**: sample 22349, EF D40-2.

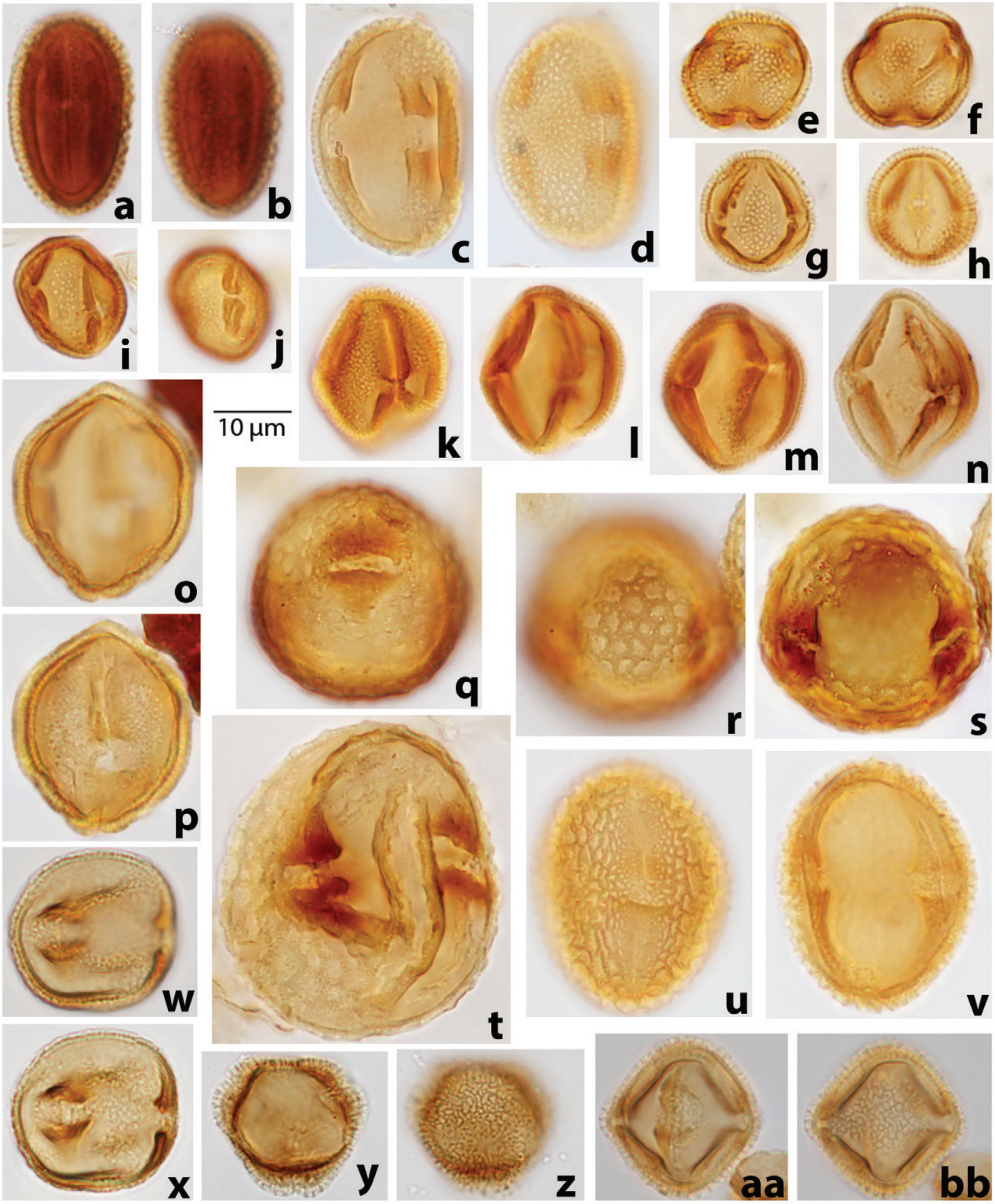
a
b
c
d
e
f
g
h
i
j
k
l
m
n
10 µm
o
p
q
r
s
t
u
v
w
x
y
z
aa
bb

PLATE 19. (*Opposite page*)

(**a, b**) *Rhoipites apertus* sp. nov. (Holotype), sample 22506, EF N14-1/2;

(**c, d**) *Rhoipites oblatus* Hoorn, 1994b, comb. nov., samples 22290, EF S45;

(**e, f**) *Rhoipites pseudoscabratus* sp. nov. (Holotype), sample 22518, EF G9;

(**g, h**) *Rhoipites lolongatus* sp. nov. (Holotype), sample 22386, EF T10-2;

(**i**) *Rhoipites protoguttatus* sp. nov. (Holotype), sample 22518, EF M17-3;

(**j, k**) *Rhoipites protoguttatus* sp. nov. (Paratype), sample 22522, EF O13-2;

(**l, m**) *Rhoipites pseudocrassopolaris* sp. nov. (Holotype), sample 22140, EF W10-4;

(**n, o**) *Rhoipites pseudopilatus* sp. nov. (Holotype), sample 22320, EF L44-3/4;

(**p, q**) *Rhoipites quantulus* sp. nov. (Holotype), sample 22287, EF T17-3;

(**r, s**) *Rhoipites ticuneorum* Hoorn, 1993, comb. nov., sample 22140, EF L14-2;

(**t, u**) *Rugutricolporites arcus* Hoorn, 1993, sample 22140, EF R24-2;

(**v–y**) *Rugutricolporites felix* González-Guzmán, 1967; **v, w**: samples 22290, EF K8-13; **x, y**: sample 22290, EF S31-3.

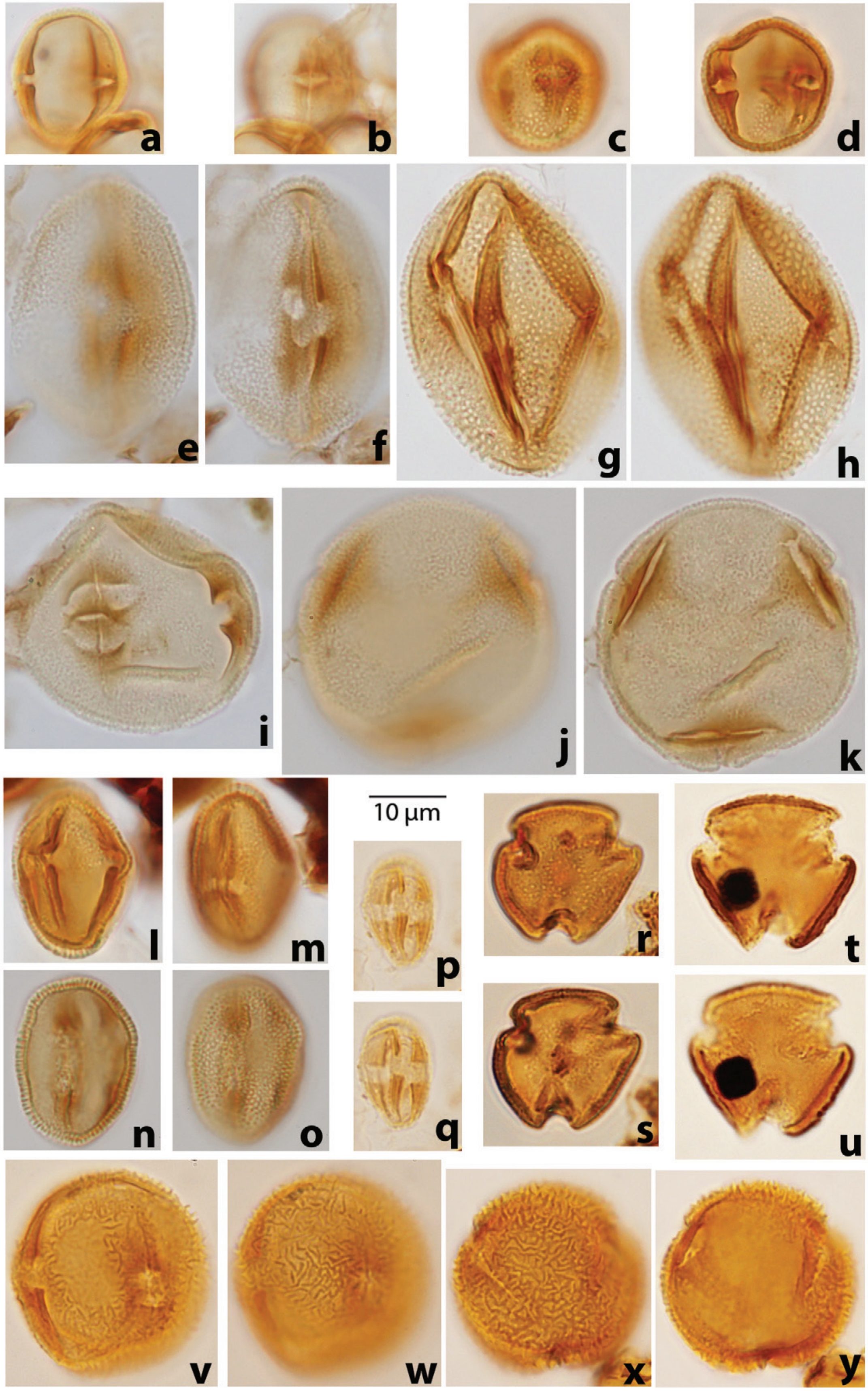
a
b
c
d
e
f
g
h
i
j
k
l
m
10 µm
p
r
t
n
o
q
s
u
v
w
x
y

PLATE 20. (*Opposite page*)

(**a, b**) *Siltaria dilcheri* Silva-Caminha et al., 2010, sample 22140, EF E7-2;

(**c, d**) *Siltaria santaisabelensis* (Hoorn, 1994b) Silva-Caminha et al., 2010, sample 22158, K20-1/2;

(**e–g**) *Striasyncolpites anastomosatus* Silva-Caminha et al., 2010, **e, f**: sample 22158, EF P35-4; **g**: sample 22158, EF P35-4;

(**h, i**) *Striatopollis catatumbus* (González-Guzmán, 1967) Takahashi and Jux, 1989, sample 22381, EF R15-3;

(**j, k**) *Striatopollis crassitectatus* sp. nov. (Holotype), sample 22140, EF Q7-3;

(**l**) *Striatopollis crassitectatus* sp. nov. (Paratype), sample 22282, EF H11-4;

(**m, n**) *Striatopollis poloreticulatus* Silva-Caminha et al., 2010, sample 22272, EF L8-2;

(**o, p**) *Syncolporites foveolatus* sp. nov. (Holotype), sample 22354, EF N9;

(**q, r**) *Syncolporites tenuicolpatus* sp. nov. (Holotype), sample 22290, EF E11-4;

(**s**) *Syncolporites tenuicolpatus* sp. nov. (Paratype), sample 22386, EF D23;

(**t, u**) *Syncolporites triangularis* Regali et al. 1974, sample 22354, EF K22-2.

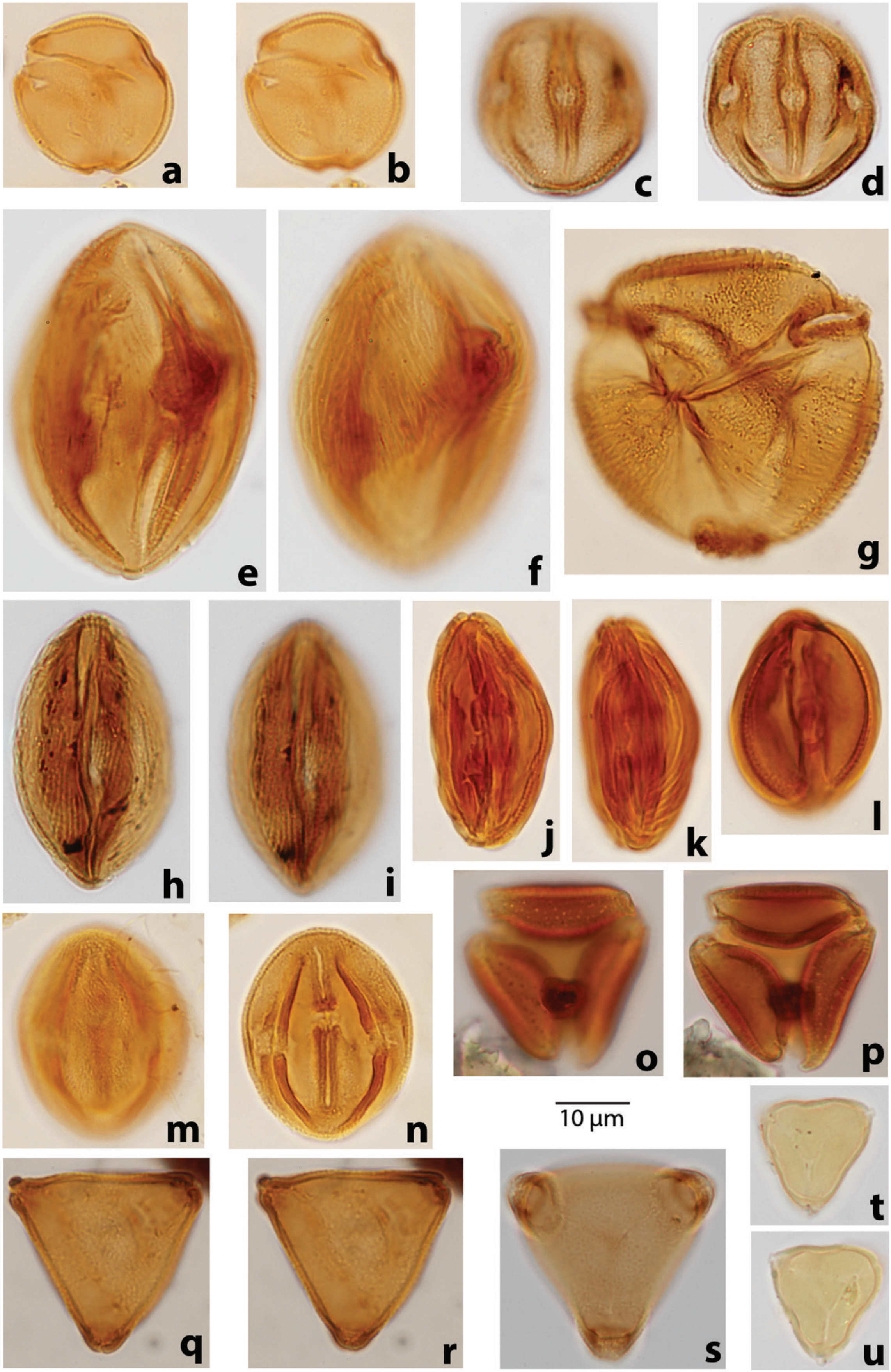
a
b
c
d
e
f
g
h
i
j
k
l
m
n
o
p
10 µm
q
r
s
t
u

PLATE 21. (*Opposite page*)

(**a**) *Tetracolporopollenites labiatus* Hoorn, 1993, comb. nov., sample 22140, L16-4;

(**b, c**) *Tetracolporopollenites magniporatus* Hoorn, 1993, comb. nov., sample 22336, EF E43-4;

(**d**) *Tetracolporopollenites nanus* sp. nov. (Holotype), sample 22320, EF D48;

(**e, f**) *Tetracolporopollenites obesus* Hoorn, 1993, comb. nov., sample 22140, EF V22-2;

(**g–j**) *Tetracolporopollenites silvaticus* Hoorn, 1993, comb. nov.; **g, h**: sample 22320, EF R13; **i, j**: sample 22170, EF R33-1;

(**k–m**) *Tetracolporopollenites xatanawensis* sp. nov. (Holotype), sample 22140, EF W35-1;

(**n**) *Tetracolporopollenites xatanawensis* sp. nov. (Paratype), sample 22256, EF O40-3-4;

(**o, p**) *Verrutricolporites pusillus* sp. nov. (Holotype), sample 22140, EF N37;

(**q, r**) *Verrutricolporites simplex* sp. nov. (Holotype), sample 22482, EF F10;

(**s, t**) *Verrutricolporites simplex* sp. nov. (Paratype), sample 22481, EF F48;

(**u, v**) *Verrutricolporites rotundiporus* Van der Hammen and Wymstra, 1964, sample 22140, EF K15;

(**w, x**) *Zonocostites ramonae* Germeraad et al., 1968, sample 22320, EF F11-2-4;

(**y, z**) *Byttneripollis rugulatus* nov. sp. (Holotype), sample 22277, EF L13-3;

(**aa, bb**) *Byttneripollis rugulatus* nov. sp. (Paratype), sample 22158, EF G20-1;

(**cc, dd**) *Byttneripollis ruedae* Silva-Caminha et al., 2010, sample 22422, EF O38-2.

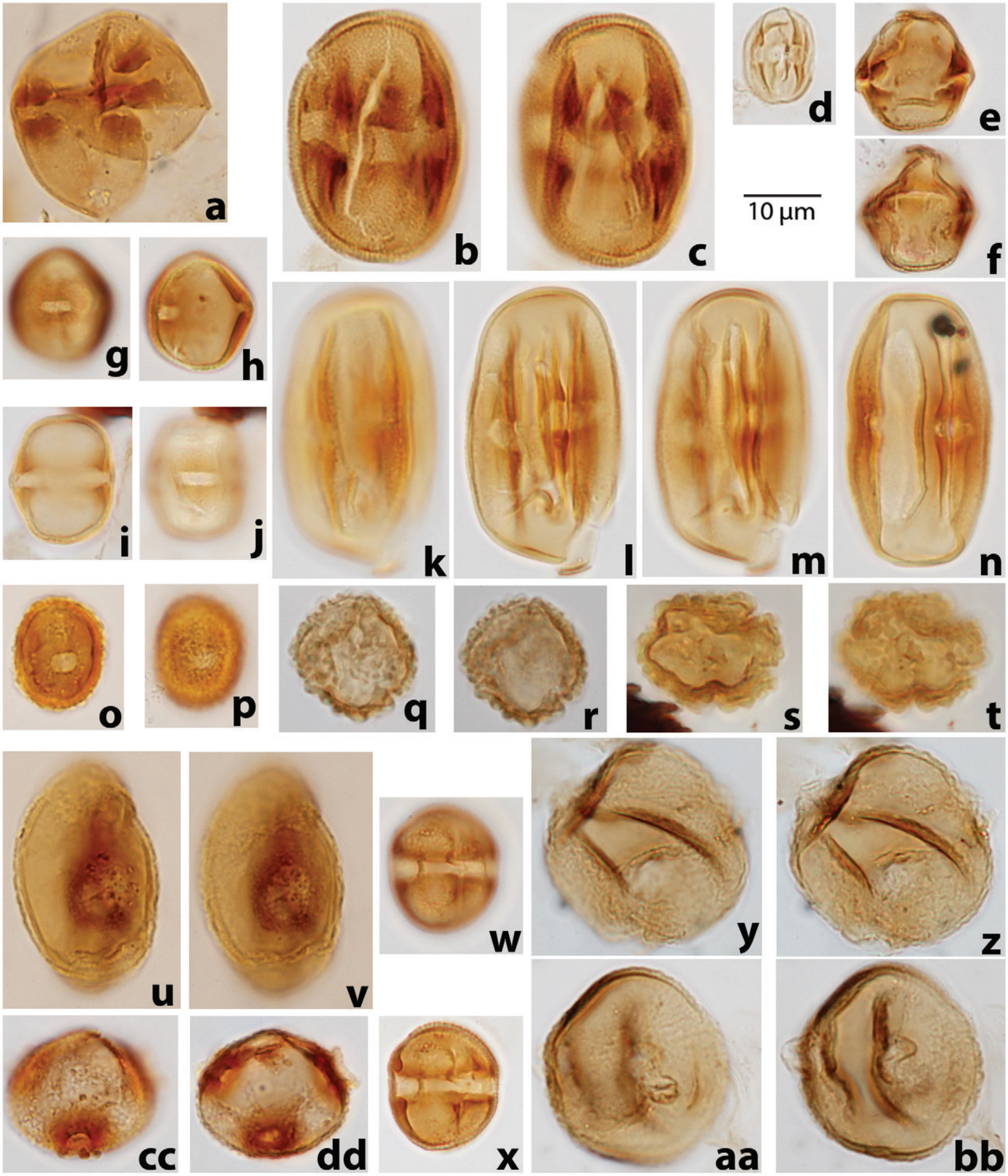
a
b
c
d
e
10 µm
f
g
h
i
j
k
l
m
n
o
p
q
r
s
t
u
v
w
y
z
cc
dd
x
aa
bb

PLATE 22. (*Opposite page*)

(**a**) *Corsinipollenites collaris* Silva-Caminha et al., 2010, sample 22398, EF M33-2;

(**b, c**) *Corsinipollenites oculusnoctis* (Thiergart, 1940) Nakoman, 1965, sample 22294, EF U46-2;

(**d**) *Corsinipollenites scabratus* Silva-Caminha et al., 2010, sample 22398, EF U36-2;

(**e, f**) *Echitriporites jolyi* Leite et al., 2021, sample 22164, EF T17;

(**g, h**) *Florschuetzia impostora* sp. nov. (Holotype), sample 22460, EF X8-3;

(**i**) *Florschuetzia impostora* sp. nov. (Paratype), sample 22460, EF V7-3;

(**j, k**) *Florschuetzia impostora* sp. nov. (specimen), sample 22460, EF C8-3;

(**l, m**) *Proteacidites poriscabratus* sp. nov. (Holotype), sample 22330, EF G41-1;

(**n**) *Proteacidites poriscabratus* sp. nov. (Paratype), sample 22326, EF C20-3;

(**o**) *Proteacidites pseudodehaanii* sp. nov. (Holotype), sample 22412, EF L9-1/3.

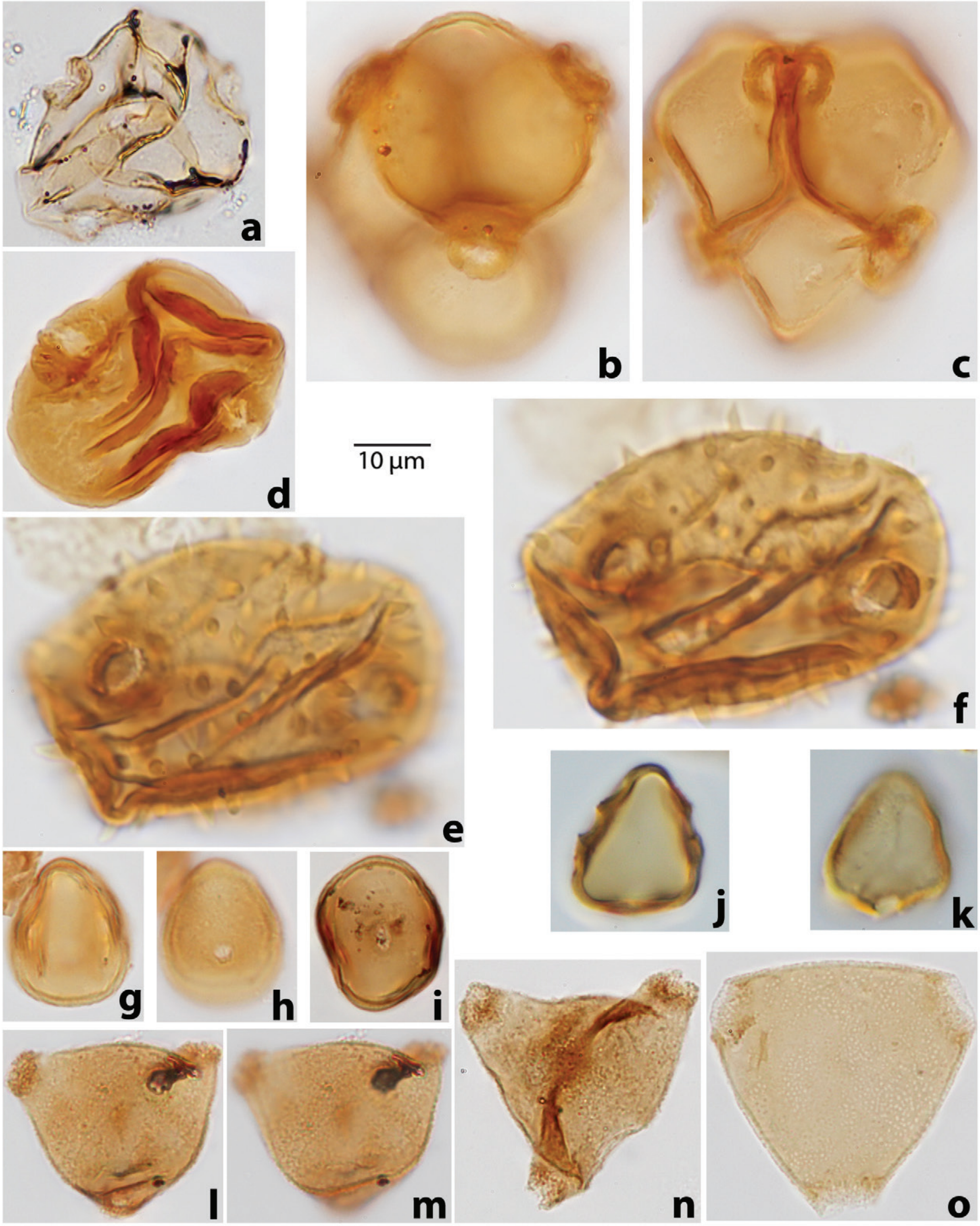
a
b
c
d
10 µm
f
e
j
k
g
h
i
l
m
n
o

PLATE 23. (*Opposite page*)

(**a**) *Proteacidites triangulatus* Lorente, 1986, sample 22445, EF E7-1;

(**b**) *Psilatriporites minimus* sp. nov. (Holotype), sample 22506, EF S4/3;

(**c, d**) *Psilatriporites minimus* sp. nov. (Paratype), sample 22303, EF U22-2;

(**e**) *Psilatriporites desilvae* Hoorn, 1993, sample 22438, EF F15-2;

(**f–i**) *Retitriporites crotonicolumellatus* Jaramillo et al., 2011, comb. nov. et emend., **f, g**: sample 22436, EF S21-4; **h, i**: sample 22436, EF N13-3;

(**j, k**) *Retitriporites discretus* sp. nov. (Holotype), sample 22518, EF V17;

(**l, m**) *Retitriporites discretus* sp. nov. (Paratype), sample 22522, EF S47-1/2;

(**n, o**) *Retitriporites sifonis* sp. nov. (Holotype), sample 22290, EF F42-2;

(**p, q**) *Retitriporites typicus* González-Guzmán, 1967, sample 22277, EF F19-4;

(**r–t**) *Ctenolophinidites suigeneris* Silva-Caminha et al., 2010; **r, s**: sample 22164, EF R37-2; **t**: sample 22445, EF L25;

(**u**) *Jandufouria minor* Jaramillo and Dilcher, 2001, sample 22518, EF X12.

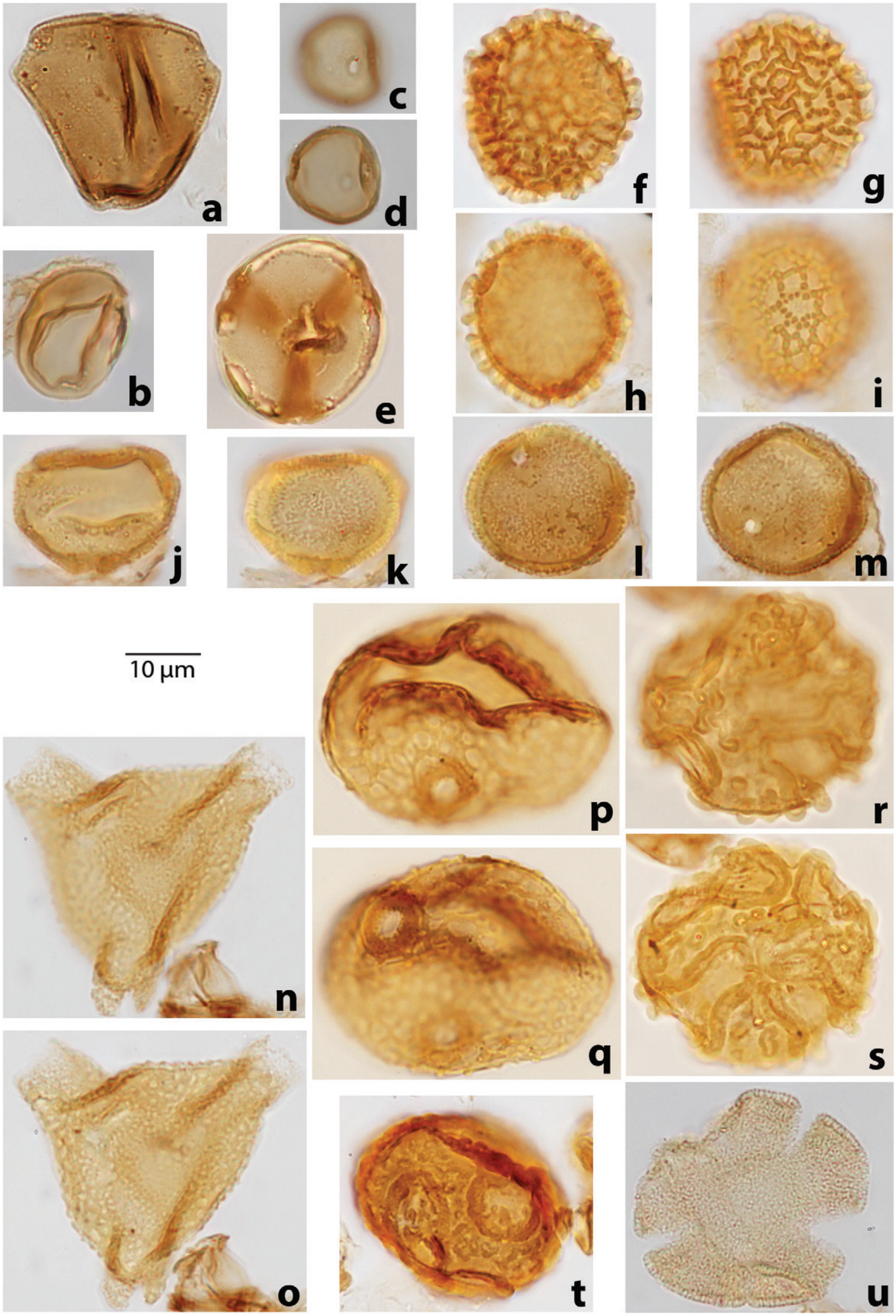
a
b
c
d
e
f
g
h
i
j
k
l
m
10 µm
n
o
p
q
r
s
t
u

PLATE 24. (*Opposite page*)

(**a, b**) *Passifloriidites pseudoperculatus* gen. et sp. nov. (Holotype), sample 22365, EF P10-3;

(**c, d**) *Passifloriidites pseudoperculatus* gen. et sp. nov. (Paratype), sample 22422, EF F35;

(**e, f**). *Passifloriidites pseudoperculatus* gen. et sp. nov. (pseudoperculum), sample 22518, EF Q15-3;

(**g, h**) *Perfotricolpites hexacolpatus* sp. nov. (Holotype), sample 22354, EF W42-2;

(**i, j**) *Perfotricolpites hexacolpatus* sp. nov. (Paratype), sample 22438, EF K45-1.

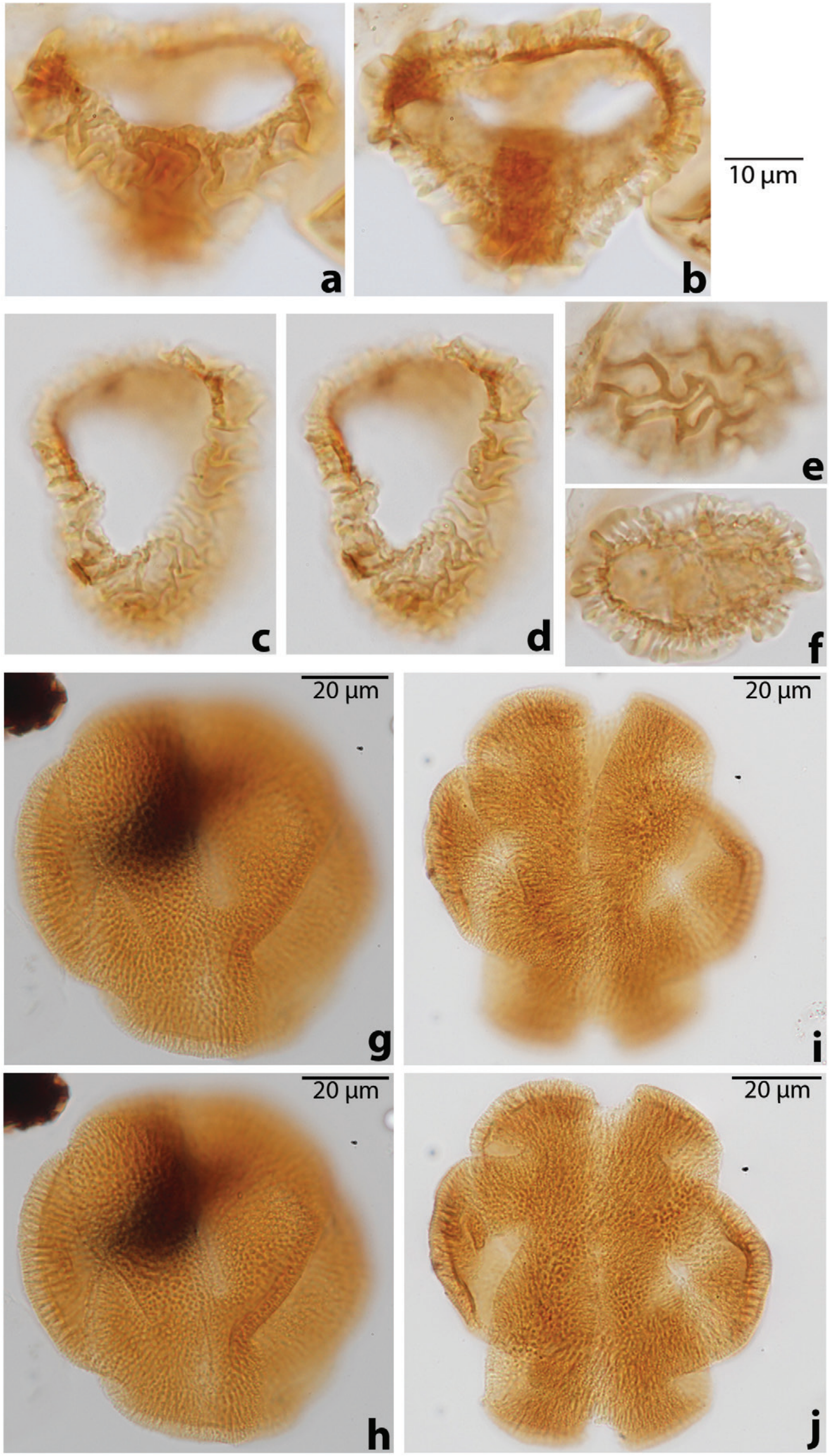
a
b
10 µm
c
d
e
f
20 µm
g
20 µm
i
20 µm
h
20 µm
j

PLATE 25. (*Opposite page*)

(**a–c**) *Retistephanocolpites curvimuratus* Leite et al., 2021; **a, b**: sample 22386, EF L46-2; **c**: sample 22422, EF E30;

(**d, e**) *Retistephanocolpites liberalis* sp. nov. (Holotype), sample 22282, EF L14/2;

(**f**) *Retistephanocolpites liberalis* sp. nov. (Paratype), sample 22287, EF S17-1;

(**g–i**) *Retistephanocolpites pardoi* Leite et al.; 2021; **g, h**: sample 22261, EF H38-3/4; **i**: sample 22272, EF G6-4;

(**j, k**) *Retistephanocolpites angeli* Leidelmeyer, 1966, sample 22518, EF F6-1;

(**l, m**) *Heterocolpites incomptus* Hoorn, 1993, sample 22290, EF Q70-2;

(**n**) *Heterocolpites rotundus* Hoorn, 1993, sample 22170, EF F20-4;

(**o, p**) *Heterocolpites verrucosus* Hoorn, 1993, sample 22272, EF W15-4;

(**q, r**) *Psilastephanocolporites ectoporatus* sp. nov. (Holotype), sample 22140, EF L22-1/3;

(**s**) *Psilastephanocolporites ectoporatus* sp. nov. (Paratype), sample 22140, EF X32;

(**t**) *Psilastephanocolporites fissilis* Leidelmeyer, 1966, sample 22290, EF Q14;

(**u, v**) *Psilastephanocolporites marinamensis* Hoorn, 1994b, sample 22460, EF M8-1/3.

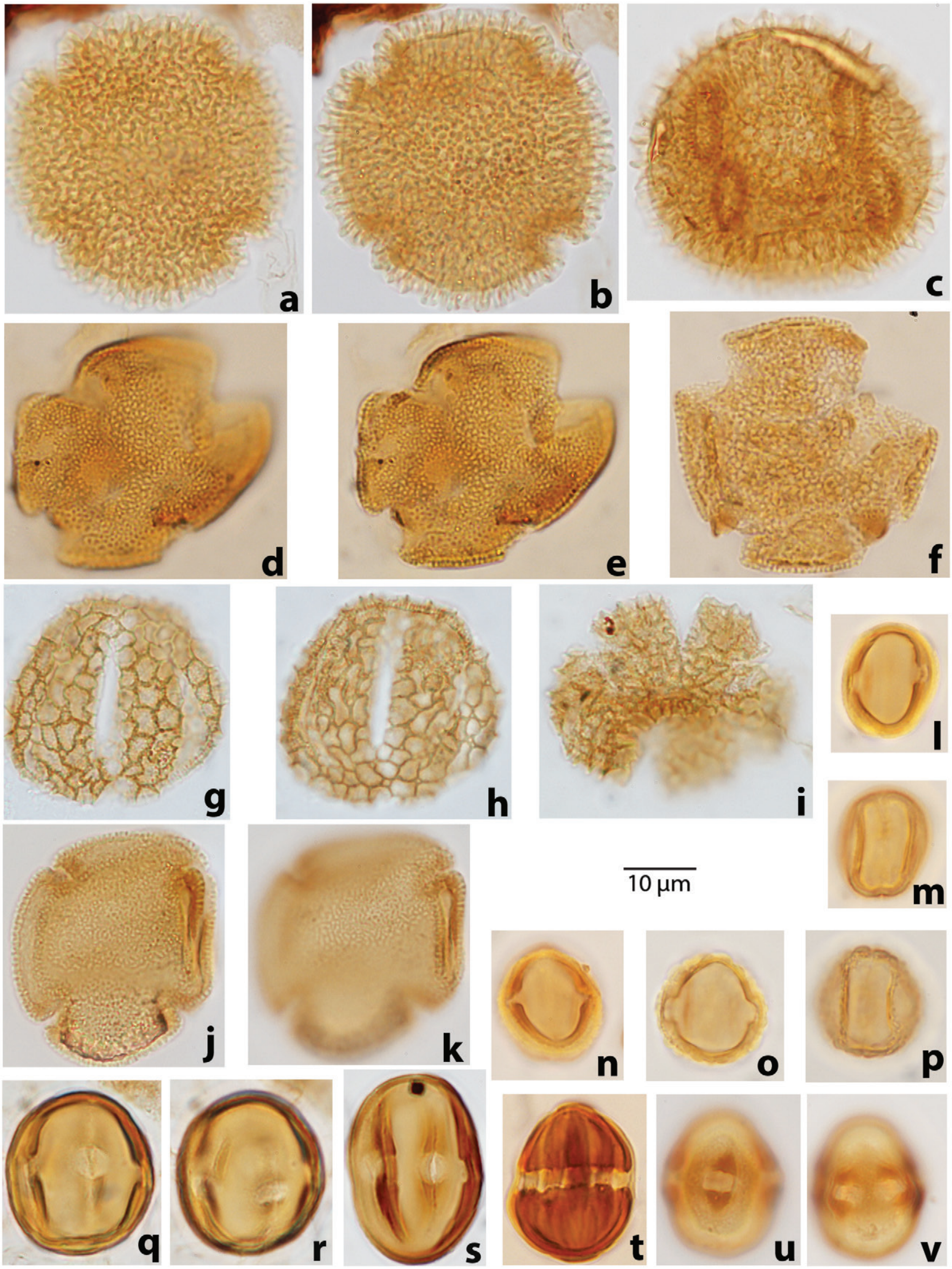
a
b
c
d
e
f
g
h
i
l
10 μm
m
j
k
n
o
p
q
r
s
t
u
v

PLATE 26. (*Opposite page*)

(**a, b**) *Psilastephanocolporites pseudomarinamensis* sp. nov. (Holotype), sample 22282, EF T16-1;

(**c–e**) *Retistephanocolporites loxocolpatus* sp. nov. (Holotype), sample 22140, EF J40-4;

(**f, g**) *Retistephanoporites minutiporus* Jaramillo and Dilcher, 2001; **f**: sample22460, EF N18-2; **g**: sample 22482, EF R6-2;

(**h**) *Psilastephanoporites herngreenii* Hoorn, 1993, sample 2290, EF J19-3/4;

(**i–k**) *Retistephanoporites crassiannulatus* Lorente, 1986, **i, j**: sample 22277, EF F19-4; **k**: sample 22456, EF K45;

(**l, m**) *Verrustephanoporites circularis* sp. nov. (Holotype), sample 22415, EF M13-2/4;

(**n**) *Verrustephanoporites intraverrucosus* sp. nov. (Holotype), sample 22381, EF S-37-3;

(**o**) *Verrustephanoporites intraverrucosus* sp. nov. (Paratype), sample 22381, EF G9-2/4;

(**p, q**) *Malvacipollis spinulosa* Frederiksen, 1983; **p**: sample 22164, EF Y49-1; **q**: sample 22290, EF T13-2/4.

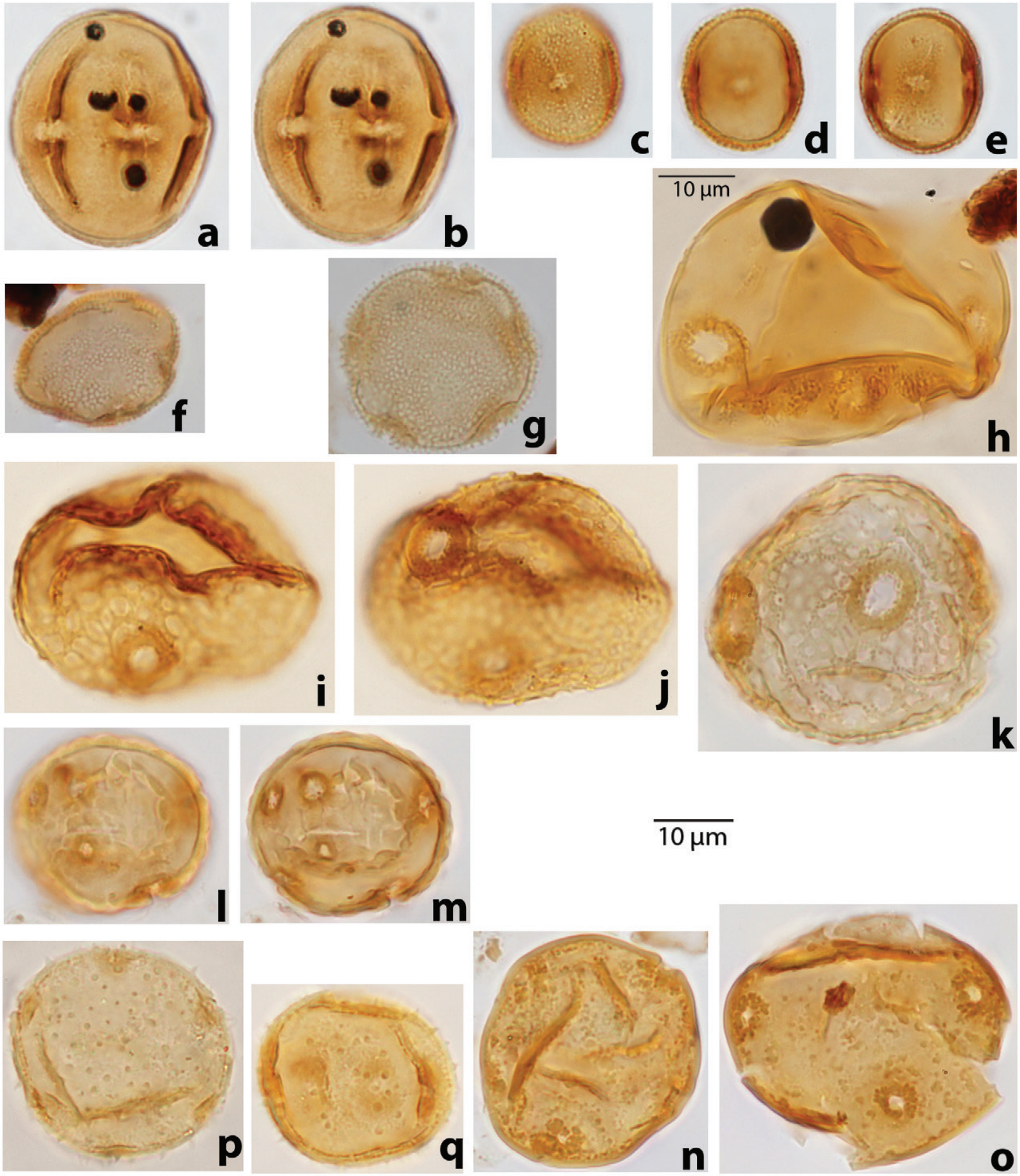
a
b
c
d
e
10 µm
f
g
h
i
j
k
l
m
10 µm
p
q
n
o

PLATE 27. (*Opposite page*)

(**a, b**) *Lymingtonia splendida* sp. nov. (Holotype), sample 22506, EF O48-3/4;

(**c–h**) *Perisyncolporites pokornyi* Germeraad et al., 1968; **c, d**: sample 22282, EF O10; **e, f**: sample 22279, EF V22-1; **g, h**: sample 22287, EF S17-4 (tectum is lost);

(**i**) *Cyperaceaepollenites wesselinghii* sp. nov. (Holotype), sample 22256, EF L46;

(**j, k**) *Cyperaceaepollenites wesselinghii* sp. nov. (Paratype), sample 22321, EF H8-3.

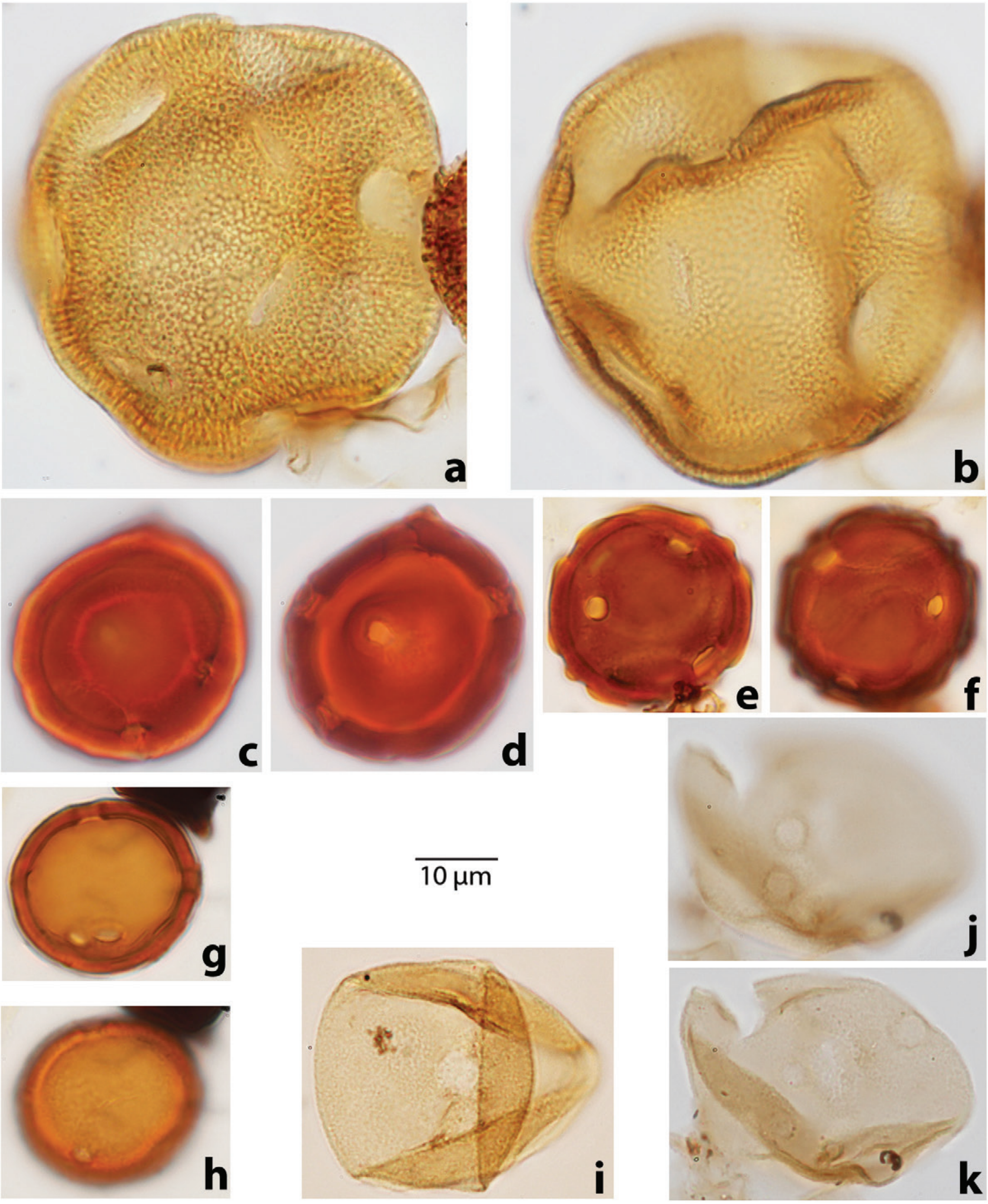
a
b
c
d
e
f
g
10 µm
j
h
i
k

PLATE 28. (*Opposite page*)

(**a**) *Echiperiporites estelae* Germeraad et al., 1968, sample 22344, EF K10;

(**b, c**) *Echiperiporites germeraadii* Leite et al., 2021, sample 22158, EF U14-3;

(**d**) *Echiperiporites intectatus* Silva-Caminha et al., 2010, sample 22140, EF Q8;

(**e, f**) *Echiperiporites titanicus* Leite et al., 2021; **e**: sample 22318, EF L30-2; **f**: sample 22318, EF E43-3;

(**g, h**) *Echiperiporites jutaiensis* Silva-Caminha et al., 2010, sample 22140, EF F9;

(**i, j**) *Echiperiporites lophatus* Silva-Caminha et al., 2010; **i**: sample 22398, EF J37; **j**: sample 22278, EF E39-1/2;

(**k**) *Glencopollis curvimuratus* Silva-Caminha et al., 2010, sample 22278, EF K11-3/4.

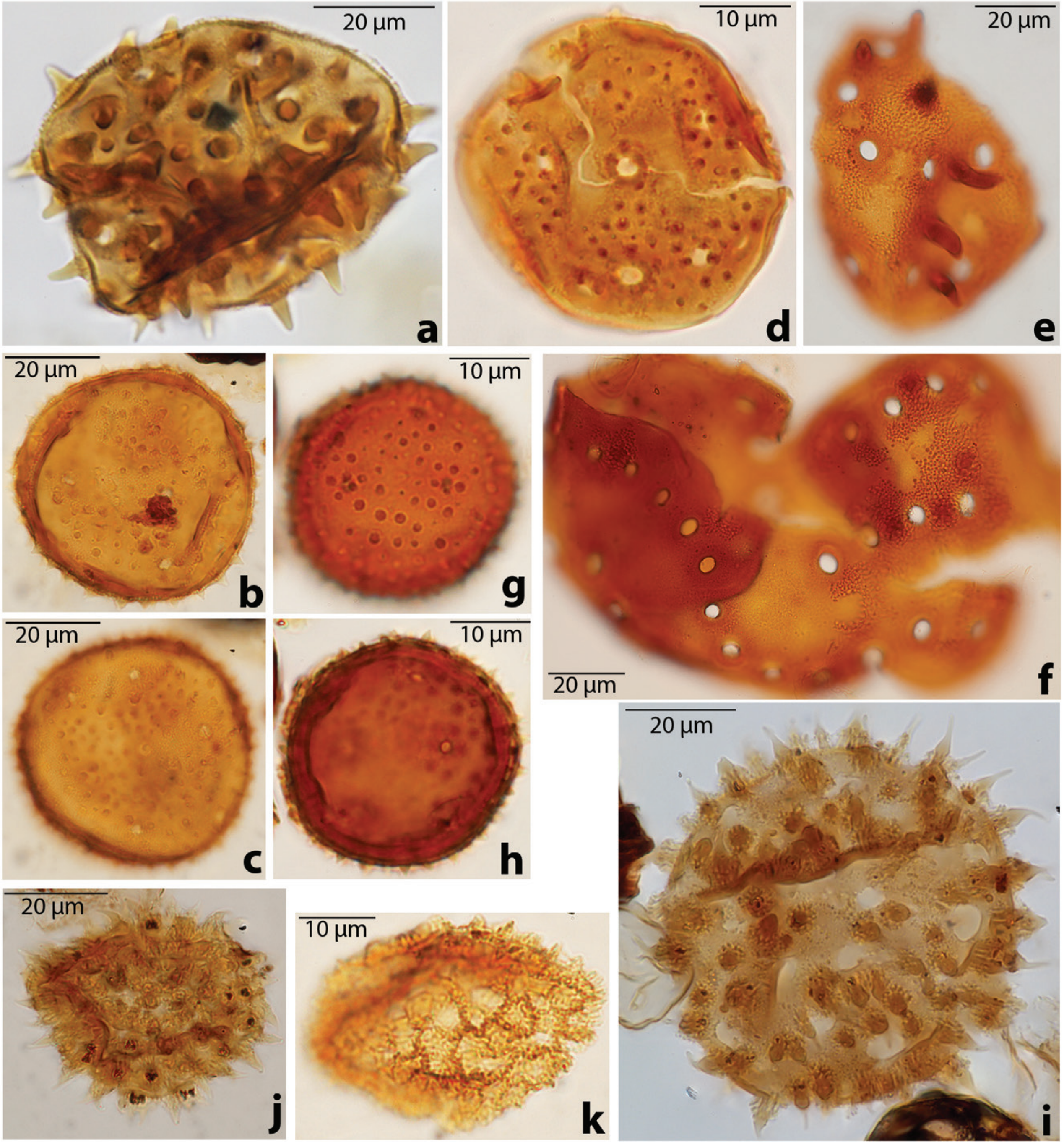
20 µm
a
10 µm
d
20 µm
e
20 µm
b
10 µm
g
20 µm
f
20 µm
c
10 µm
h
20 µm
i
20 µm
j
10 µm
k

PLATE 29. (*Opposite page*)

(**a**) *Multiporopollenites crassinexinatus* Silva-Caminha et al., 2010, sample 22354, EF K5;

(**b, c**) *Multiporopollenites intermedius* sp. nov. (Holotype), sample 22164, EF J10-1;

(**d**) *Parsonsidites? brenacii* Silva-Caminha et al., 2010, sample 22279, EF U25-4;

(**e**) *Parsonsidites? minibrenacii* sp. nov. (Holotype), sample 22518, EF E43-4;

(**f**) *Parsonsidites? minibrenacii* sp. nov. (Paratype), sample 22506, EF R6-1/2;

(**g, h**) *Psilaperiporites depressus* sp nov. (Holotype), sample 22279, EF V12;

(**i, j**) *Psilaperiporites depressus* sp nov. (Paratype), sample 22278, EF O32;

(**k**) *Psilaperiporites multiporatus* Hoorn, 1994a, sample 22358, EF B49;

(**l, m**) *Psilaperiporites circinatus* sp. nov. (Holotype), sample 22349, EF J11-1;

(**n–p**) *Retiperiporites retiporatus* sp. nov. (Holotype), sample 22298, EF G12-3;

(**q, r**) *Thymelipollis amazonicus* sp. nov. (Holotype), sample 22506, EF P17;

(**s**) *Botryococcus* spp., sample 22170, EF S17;

(**t**) *Pediastrum*/*Pseudopediastrum* spp., sample 22272, EF G35-2/4;

(**u**) foraminiferal lining, sample 22277, EF D13.

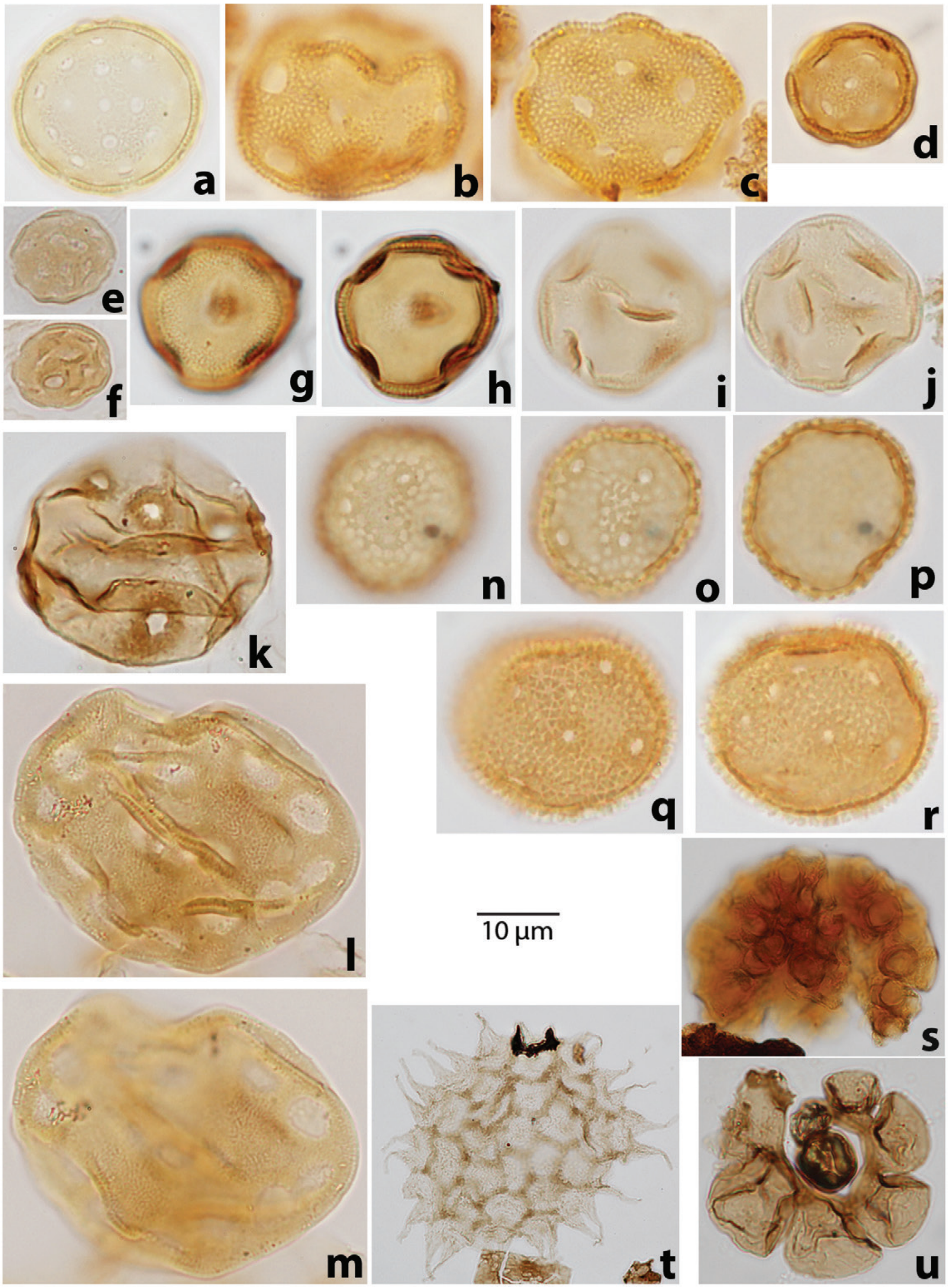
a
b
c
d
e
f
g
h
i
j
k
n
o
p
q
r
l
10 µm
s
m
t
u

PLATE 30. (*Opposite page*)

(**a**) *Apteodinium? vescum* Matsuoka, 1983, sample 22454, EF H44-1/3;

(**b**) rounded brown cysts (RBCs), sample 22158, EF U18-4;

(**c, d**) *Cleistosphaeridium ancyreum* (Cookson and Eisenack, 1965) Eaton et al., 2001, sample 22460, EF U47;

(**e, f**) *Cleistosphaeridium placacanthum* (Deflandre and Cookson, 1955) Eaton et al., 2001, sample 22454, EF X23;

(**g**) *Cribroperidinium* sp., sample 22451, EF U5/2;

(**h**) *Cyclopsiella elliptica/granosa* complex sensu de Verteuil and Norris, 1996, sample 22158, EF 23-1;

(**i, j**) *Hystrichokolpoma rigaudiae* Deflandre and Cookson, 1955, sample 22460, EF E18-2;

(**k, l**) *Hystrichokolpoma* spp., sample 22454, EF J22-2/4;

(**m, n**) *Impletosphaeridium prolatum* Head et al., 1989, sample 22277, EF K37-3;

(**o***) *Leiosphaeridia* "scabrate," sample 22290, EF P45-1/2;

(**p***) *Leiosphaeridia* spp., sample 22277, EF T40.

*Taken with DIC (differential interference contrast).

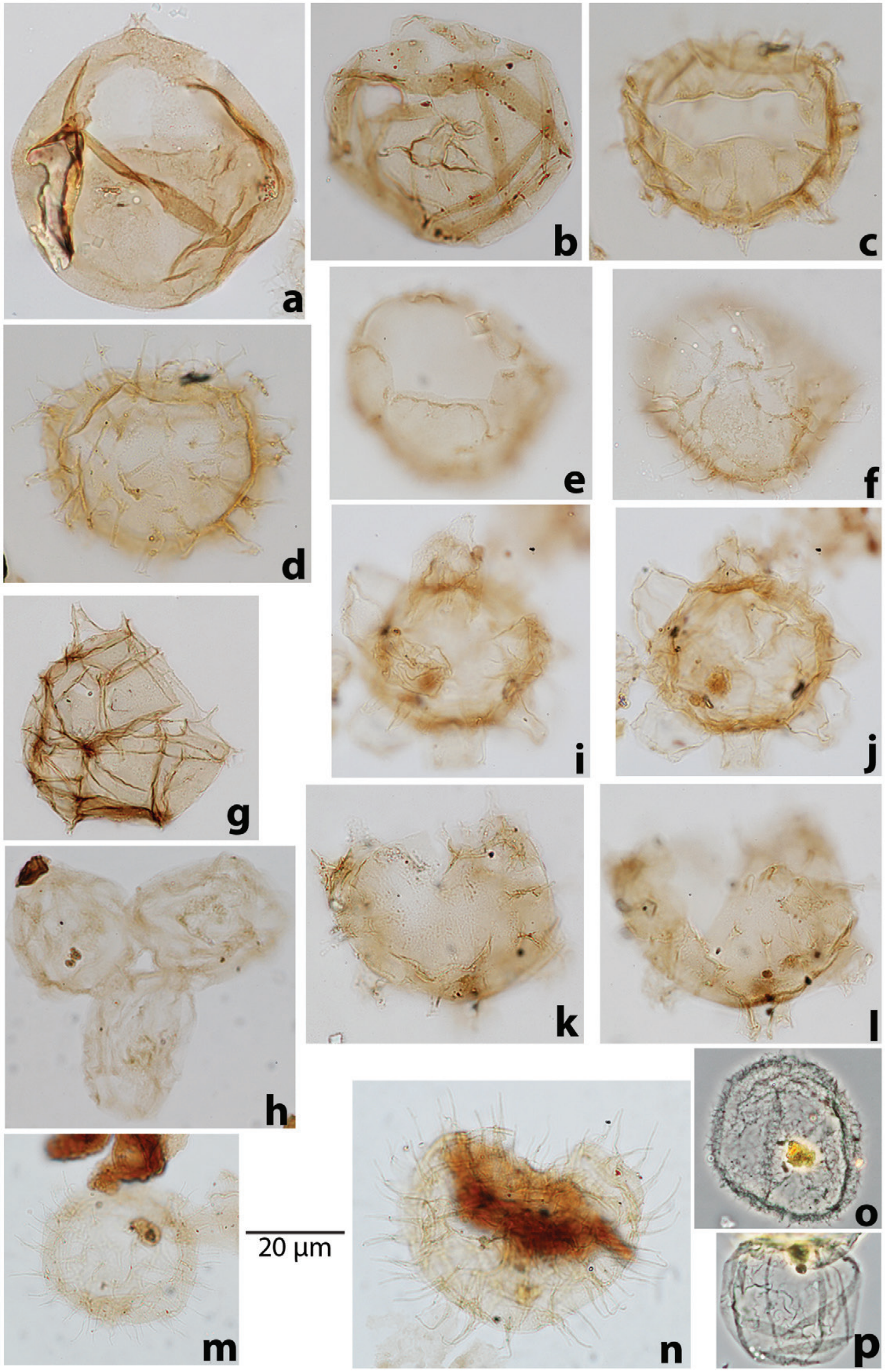
a
b
c
d
e
f
g
i
j
h
k
l
m
20 µm
n
o
p

PLATE 31. (*Opposite page*)

(**a–c**) *Lingulodinium machaerophorum* (Deflandre and Cookson, 1955) Wall, 1967; **a, b**: sample 22294, EF S18; **c**: sample 22294, EF V8-2;

(**d**) *Operculodinium israelianum* (Rossignol, 1962) Wall, 1967, sample 22454, EF K9-2;

(**e, f**) *Quadrina*? *condita* de Verteuil and Norris, 1996; **e**: sample 22295, EF W40-2; **f**: sample 22319, EF E48;

(**g**) *Quadrina*? "*incerta*" (= Dinocyst XI of Lenoir and Hart, 1986), sample22454, EF E41-4;

(**h–n**) *Spiniferites* spp.*;* **h, i**: sample 22451, EF Q14-2; **j, k**: sample 22451, EF F21-2/4; **l, m**: sample 22480, EF L25-1/2; **n**: sample 22451, EF D20-2;

(**o**) *Trinovantedinium ferugnomatum* de Verteuil and Norris, 1996, sample 22295, EF Q38-2;

(**p**) *Trinovantedinium*? *xylochoporum* de Verteuil and Norris, 1996, sample 22158, EF U9-1;

(**q**) *Tuberculodinium vancampoae* (Rossignol, 1962) Wall, 1967, sample 22451, EF O46-1.

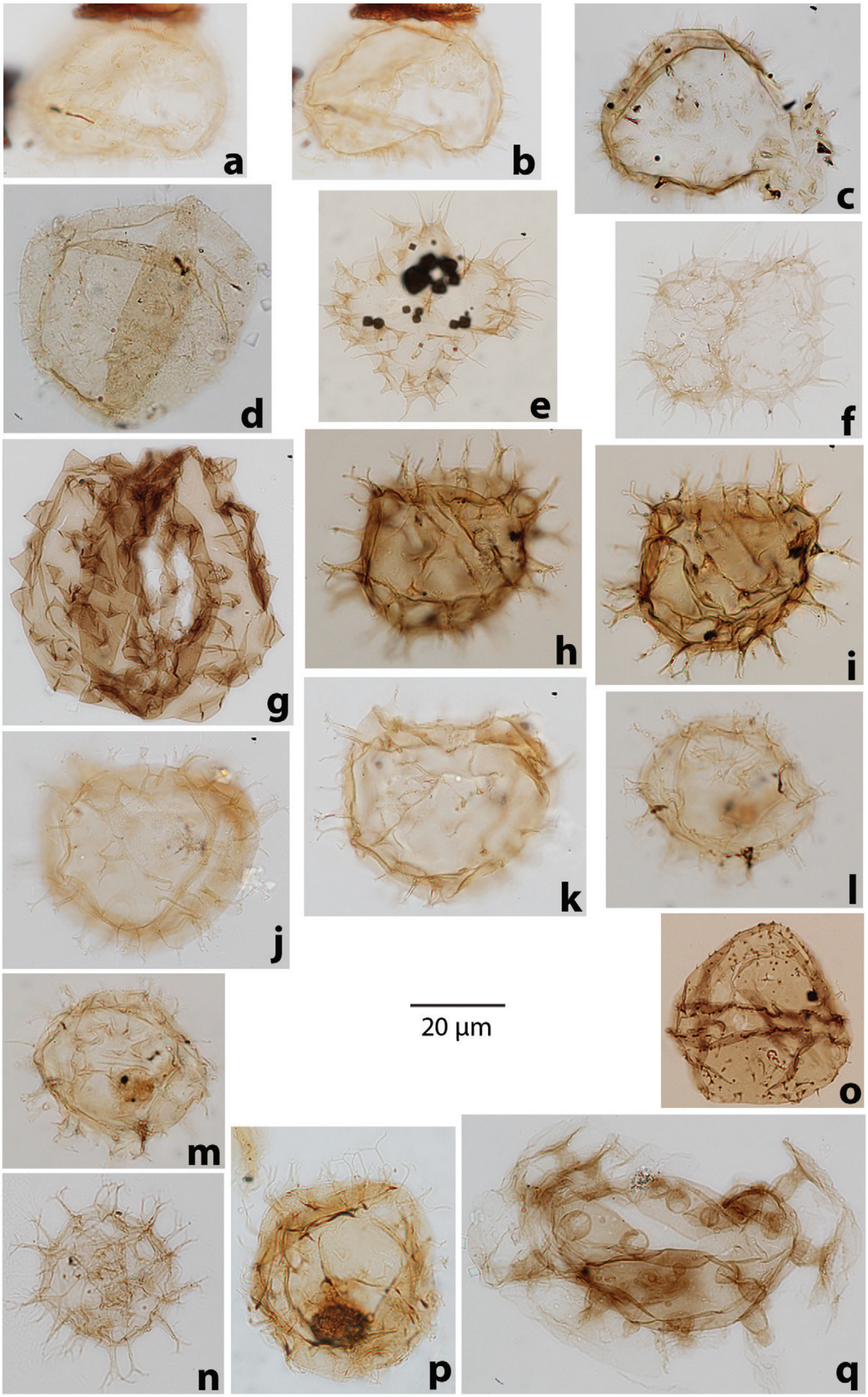
a
b
c
d
e
f
g
h
i
j
k
l
20 µm
o
m
n
p
q

References

Absy, M. L. 1979. A Palynological Study of Holocene Sediments in the Amazon Basin. Ph.D. diss., University of Amsterdam, Netherlands.

Adegoke, O. S., R. E. Jan du Chêne, E. A. Agumanu, and P. O. Ajayi. 1978. Palynology and Age of the Kerikeri Formation, Nigeria. *Revista Española de Micropaleontología*, 10(2): 267–283.

Akabane, T. K., A. O. Sawakuchi, C. M. Chiessi, A. K. Kern, J. L. D. Pinaya, G. C. T. Ceccantini, and P. E. De Oliveira. 2020. Modern Pollen Signatures of Amazonian Rivers and New Insights for Environmental Reconstructions. *Palaeogeography, Palaeoclimatology, Palaeoecology*, 554: 109802. https://doi.org/10.1016/j.palaeo.2020.109802

Anderson, R. Y. 1960. Cretaceous-Tertiary Palynology, Eastern Side of the San Juan Basin, New Mexico. *New Mexico Bureau of Mines and Mineral Resources Memoir*, 6: 1–58.

Antoine, P.-O., M. A. Abello, S. Adnet, A. J. A. Sierra, P. Baby, G. Billet, M. Boivin, Y. Calderóne, A. Candela, J. Chabain, F. Corfui, D. A. Croft, M. Ganerød, C. Jaramillo, S. Klaus, L. Marivaux, R. E. Navarrete, M. J. Orliac, F. Parra, M. E. Pérez, F. Pujos, J.-C. Rage, A. Ravel, C. Robinet, M. Roddaz, J. V. Tejada-Lara, J. Vélez-Juarbe, F. P. Wesselingh, and R. Salas-Gismondi. 2016. A 60-Million-Year Cenozoic History of Western Amazonian Ecosystems in Contamana, Eastern Peru. *Gondwana Research*, 31: 30–59. https://doi.org/10.1016/j.gr.2015.11.001

Antoine, P.-O., P. Baby, M. Benammi, S. Brusset, D. De Franceschi, N. Espurt, C. Goillot, F. Pujos, R. Salas Gismondi, J. Tejada, and M. Urbina. 2007. "The Laventan Fitzcarrald Local Fauna, Amazonian Peru". *In* Proceedings of the Fourth European Meeting on Paleontology and Stratigraphy of Latin America, Madrid, Spain, 12–14. *Cuadernos del Museo Geominero,* 8 (September): 19–24.

Antoine, P.-O., D. Franceschi, J. J. Flynn, A. Nel, P. Baby, M. Benammi, Y. Calderón, N. Espurt, A. Goswami, and R. Salas-Gismondi. 2006. Amber from Western Amazonia Reveals Neotropical Diversity during the Middle Miocene. *Proceedings of the National Academy of Sciences,* 103(37): 13595–13600. https://doi.org/10.1073/pnas.0605801103

Archangelsky, S., and L. Villar de Seoane. 1998. Estudios Palinológicos de la Formación Baqueró (Cretácico), Provincia de Santa Cruz, Argentina. VIII [Palynological Studies of the Baqueró Formation (Cretaceous), Santa Cruz Province, Argentina. VIII]. *Ameghiniana*, 35(1): 7–19.

Aureliano, T., A. M. Ghilardi, E. Guilherme, J. P. Souza-Filho, M. Cavalcanti, and D. Riff. 2015. Morphometry, Bite-Force, and Paleobiology of the Late Miocene Caiman *Purussaurus brasiliensis*. *PLOS ONE*, 10 (2): e0117944. https://doi.org/10.1371/journal.pone.0117944

Balme, B. E. 1957. Spores and Pollen Grains from the Mesozoic of Western Australia. *Commonwealth Scientific and Industrial Research Organisation, Coal Research Section T.C. 25*, Australia.

Beerling, D. J., and D. L. Royer. 2011. Convergent Cenozoic CO2 History. *Nature Geoscience*, 4: 418–420. https://doi.org/10.1038/ngeo1186

Behling, H., J. C. Berrio, and H. Hooghiemstra. 1999. Late Quaternary Pollen Records from the Middle Caquetá River Basin in Central Colombian Amazon. *Palaeogeography, Palaeoclimatology, Palaeoecology*, 145: 193–213. https://doi.org/10.1016/S0031-0182(98)00105-9

Biswas, R. R. 1962. Stratigraphy of the Mahadev, Langpar, Cherra and Tura Formations, Assam. *Bulletin of the Geological, Mining and Metallurgical Society of India*, 25: 1–48.

Bogotá-Ángel, G., H. Huang, P. E. Jardine, N. Chazot, S. Salamanca, H. Banks, A. Pardo-Trujillo, A. Plata, H. Dueñas, W. Star, R. Langelaan, A. Eisawi, O. P. Umeji, L. O. Enuenwemba, S. Parmar, R. R. da Silveira, J. Y. Lim, V. Prasad, R. J. Morley, C. D. Bacon, and C. Hoorn. 2021. Climate and Geological Change as Drivers of Mauritiinae Palm Biogeography. *Journal of Biogeography*, 29 March, 1–22. https://doi.org/10.1111/jbi.14098

Boltenhagen, E. 1967. Spores et pollen du Crétace Supérieur Gabon [Spores and Pollen of the Upper Cretaceous of Gabon]. *Pollen et Spores*, 9: 335–355.

Boltenhagen, E. 1976. Pollen et spores Sénoniens du Gabon [Pollen and Spores of the Senonian of Gabon]. *Cahier de Micropaléontologie*, 3: 3–21.

Boonstra, M., M. I. F. Ramos, E. I. Lammertsma, P.-O. Antoine, and C. Hoorn. 2015. Marine Connections of Amazonia: Evidence from Foraminifera and Dinoflagellate Cysts (Early to Middle Miocene, Colombia/Peru). *Palaeogeography, Palaeoclimatology, Palaeoecology*, 417: 176–194. https://doi.org/10.1016/j.palaeo.2014.10.032

Brenner, G. J. 1963. The Spores and Pollen of the Potomac Group of Maryland. *Maryland Department of Geology, Mines and Water Resources Bulletin*, 27, Baltimore, USA.

Brenner, G. J., and I. S. Bickoff. 1992. Palynology and Age of the Lower Cretaceous Basal Kurnub Group from the Coastal Plain to the Northern Negev of Israel. *Palynology*, 16: 137–185. https://doi.org/10.1080/01916122.1992.9989411

Burger, D. 1976. Some Early Cretaceous Plant Microfossils from Queensland. *Bulletin of the Bureau of Mineral Resources, Geology and Geophysics, Australia*, 160: 1–22.

Cadena, E., T. M. Scheyer, J. D. Carrillo-Briceño, R. Sánchez, R., O. A. Aguilera-Socorro, A. Vanegas, M. Pardo, D. M. Hansen, and M. R. Sánchez-Villagra. 2020. The Anatomy, Paleobiology, and Evolutionary Relationships of the Largest Extinct Side-Necked Turtle. *Science Advances*, 6(7): eaay4593. https://doi.org/10.1126/sciadv.aay4593

Caputo, M. V. 1973. Relatório Preliminar de Exploração—Bacia do Acre [Preliminar Exploration Report—Acre Basin]. *Relatório 665-A da Petrobrás*, Belém, Brazil.

Cassino, R. F., C. T. Martinho, and S. A. F. Silva-Caminha. 2015. Modern Pollen Spectra of the Cerrado Vegetation in Two National Parks of Central Brazil, and Implications for Interpreting Fossil Pollen Records. *Review of Palaeobotany and Palynology*, 223: 71–86. https://doi.org/10.1016/j.revpalbo.2015.09.002

Cernusak, L. A., V. Haverd, O. Brendel, D. Le Thiec, J.-M. Guehl, and M. Cuntz. 2019. Robust Response of Terrestrial Plants to Rising CO_2. *Trends in Plant Science*, 24(7): 578–586. https://doi.org/10.1016/j.tplants.2019.04.003

Cernusak, L. A., K. Winter, C. Martínez, E. Correa, J. Aranda, M. Garcia, C. Jaramillo, and B. L. Turner. 2011. Responses of Legume Versus Non-legume Tropical Tree Seedlings to Elevated CO_2 Concentration. *Plant Physiology*, 157: 372–85. https://doi.org/10.1104/pp.111.182436

Chao, A., R. L. Chazdon, R. K. Colwell, and T.-J. Shen. 2005. A New Statistical Approach for Assessing Similarity of Species Composition with Incidence and Abundance Data. *Ecology Letters*, 8: 148–159. https://doi:10.1111/j.1461-0248.2004.00707.x

Chao, A., N. J. Gotelli, T. C. Hsieh, E. L. Sander, K. H. Ma, R. K. Colwell, and A. Ellison. 2014. Rarefaction and Extrapolation with Hill Numbers: A Framework for Sampling and Estimation in Species Diversity Studies. *Ecological Monographs*, 84(1): 45–67. https://doi.org/10.1890/13-0133.1

Chao, A., and L. Joost. 2012. Coverage-based Rarefaction and Extrapolation: Standardizing Samples by Completeness Rather than Size. *Ecology*, 93(12): 2533–2547. https://doi.org/10.1890/11-1952.1

Clarke, K. R. 1993. Non-parametric Multivariate Analyses of Changes in Community Structure. *Australian Journal of Ecology*, 18: 117–143. https://doi.org/10.1111/j.1442-9993.1993.tb00438.x

Colinvaux, P. A., P. E. De Oliveira, AND J. E. Moreno. 1999. Amazon Pollen Manual and Atlas. New York: Harwood Academic Press.

Cookson, I. C. 1950. Fossil Pollen Grains of Proteaceous Type from Tertiary Deposits in Australia. *Australian Journal of Science, series B*, 3(2): 166–177. https://doi.org/10.1071/BI9500166

Cookson, I. C. 1953. Difference in Microspore Composition of Some Samples from a Bore at Comaum, South Australia. *Australian Journal of Botany*, 1: 462–473. https://doi.org/10.1071/BT9530462

Cookson, I. C., and M. E. Dettmann. 1958. Some Trilete Spores from the Upper Mesozoic Deposits in the Eastern Australian Region. *Proceedings of the Royal Society of Victoria*, 70: 95–128.

Cookson, I. C., and A. Eisenack. 1965. Microplankton from the Browns Creek Clays, Southwestern Victoria. *Proceedings of the Royal Society of Victoria*, 79: 119–13l.

Couper, R. A. 1953. Upper Mesozoic and Cainozoic Spores and Pollen Grains from New Zealand. *New Zealand Geological Survey Palaeontological Bulletin*, 22.

Couper, R. A. 1958. British Mesozoic Microspores and Pollen Grains. A Systematic and Stratigraphic Study. *Palaeontographica Abteilung B*, 103: 75–179.

Couper, R. A. 1960. New Zealand Mesozoic and Cainozoic Plant Microfossils. *New Zealand Geological Survey Palaeontological Bulletin*, 32.

Cozzuol, M. 2006. The Acre Vertebrate Fauna: Diversity, Geography and Time. *Journal of South American Earth Sciences*, 21: 185–203. https://doi.org/10.1016/j.jsames.2006.03.005

Cruz, N. M. C. 1984. Palinologia do Linhito do Solimões no Estado do Amazonas. [Palynology of the Solimões Lignite in the State of Amazonas]. Proceedings of the Simpósio de Geologia da Amazônia 2, Manaus, Amazonas, Brazil. *Departamento Nacional de Produção Mineral*, 473–480.

Cunha, N. L., M. Delatorre, R. B. Rodrigues, C. Vidotto, F. Gonçalves, E. Scremin-Dias, G. Damasceno-Júnior, V. J. Pott, and A. Pott. 2012. Structure of Aquatic Vegetation of a Large Lake, Western Border of the Brazilian Pantanal. *Brazilian Journal of Biology*, 72(3): 519–531. https://doi.org/10.1590/S1519-69842012000300015

D'Apolito, C., M. L. Absy, and E.M. Latrubesse. 2017. The Movement of Pre-Adapted Cool Taxa in North-Central Amazonia during the Last Glacial. *Quaternary Science Reviews*, 169(1): 1–12. https://doi.org/10.1016/j.quascirev.2017.05.017

D'Apolito, C., S. A. F. Silva-Caminha, C. Jaramillo, R. Dino, and E. A. A. Soares. 2019. The Pliocene–Pleistocene Palynology of the Negro River, Brazil. *Palynology*, 43: 223–243. https://doi.org/10.1080/01916122.2018.1437090

Deflandre, G., and I. C. Cookson. 1955. Fossil Microplankton from Australian Late Mesozoic and Tertiary Sediments. *Australian Journal of Marine and Freshwater Research*, 6(2): 242–313. https://doi.org/10.1071/MF9550242

de Jersey, N. J. 1962. Triassic Spores and Pollen Grains from the Ipswich Coalfield. *Geological Survey of Queensland Publication*, 307: 1–18.

Delcourt, A., and G. Sprumont. 1955. Les spores et grains de pollen du Wealdien du Hainaut [Spores and Pollen Grains of the Wealdien of Hainaut]. *Memoires de la Societe Geologique de Belgique*, nouvelle series (in quarto) 5: 1–73.

Dessaune-Rodrigues, I., M. L. Absy, S. A. F. Silva-Caminha, V. G. Esteves, C. B. F. Mendonça, M. G. Ferreira, and C. O. Moura. 2016. Pollen Morphology of 25 Apocynaceae Species in the Adolpho Ducke Forest Reserve, Amazonas (Brazil). *Palynology*, 41(2): 278–296. https://doi.org/10.1080/01916122.2016.1146173

Dettmann, M. E. 1963. Upper Mesozoic Microfloras from South-Eastern Australia. *Proceedings of Royal Society of Victoria*, 77: 1–148.

de Verteuil, L., and G. Norris. 1996. Miocene Dinoflagellate Stratigraphy and Systematics of Maryland and Virginia. *Micropaleontology*, 42: 1–172.

De Vleeschouwer, D., M. Vahlenkamp, M. Crucifix, and H. Pälike. 2017. Alternating Southern and Northern Hemisphere Response to Astronomical Forcing during the Past 35 Million Years. *Geology*, 45: 375–378. https://doi.org/10.1130/G38663.1

Dick, W. C., S. L. Lewis, M. Maslin, M., and E. Bermingham. 2013. Neogene Origins and Implied Warmth Tolerance of Amazon Tree Species. *Ecology and Evolution*, 3(1): 162–169. https://doi:10.1002/ece3.441

Dinno, A. 2017. dunn.test: Dunn's Test of Multiple Comparisons Using Rank Sums. R package version 1.3.5. https://CRAN.R-project.org/package=dunn.test [Permanent link.]

Döring, H. 1964. Trilete Sporen aus dem Oberen Jura und dem Wealden Norddeutschlands [Trilete spores from the Upper Jura and the Wealden of Northern Germany]. *Geologie Beihefte*, 13(9): 1009–1129.

Draper, F. C., E. N. Honorio-Coronado, K. H. Roucoux, I. T. Lawson, N. C. A. Pitman, P. V. A. Fine, O. L. Phillips, L. A. Torres-Montenegro, E. Valderrama-Sandoval, I. Mesones, R. García-Villacorta, F. R. R. Arévalo, and T. R. Baker. 2018. Peatland Forests Are the Least Diverse Tree Communities Documented in Amazonia, but Contribute to High Regional Beta-Diversity. *Ecography*, 41: 1256–1269. https://doi:10.1111/ecog.03126

Drugg, W. S. 1967. Palynology of the Upper Moreno Formation (Late Cretaceous-Paleocene) Escarpado Canyon, California. *Palaeontographica Abteilung B*, 120: 1–71.

Dueñas, H. 1980. Palynology of Oligocene-Miocene Strata of Borehole Q-E-22, Planeta Rica, Northern Colombia. *Review of Palaeobotany and Palynology*, 10: 318–328. https://doi.org/10.1016/0034-6667(80)90016-0

Dueñas, H. 1986. Geología y palinología de la Formación Ciénaga de Oro, Región Caribe Colombiana [Geology and Palynology of the Ciénaga de Oro Formation, Colombian Caribbean Region]. *Publicaciones Geologicas Especiales del Ingeominas*, 18: 1–51.

Dutta, S. K., and S. C. D. Sah. 1970. Palynostratigraphy of the Tertiary Sedimentary Formations of Assam: 5. Stratigraphy and Palynology of South Shillong Plateau. *Palaeontographica Abteilung B*, 131: 1–72.

Eaton, G. L., R. A. Fensome, J. B. Riding, and G. L. Williams. 2001. Re-evaluation of the Status of the Dinoflagellate Cyst Genus. *Cleistosphaeridium. Neues*

Jahrbuch für Geologie und Paläontologie, 219: 171–205. https://doi.org/10.1127/njgpa/219/2001/171

Eiras, J. F., C. R. Becker, E. M. Souza, F. G. Gonzaga, J. G. F. Silva, L. M. F. Daniel, N. S. Matsuda, and F. J. Feijó. 1994. Bacia do Solimões [Solimões Basin]. *Boletim de Geociências da Petrobrás*, 8(1): 17–45.

Elsik, W. C. 1968. Palynology of a Paleocene Rockdale Lignite, Milam County, Texas. II. Morphology and Taxonomy. *Pollen et Spores*, 10: 559–664.

Erdtman, G. 1960. On Three New Genera from the L. Headon Beds. *Botaniska Notiser*, 113: 46–48.

Erdtman, G., and H. Straka. 1961. Cormophyte Spore Classification. *Geologiska Föreningen i Stockholm Förhandlingar*, 83(1): 65–78. https://doi.org/10.1080/11035896109449582

Espinosa, B. S., C. D'Apolito, S. A. F. Silva-Caminha, M. G. Ferreira, and M. L. Absy. 2020. Neogene Paleoecology and Biogeography of a Malvoid Pollen in Northwestern South America. *Review of Palaeobotany and Palynology*, 273: 104131. https://doi.org/10.1016/j.revpalbo.2019.104131

Ferraz-Vicentini, K. R., and M. L. Salgado-Labouriau. 1996. Palynological Analysis of a Palm Swamp in Central Brazil. *Journal of South American Earth Sciences*, 9(3–4): 207–219. https://doi.org/10.1016/0895-9811(96)00007-7

Figueiredo, F. O. G., G. Zuquim, H. Tuomisto, G. M. Moulatlet, H. Balslev, and F. R. C. Costa. 2018. Beyond Climate Control on Species Range: The Importance of Soil Data to Predict Distribution of Amazonian Plant Species. *Journal of Biogeography*, 45: 190–200. https://doi.org/10.1111/jbi.13104

Flora do Brasil. 2020. Jardim Botânico do Rio de Janeiro. http://floradobrasil.jbrj.gov.br/ (accessed 7 July 2021).

Fontes, D., C. Jaramillo, and E. Moreno. 2020. Pollen Morphology of the Amacayacu Forest Dynamics Plot, Western Amazon, Colombia. *Palynology*, 44: 32–79. https://doi.org/10.1080/01916122.2018.1538024

Foote, M. 2000. Origination and Extinction Components of Taxonomic Diversity: General Problems. In *Deep Time: Paleobiology's Perspectives,* ed. D. H. Erwin and S. L. Wing, pp. 74–105. Lawerence: Paleontological Society.

Frederiksen, N. O. 1983. *Middle Eocene Palynomorphs from San Diego, California. Part II. Angiosperm Pollen and Miscellanea*. American Association of Stratigraphic Palynologists contribution series, no. 12. Dallas: American Association of Stratigraphic Palynologists Foundation.

Frederiksen, N. O. 1988. *Sporomorph Biostratigraphy, Floral Changes, and Paleoclimatology, Eocene and Earliest Oligocene of the Eastern Gulf Coast*. Washington, D.C.: U.S. Geological Survey Professional Paper 1448.

Gentry, A. 1993. *A Field Guide to the Families and Genera of Woody Plants of Northwest South America (Colombia, Ecuador, Peru) with Supplementary Notes on Herbaceous Taxa*. Washington, D.C.: Conservation International.

Germeraad, J. H., C. A. Hopping, and J. Muller. 1968. Palynology of Tertiary Sediments from Tropical Areas. *Review of Palaeobotany and Palynology*, 6: 189–348. https://doi.org/10.1016/0034-6667(68)90051-1

Gilinsky, N. L. 1991. Bootstrapping and the Fossil Record. In *Analytical Paleobiology*, ed. N. L. Gilinsky and P. W. Signor, pp. 185–206. Pittsburgh: Paleobiology Society.

Goldner, A., N. Herold, and M. Huber. 2014. The Challenge of Simulating the Warmth of the Mid-Miocene Climatic Optimum in CESM1. *Climate of the Past*, 10: 523–536. https://doi.org/10.5194/cp-10-523-2014

Gomes, B. T., M. L. Absy, C. D'Apolito, C. Jaramillo, and R. Almeida. 2021. Compositional and Diversity Comparisons between the Palynological Records of the Neogene (Solimões Formation) and Holocene Sediments of Western Amazonia. *Palynology*, 45(1). https://doi.org/10.1080/01916122.2019.1692314

González-Guzmán, A. E. 1967. *A palynological Study on the Upper Los Cuervos and Mirador Formations (Lower and Middle Eocene; Tibu area, Colombia)*. Leiden: E. J. Brill.

Gorini, C., B. U. Haq, A. T. Reis, C. G. Silva, A. Cruz, E. Soares, and D. Granjeon. 2014. Late Neogene Sequence Stratigraphic Evolution of the Foz do Amazonas Basin, Brazil. *Terra Nova*, 26: 179–185. https://doi.org/10.1111/ter.12083

Gross, M., W. E. Piller, M. I. Ramos, and J. D. Silva Paz. 2011. Late Miocene Sedimentary Environments in South-Western Amazonia (Solimões Formation; Brazil). *Journal of South American Earth Sciences*, 32: 169–181. https://doi.org/10.1016/j.jsames.2011.05.004

Gross, M., M. I. Ramos, M. Caoraletti, and W. E. Piller. 2013. Ostracods (Crustacea) and Their Palaeoenvironmental Implication for the Solimões Formation (Late Miocene; Western Amazonia/Brazil). *Journal of South American Earth Sciences*, 42: 216–241. https://doi.org/10.1016/j.jsames.2012.10.002

Gross, M., M. I. Ramos, and W. E. Piller. 2015. A Minute Ostracod (Crustacea: Cytheromatidae) from the Miocene Solimões Formation (Western Amazonia, Brazil): Evidence for Marine Incursions? *Journal of Systematic Palaeontology*, 14(7): 581–602. https://doi.org/10.1080/14772019.2015.1078850

Head, M. J., G. Norris, and P. J. Mudie. 1989. Palynology and Dinocyst Stratigraphy of the Miocene in ODP Leg 105, Hole 645E, Baffin Bay. *Proc. ODP, Sci. Results,* 105: 467–514. (Ocean Drilling Program, College Station, Tex.)

Hedlund, R. W. 1966. Palynology of the Red Branch Member (Woodbine Formation). *Oklahoma Geological Survey Bulletin*, 112: 1–69.

Herngreen, G. F. W. 1973. Palynology of Albian-Cenomanian Strata of Borehole 1-QS-1-MA, State of Maranhão, Brazil. *Pollen et Spores*, 15(3–4): 515–555.

Herngreen, G. F. W. 1975. An Upper Senonian Pollen Assemblage of Borehole 3-Pia-10Al State of Alagoas, Brazil. *Pollen et Spores*, 17: 93–140.

Higgins, M. A., K. Ruokolainen, H. Tuomisto, N. Llerena, G. Cardenas, O. L. Phillips, R. Vásquez, and M. Räsänen. 2011. Geological Control of Floristic Composition in Amazonian Forests. *Journal of Biogeography*, 38: 2136–2149. https://doi.org/10.1111/j.1365-2699.2011.02585.x

Hoorn, C. 1993. Marine Incursions and the Influence of Andean Tectonics on the Miocene Depositional History of Northwestern Amazonia: Results of a Palynostratigraphic Study. *Palaeogeography, Palaeoclimatology, Palaeoecology*, 105: 267–309. https://doi.org/10.1016/0031-0182(93)90087-Y

Hoorn, C. 1994a. An Environmental Reconstruction of the Palaeo-Amazon River System (Middle–Late Miocene, NW Amazonia). *Palaeogeography, Palaeoclimatology, Palaeoecology*, 112: 187–238. https://doi.org/10.1016/0031-0182(94)90074-4

Hoorn, C. 1994b. Fluvial Palaeoenvironments in the Intracratonic Amazonas Basin (Early Miocene–Early Middle Miocene, Colombia). *Palaeogeography, Palaeoclimatology, Palaeoecology*, 109: 1–54. https://doi.org/10.1016/0031-0182(94)90117-1

Hoorn, C. 2006. Mangrove Forests and Marine Incursions in Neogene Amazonia (Lower Apaporis River, Colombia). *Palaios*, 21(2): 197–209. http://dx.doi.org/10.2110/palo.2005.p05-131

Hoorn, C., G. R. Bogotá-A, M. Romero-Baez, E. I. Lammertsma, S. G. Flantua, E. L. Dantas, R. Dino, D. A. Carmo, and F. Chemale. 2017. The Amazon at Sea: Onset and Stages of the Amazon River from a Marine Record, with Special Reference to Neogene Plant Turnover in the Drainage Basin. *Global and Planetary Change*, 153: 51–65. https://doi.org/10.1016/j.gloplacha.2017.02.005

Hoorn, C., R. van der Ham, F. de la Parra, S. Salamanca, H. ter Steege, H. Banks, W. Star, B. J. van Heuven, R. Langelaan, F. A. Carvalho, G. Rodríguez-Forero, and L. P. Lagomarsino. 2019. Going North and South: The Biogeographic History of Two Malvaceae in the Wake of Neogene Andean Uplift and Connectivity between the Americas. *Review of Palaeobotany and Palynology*, 264: 90–109. doi.org/10.1016/j.revpalbo.2019.01.010

Hoorn, C., F. P. Wesselingh, H. ter Steege, M. A. Bermudez, A. Mora, J. S. I. Sanmartín, A. Sanchez-Meseguer, C. L. Anderson, J. P. Figueiredo, C. Jaramillo, D. D. Riff, F. R. Negri, H. Hooghiemstra, J. Lundberg, T. Stadler, T. Sarkinen, and A. Antonelli. 2010. Amazonia through Time: Andean Uplift, Climate Change, Landscape Evolution and Biodiversity. *Science*, 330: 927–931. https://doi.org/10.1126/science.1194585

Horbe, A. M. C., M. Roddaz, L. B. Gomes, R. T. Castro, E. L. Dantas, and D. A. Carmo. 2019. Provenance of the Neogene Sediments from the Solimões Formation (Solimões and Acre Basins), Brazil. *Journal of South American Earth Sciences*, 93: 232–241. https://doi.org/10.1016/j.jsames.2019.05.004

Householder, J. E., and F. Wittmann. 2016. Floristic Diversity of *Mauritia flexuosa* Wetlands in the Brazilian Amazon. In *Morichales, canangucháles y otros palmares inundables de Suramérica. Parte II: Colombia, Venezuela, Brasil, Perú, Bolivia, Paraguay, Uruguay y Argentina. Serie editorial recursos hidrobiológicos y pesqueros continentales de Colombia*, ed. C. A. Lasso, G. Colonnello, and M. Moraes, pp. 241–252. Bogotá: Instituto de Investigación de los Recursos Biológicos Alexander von Humboldt (IAvH).

Hsieh, T. C., K. H. Ma, and A. Chao. 2019. iNEXT: iNterpolation and EXTrapolation for Species Diversity. R package version 2.0.19. https://cran.r-project.org/web/packages/iNEXT/index.html [Permanent link.]

Ibrahim, A. C. 1933. *Sporenformen des Aegir-horizonts des Ruhr-Reviers* [Spore forms of the Aegir horizon of the Ruhr area]. Wurzburg: University of Berlin.

Irion, G., M. B. Bush, J. A. Nunes de Mello, D. Stüben, T. Neumann, G. Müller, J. O. Morais, and J. W. Junk. 2006. A Multiproxy Palaeoecological Record of Holocene Lake Sediments from the Rio Tapajós, Eastern Amazonia. *Palaeogeography, Palaeoclimatology, Palaeoecology*, 240: 523–535. https://doi.org/10.1016/j.palaeo.2006.03.005

Jan du Chêne, R. E., I. Klasz, and E. E. Archibong. 1978. Biostratigraphic Study of the Borehole Ojo-1, SW Nigeria, with Special Emphasis on the Cretaceous Microflora. *Revue de Micropaléontologie*, 21: 123–139.

Jansonius, J., and L. V. Hills. 1976. Genera File of Fossil Spores and Pollen. 3287 cards. *Department of Geology, Special Publication.* Calgary, Alberta: University of Calgary.

Jansonius, J., and L. V. Hills. 1990. Genera File of Fossil Spores. Supplement. Cards 4585–4811. *Department of Geology, Special Publication.* Calgary, Alberta, Canada: University of Calgary.

Jaramillo, C., G. Bayona, A. Pardo-Trujillo, M. Rueda, V. Torres, G. Harrington, and G. Mora. 2007. The Palynology of the Cerrejón Formation (Upper Paleocene) of Northern Colombia. *Palynology*, 31: 153–189. https://doi.org/10.1080/01916122.2007.9989641

Jaramillo, C., and D. L. Dilcher. 2001. Middle Paleogene Palynology of Central Colombia, South America: A Study of Pollen and Spores from Tropical Latitudes. *Palaeontographica Abteilung B*, 258: 87–213.

Jaramillo, C., C. Hoorn, S. A. F. Silva, F. Leite, F. Herrera, L. Quiroz, R. Dino, R., and L. Antonioli. 2010a. The Origin of the Modern Amazon Rainforest: Implications of the Palynolgical and Palaeobotanical Record. In *Amazonia: Landscape and Species Evolution—A Look into the Past*, ed. C. Hoorn and F. P. Wesselingh, pp. 317–334. Oxford: Blackwell Publishing.

Jaramillo, C., E. Moreno, V. Ramírez, S. A. F. Silva, A. Barrera, C. Sánchez, S. Morón, F. Herrera, J. Escobar, R. Koll, S. R. Manchester, and N. Hoyos. 2014. Palynological Record of the Last 20 Million Years in Panama. In *Paleobotany and Biogeography: A Festschrift for Alan Graham in His 80th Year,* ed. W. D. Stevens, O. M. Montiel, and P. Raven, pp. 134–251. St. Louis: Missouri Botanical Garden Press.

Jaramillo, C., D. Ochoa, L. Contreras, M. Pagani, H. Carvajal-Ortiz, L. M. Pratt, S. Krishnan, A. Cardona, M. Romero, L. Quiroz, G. Rodríguez, M. J. Rueda, F. de la Parra, S. Morón, W. Green, G. Bayona, C. Montes, O. Quintero, R. Ramírez, G. Mora, S. Schouten, H. Bermúdez, R. Navarrete, F. Parra, M. Alvarán, J. Osorno, J. L. Croley, V. Valencia, and J. Vervoort. 2010b. Effects of Rapid Global Warming at the Paleocene-Eocene Boundary on Neotropical Vegetation. *Science*, 330: 957–61. https://doi.org/10.1126/science.1193833

Jaramillo, C., I. Romero, C. D'Apolito, G. Bayona, E. Duarte, S. Louwye, J. Escobar, J. Luque, J. D. Carrilo-Briceño, V. Zapata, A. Mora, S. Schouten, M. Zavada, G. Harrington, J. Ortiz, and F. P. Wesselingh. 2017. Miocene Flooding Events of Eastern Amazonia. *Science Advances*, 3(5): e1601693. https://doi.org/10.1126/sciadv.1601693

Jaramillo, C., and M. J. Rueda. 2020. A Morphological Electronic Database of Cretaceous-Tertiary and Extant Pollen and Spores from Northern South America, v. 2020. *Smithsonian Tropical Research Institute*. http://biogeodb.stri.si.edu/jaramillosdb/web/morphological/ (accessed 20 October 2020).

Jaramillo, C., M. Rueda, and G. Mora. 2006. Cenozoic Plant Diversity in the Neotropics. *Science*, 311: 1893–1896. https://doi.org/10.1126/science.1121380

Jaramillo, C.A., M. Rueda, and V. Torres. 2011. A Palynological Zonation for the Cenozoic of the Llanos and Llanos Foothills of Colombia. *Palynology*, 35: 46–84. https://doi.org/10.1080/01916122.2010.515069

Jaramillo, C., Zavada, M., Ortiz, J., Pardo, A., and D. Ochoa. 2013. The Biogeography of the Araucarian Dispersed Pollen *Cyclusphaera*. *International Journal of Plant Sciences*, 174(3): 489–498. https://doi.org/10.1086/668869

Jorge, V., C. D'Apolito, and S. A. F. da Silva-Caminha. 2019. Exploring Geophysical and Palynological Proxies for Paleoenvironmental Reconstructions in the Miocene of Western Amazonia (Solimões Formation, Brazil). *Journal of South American Earth Sciences*, 94: 102223. https://doi.org/10.1016/j.jsames.2019.102223

Junk, W. J., and M. T. F. Piedade. 1997. Plant Life in the Floodplain with Special Reference to Herbaceous Plants. In *The Central Amazon Floodplain: Ecology of a Pulsating System,* ed. W. J. Junk, pp. 147–185. Volume 126. Berlin: Springer, Ecological Studies.

Kaandorp, R. J. G., H. B. Vonhof, F. P. Wesselingh, L. Romero Pittman, D. Kroon, and J. E. van Hinte. 2005. Seasonal Amazonian Rainfall Variation in the Miocene Climate Optimum. *Palaeogeography, Palaeoecology, Paleoclimatology*, 221: 1–6. https://doi.org/10.1016/j.palaeo.2004.12.024

Kachinasz, K. R., and S. A. F. Silva-Caminha. 2016. Palinoestratigrafia da Formação Solimões: Comparação entre bioestratigrafia tradicional e o método de associações unitárias [Palynostratigraphy of the Solimões Formation: Comparison between Traditional Biostratigraphy and the Unitary Associations Method]. *Revista Brasileira de Paleontologia*, 19(3): 481–490. http://dx.doi.org/10.4072/rbp.2016.3.12

Kedves, M. 1995. *Upper Cretaceous Spores from Egypt*. Hungary: Szeged.

Kedves, M., and N. Solé de Porta. 1963. Comparación de las esporas del género *Cicatricosisporites* R. Pot y Gell, 1933 de Hungría y Colombia [Comparison between Spores of the Genus *Cicatricosisporites* R. Pot y Gell, 1933 from Hungry and Colombia]. Algunos problemas referentes a su significado estratigráfico. *Boletin Geologico*, 12: 51–76.

Kern, A. K., M. Gross, C. P. Galeazzi, F. N. Pupim, A. O. Sawakuchi, R. P. Almeida, W. E. Piller, G. G. Kuhlmann, and M. A. S. Basei. 2020. Re-investigating Miocene Age Control and Paleoenvironmental Reconstructions in Western Amazonia (Northwestern Solimões Basin, Brazil). *Palaeogeography, Palaeoclimatology, Palaeoecology*, 545: 109652. https://doi.org/10.1016/j.palaeo.2020.109652

Khan, A. M., and A. R. H. Martin. 1972. A Note on Genus *Polypodiisporites* R. Potonié. *Pollen et Spores*, 13: 475–480.

Klaus, W. 1960. Sporen der Karnischen Stufe der ostalpinen Trias [Spores of the Carnian Stage of the Eastern Alpine Triassic]. *Jahrbuch der Geologischen Bundesanstalt*, 5: 107–184.

Konzalová, M. 1976. Micropalaeobotanical (Palynogical) Research of the Lower Miocene of Northern Bohemia. *Rozpravy Ceskoslovenské Akademie Ved*, 86(12): 1–75.

Krause, G., H. K. Winter, B. Krause, P. Jahns, M. García, J. Aranda, and A. Virgo. 2010. High Temperature Tolerance of a Tropical Tree, *Ficus insipida*: Methodological Reassessment and Climate Change Considerations. *Functional Plant Biology*, 37: 890–900. https://doi.org/10.1071/FP10034

Krutzsch, W. 1959. Mikropaläontologische (sporenpaläontologische) Untersuchungen in der Braunkohle des Geiseltales—[Part] I, Die Sporen und die Sporenartigen sowie ehemals im Geiseltal zu Sporites gestellten Formeinheiten der Sporae dispersae der mitteleozänen Braunkohle des mittleren Geisel tales (Tagebau Neumark-West i.w.S.) unter Berücksichtigung und Revision weiterer Sporenformen aus der bisherigen Literatur [Micropalaeontological (spore-paleontological) investigations in the lignite of the Geiseltales—[Part] I, The Spore and the Spore-like as Well as Units of the Sporae Dispersae of the Middle Eocene Lignite of the Middle Geisel Valley (Neumark-West Opencast Mine), Taking into Account and Evaluating Further Spore Forms from Previous Literature]. *Geologie*, 8 (21/22).

Krutzsch, W. 1963. *Atlas der mittel- und jungtertiaren dispersen Sporen und Pollen-sowie der Mikroplanktonformen des nordlichen Mitteleuropas. Lieferung 3: Sphagnaceoide und Selaginellaceoide Sporenformen* [Atlas of the Middle and Early Tertiary Dispersed Spores and Pollen as Well as the Microplankton Forms of Northern Central Europe. Delivery 3: Sphagnaceoide and Selaginellaceoide Spore Forms]. Jena/Berlin: Veb Gustav Fischer Verlag.

Krutzsch, W. 1966. Zur kenntnis des praquartaren periporaten pollenformen [Study of pre-Quaternary Periporate Pollen Grains]. *Geologie*, 55: 16–71.

Krutzsch, W. 1967. *Atlas der mittel- und jungtertiaren dispersen Sporen und Pollen-sowie der Mikroplanktonformen des nordlichen Mitteleuropas. Lieferung 4 und 5: Weitere azonotrilete (apiculate, murornate), monolete und alete Sporenformen* [Atlas of the Middle and Early Tertiary Dispersed Spores and Pollen as Well as the Microplankton Forms of Northern Central Europe. Delivery 4 and 5: Further Azonotrilete (Apiculate, Murornate), Monolete and Alete Spore Forms]. Jena/Berlin: Veb Gustav Fischer Verlag.

Krutzsch, W. 1970. *Atlas der mittel- und jungtertiaren dispersen Sporen- und Pollen-sowie der Mikroplanktonformen des nordlichen Mitteleuropas. Lieferung 7: Monoporate, monocolpate, longicolpate, dicolpate und ephedroide (polyplicate) Pollenformen* [Atlas of the Middle and Early Tertiary Disperse Spore and Pollen as Well as the Microplankton Forms of Northern Central Europe. Delivery 7: Monoporate, Monocolpate, Longicolpate, Dicolpate and Ephedroid (Polyplicate) Pollen Forms]. Jena/Berlin: Veb Gustav Fischer Verlag.

Latrubesse, E. M., M. Cozzuol, S. A. F. Silva-Caminha, C. A. Rigsby, M. L. Absy, and C. Jaramillo. 2010. The Late Miocene Paleogeography of the Amazon Basin and the Evolution of the Amazon River System. *Earth-Science Reviews*, 99: 99–124. https://doi.org/10.1016/j.earscirev.2010.02.005

Latrubesse, E. M., S. A. F. Silva-Caminha, M. Cozzuol, and M. L. Absy. 2007. Late Miocene Continental Sedimentation in the Southwestern Amazonia and Its Regional Significance: Biotic and Geological Evidence. *Journal of South American Earth Sciences*, 23: 61–80. https://doi.org/10.1016/j.jsames.2006.09.021

Leandro, L. M., C. E. L. Vieira, A. Santos, and G. Fauth. 2019. Palynostratigraphy of Two Neogene Boreholes from the Northwestern Portion of the Solimões Basin, Brazil. *Journal of South American Earth Sciences*, 89: 211–218. https://doi.org/10.1016/j.jsames.2018.11.016

Legoux, O. 1978. Quelques espèces de pollen caractéristiques du Néogène du Nigéria [Some Characteristic Species of Pollen from the Neogene of Nigeria]. *Bulletin des Centres de Recherche Exploration-Production Elf-Aquitaine*, 2: 265–317.

Leidelmeyer, P. 1966. The Paleogene and Lower Eocene Pollen Flora of Guyana. *Leidse Geologische Mededelingen*, 38: 49–70.

Leite, F. P. R., J. Paz, D. A. Carmo, and S. A. F. Silva-Caminha. 2017. The Effects of the Inception of Amazonian Transcontinental Drainage during the Neogene on the Landscape and Vegetation of the Solimões Basin, Brazil. *Palynology*, 41(3): 412–422. https://doi.org/10.1080/01916122.2016.1236043

Leite, F. P. R., S. A. F. Silva-Caminha, and C. D'Apolito. 2021. New Neogene Index Pollen and Spore Taxa from the Solimões Basin (Western Amazonia), Brazil. *Palynology*, 45(1): 115–141. https://doi.org/10.1080/01916122.2020.1758971

Lenoir, E. A., and G. F. Hart. 1986. Burdigalian (Early Miocene) Dinocysts from Off-Shore Louisiana. In *Papers from the First Symposium on Neogene Dinoflagellate Cyst Biostratigraphy*, ed. J. H. Wrenn, S. L. Duffield, and J. A. Stein, pp. 59–81. Contribution Series 17. Dallas: American Association of Stratigraphic Palynologists.

León-García, I. V., and E. Lasso. 2019. High Heat Tolerance in Plants from the Andean Highlands: Implications for Paramos in a Warmer World. *PLOS ONE*, 14(11): e0224218. https://doi.org/10.1371/journal.pone.0224218

Linhares, A. P., V. C. S. Gaia, and M. I. F. Ramos. 2017. The Significance of Marine Microfossils for Paleoenvironmental Reconstruction of the Solimões Formation (Miocene), Western Amazonia, Brazil. *Journal of South American Earth Sciences*, 79: 57–66. http://dx.doi.org/10.1016/j.jsames.2017.07.007

Linhares, A. P., M. I. F. Ramos, V. C. S. Gaia, and Y. S. Frias. 2019. Integrated Biozonation Based on Palynology and Ostracods from the Neogene of Solimões Basin, Brazil. *Journal of South American Earth Sciences*, 91: 57–70. https://doi.org/10.1016/j.jsames.2019.01.015

Lloyd, J., and G. D. Farquhar. 2008. Effects of Rising Temperatures and [CO$_2$] on the Physiology of Tropical Forest Trees. *Philosophical Transactions of the Royal Society B*, 363: 1811–1817. https://doi.org/10.1098/rstb.2007.0032

Londoño, L., D. L. Royer, C. Jaramillo, J. Escobar, D. A. Foster, A. L. Cárdenas-Rozo, and A. Wood. 2018. Early Miocene CO$_2$ Estimates from a Neotropical Fossil Leaf Assemblage Exceed 400 ppm. *American Journal of Botany*, 105(11): 1–9. https://doi.org/10.1002/ajb2.1187

Lorente, M. A. 1986. *Palynology and Palynofacies of the Upper Tertiary in Venezuela*. Dissertatione Botanicae, Band 99. Berlin: Cramer.

Lorente, F. L., A. A. Buso-Junior, P. E. De Oliveira, and L. C. R. Pessenda. 2017. *Atlas Palinológico: Laborátório 14C–CENA/USP*. Piracicaba, SP, Brazil: FEALQ.

Lundberg, J. G., J. G. Marshall, J. Guerrero, B. Horton, M. C. S. L. Malabarba, and F. P. Wesselingh. 1998. The Stage for Neotropical Fish Diversification: A History of Tropical South American Rivers. In *Phylogeny and Classification of Neotropical Fishes*, ed. L. R. Malabarba, R. E. Reis, R. P. Vari, Z. M. S. Lucena, and C. A. S. Lucena, pp. 13–48. Porto Alegre, Brazil: EDIPUCRS.

Lundberg, J. G., M. H. Sabaj Pérez, W. M. Dahdul, and O. A. Aguilera. 2010. The Amazonian Neogene Fish Fauna. In *Amazonia: Landscape and Species Evolution—A Look into the Past*, ed. C. Hoorn and F. P. Wesselingh, pp. 281–301. Oxford: Blackwell Publishing.

Magurran, A. E. 2004. *Measuring Biological Diversity*. Malden, Mass.: Blackwell Publishing.

Maia, R. G., H. K. Godoy, H. S. Yamaguti, P. A. Moura, F. S. Costa, M. A. Holanda, and J. Costa. 1977. *Projeto de carvão no Alto Solimões. Relatório final* [Coal Project in the Upper Solimões. Final Report]. Manaus, Brazil: CPRM-DNPM.

Mathur, Y. K. 1966. On the Microflora in the Supratrappeans of Western Kutch, India. *Quarterly Journal. The Geological, Mining and Metallurgical Society of India*, 38: 33–51.

Mathur, Y. K., and A. K. Jain. 1980. Palynology and Age of the Dras Volcanics near Shergol, Ladakh, Jammu and Kashmir, India. *Geoscience Journal*, 1: 55–74.

Matsuoka, K. 1983. Late Cenozoic Dinoflagellates and Acritarchs in the Niigata District, Central Japan. *Paleontographica B*, 187: 89–154.

Melack, J. M., and L. L. Hess. 2010. Remote Sensing of the Distribution and Extent of Wetlands in the Amazon Basin. In *Amazonian Floodplain Forests*, ed W. J. Junk, M. T. F. Piedade, F. Wittmann, J. Schöngart, P. Parolin, pp. 43–59. Dordrecht: Springer. https://doi.org/10.1007/978-90-481-8725-6_3

Merino, E. R., and M. L. Assine. 2020. Hidden in Plain Sight: How Finding a Lake in the Brazilian Pantanal Improves Understanding of Wetland Hydrogeomorphology. *Earth Surfaces: Processes and Landforms*, 45: 440–458. https://doi.org/10.1002/esp.4745

Monsch, K. A. 1998. Miocene Fish Faunas from the Northwestern Amazonia Basin (Colombia, Peru, Brazil) with Evidence of Marine Incursions. *Palaeogeography, Palaeoclimatology, Palaeoecology*, 143(1): 31–50. https://doi.org/10.1016/S0031-0182(98)00064-9

Muller, J. 1959. Palynology of Recent Orinoco Delta and Shelf Sediments: Reports of the Orinoco Shelf Expedition. *Micropaleontology*, 5(1): 1–32.

Muller, J., E. Giacomo, and A. W. Van Erve. 1987. *A Palynological Zonation for the Cretaceous, Tertiary and Quaternary of Northern South America*. Contribution Series 19. Dallas: American Association of Stratigraphic Palynologists Foundation.

Muñoz-Torres, F. A., R. C. Whatley, and D. van Harten. 2006. Miocene Ostracod (Crustacea) Biostratigraphy of the Upper Amazon Basin and Evolution of the Genus *Cyprideis*. *Journal of South American Earth Sciences*, 21: 75–86. https://doi.org/10.1016/j.jsames.2005.08.005

Nakoman, E. 1965. Description d'un noveau genre de form: *Corsinipollenites* [Description of a New Form Genus: *Corsinipollenites*]. *Annales de la Société Géologique du Nord*, 85: 155–158.

Negri, F. R., J. Bocquentin-Villanueva, J. Ferigolo, and P.-O. Antoine. 2010. A Review of Tertiary Mammal Faunas and Birds from Western Amazonia. In *Amazonia: Landscape and Species Evolution—A Look into the Past*, ed. C. Hoorn and F. P. Wesselingh, pp. 245–258. Oxford: Blackwell Publishing.

Nichols, D. J., H. T. Ames, and A. Traverse. 1973. On *Arecipites* Wodehouse, *Monocolpopollenites* Thomson & Pflug, and the Species "*Monocolpopollenites tranquillus*." *Taxon*, 22: 241–56.

Nogueira, A. C. R., R. R. Silveira, and J. T. F. Guimarães. 2013. Neogene-Quaternary Sedimentary and Paleovegetation History of Eastern Solimões Basin, Central Amazon Region. *Journal of South American Earth Sciences*, 46: 89–99. http://dx.doi.org/10.1016/j.jsames.2013.05.004

Norris, G. 1967. Spores and Pollen from the Lower Colorado Group (Albian–?Cenomanian) of Central Alberta. *Palaeontographica Abteilung B*, 120: 72–115.

Oksanen, J., F. G. Blanchet, M. Friendly, R. Kindt, P. Legendre, D. McGlinn, P. R. Minchin, R. B. O›Hara, G. L. Simpson, P. Solymos, M. H. H. Stevens, E. Szoecs, and H. Wagner. 2019. Vegan: Community Ecology Package. R package version 2.5-5. https://CRAN.R-project.org/package=vegan [Permanent link.]

Ortiz, J., and C. Jaramillo. 2020. SDAR: A Toolkit for Stratigraphic Data Analysis. R package version 0.9-55. https://CRAN.R-project.org/package=SDAR [Permanent link.]

Palazzesi, L., V. D. Barreda, J. I. Cuitiño, M. V. Guler, M. C. Tellería, and V. Santos. 2014. Fossil Pollen Records Indicate That Patagonian Desertification Was Not Solely a Consequence of Andean Uplift. *Nature Communications*, 5: 3558. https://doi.org/10.1038/ncomms4558

Pant, D. D. 1954. Suggestions for the Classification and Nomenclature of Fossil Spores and Pollen Grains. *Botanical Review*, 20: 33–60.

Pflanzl, G. 1956. Das Alter der Braunkohlen des Meißners, der Flöze 2 und 3 des Hirschberger und eines benachbarten Kohlenlagers bei Laudenbach [The Age of the Lignite from the Meissner, the Seams 2 and 3 of the Hirschberger and a Neighboring Coal Store Near Laudenbach]. *Notizlatt des Hessischen Landesamtes für Amt Bodenforsch zu Wiesbaden*, 84: 232–244.

Pflug, H. D. 1953. Zur Entstehung und Entwicklung des angiospermiden pollens in der Erdgeschichte [On the Origin and Development of Angiosperm Pollen in the History of the Earth]. *Palaeontographica Abteilung B*, 95: 60–171.

Pianka, E. R. 1966. Latitudinal Gradients in Species Diversity: A Review of Concepts. *American Naturalist*, 100 (910): 33–46. https://doi.org/10.1086/282398

Pierce, R. L. 1961. Lower Upper Cretaceous Plant Microfossils from Minnesota. *Minnesota Geological Survey Bulletin*, 42.

Pocknall, D. T., and Y. M. Crosbie. 1982. Taxonomic Revision of Some Tertiary Tricolporate and Tricolpate Pollen Grains from New Zealand. *New Zealand Journal of Botany*, 20: 7–15. https://doi.org/10.1080/0028825X.1982.10426401

Pocknall, D., T., and D. M. Jarzen. 2012. *Grimsdalea magnaclavata* Germeraad, Hopping & Muller: An Enigmatic Pollen Type from the Neogene of Northern South America. *Palynology*, 36(1): 134–143. http://dx.doi.org/10.1080/01916122.2011.642258

Pocknall, D. T., and D. C. Mildenhall. 1984. Late Oligocene-Early Miocene Spores and Pollen from Southland, New Zealand. *New Zealand Geological Survey Paleontological Bulletin*, 51: 1–66.

Pocock, S. A. J. 1962. Microfloral Analysis and Age Determinations of Strata at the Jurassic Cretaceous Boundary in the Western Canada Plains. *Palaeontographica Abteilung B*, 111: 1–95.

Por, F. D. 1995. *The Pantanal of Mato Grosso (Brazil)—World's Largest Wetlands*. Dordrecht: Kluwer Academic Publishers. https://doi.org/10.1007/978-94-011-0031-1

Potonié, R. 1931. Zur Mikroskopie der Braunkohlen. Tertiäre Blütenstaubformen [Microscopy of Brown Coals. Tertiary Pollen Forms]. *Braunkohle*, 30(16): 325–333.

Potonié, R. 1934. Zur Mikrobotanik des eozänen Humodils des Geiseltals [On the Microbotany of the Eocene Humodile of the Geiseltal]. *Arbeiten aus dem Institut für Paläeobotanik und Petrographie der Brennsteine*, 4: 25–125.

Potonié, R. 1956. *Synopsis der Gattungen der Sporae dispersae. I. Teil: Sporites* [Synopsis of the Genera of Sporae Dispersae. Part I: Sporites]. Hannover: Beihefte zum Geologischen Jahrbuch, 23.

Potonié, R. 1958. *Synopsis der Gattungen der Sporae dispersae. II. Teil: Sporites (Nachtrage), Saccites, Aletes, Praecolpates, Polyplicates, Monocolpates* [Synopsis of the Genera of Sporae Dispersae. Part II: Sporites (Addendum), Saccites, Aletes, Praecolpates, Polyplicates, Monocolpates]. Hannover: Beihefte zum Geologischen Jahrbuch, 31.

Potonié, R. 1966. *Synposis der Gattungen der Sporae dispersae. IV. Teil: Nachtrage zu allen Gruppen (Turmae)* [Synposis of the Genera of the Sporae Dispersae. Part IV: Addendum to All Groups (Turmae)]. Hannover: Beihefte zum Geologischen Jahrbuch 72.

Potonié, R., and J. Gelletich. 1933. Uber Pteridophyten-sporen einer eozanen Braunkohle aus Dorog in Ungarn [On Pteridophyte Spores of an Eocene Brown Coal from Dorog in Hungary]. *Sitzungsberichte der Gesellschaft naturforschender Freundes zu Berlin*, 33: 517–523.

Potonié, R., and A. Venitz. 1934. Zur Mikrobotanik des miozanen Humodils der niederrheinischen Bucht [On the Microbotany of the Miocene Humodile of the Lower Rhine Bay]. *Arbeiten aus dem Institut fur Paläobotanik und Petrographie der Brennsteine*, 5: 5–54.

Pott, A., A. K. M. Oliveira, G. A. Damasceno-Június, and J.S.V. Silva. 2011. Plant Diversity of the Pantanal Wetland. *Brazilian Journal of Biology*, 71(1): 265–273. https://doi.org/10.1590/S1519-69842011000200005

Pott, V. J., and A. Pott. 2000. *Plantas aquáticas do Pantanal* [Aquatic Plants from Pantanal]. Brasília, Brazil: Embrapa.

Punt, W., P. P. Hoen, S. Blackmore, S. Nilsson, and A. Le-Thomas. 2007. Glossary of Pollen and Spore Terminology. *Review of Paleobotany and Palynology*, 143: 1–81. https://doi.org/10.1016/j.revpalbo.2006.06.008

Punyasena, S. W., J. W. Dalling, C. Jaramillo, and B. L. Turner. 2011. Comment on "The Response of Vegetation on the Andean Flank in Western Amazonia to Pleistocene Climate Change." *Science*, 333: 1825a–b. https://doi.org/10.1126/science.1207525

Puri, G. S. 1963. Some Plant Microfossils from the Cretaceous and Paleocene of Nigeria. *University of Ibadan Botanical Studies*, 10: 1–142.

Quesada, C. A., O. L. Phillips, M. Schwarz, C. I. Czimczik, T. R. Baker, S. Patiño, N. M. Fyllas, M. G. Hodnett, R. Herrera, S. Almeida, E. Alvarez Dávila, A. Arneth, L. Arroyo, K. J. Chao, N. Dezzeo, T. Erwin, A. di Fiore, N. Higuchi, E. Honorio Coronado, E. M. Jimenez, T. Killeen, A. T. Lezama, G. Lloyd, G. López-González, F. J. Luizão, Y. Malhi, A. Monteagudo, D. A. Neill, P. Núñez Vargas, R. Paiva, J. Peacock, M. C. Peñuela, A. Peña Cruz, N. Pitman, N. Priante Filho, A. Prieto, H. Ramírez, A. Rudas, R. Salomão, A. J. B. Santos, J. Schmerler, N. Silva, M. Silveira, R. Vásquez, I. Vieira, J. Terborgh, J. Lloyd. 2012. Basin-Wide Variations in Amazon Forest Structure and Function Are Mediated by Both Soils and Climate. *Biogeosciences*, 9: 2203–2246. https://doi.org/10.5194/bg-9-2203-2012

Raine, J. I. 1981. *Palynological Correlation of the Dunollie/Rewanui Member Boundary in Drillholes 621 and 622, Greymouth Coalfield*. New Zealand Geological Survey Report, 47.

Ramanujam, C. G. K. 1966. Pteridophytic Spores from the Miocene Lignite of South Arcot District, Madras. *Palynological Bulletin*, 2–3: 29–40.

R Core Team. 2019. R: A Language and Environment for Statistical Computing. R Foundation for Statistical Computing, Vienna, Austria. URL https://www.R-project.org/

Regali, M. S., N. Uesegui, and A. Santos. 1974. Palinologia dos sedimentos Meso–Cenozoicos do Brasil (I) [Palynology of Meso-Cenozoic sediments from Brazil (I)]. *Boletim Técnico da Petrobras*, 17: 263–362.

Reichgelt, T., W. J. D'Andrea, A. C. Valdivia-McCarthy, B. R. S. Fox, J. M. Bannister, J. G. Conran, W. G. Lee, and D. E. Lee. 2020. Elevated CO_2, Increased Leaf-Level Productivity, and Water-Use Efficiency during the Early Miocene. *Climate of the Past*, 16: 1509–1521. https://doi.org/10.5194/cp-16-1509-2020

Riff, D., P. S. R. Romano, G. R. Oliveira, and O. A. Aguilera. 2010. Neogene Crocodile and Turtle Fauna in Northern South America. In *Amazonia: Landscape and Species Evolution—A Look into the Past*, ed. C. Hoorn and F. P. Wesselingh, pp. 259–280. Oxford: Blackwell Publishing.

Roddaz, M., P. Baby, S. Brusset, W. Hermoza, and J. M. Darrozes. 2005. Forebulge Dynamics and Environmental Control in Western Amazonia: The Case Study of the Arch of Iquitos (Peru). *Tectonophysics*, 399: 87–108. https://doi.org/10.1016/j.tecto.2004.12.017

Rodríguez-Zorro, P., B. Turcq, R. Cordeiro, L. Moreira, R. Costa, C. McMichael, and H. Behling. 2018. Forest Stability during the Early and Late Holocene in the Igapó Floodplains of the Rio Negro, Northwestern Brazil. *Quaternary Research*, 89(1): 75–89. https://doi.org/10.1017/qua.2017.99

Romero, I. C., S. Kong, C. C. Fowlkes, C. A. Jaramillo, M. A. Urban, F. Oboh-Ikuenobed, C. D'Apolito, and S. W. Punyasena. 2020. Improving the Taxonomy of Fossil Pollen Using Convolutional Neural Networks and Superresolution Microscopy. *Proceedings of the National Academy of Sciences*, 117(45): 202007324. https://doi.10.1073/pnas.2007324117

Rossignol, M. 1962. Analyse pollinique de sédiments marins quaternaires en Israël II—Sédiments Pleistocènes [Pollen Analyses of Quaternary Marine Sediments in Israel II—Pleistocene Sediments]. *Pollen et Spores*, 4(1): 121–148.

Roubik, D.W., and J. E. Moreno. 1991. *Pollen and Spores of Barro Colorado Island*. St. Louis: Missouri Botanical Garden.

Roucoux, K. H., I. T. Lawson, T. D. Jones, T. R. Baker, E. N. Honorio-Coronado, W. D. Gosling, and O. Lähteenoja. 2013. Vegetation Development in an Amazonian Peatland. *Palaeogeography, Palaeoclimatology, Palaeoecology*, 374: 242–255. https://doi.org/10.1016/j.palaeo.2013.01.023

Rull, V. 1997. Oligo-Miocene Palynology of the Rio Chama Sequence (Western Venezuela), with Comments on Fossil Assemblages as Paleoenvironmental Indicators. *Palynology*, 21: 213–229. https://doi.org/10.1080/01916122.1997.9989497

Rull, V. 1998. Biogeographical and Evolutionary Considerations of *Mauritia* (Arecaceae), Based on Palynological Evidence. *Review of Palaeobotany and Palynology*, 100: 109–122. https://doi.org/10.1016/S0034-6667(97)00060-2

Sá, N. P., M. L. Absy, and E. A. A Soares. 2016. Late Holocene Paleoenvironments of the Floodplain of the Solimões River, Central Amazonia, Based on the Palynological Record of Lake Cabaliana. *Acta Botanica Brasilica*, 30(3): 473–485. https://doi.org/10.1590/0102-33062016abb0250

Sá, N. P., M. A. Carvalho, and G. C. Correia. 2020. Miocene Paleoenvironmental Changes in the Solimões Basin, Western Amazon, Brazil: A Reconstruction Based on Palynofacies Analysis. *Palaeogeography, Palaeoclimatology, Palaeoecology*, 537: 109450. https://doi.org/10.1016/j.palaeo.2019.109450

Sacek, V. 2014. Drainage Reversal of the Amazon River Due to the Coupling of Surface and Lithospheric Processes. *Earth and Planetary Science Letters*, 401: 301–312. https://doi.org/10.1016/j.epsl.2014.06.022

Sah, S. C. D. 1967. *Palynology of an Upper Neogene Profile from Rusizi Valley (Burundi)*. Annales du Musée Royal de l'Afrique Centrale, Tervuren Series 8, 57.

Sah, S. C. D., and S. K. Dutta. 1966. Palynostratigraphy of the Sedimentary Formations of Assam-1. Stratigraphical Position of the Cherra Formation. *Palaeobotanist*, 15 (1-2): 72–86.

Salamanca-Villegas, S., E. Van Soelen, M. L. T. Van Manen, S. G. A. Flantua, R. V. Santos, M. Roddaz, E. L. Dantas, E. Van Loon, J. S. S. Damsté, J. H. Kim, and C. Hoorn. 2016. Amazon Forest Dynamics under Changing Abiotic Conditions in the Early Miocene (Colombian Amazonia). *Journal of Biogeography*, 43: 2424–2437. https://doi.org/10.1111/jbi.12769

Salard-Cheboldaeff, M. 1974. Pollens tertiaries du Cameroun rapportés a la famille des Hippocratéacées [Pollen from Cameroon related to the Hippocrateaceae Family]. *Pollen et Spores*, 16(4): 499–506.

Salard-Cheboldaeff, M. 1978. Sur la palynoflore maestrichtienne et tertiaire du basin sédimentaire littoral du Cameroun [On the Maastrihtian and Tertiary Palynoflora of the Littoral Sedimentary Basin of Cameroon]. *Pollen et Spores*, 20(2): 215–260.

Salas-Gismondi, R., P. Baby, P.-O. Antoine, F. Pujos, M. Benammi, N. Espurt, S. Brusset, M. Urbina, and D. De Franceschi. 2006. "Late Middle Miocene Vertebrates from the Peruvian Amazonian Basin (Inuya and Mapuya Rivers, Ucayali): Fitzcarrald Expedition 2005." Proceedings of the XIII Congreso Peruano de Geología. Lima, Peru, 17–20 October. *Publicación especial (Sociedad Geológica del Perú)*, 7: 643–646.

Salas-Gismondi, R., J. J. Flynn, P. Baby, J. V. Tejada-Lara, F. P. Wesselingh, and P.-O. Antoine. 2015. A Miocene Hyperdiverse Crocodilian Community

Reveals Peculiar Trophic Dynamics in Proto-Amazonian Mega-Wetlands. *Proceedings of the Royal Society B*, 282: 20142490. http://dx.doi.org/10.1098/rspb.2014.2490

Samoilovich, S. R., and N. D. Mtchedlishvili, eds. 1961. *Pyl'tsa i spory zapadnoi Sibiri:yura-Paleotsen.* [Pollen and Spores from Western Siberia: Jurassic-Paleocene]. Leningrad, Russia: Vserossiyskiy Neftyanoy Nauchno-Issledovatel›skiy Geologorazvedochnyy Institut, No. 177.

Sanders, H. L. 1968. Marine Benthic Diversity: A Comparative Study. *American Naturalist*, 102(925): 243–282.

Sarmiento, G. 1992. Palinología de la Formación Guaduas—Estratigrafía y sistemática [Palynology of the Guaduas Formation—Stratigraphy and Systematics]. *Boletín Geológico*, 32: 45–126.

Schrank, E. 1994. Palynology of the Yesomma Formation in Northern Somalia: A Study of Pollen, Spores and Associated Phytoplankton from the Late Cretaceous Palmae Province. *Palaeontographica Abteilung B*, 231: 63–112.

Schuler, M., and J. Doubinger. 1970. Observations palynologiques dans le Basin d'Amaga (Colombie) [Palynological Observations of the D'Amaga Basin (Colombia)]. *Pollen et Spores*, 12(3): 429–450.

Selling, O. H. 1944. Studies in the Recent and Fossil Species of *Schizaea*, with Particular Reference to Their Spore Characters. *Meddelanden fran Goteborgs Botaniska Tradgard*, 16: 1–112.

Selling, O. H. 1946. Studies in Hawaiian pollen statistics. Part 1. The spores of the Hawaiian pteridophtyes. *Bernice P. Bishop Museum Special Publication*, 37.

Silva, M. P., R. Mauro, G. Mourão, and M. Coutinho. 2000. Distribuição e quantificação de classes de vegetação do pantanal através de levantamento aéreo [Distribution and Quantification of Vegetation Classes in the Pantanal using Aerial Survey]. *Revista Brasileira de Botânica*, 23(2): 143–152. https://doi.org/10.1590/S0100-84042000000200004

Silva-Caminha, S. A. F., C. D'Apolito, C. Jaramillo, B. S. Espinosa, and M. Rueda. 2020. Palynostratigraphy of the Ramon and Solimões Formations in the Acre Basin, Brazil. *Journal of South American Earth Sciences*, 103: 102720. https://doi.org/10.1016/j.jsames.2020.102720

Silva-Caminha, S. A. F., C. Jaramillo, M. L. Absy. 2010. Neogene Palynology of the Solimões Basin, Brazilian Amazonia. *Palaeontographica Abteilung B*, 283 (1–3): 1–67. https://doi.org/10.1127/palb/284/2010/13

Singh, C. 1971. *Lower Cretaceous Microflora of the Peace River Area, Northwestern Alberta*. Research Council of Alberta Bulletin, 28: 1–586.

Singh, C. 1983. *Cenomanian Microfloras of the Peace River Area, Northwestern Alberta*. Alberta Geological Survey Bulletin, 44.

Srivastava, S. K. 1969. Some Angiosperm Pollen from the Edmonton Group (Maestrichtian), Alberta, Canada. In *J. Sen Memorial Volume, Special Publication,* ed. H. Santapau, A. K. Ghosh, S. Chanda, S. K. Roy, and S. K. Chaudhuri, pp. 47–67. Calcutta: J. Sen Memorial Committee and Botanical Society of Bengal.

Srivastava, S. K. 1971. Monolete Spores from the Edmonton Formation (Maastrichian), Alberta, Canada. *Review of Palaeobotany and Palynology*, 11: 251–265. https://doi.org/10.1016/0034-6667(71)90006-6

Stein, A., K. Gerstner, and H. Kreft. 2014. Environmental Heterogeneity as a Universal Driver of Species Richness Across Taxa, Biomes and Spatial Scale. *Ecology Letters*, 17: 866–880. https://doi.org/10.1111/ele.12277

Sugihara, G. 1980. Minimal Community Structure: An Explanation of Species Abundance Patterns. *American Naturalist*, 116(6): 770–787.

Sugita, S. 1994. Pollen Representation of Vegetation in Quaternary Sediments: Theory and Method in Patchy Vegetation. *Journal of Ecology*, 82(4): 881–897.

Takahashi, K., and U. Jux. 1989. Palynology of Middle Tertiary Lacustrine Deposits from the Jos Plateau, Nigeria. *Bulletin of the Faculty of Liberal Arts, Nagasaki University (Natural Science)*, 29(2): 181–367.

Tews, J., U. Brose, V. Grimm, K. Tielborger, M. C. Wichmann, M. Schwager, and F. Jeltsch. 2004. Animal Species Diversity Driven by Habitat Heterogeneity/Diversity: The Importance of Keystone Structures. *Journal of Biogeography*, 31: 79–92. https://doi.org/10.1046/j.0305-0270.2003.00994.x

Thiergart, F. 1938 [1937]. Die Pollenflora der Niederlausitzer Braunkohle, besonders im Profil der Grube Marga bei Senftenberg [The Pollen Flora of the Niederlausitz Lignite, Especially in the Profile of the Marga Mine Near Senftenberg]. *Jahrbuch der Preussische geologischen Landesanstalt und Bergakademie zu Berlin*, 58: 282–356.

Thiergart, F. 1940. Die mikropalaontologie als Pollenanalyse in dienst der Braunkohlenforschung [Micropaleontology as Pollen Analysis in the Service of Lignite Research]. *Brennstoff-Geologie*, 13: 1–82.

Thomson, P. W., and H. Pflug. 1953. Pollen und Sporen des mitteleuropaischen Tertiars [Pollen and Spore from the Central European Tertyary]. *Palaeontographica Abteilung B*, 94: 1–138.

Toivonen, T., S. Maki, and R. Kalliola. 2007. The Riverscape of Western Amazonia—A Quantitative Approach to the Fluvial Biogeography of the Region. *Journal of Biogeography*, 34(8):1374–1387. https://doi.org/10.1111/j.1365-2699.2007.01741.x

Traverse, A. 1955. *Pollen Analysis of the Brandon Lignite of Vermont*. U.S. Bureau of Mines, Report of Investigations, 5151.

Tuomisto, H., G. M. Moulatlet, H. Balslev, T. Emilio, F. O. G. Figueiredo, D. Pedersen, and K. Ruokolainen. 2016. A Compositional Turnover Zone of Biogeographical Magnitude within Lowland Amazonia. *Journal of Biogeography*, 43: 2400–2411. https://doi.org/10.1111/jbi.12864

Turland, N. J., J. H. Wiersema, F. R. Barrie, W. Greuter, D. L. Hawksworth, P. S. Herendeen, S. Knapp, W.-H. Kusber, D.-Z. Li, K. Marhold, T. W. May, J. McNeill, A. M. Monro, J. Prado, M. J. Price, and G. F. Smith. 2018. *International Code of Nomenclature for Algae, Fungi, and Plants (Shenzhen Code) Adopted by the Nineteenth International Botanical Congress Shenzhen, China, July 2017. Regnum Vegetabile 159*. Glashütten, Germany: Koeltz Botanical Books. https://doi.org/10.12705/Code.2018

Urrego, L. E., C. González, G. Urán, and J. Polanía. 2010. Modern Pollen Rain in Mangroves from San Andres Island, Colombian Caribbean. *Review of Palaeobotany and Palynology*, 162: 168–182. https://doi.org/10.1016/j.revpalbo.2010.06.006

Vajda-Santivanez, V. 1999. Miospores from Upper Cretaceous-Paleocene Strata in Northwestern Bolivia. *Palynology*, 23: 181–196. https://doi.org/10.1080/01916122.1999.9989527

Van der Hammen, T. 1954. The Development of Colombian Flora throughout Geologic Periods: I, Maestrichtian to Lower Tertiary. *Boletín Geológico*, 2: 49–106.

Van der Hammen, T. 1956a. Description of Some Genera and Species of Fossil Pollen and Spores. *Boletín Geológico*, 4: 103–109.

Van der Hammen, T. 1956b. A Palynological Systematic Nomenclature. *Boletín Geológico*, 4: 63–101.

Van der Hammen, T., and D. Burger. 1966. Pollen Flora and Age of the Takutu Formation (Guyana). *Leidse Geologische Mededelingen*, 38: 173–180.

Van der Hammen, T., and C. García. 1966. The Paleocene Pollen Flora of Colombia. *Leidse Geologische Mededelingen*, 35: 105–114.

Van der Hammen, T., and T. A. Wymstra. 1964. A Palynological Study on the Tertiary and Upper Cretaceous of British Guayana. *Leidse Geologische Mededelingen*, 30: 183–241.

Van der Kaars, W. A. 1983. A Palynological-Paleoecological Study of the Lower Tertiary Coal-Bed Sequence from El Cerrejón (Colombia): *Geología Norandina*, 8: 33–48.

Van Hoeken-Klinkenberg, P. M. J. 1964. A Palynological Investigation of Some Upper Cretaceous Sediments in Nigeria. *Pollen et Spores*, 6: 209–231.

Van Hoeken-Klinkenberg, P. M. J. 1966. Maastrichtian Paleocene and Eocene Pollen and Spores from Nigeria. *Leidse Geologische Mededelingen*, 38: 37–48.

Wall, D. 1967. Fossil Microplankton in Deep-Sea Cores from the Caribbean Sea. *Palaeontology*, 10(1): 95–123.

Weng, C., M. B. Bush, and M. R. Silman. 2004. An Analysis of Modern Pollen Rain on an Elevational Gradient in Southern Peru. *Journal of Tropical Ecology*, 20: 113–124. https://doi.org/10.1017/S0266467403001068

Wesselingh, F. P. 2006. Molluscs from the Miocene Pebas Formation of Peruvian and Colombian Amazonia. *Scripta Geologica*, 133: 19–290.

Wesselingh, F. P., J. Guerrero, M. Räsänen, L. Romero-Pitmann, and H. Vonhof. 2006a. Landscape Evolution and Depositional Processes in the Miocene Amazonian Pebas Lake/Wetland System: Evidence from Exploratory Boreholes in Northeastern Peru. *Scripta Geologica*, 133: 323–361.

Wesselingh, F. P., C. Hoorn, J. Guerrero, M. Räsänen, L. Romero-Pitmann. 2006b. The Stratigraphy and Regional Structure of Miocene Deposits in Western Amazonia (Peru, Colombia and Brazil), with Implications for Late Neogene Landscape Evolution. *Scripta Geologica*, 133: 291–322.

Wesselingh, F. P., and M. I. Ramos. 2010. Amazonian Aquatic Invertebrate Faunas (Mollusca, Ostracoda) and Their Development Over the Past 30 Million Years. In *Amazonia: Landscape and Species Evolution—A Look into the Past*, ed. C. Hoorn and F. P. Wesselingh, pp. 302–316. Oxford: Blackwell Publishing.

Wesselingh, F. P., M. E. Räsänen, G. Irion, H. B. Vonhof, R. Kaandorp, W. Renema, L. Romero Pittman, and M. Gingras. 2002. Lake Pebas: A Palaeoecological Reconstruction of a Miocene, Long-Lived Lake Complex in Western Amazonia. *Cainozoic Research*, 1: 35–81.

Weyland, H. and W. Krieger. 1953. Die Sporen und Pollen der Aachener Kreide und ihre Bedeutung fur die Charakterisierung des Mittleren Senons [The Spores and Pollen of the Aachen Chalk and Their Significance for the Characterization of the Middle Senonian]. *Palaeontographica Abteilung B*, 95: 6–29.

Wittmann, F., J. Schöngart, J. C. Montero, T. Motzer, W. J. Junk, M. T. F. Piedade, H. L. Queiroz, and M. Worbes. 2006. Tree Species Composition and Diversity Gradients in White-Water Forests across the Amazon Basin. *Journal of Biogeography*, 33(8): 1334–1347. https://doi.org/10.1111/j.1365-2699.2006.01495.x

Wodehouse, R. P. 1933. The Oil Shales of the Eocene Green River Formation. *Bulletin of the Torrey Botanical Club*, 60: 479–535.

Wood, G. D., A. M. Gabriel, and J. C. Lawson. 1996. Palynological Techniques—Processing and Microscopy. In *Palynology: Principles and Applications* ed. J. Jansonius and D. C. McGregor, pp. 29–50. Volume 1. Dallas, Tex.: American Association of Stratigraphic Palynologists Foundation.

You, Y., M. Huber, R. D. Müller, C. J. Poulsen, and J. Ribbe. 2009. Simulation of the Middle Miocene Climate Optimum. *Geophysical Research Letters*, 36: L04702. https://doi.org/10.1029/2008GL036571

Zhang, Y. G., M. Pagani, Z. Liu, S. M. Bohaty, and R. DeConto. 2013. A 40-Million-Year History of Atmospheric CO2. *Philosophical Transactions of the Royal Society A*, 371: 20130096. http://dx.doi.org/10.1098/rsta.2013.0096

Index of Algae and Dinoflagellate Cysts, Spores, and Pollen

Algae and Dinoflagellate Cysts

SPORES

POLLEN

SUMMARY OF REQUIREMENTS FOR SMITHSONIAN CONTRIBUTIONS SERIES

For comprehensive guidelines and specifications, visit https://scholarlypress.si.edu.

ABSTRACTS must not exceed 300 words.

TEXT must be prepared in a recent version of Microsoft Word; use a Times font in 12 point for regular text; be double-spaced; and have 1” margins.

REQUIRED ELEMENTS are title page, abstract, table of contents, main text, and references.

FIGURES must be numbered sequentially (1, 2, 3, etc.) in the order called out; have components lettered consistently (in size, font, and style) and described in captions; include a scale bar or scale description, if appropriate; include any legends in or on figures rather than in captions. Figures must be original and must be submitted as individual TIF or EPS files.

FIGURE FILES must meet all required specifications in the Digital Art Preparation Guide. Color images should be requested only if required.

TAXONOMIC KEYS in natural history manuscripts should use the aligned-couplet form for zoology. If cross referencing is required between key and text, do not include page references within the key, but number the keyed-out taxa, using the same numbers with their corresponding heads in the text.

SYNONYMY IN ZOOLOGY must use the short form (taxon, author, year:page), with full reference at the end of the manuscript under “References.”

REFERENCES should be in alphabetical order, and in chronological order for same-author entries. Each reference should be cited at least once in main text. Complete bibliographic information must be included in all citations. Examples of the most common types of citations can be found at SISP’s website under Resources/Guidelines & Forms.